UNIVERSITÀ DEGLI STUDI DI MILANO

Faculty of Veterinary Medicine

Graduate School of Animal Health and Production:
Science, Technology and Biotechnologies
Department of Health, Animal Science and Food Safety

PhD Course in Biotechnologies Applied to Veterinary and
Animal Husbandry Sciences
Class XXVIII

Improving in vitro embryo production: the use of oocyte chromatin configuration and cumulus cell gene expression profile to set up customized pre-IVM protocol.

PhD Candidate: Cecilia DIECI
Nr. R09996

Tutor: Prof. Alberto Maria LUCIANO, PhD
Co-Tutor: Prof.ssa Valentina LODDE, PhD

PhD program coordinator: Prof. Fulvio GANDOLFI

Academic Year 2017-2018

"So, remember, look at the stars and not at your feet. However difficult life may seem, there is always something you can do and succeed at. It matters that you don't just give up"

S. Hawking

Dedicated to the strongest person I know: my husband, Frediano.

RIASSUNTO

L'efficienza delle tecnologie di produzione di embrioni in vitro (IVP) è ancora limitata sia in ambito zootecnico che in clinica umana. L'IVP consiste in 4 fasi principali in cui si verificano in laboratorio gli eventi chiave dello sviluppo di un nuovo organismo: 1) il recupero di ovociti immaturi (arrestati in profase I della divisione meiotica) da donatrici vive o isolati da ovaie raccolte da animali macellati; 2) la maturazione in vitro (IVM), cioè la coltura degli ovociti fino allo stadio di metafase II della meiosi; 3) la fecondazione in vitro (IVF) e 4) la coltura in vitro dell'embrione (IVC), durante la quale, gli embrioni di nuova formazione, raggiungono lo stadio di blastocisti. Dopo la fecondazione in vitro, gli embrioni possono essere trasferiti in riceventi attraverso il trasferimento embrionario o essere congelati per un uso successivo. Nonostante i potenziali progressi offerti dai sistemi IVP, la percentuale di successo nella specie bovina è rimasta pressoché stabile negli ultimi 30 anni ed è limitata ad un terzo degli ovociti isolati dall'ovaio che raggiungono lo stadio di blastocisti. Questa condizione è purtroppo comune ad altre specie. La qualità degli ovociti è cruciale per l'efficienza dei protocolli di IVP e la maturazione dell'ovocita rappresenta il primo processo limitante di tutto il sistema.

Al momento della rimozione dai follicoli ovarici antrali, gli ovociti si trovano arrestati alla profase della prima divisione meiotica, la cosiddetta fase della vescicola germinale (GV), in cui la cromatina è racchiusa all'interno dell'involucro nucleare. Gli ovociti allo stadio GV abitualmente utilizzati nelle pratiche di IVP sono raccolti da follicoli antrali di medie dimensioni e, in quanto tali, devono ancora completare i passaggi finali di crescita e differenziamento necessari ad acquisire la cosiddetta "competenza di sviluppo", ossia il corredo di organuli e molecole necessario a sostenere la fecondazione e lo sviluppo dell'embrione. Inoltre, poiché lo sviluppo dei follicoli dei mammiferi avviene a ondate successive, uno dei fattori limitanti è rappresentato dall'eterogeneità intrinseca degli ovociti sottoposti a IVM e dalla mancanza di approcci in vitro dedicati per finalizzare il loro processo di differenziamento.

Gli studi condotti durante il programma di dottorato mirano a definire parametri morfologici e funzionali non invasivi che possano essere utilizzati come marker del differenziamento degli ovociti e che possano essere considerati per migliorare l'efficienza delle tecniche attuali. Gli studi sono stati condotti sui modelli animali suino e bovino. In entrambe le specie, i cambiamenti progressivi nella configurazione su larga scala della cromatina, che caratterizzano il processo di differenziamento degli ovociti, sono stati utilizzati come marker di acquisizione della competenza allo sviluppo

embrionale. In particolare, l'ipotesi di lavoro principale è stata quella di utilizzare la configurazione della cromatina come indicatore dell'eterogeneità della popolazione di ovociti sottoposti a IVM e di mettere a punto protocolli personalizzati di maturazione con maggiore efficienza ed efficacia, che consentissero di massimizzare lo sfruttamento della riserva ovarica.

Nella prima parte di studi, sono stati caratterizzati i diversi pattern di configurazione della cromatina GV negli ovociti suini e queste informazioni sono state utilizzate per realizzare un protocollo di prematurazione in grado di migliorare la competenza allo sviluppo dell'ovocita. Nella seconda parte, nel modello bovino, sono stati studiati i profili di trascrizione delle cellule del cumulo basati sulla configurazione della cromatina nell'ovocita allo stadio di GV quali marker di competenza allo sviluppo embrionale. In questi studi, l'uso combinato dei parametri morfologici insieme all'analisi dei profili trascrittomici delle cellule del cumulo, ci ha permesso di convalidare un protocollo di coltura di base per la prematurazione dell'ovocita bovino.

In conclusione, i nostri dati indicano che il miglioramento dell'efficienza dei protocolli di IVP richiede la selezione di una popolazione di ovociti più omogenea, che deve essere trattata considerando specifici bisogni colturali dell'ovocita, quindi progettando un sistema di prematurazione personalizzato. In particolare, i nostri risultati contribuiscono all'identificazione di specifici biomarcatori non invasivi dello stato di differenziamento e di salute dell'ovocita che possono fornire strumenti utili per la selezione di ovociti di buona qualità e per migliorare il potenziale riproduttivo nei mammiferi di interesse zootecnico.

ABSTRACT

The efficiency of in vitro embryo production (IVP) technologies is still limited in both livestock and humans. IVP consists of 4 major steps in which the key events of the development of a new organism occur in the laboratory: 1) the recovery of immature (prophase I arrested) oocytes from live donors or from isolated ovaries collected from dead animals; 2) the in vitro maturation (IVM), i.e. the culture of oocytes up to the metaphase II stage of meiosis; 3) the in vitro fertilization (IVF) and 4) the in vitro embryo culture (IVC), during which the newly formed embryos reach the blastocyst stage of development. After IVC, the embryos can be transferred to female recipients through embryo transfer or be frozen for later use. Despite the potential advances offered by IVP systems, the percentage of success in cow remained stunning stable over the last 30 years and is restricted to one third of the oocytes isolated from the ovary reaching the blastocyst stage of embryonic development. This limitation is similar in other species. The quality of the oocytes is crucial for IVP efficiency and the maturation of the oocyte represents the first key limiting step of the system. At the time of removal from the ovarian antral follicles, the oocytes are arrested at the prophase of the first meiotic division, the so called Germinal Vesicle (GV) stage, in which the chromatin is enclosed within the nuclear envelope. GV stage oocytes routinely used in IVP settings are collected from middle sized antral follicles and, as such, would still need to complete the final growth and differentiation steps, necessary to provide the so-called 'developmental competence', i.e. the machinery required to sustain fertilization and embryo development. Moreover, since mammalian follicle development occurs in waves, some of the limiting factors lie in the intrinsic heterogeneity of the oocytes that are subjected to IVM and in the lack of dedicated in vitro approaches to finalize their differentiation process.

Studies conducted during the doctorate program aimed at defining morphological and functional non-invasive parameters that can be used as marker of oocyte differentiation and that can be considered to improve the efficiency of current techniques. The studies were conducted in porcine and bovine animal models. In both species, the progressive changes in large-scale chromatin configuration, that characterize the oocyte differentiation process, were used as a marker of differentiation and developmental potential acquisition. In particular, the main assumption was to utilize the chromatin configuration as an indicator of the heterogeneity of the oocyte population subjected to IVM and design customized IVM protocols with increased efficiency and efficacy, that would allow to maximize the exploitation of the oocyte reservoir.

In the first part, the porcine oocyte GV chromatin configuration patterns were characterized, and this information was utilized for testing a pre-IVM protocol able to improve oocyte developmental competence. In the second part, the cumulus cells transcriptomic profiles based on the GV chromatin configuration as a marker of oocyte developmental competence were studied in the bovine model. In these studies, the combined use of morphological parameters together with the analysis of the transcriptomic profiles of cumulus cells allowed us to validate a basic oocyte culture protocol.

In conclusion, our data indicate that the improvement of IVP outcome requires the selection of a more homogeneous oocyte population that must be treated considering specific oocyte cultural needs, so designing customized pre-IVM culture system. In particular, our findings contribute to the identification of specific non-invasive biomarker(s) of oocyte health status and final differentiation that can provide useful tools for the selection of good quality oocyte and to improve the reproductive potential in animal breeding.

ACKNOWLEDGEMENTS

My thanks equally go to my parents-in–law, **Pietro e Cristina Sebastiani**, and all their wonderful family, for treating me like one of their own. I owe them huge thanks not only for their constant support, but also for being such a wonderful grandparent.

Words fail me to express my totally appreciation to my lovely husband, my best friend and amazing father of my kids **Frediano**. Where would I be without you? You have been a true and great supporter and have unconditionally loved me during my good and bad times. You have been non-judgmental of me and instrumental in instilling confidence. You always take my problems as your own, help me to overcome them, and encourage me to achieve the highest level. You have faith in me and in my intellect even when I felt like digging hole. I truly thank you for always sticking by my side. The amount of patience you had with me in the last years was incredible. This thesis is in large part due to your indefinite help in the crucial moments where I was discouraging. You are my rock. There are no words to convey how much I love you.

Last, but not least, a huge thank to the three "masterpieces I produced" during my PhD, my lovely sons **Leone, Sveva e Irene.** Kids do not make things easier. But they do give you a reason to keep going. Thanks kids for teaching me that IMPOSSIBLE IS NOTHING… if you are surrounded with unconditional love and a certain amount of Lego! Being your mother is a great honor and has made my heart grow bigger than I ever knew it could be.

Kids, if you read this when you are older, we love you and we will make sure you get to follow your dreams just as we could.

TABLE OF CONTENT

LIST OF ABBREVIATIONS

3'UTR	3 prime untranslated region
5'UTR	5 prime untranslated region
ADAMTS1	disintegrin and metalloproteinase with thrombospondin type 1 motif, member 1
AREG	amphiregulin
ART	assisted reproductive technology
bFGF	basic fibroblast growth factor
BMP15	bone morphogenic protein 15
BTC	betacellulin
cAMP	cyclic adenosine monophosphate
CASP	caspase
CC	cumulus cell
CD44	CD44 antigen /gene
CDK1	cyclin dependent kinase one
cDNA	complementary DNA
cGMP	cyclic guanosine monophosphate
CL	corpus luteum
COC	cumulus oocyte complex
CREB	cAMP response element binding
CTRL	control
cx	connexin
CYP19A1	cytochrome P450, family 19, subfamily A, polypeptide 1
DAG	diacyl glycerol
DNA	deoxyribonucleic acid
DO	denuded oocyte
E2	estradiol
ECM	extracellular matrix
EGF	epidermal growth factor
EGF –Like	epidermal growth factor like
ER	endoplasmic reticulum
EREG	epiregulin

ERK1/2	extracellular signal related kinase
FF	follicular fluid
FSH	follicle stimulating hormone
FSHR	follicle stimulating hormone receptor
GC	granulosa cell
GDF9	growth differentiation factor 9
GJC	gap junction communication
GnRH	gonadotropin releasing hormone
GSH	glutathione
GTP	guanosine-5'-triphosphate
GV	germinal vesicle
GVBD	germinal vesicle breakdown
HA	hyaluronic acid
HAS2	hyaluronan synthase two
HCG	human corhionic gonadotropin
IETS	international embryo transfer society
IGF-I	insulin growth factor one
IVC	in vitro colture
IVF	in vitro fertilization
IVM	in vitro maturation
IVP	in vitro embryo production
Ial	inter-a-trypsin inhibitor
kDa	kilodalton
KO	knockout
LH	luteinizing hormone
LHR	luteinizing hormone receptor
MAPK	mitogen-activated protein kinase
MGC	mural granulosa cell
MI	metaphase One
MII	metaphase Two
Mos	moloney murine sarcoma viral oncogene homolog
MPF	maturation promoting factor
mRNA	messenger ribonucleic acid

NCBI	National Center for Biotechnology Information
NO	nitric oxide
NSN	non-surrounded nucleus
OPU	ovum pick-up
OSF	oocyte secreted factor
P4	progesterone
PCR	polymerase chain reaction
PDE	phosphodiesterase
PDGF	platelet derived growth factor
p-f	post-fertilization
PGC	primordial germ cell
PG	prostaglandin
PI3K	phosphatidyl inositol 3-kinase
PIP2	phosphatidylinositol 4,5-bisphosphate
PKA	protein kinase A
PKB	protein kinase B
PKC	protein kinase C
PLC	phospholipase C
PTX3	pentraxin 3
qRT-PCR	quantitative real-time PCR
RNA	ribonucleic acid
ROS	reactive oxygen species
rRNA	ribosomal RNA
RT	reverse transcriptase
SC	singly condensed
SCF	stem cell factor
SCNT	somatic cell nuclear transfer
siRNA	small interferring RNA
SN	surrounded nucleus
TGF	transforming growth factor
TNFAIP6	tumor necrosis factor-induced protein-6
TZP	tranzonal projection
ZP	zona pellucida

FOREWORD

In the first chapter, we firstly introduce the infertility issue. We then report a literature review focused on mammalian ovarian origin and functions, on oocyte maturation and developmental competence acquisition, as well as on cumulus cells differentiation and possible contribution to oocyte maturation, ovulation and fertilization. Finally, there is also a quick overview of the state of art of assisted reproductive technologies (ARTs).

Subsequent chapters represent two different parts of this PhD project. In particular, chapter 2 and 3 are published papers on international journals. They are therefore presented with their individual bibliography.

The last section contains a general discussion on the obtained results. Moreover, we provide our view on the future perspective of such a type of approach, aimed at selecting the best population of oocyte that could be efficiently used in in vitro embryo production (IVP).

The appendix section includes all the published papers in which I collaborated during my PhD.

CHAPTER 1: Literature Review

SECTION 1: THE SUBFERTILITY ISSUE

In the economics of livestock industry, the maintenance of fertility in animals is of considerable interest. As a matter of fact, infertility means heavy economic losses for the industry. In cattle, in the last 50 years we assisted to a constant decline in worldwide dairy cow fertility. This could be expressed as pregnancy rates to first insemination [1], calving interval, duration from calving to conception or number of insemination for conception [2]. Generally, subfertility is described as any condition leading to failure to establish a pregnancy following completion of uterine involution at 40–50 days post- partum [3]. Being the major cause for culling animals it has a great impact on dairy economics. In addition, the lost income from milk sale, the cost of semen needed for repeated attempts to artificially inseminate cows and the replacement of culled animals are all factors contributing to economic loss. Furthermore, it also has obvious animal welfare implications [3].

Interestingly, high selection to achieve increased milk yields has been considered to have a negative on the reproductive efficiency. However, higher milk production does not seem to be the unique feature to blame. Thus, reproductive success relates to follicular development, estrus onset, successful ovulation, fertilization, implantation, and the development and delivery of a healthy fetus. Anything interfering with these routines, such as diseases, poor nutrition, inadequate herd management, genetical or epigenetics factors, hormonal disturbances or environmental changes, could makes the animal infertile, if only temporarily.

Trying to overcome this type of problems, in the last decades, important results in ARTs have been achieved, thus improving in vitro embryo production (IVP). Milestones are for example the in vitro oocyte maturation (IVM), fertilization (IVF), intracytoplasmic sperm injection (ICSI), somatic cells nuclear transfer (SCNT) and dedicated embryo culture (IVC) system in different mammalian species, just to mention a few.
However, despite the many scientific advances, the IVP remains deeply inefficient, both in bovine and in pigs as well as in human clinical applications. The development of specific protocol for IVM that could produce high quality oocyte is a major challenge in ART [4]. It is widely agreed, for example, that low efficiencies of pig IVP and SCNT are at least in part due to a suboptimal IVM [5, 6]. Indeed, IVM approaches are still not able to provide a milieu that reflects the naturally changing environment of the follicle and to support the cellular changes taking place in the oocyte nuclear and cytoplasmic compartments.

Moreover, the information obtained studying different animal model should be a fundamental prerequisite to test new approaches or techniques before their preclinical trial in human.

It is important to remember that more than 80 millions of people are experiencing infertility troubles worldwide. One of the most studied animal in reproductive field is the mouse since it is easier and less expensive to achieve gene knock out (KO). The specie prolificacy, pubertal age, short follicular cycle and pregnancy duration have also contributed to this choice. However, the mouse model shows some major physiological differences compared to both large mammals and human. In fact, it is a polyovulatory specie with «accelerated» physiological processes [7], reflecting probably different signaling pathways and molecular regulation. The use of large mammals' model to study fundamental mechanism and new technologies before clinical investigation has offered a valuable solution. Actually, the choice of these models has solid arguments mainly interesting similarities with human. This includes the similar ovarian size, mature follicle diameter and corpus luteum (CL) dimension and in some cases the common monovulatory characteristic. The ovarian anatomy (superficial cortex, central stroma) and even the reproductive pathology (polycystic ovaries) were also comparable. Interestingly, the follicular waves, the physiology of ovulation and lactation as well as the early embryo chronology are analogous and are well studied and documented [8].

Clearly, all the studies regarding mammals or even human could help in a better characterization of the molecular determinants of oocyte quality thus permitting a better understanding of the reproductive process and ultimately improve IVP efficiency.

SECTION 2: THE OVARY

2.1 Ovarian development and differentiation

The word "ovary" derives from the Latin word "ovum," that means egg. The mammalian ovary is the organ responsible for the production of germ cells (oocytes). This organ has also an important endocrine function. These two aspects are fundamental in order to ensure a successful reproductive outcome. In this section, we depict how the germ cells arise and reach the undifferentiated gonad.

In mammals, the whole germ cell compartment of the ovary derives from a group of embryonic stem cells called primordial germ cells (PGC). PGCs are still diploid cells originated from the epiblast and then migrate into the posterior endoderm where they are detected in the yolk sac near the caudal end of the primitive streak and the allantois [9]. They are round shape and enclose enough energy reserves as lipid droplets and glycogen, especially at the beginning of their migration along the hindgut to the genital ridges [10, 11].

Initially, they move passively to the gut epithelium. They then, start moving actively by amoeboid movements influenced by chemotactic substances present in mammal embryonic microenvironment [12, 13].

After reaching the ventromedial face of the mesonephros, PGCs lose their motility, become even more proliferative undergoing intensive mitotic divisions. Then, they colonize the coelomic epithelium and start differentiation either in oogonia or spermatogonia (depending on the embryo genotype). The somatic compartment seems to be generated by segregating cells of the coelomic epithelium either from the mesenchyme of the ovary or from the mesonephros [14, 15]

The primordial gonadal tissue becomes oval shaped and separates its self in a bi-compartment structure: the central zone which is dense and the cortex that looks clearer and shows the first signs of sexual differentiation [16, 17]. Dividing oogonia are clustered and interconnected giving rise to the cortical sex cords.

Notably, the precise factors that are able to induce the conversion of oogonia to primary oocytes, through the induction of meiosis, come from somatic cells [18, 19]. This first meiotic event, sets forth the beginning of folliculogenesis.

2.2 Folliculogenesis

Folliculogenesis is the set of physiological and molecular events that drive the development of the small primordial follicles into preovulatory follicles that undergo atresia or ovulation [20].

As described in the previous paragraph, some oogonia start meiosis through the preleptotene stage. This step, that marks the conversion of oogonia to primary oocytes, is characterized by DNA replication and meiosis preparation. Thereafter, the oocyte moves through the events of the prophase I stage (i.e. including leptotene, zygotene, and pachytene) before arresting until puberty [21]. The beginning of the prophase I is variable among mammalian species. For example, it occurs during the fetal stage at the 9 to 10th week p-f for woman and cow.

Together with the meiosis's initiation primary oocytes, surrounded by a single layer of flattened pre-granulosa cells (GCs), become enclosed in a basement membrane [22]. Forming an independent entity named the **primordial follicle** (Fig. 1). These follicles are located in the periphery of the ovarian cortex and are considered as the structural and functional unit of the mammalian ovary. From which will derive all the subsequent follicular development stages pre- and post-natally. In cattle, their diameter is equal or less than 40 μm [23]. It is established that both intermediate junctions and gap junctions are already present between GCs. However, only intermediate junctions are present between granulosa and oocyte, at this stage [24] There is strong evidence that oocyte growth starts before follicle formation and continues along the folliculogenesis.

These meiotic arrested oocytes represent the definitive pool of oocytes of an individual. These, wait to be recruited for development, that could happen months or even years later depending on the species [25, 26]. After puberty, few of the arrested primordial follicles at a time enter the nonreversible growing phase during which GCs become cuboidal and restart mitosis.

When the oocyte is surrounded by a single layer of cuboidal GCs, the follicle reaches the **primary stage.** At this stage, the establishment of first gap junctions between the corona radiata cells and the oocyte is reported. The origin and the type of factors that induce the development of some primordial follicle are still undetermined. Although, in the mouse model some candidate genes have been reveled: The epidermal growth factor (EGF), the stem cell factor (SCF), the c-kit protein and its ligand (KL), bone morphogenetic protein-15 (BMP-15) and the growth differentiation factor-9 (GDF-9) [27]. At this stage, the zona pellucida (ZP) begins to form.

The **secondary stage** is characterized by the presence of at least two layers of cuboidal GCs

surrounding the oocyte. Interestingly, the inner most layer of GCs also exhibit processes that project across the ZP towards the oolemma termed tranzonal projections (TZPs). Moreover, at this stage gap junctions begin to form between the oocyte and the GCs [28]. A peripheral theca cell layer develops. There are several chemicals from the GCs, like platelet derived growth factor (PDGF) and basic fibroblast growth factor (bFGF), that are able to increase the expression of KL. This, promotes the acquisition of mesenchymal cells that become the theca layers, to the basil lamina of the follicle [29]. The theca cells form two different layers, the interna and the externa. The theca interna becomes very vascularized and is useful for clearing waste and transporting nutrients. The theca externa is a more loosely associated group of cells that contain smooth muscles cells [30]. Briefly, this follicular stage is marked by a growing oocyte, still at the diplotene stage, surrounded by mitotically active GCs [22, 31].

Finally, growing follicles reach the **tertiary or antral stage**. The follicles are then marked by the formation of a follicular fluid-filled cavity: the antrum. Its volume increases concomitantly with an active mitosis in the somatic compartment [32]. GCs create an osmotic gradient, by producing hyaluronan and versican, that draws the fluid inside the follicle [33]. At this stage, GCs can be classified as cumulus cells, closely associated to the oocyte (which inner layer is defined as the corona radiata) or more distant mural granulosa cells [34]. Cumulus cells and the female gamete form the cumulus cell-oocyte complex (COC). Surrounding the granulosa cells there is a basil lamina encircled by the theca cell layers

During follicle development, the enclosed oocyte resume transcription and grow in size until transcription stops and the oocytes reach the full size. In cow, when oocytes have reached their full size (greater than 120 µm in diameter) and the follicle diameter is about 3 mm, the level of transcriptional activity is immaterial if not completely absent [35]. These events are mainly driven by follicle stimulating hormone (FSH) stimulation [36]. Knowing that antral follicles were found at birth in women and cattle, follicular recruitment and growth look to begin in fetal life [37]). These early tertiary follicles are ready for follicular waves' recruitment. During a cattle's estrus cycle (discussed later), these follicular dynamics may include one to four waves of follicular synchronized cohorts. This could lead to the development the selection of the dominant preovulatory follicle [38]. Just prior to ovulation, GCs acquire the LH receptors and the perivitelline space is formed.
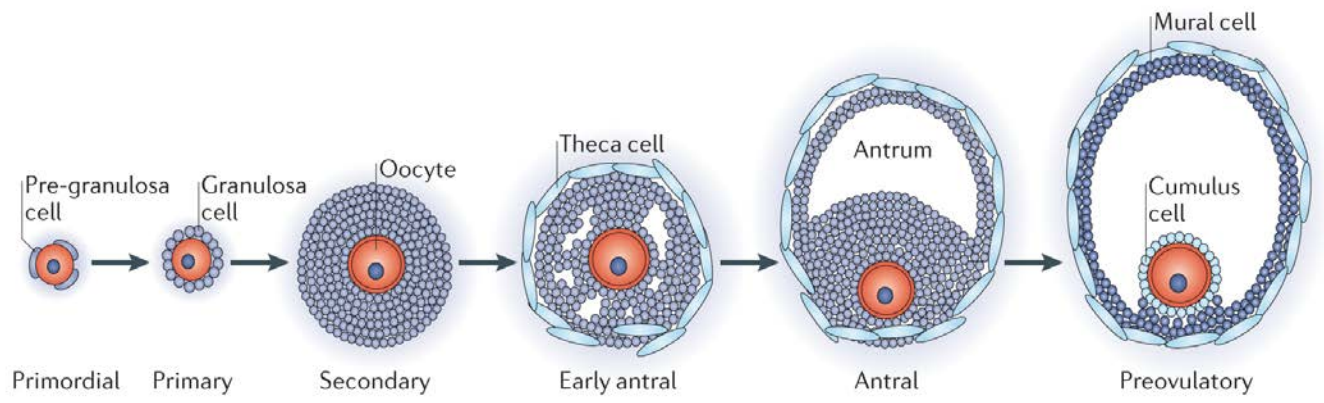
Fig. 1 Different stages of folliculogenesis [39]

2.3 Follicular waves and atresia

Follicular development occurs in waves. During the luteal estrus cycle, two or three cohorts of antral follicles are recruited to grow (Fig. 2). For example, bovine cycle has two or three follicular waves during a period of 21 (2 waves)-23 days (three waves), and only the final one is ovulatory [40]. Each wave consists of 3-to-5-synchronously-developing follicles [41-43].

The final follicular growth in mammals is a process that includes three main steps: recruitment, selection and dominance. Recruitment is the entrance into the gonadotropin-dependent phase of a cohort of follicles. A rise in FSH allows a medium antral follicle (> 5 mm) pool to undergo further growth. This first step seems to be mainly dependent on the follicle diameter and on the availability of functional gonadotropin receptors in its somatic compartment.

To permit large follicle growth to proceed, insulin-like growth factor (IGF) signaling is essential [44, 45]. In the end of the luteal phase, FSH concentrations appear to be higher in one medium sized follicle. Driving further growth and an earlier transition to LH responsiveness [46].

The selected follicle starts producing estradiol and inhibin to suppress the other follicles' growth, allowing it to become the only preovulatory follicle. In the case of poly ovulatory species, such as porcine, where many follicles ovulate simultaneously, the suppression is generated by a number of large follicles instead of one [47]. Unfortunately, the exact mechanism of selection is not fully understood, but certainly, a progressive switch of the future dominant follicle from FSH to LH dependence occurs [48]. The timing of mRNA expression of LH receptors in granulosa cells appears to be partially responsible for this switch [49]. Follicular growth will continue during the dominance phase until the follicle has reached a species and breed specific diameter [50]. In the end, the increase of the estradiol concentration stimulates the LH peak and the ovulation of the dominant follicle [51, 52].

After ovulation, the follicle luteinizes and the granulosa and theca cells, will form a CL that will secrete progesterone (P4). This hormone primes the uterus in case a pregnancy occurs [32]. It takes 15 days for the cow to recognize pregnancy thanks to the production of interferon tau [53]. In humans, the agent of recognition is chorionic gonadotropin [54]. If no pregnancy is detected, the uterus starts producing prostaglandin F 2-alpha to cause CL regression in preparation for the next period of estrus [32].

It is important to underline that among the large initial number of primordial follicles, only very few oocytes ovulate (the number varies by species). This is due to a process called follicular atresia. As mentioned above, each ovarian cycle requires the recruitment of a certain number of oocytes to grow simultaneously. However, these never ovulate even after reaching a certain diameter. [55] The subordinate follicles regress in favor of the dominant one. This may seem to be an inefficient process. However, such process may be useful to select the follicle containing the most developmental competent oocyte.

The programmed-cell death leading to atresia is a molecular process that can occur at any stage of the lifespan. Once the initial pool of follicles is established, any insufficient exchanges of molecules between the female gamete and the somatic compartment could be lethal. Even if not completely understood, some factors were reported to be involved in apoptosis of follicular cells. For example, the process seems to be regulated by members of the Bcl-2 family and by tumor necrosis factor family member cytokines [56], that in the end will activate the caspase cascade causing the programmed cell death [57], ultimately leading to follicular atresia.

Reactive oxygen species (ROS) signaling may also play a role in atresia. Typically, ROS accumulate in the cell and, when reaching an excessive level, could damage the DNA or even the protein structures [58]. Lund et al. have suggested that these negative effects can be partially neutralized by estradiol [59] in the dominant follicle. However, even the dominant follicle displays some level of atresia in the granulosa cells [60] [61], which is considered a process normally affecting 1-2% of granulosa cells of healthy follicles [62].
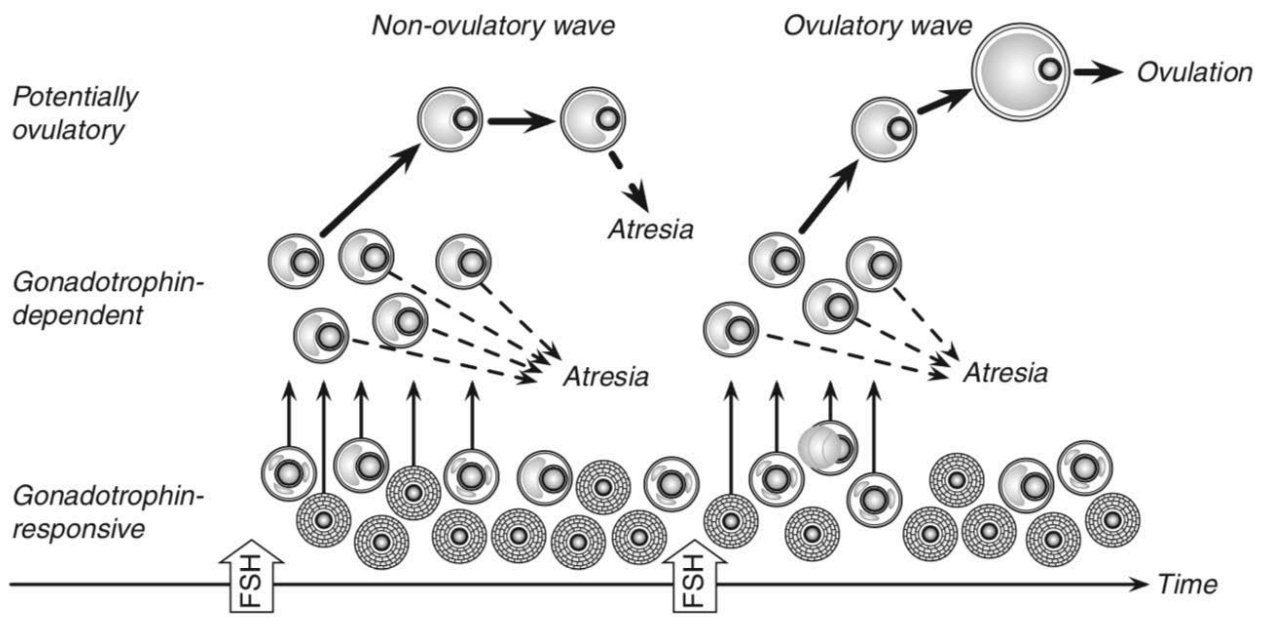
Fig. 2 The wave-like pattern in the terminal stages of follicle growth in bovine [63].

2.4 The estrous cycle

Estrous cycle consists of two main stages separated by the ovulation. A first proliferative event called follicular phase followed by a secretory one, called the luteal phase (Fig.3). In particular, in bovine, two to three follicular waves were detected during each estrous cycle [41, 42, 64]

The estrous cycle starts at puberty; i.e. between 8 to 12 months in heifers and 6 to 8 months in gilts. It includes four stages. The first one is proestrus, in which the final growth of one preovulatory follicle takes place. This stage is characterized also by the CL regression and by the decline in progesterone level. In contrast, estradiol level increases. The second stage is estrus, where ovulation occurs. The last two stages are metestrus, during which CL develops, and diestrus where the CL reaches its optimal progesterone secretory function. While the proestrus and estrus form the follicular phase, metestrus togheter with the diestrus constitute the luteal phase.

Normally, in cow and swine, each estrous cycle lasts on average 21 days starting by the estrus phase. Finally, if fertilization does not occur, the CL regresses and the level of FSH increases stimulating a new follicular wave.
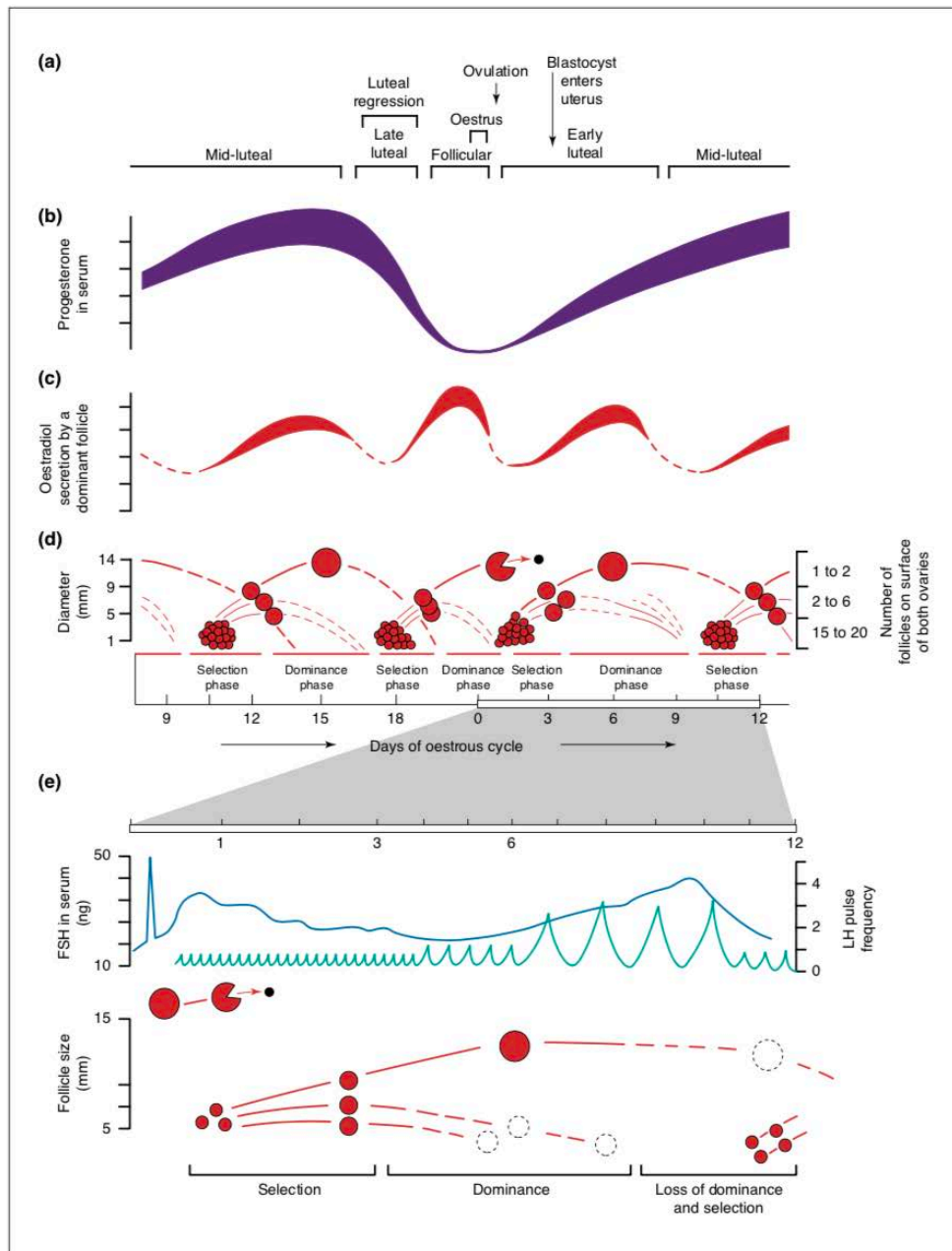
Fig. 3 Main endocrine patterns of the bovine estrous cycle (a) The stage of the bovine estrous cycle when selection, dominance and loss of dominance occur during each developmental wave of turnover of follicles. (b) Activity of the corpus luteum in terms of its progesterone output. (c) Correlation of estradiol production with the development of the dominant follicle in each wave. (d) The waves of follicular development throughout the cycle. Cohorts of follicles arise, and while one is selected to become dominant, the others become atretic. In the early and mid-luteal phases, the dominant follicle also atrophies, but in the cohort, that develops in the late luteal phase, the dominant follicle ovulates. (e) Events that take place in the different phases (selection, dominance, loss of dominance) in turnover of the first-wave dominant follicle (days 0–12 of the cycle,

corresponding to the bar on the axis in (d)) [42]

SECTION 3: THE OOCYTE

3.1 Oogenesis

The female reproductive system propagates life by producing a good quality oocyte that will become an embryo after fertilization. The most important difference between oocyte and sperm role in reproduction is that the sperm makes only a complementary genetic contribution to the zygote, meanwhile the oocyte is of course a genetic but also a cytoplasmic donor, contributing nearly all the organelles and non-chromosomal molecules needed for early embryonic development, up to the embryonic genome activation. These occurrences outline the incredible importance centering on the oocyte in the reproduction process.

The process that lead to the generation of the female gamete is termed oogenesis. This term describes the complete process of oocyte development and differentiation ranging from the migration of the first germ cells to the genital ridge until the formation of haploid, mature and developmentally competent female gamete [65]. As stated in the previous paragraph, the oocyte grows and differentiates within the ovarian follicle; thus, folliculogenesis process influences the oocyte growth, maturation and developmental competence acquisition [66]. It is obvious that, oogenesis and folliculogenesis are two strictly interconnected events, and their precise coordination is fundamental for obtaining a good quality gamete [67, 68].

As described before, the PGC (2n) start active mitosis once they reach the genital ridge becoming oogonia. This mitotic activity is crucial for the size of the initial oocyte reserve that will serve during the whole reproductive career of mammalian species. However, the key process in oogenesis is meiosis, which permit the transformation of the oogonia into oocytes. The mechanism and molecular factors involved in triggering the meiotic initiation are still poorly understood. Starting with a DNA synthesis phase, the oocytes progress with duplicated chromosomes through leptotene, zygotene and pachytene of the prophase I. This stage is characterized by the genetic material exchange between maternal and paternal chromatids, the so-called crossing-over. Each chromosome starts to condense, becomes thicker and lines up with its homologous to form a tetrad structure. Following the synaptonemal complex degradation, the bivalents remain attached via the chiasma. All the oocyte reserve is blocked at the diplotene stage, called also the germinal vesicle (GV), which refers to the oocyte's nucleus, prior to birth for both woman and cow [69]. It is

important to note that meiosis arrest is maintained for many years depending on species. Concomitantly with the follicle growth, the oocyte starts DNA transcription and increases its volume. During this period, the oocytes accumulates molecules that will drive the subsequent stages of oogenesis, fertilization and embryonic development, up to embryonic genome activation. Transcription ceases when he oocytes reaches its full size before meiotic resumption.

After the LH surge and prior to ovulation, the oocyte resumes meiosis (GV breakdown, GVBD) and achieves its first meiotic division and continues into the second meiotic division and arrests again at the metaphase II stage. The transition from the Prophase I to the metaphase II stage is referred to as 'oocyte maturation'. Meiosis resumes again at fertilization, when ana- and telophase II occur, and the second polar body is emitted. In the end oocyte involved in fertilization is a haploid cell.
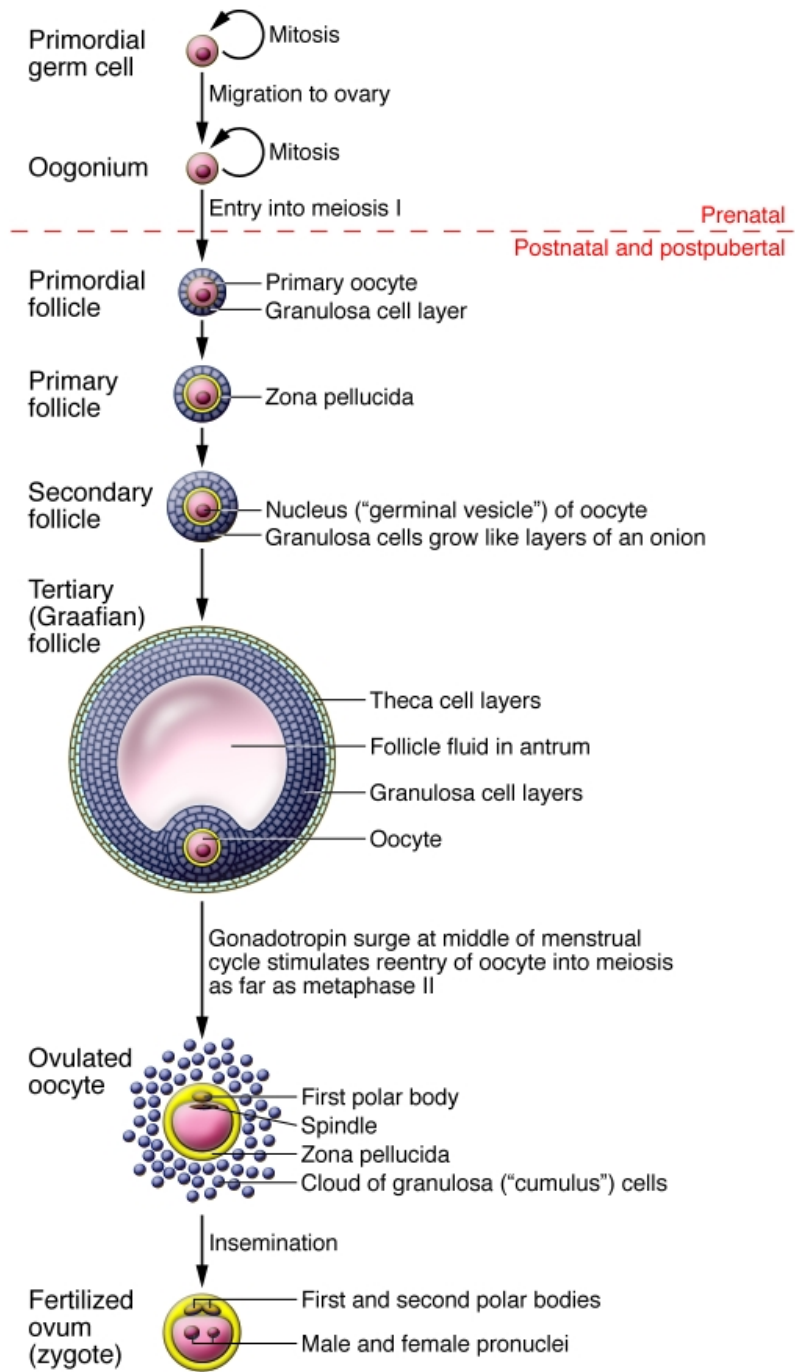
Figure 4. Schematic diagram of follicle and oocyte maturation and in the ovary ([66])

3.2 Oocyte growth, maturation and developmental competence acquisition

Oocyte competence is defined as the capability of the female gamete to mature, be fertilized and produce a good quality and transferable embryo able to give viable and healthy progeny. Many studies documented that oocyte maturation is the key step in the competence acquisition [70-72]. Oocyte maturation involves nuclear, cytoplasmic and molecular events.

The key event in nuclear maturation is mainly the meiotic process. The oocyte starts nuclear maturation as a cell that has been blocked at prophase I for a long time. Then, it goes through the breakdown of the nuclear envelope (also termed GV break down, GVBD), association of the homologous chromosomes, chromosome segregation and first PB extrusion, until the second meiotic arrest at MII stage. The second meiotic resumption will occur during fertilization process [73]. The meiotic progression is very exceptional in term of duration as well as regulation complexity.

In the immature oocyte, the nuclear chromatin is separated from the rest of the cytoplasm by nuclear envelope, which is a very selective membrane. Its inner face contains the nuclear lamina which have high affinity to chromatin and whose phosphorylation by the maturation promoting factor (MPF) causes their depolymerisation into small vesicles (GVBD) [74]. Histones have a very important role in nuclear maturation (H2A, H2B, H3, H4 and HI). Thanks to their positive charge, they can interact by electrostatic force with the phosphoric acid groups of the DNA, becoming responsible of the structural organization of the DNA. Moreover, if phosphorylated, they serve as transcription regulators. [75]

During follicular growth, the GV oocyte synthetize a large amount of ribosomal RNA (rRNA) as well as an increasing quantity of mRNAs stabilized by a poly(A) tail. In the end, the occurrence of GVBD signs the arrest of most if not all the transcriptional activity until the embryo genome activation [22, 76].

Cytoplasmic maturation refers to all the ultrastructural modifications that happen in the ooplasma starting some days before the LH surge to final nuclear maturation and that are in part responsible for a successful fertilization, cleavage and early embryo development [72, 77]. Unfortunately, there is no available direct measure of this type of maturation. That's why the meiotic maturation is commonly used as an indirect reference to the cytoplasmic one. The cytoplasmic maturation focuses mostly on ultrastructural and morphological aspects. With the oocyte maturation

progression, some visible cytoplasmic events happen. Firstly, Golgi membranes start to disappear leaving an area in between with very few organelles except for a large network of smooth endoplasmic reticulum (ER). Secondly, cortical granules move to the periphery thus becoming an effective barrier against polyspermy at the fertilization [28, 78, 79]. The ZP thickness and differentiation, as well as the nucleus dimension and the first polar body extrusion are other criteria used to assess oocyte cytoplasmic maturation [77]. However, the so-called molecular maturation is the one that most closely concerns the oocyte's embryonic developmental competence and that still represents the poorly characterized aspect (reviewed [80]).

During oocyte growth, the oocyte diameter increases notably, due in part to an intense metabolic activity. Effectively, the female gamete synthetizes and accumulates many molecules (mRNA, ribosomes, proteins) that contribute in maturation fulfillment and further embryonic development after fertilization. Molecular maturation includes all the molecular processes that occur both in the nucleus and ooplasma compartments. Although still poorly defined, molecular maturation is needed to accurately assess the oocyte maturation status. [81]. Its importance increases especially if we consider the limits of the morphological criteria used to evaluate oocyte competence. One of the main events in molecular maturation is mRNA transcription and storage. For example, many studies have shown a significant synthesis of mRNA during bovine oocyte growth [82, 83]measured through uridine triphosphate 35S-UTP incorporation method. The transcription level is reported to be high during the GV stage, when the chromatin has a permissive state [78]. Moreover, it is important to notice that the oocyte is able to store its mRNAs in an inactive translational state for long periods of times protecting them from degradation, thanks to the presence of the tail Poly (A) and RNA binding proteins, which safeguard them from the RNases enzymes. Certainly, the most notable process for meiotic resumption is the translation. As a matter of fact, if we treat oocyte with cycloheximide in order to inhibit protein synthesis, meiotic resumption will not occur.

Protein synthesis is achieved through a selective process based mainly on the poly (A) tail length [84, 85]. Untranslated region (3'UTR) appears to influence the stability, storage and translation of mRNA [86]. In bovine species, the synthesis of the proteins was maximum around the GVBD stage, three times more than its level at GV stage, before decreasing again around the MII stage [87] Moreover, post-translational modifications mainly phosphorylation are reported in the bovine oocyte during the G2/M transition [88]. There are many enzymes involved in this process as: Phosphatase (1 and 2A) [89] and many kinases such as Mos Kinases, the phosphatidylinositol 3 (PI3)-kinase, PKA, PKB, PKC and MAP kinases. Finally, we have to underline that there is an active metabolic activity within oocyte characterized by a significant increase in glycolysis

including pyruvate, glutamine and lactate, which seems to have a positive effect on nuclear maturation and developmental competence acquisition [90] [91, 92]Fan, 2004 #1223}.

In conclusion, a competent oocyte is a gamete that is able to achieve nuclear, cytoplasmic and molecular maturation, to get fertilized and go across early stages of embryo development until the blastocyst stage, and to lead to a viable and healthy offspring [81]. It is important to notice that a partial or total failure of any maturation type should affect the final competence achievement. On the contrary, successful achievement of previous maturation steps don't guarantee the followings. Due to its complexity, there is not a completely reliable way to measure the oocyte competence. Nowadays, the approaches used are based on oocyte or cumulus-oocyte complex (COC) morphology, but these markers are poorly predictive.

3.3 Large-scale Chromatin Remodeling Process

The process of oocyte chromatin remodeling, occurring in the nucleus towards the end of gamete differentiation and before meiotic resumption, has been studied in several mammalian species. Interestingly, this process seems to be positively related to the progressive oocyte competence acquisition.

As indicated before, the nucleus of oocytes arrested at the diplotene I stage shows an intact nuclear envelope that is named **germinal vesicle** (**GV**), while the breakdown of this envelope, which occurs after the resumption of meiosis is known as GV breakdown (GVBD).

During the last phase of the oocyte growth, the chromatin enclosed within the GV is subjected to several levels of regulation regarding both its structure and function. These events include mechanisms acting both locally, on specific loci, and on a large-scale to remodel wide portions of the genome. Morphologically, the chromosomes lose their typical appearance and form a loose chromatin mass [93], which undergoes dynamic rearrangements within the GV before meiotic resumption.

In 1990 Matson and Albertini [94] described these changes in the organization of the mouse oocyte's chromatin in correlation to progressive stages of follicular development. In their study, chromatin organization was classified into discrete patterns. Initially, the chromatin mass is dispersed throughout the nucleoplasm and appears mainly decondensed, with the exception of some aggregates of condensed chromatin. Thereafter, chromatin starts to condensate, and few chromatin foci start to associate with the nucleolar periphery until a complete rim of heterochromatin appears in close apposition to the nucleolus, which is not active at this stage (nucleolar remnant). Further studies confirmed these observations. Consequently, the presence or absence of a complete rim of heterochromatin around the nucleolus is considered to be the main morphological criteria for the classification of mouse GV oocytes. The configuration in which the perinucleolar chromatin rim is absent is named 'Non Surrounded Nucleolus' (NSN), while the configuration where the perinucleolar chromatin rim is present is termed 'Surrounded Nucleolus' (SN) [95-97]. Intermediate configurations have been defined as 'partly NSN' and 'partly SN' [98]. Notably, NSN type configuration is typical of oocytes collected from primordial to growing preantral follicles; nonetheless, NSN oocytes are also found in antral follicles that indeed enclose both NSN and SN oocytes. The percentage of SN oocytes increases with the expansion of the follicle diameter.

Starting from studies in the mouse model, GV chromatin configurations have been studied in several mammalian species by means of fluorescence microscopy analysis (Fig. 5). Thus, changes of the large-scale chromatin organization during oocyte growth and differentiation have been reported in monkey[99], pig[100, 101],human[102, 103], horse [104]-[105], cattle [106-108], goat[109], sheep[110], rabbit [111], buffalo[112], dog[113, 114], ferret [115] and cat [116]. The formation of the perinucleolar rim of condensed chromatin has been reported to be a typical feature in some of the above-mentioned species, including human, pig and monkey. However, notable exceptions have also been described. For example, in cattle and horse chromatin condenses into a single compact clump instead of forming a clearly detectable rim around the nucleolus [105, 107, 117]. Further electron microscopy studies in cow, though, have revealed that chromatin in these oocytes is mainly located near the nucleolar remnant, that in turn appears to be partially or completely encapsulated by heterochromatin [118]. Nevertheless, what is clear from scientific literature is that chromatin enclosed within the GV of the prophase I-arrested mammalian oocyte condenses progressively. In the end, the chromatin mass is concentrated in a small area of the nucleoplasm, often in close association with the inactive nucleolus. The processes of chromatin condensation and spatial reorganization typically reach their highest level just before meiotic resumption. Numerous studies on different mammalian species demonstrate that the increasement of chromatin condensation is related to a progressive increase of oocyte dimension and to antrum formation [94, 96, 97, 99, 100, 103, 107, 108, 110-112, 116];[102, 119]. Moreover, oocytes showing high levels of chromatin condensation have been positively related to an increased embryonic developmental potential as indicated before.

For example, in different species it occurs that oocytes have a higher capability to mature *in vitro* when isolated from large antral follicles that enclose a big proportion of oocytes showing advanced stages of chromatin condensation [95, 99, 111, 112, 120].

Further, evidence that oocytes with condensed chromatin are more able to sustain in *vitro* early embryonic development was firstly provided in murine model. In these works, living oocytes from antral follicles were divided into NSN and SN oocytes after staining with Hoechst 33342 and then subjected to standard procedures for IVP [121, 122]. Zuccotti et al. demonstrated that after *in vitro* maturation and fertilization, NSN oocytes were incapable of any development beyond the two-cell stage, whereas SN oocytes progressed till the blastocyst stage. In cattle, a similar experimental approach gave further insights into this process [107]. Bovine oocytes were classified into four stages based on their chromatin configuration under fluorescence microscopy and cultured in vitro with a system that enables embryonic development of denuded oocytes [123]. Specifically, the GV0 stage bovine oocyte is characterized by a diffuse filamentous pattern of chromatin dispersed in the

whole nuclear area; the GV1 and GV2 configurations represent early and intermediate stages, respectively, of chromatin remodeling, a process starting with the appearance of few foci of condensation in GV1 and proceeding with the formation of distinct clumps of condensed chromatin in GV2 oocytes. The GV3 is the stage where the maximum level of condensation is reached, with chromatin organized into a single mass. Importantly, when matured *in vitro*, oocytes with a GV0 configuration showed a very limited capacity to resume and complete meiosis, while virtually all the GV1, GV2 and GV3 oocytes were able to reach MII stage. On the contrary, after *in vitro* fertilization and embryo culture, only a limited percentage of GV1 oocytes are able to reach the blastocyst stage, while GV2 and GV3 oocytes showed a higher embryonic developmental potential [107]. In pig, there is a fundamental difference in the use of the nomenclature, that must be noted. In this species, GV1 configuration represents the higher degree of chromatin condensation and it is proceeded by stringy chromatin (SC) classes and the filamentous chromatin (FC) pattern. In particular, FC is characterized by the presence of a diffuse filamentous pattern of chromatin distributed in the whole nuclear area. The SC configurations are characterized by an increased level of condensation of the chromatin that became clearly thicker and organized into clumps. Finally, in GVI configuration all the condensed chromatin mass is organized around the nucleolus [124]. Thus, GV1 oocytes already acquire the ability to mature and be fertilized in vitro. On the contrary, GV2-GV4 configurations are typical of oocytes that have already resumed meiosis, even though the nuclear envelope is still detectable [125-127]

Unfortunately, the molecular mechanisms regulating changes in large-scale chromatin configuration in the mammalian oocyte still remain poorly understood.
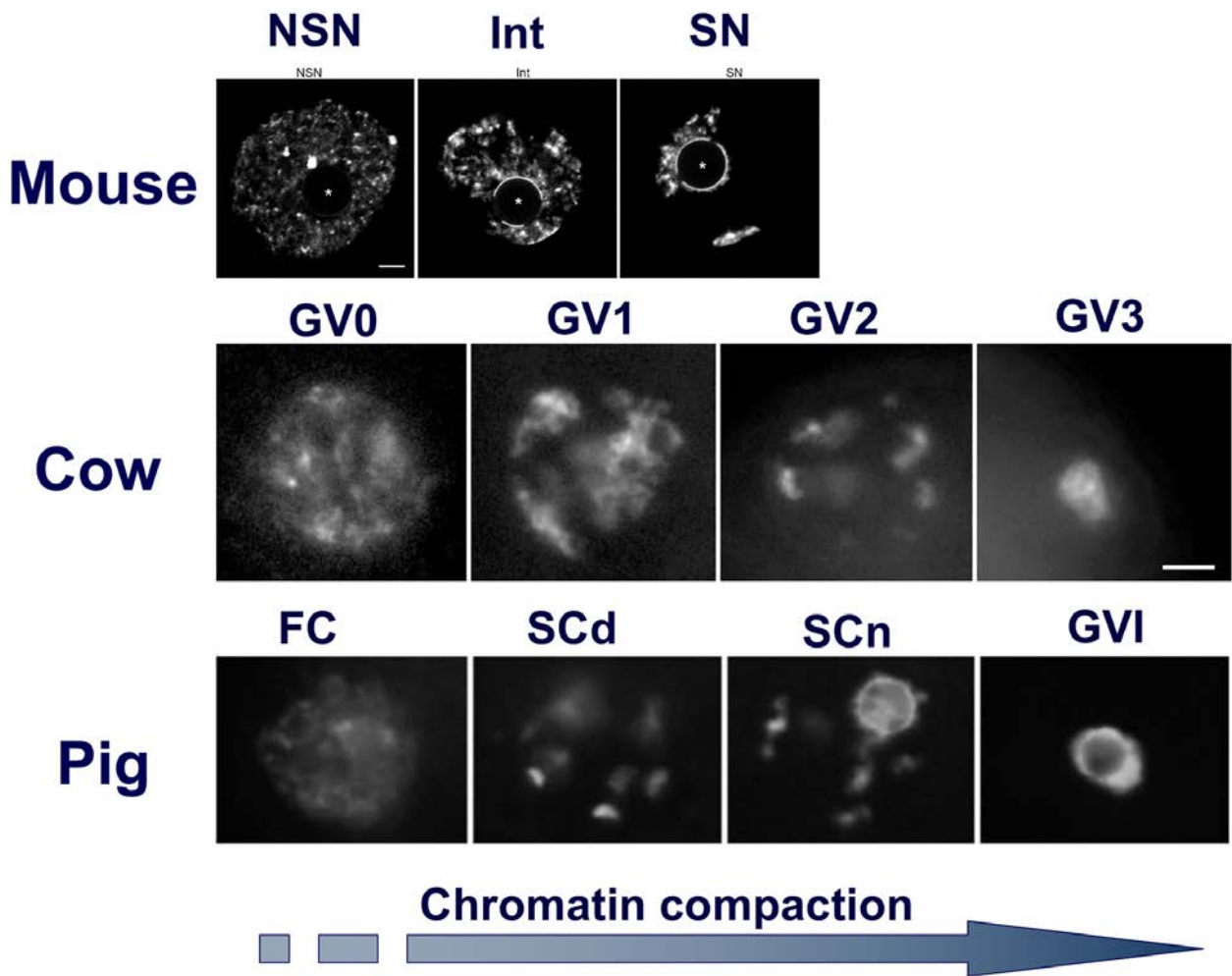
Fig. 5 Representative fluorescent images after Hoechst 33342 labeling of murine, bovine and porcine oocytes with different GV chromatin configurations [101, 107, 128]

SECTION 4: THE CUMULUS CELLS

During folliculogenesis, the female gamete is surrounded by follicular somatic cells that differentiate into mural granulosa cells (MGCs) and, starting from the tertiary follicle stage, into cumulus cells (CCs). CCs are highly specialized follicular cells that surround the oocyte and establish with it an intimate cell-to-cell communication gap-junctions (GJC) mediated. It has been established that the CCs removal or the disruption of these intercellular communications [101, 129-132], or the inhibition of their normal metabolic, transcriptional and/or translational activities[133, 134] negatively affect both oocyte maturation and developmental competence.

It is important to point out that CCs functions are deeply influenced by the follicular environments, as well as by oocyte-secreted factors (OSFs) (Fig.6).
As a matter of fact, in addition to gonadotropins, locally produced members of different growth factors families such as fibroblast growth factors (FGF), epidermal growth factors (EGF), transforming growth factors (TGF) and IGF are involved in follicular development as well as oocyte growth and maturation regulation. In particular, the EGF family stimulates granulosa cells proliferation and protein phosphorylation. The expression of both EGF and its receptor EGFR are induced by FSH in most mammalian granulosa cells. Other molecules, called EGF-like factors as epiregulin (EREG), amphiregulin (AREG) and betacellulin (BTC) are triggered also by gonadotropins. Incubation of follicles with these growth factors induced some morphological and biochemical events initiated by pituitary hormones, including CCs expansion and oocyte maturation [135]. Moreover, GDF9 and BMP15 are the most recognized OSFs. They are two members of the transforming growth factors (TGFs) superfamily[136-139]. These two factors promote granulosa and cumulus cells proliferation [140], prevent luteinization of the granulosa cells, inhibit apoptosis, and regulate metabolism. They transmit their signals through SMAD2/3 and EGFR-ERK1/2 signaling pathways to alter gene expression and cell function [141].
At the same time, several recent studies, based on physiological, metabolic or even genomic approaches, investigate how the CCs could influence oocyte maturation, competence acquisition, ovulation, fertilization and early embryo development. [142-150]. For this reason, recently CCs are used as a source of non-invasive biomarker for evaluating the quality of the female gamete in many mammalian species [151-153] However, most of the pathways and molecules involved in such a type of contribution still remain to be elucidated.

 Next section focuses on the CCs origin and differentiation in mammalian species and their intimate relationships with the female gamete.

4.1 Cumulus cells origin

Granulosa cells (GCs) are a pseudostratified epithelium that undergoes morphological and physiological changes from the secondary follicle stage until ovulation and luteinization. GCs derive from the mesonephric precursor cells although this statement has been recently revised suggesting a mesothelial origin from studies conducted in sheep [154]. In any case, since the cumulus cells line originate from GCs, they have therefore the same embryonic origin. Importantly, CCs are the result of the differentiation of preantral GCs into two cell sub-types: the mural granulosa cells (MGCs) located close to the follicular basal lamina and CCs that enclose the female gamete. At the beginning, the squamous granulosa cells of the primordial follicle become cuboidal and start to proliferate until the secondary stage follicle. Starting from the secondary stage GCs becomes FSH-responsive. Follicle and oocyte growths together until the oocyte reaches its maximal dimension. Thereafter, follicular growth becomes even faster, and the formation of pockets filled with follicular fluid (FF) occur within the GCs intercellular space [155]. The fusion of these pockets leads to the formation of the antrum. This fact determines the achievement of the tertiary follicle stage. Concomitant with GCs proliferation in mouse, GCs transcriptional activity increases and reaches its maximum just prior the formation of the antrum [156].

CCs display several ultrastructural and molecular signs of differentiation and high specialization that might be associated to their particular functions. For example, despite the presence of the LH receptor (LHR) transcripts in both granulosa and cumulus [157-159], the immunoassays revealed the lack of LHR protein both on the surface of the oocyte and on cumulus cells compared to mural GC [160].

The neo-formed CCs continue to differentiate also under the influence of oocyte-secreted factors [137, 138, 161]. The innermost layers of CCs, also called corona radiata, establish an intimate contact with the zona pellucida (ZP) allowing precise exchanges essential for the gamete maturation. These exchanges are thought to occur between the oolemma and the CCs transzonal cytoplasmic projections (TZPs) [162]. During ovulation, most of CCs will follow the oocyte in its journey through the oviduct. Conversely, the MGCs and theca cells will form the corpus luteum (CL).

The presence of cumulus cells is essential for oocyte growth, meiosis resumption, oocyte maturation and developmental competence acquisition. Relatively recent works also documented the importance of the oocyte in positively influencing the follicular cells proliferation and

differentiation. In particular, the TGF-P family are suggested to be the main responsible of these effects [130, 136]. For example, GDF9 and BMP 15 are two oocyte-secreted factors that influence CCs final differentiation prior to ovulation. These factors are reported to stimulate CCs expansion and to control gene expression during final phase of oocyte maturation [163]. To date, the main distinctive morphological characteristic for CCs is their capability to expand through the mucification process. For what it concerns transcriptomic, several studies showed that MGCs and CCs differentially respond to FSH stimulation by the selective expression of different genes [164-166]. These functional differences between MGCs and CCs are also due to intrinsic molecular pathways that allow differential gene expression and therefore distinctive functions between the two somatic cell types [167].

Considering the effect of both gonadotropins and oocyte-secreted factors on follicular compartment, one can detect a morphogen gradient that is responsible for the unique characteristics of CCs such as LH-R repression [135, 168, 169]) and ability to secrete progesterone [170-172]

To conclude, two opposite morphogen gradients are the real key players in follicular cells differentiation and specialization. A centripetal action would describe the gonadotropins effect, which predominate in theca and MGCs and decrease progressively near the oocyte. Conversely, the oocyte-secreted factors show a centrifugal effect. They are more effective on CCs than on the periphery of the follicle [173].

Cumulus cells to oocyte
e.g. Kit-ligand
FF-MAS
EGF-like peptides

Gap-junctional
cAMP
Purines/pyrimidines
Metabolites
Amino acids

Oocyte to cumulus cells
Oocyte-secreted factors
e.g. GDF-9
GDF-9B (BMP-15)
BMP-6
Activins?
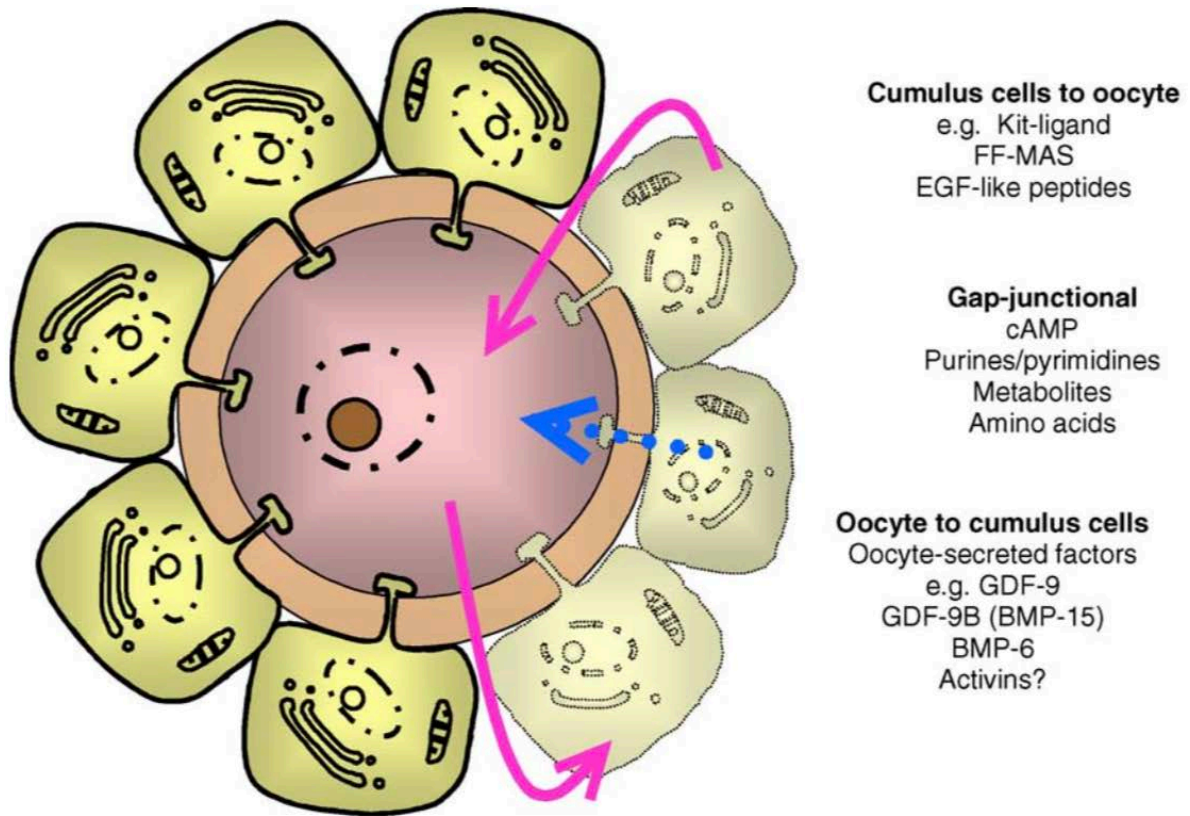
Fig. 6. Oocyte-granulosa cell communication: paracrine signaling (curved arrows) and gap-junctional exchange (straight arrow). [137]

4.2 Cumulus cells: the ability to expand

The capability of CCs to expand is mandatory for this cell type and it is a crucial step between the LH surge and the ovulation [174, 175].

Before the onset of the gonadotropins preovulatory surge, CCs form a compacted layer that enclosed the oocyte and maintain cell-cell communications both between each other and with the gamete. The process of cumulus expansion consists in complex morpho-structural changes induced by the LH surge. This process leads to the production of a mucoelastic matrix that will be deposit in the intercellular space between cumulus cells. This extracellular matrix (ECM) is composed by glycoproteins, hyaluronic acid (HA), proteoglycans. In vivo, CCs expansion is induced by LH (or by HCG) [176]. On the contrary, in vitro, CCs expansion is obtained using many factors such as: FSH, EGF superfamily (amphiregulin, AR; epiregulin, EREG; betacellulin, BTC...), IL6, and forskolin [132, 177-180].

After exposing preovulatory follicles to the LH surge, cumulus mucification starts with rapid expression of HAS2 gene and therefore an intensive production of hyaluronan acid (HA) This HA-rich matrix allows CCs distancing. The factor inter-a trypsin inhibitor (Ial) is another component of the ECM that was reported to allow protein complexes formation. It links proteins covalently to the HA molecule thus permitting ECM stabilization [181, 182].

HA binds with high affinity the tumor necrosis factor- induced factor 6 's (TNFAIP6) module domain. Domains that recognize HA were found also in other ECM proteins, such as CD44 and versican (CSPG2). The interaction of HA with the receptor CD44 is involved various biological functions. This interaction is modulated by TNFAIP6 [183, 184]. In addition to the Ial, the matrix stabilization is also promoted by pentraxin 3 (PTX3). It is a multifunctional protein playing a crucial role in the ECM assembly by possible covalent link with TNFAIP6 [185]. CCs mucification is also under the oocyte governance through the oocyte-secreted factors mainly the GDF9 and BMP 15 [138, 186] [187]. In fact, these factors are able to induce the expression of hyaluronan synthase 2 (HAS2), TNFAIP6 and PTX3 genes [188]. Interestingly, phenotypes of impaired ECM structure are accompanied by ovulation failure in each one of these three TNFAIP6-, PTX3- and ADAMTS1-null female mice [189-191].

Cumulus expansion and the consequent uncoupling between oocyte and cumulus cells relies on the

preovularory LH peak and depends by the second messenger cyclic nucleotide adenosine monophosphate (cAMP) activity. Using microinjection of fluorescent dyes, Luciano at al. reported that despite expansion, CCs remain metabolically coupled via gap junctions (GJC) even if the number of functional GJC decrease during IVM [107, 192-194]. This decrease of GJC during in vitro culture was also reported by Gilchrist Group elsewhere [195]. Importantly, Luciano and collaborators have highlighted the importance of the prolongation of the functional coupling during the IVM in the oocyte developmental competence acquisition [101, 105]. We should highlight that despite worthy information available about CCs expansion, supplementary yet unknown factors could be involved in this process.

Importantly, these results served as a conceptual basis for developing in vitro approaches aimed at increasing the time of cross-talk between the oocyte and the somatic compartment, useful for synchronizing the oocyte's nuclear and molecular maturation and increasing its embryonic developmental capability after fertilization. These protocols are named pre-maturation systems.

4.3 Cumulus Cells Metabolism and main Signaling Pathways

CCs are the elicited site for well-orchestrated processes that ensure the achievement of oocyte competence. The main characteristic of CCs is their ability to expand. This is the result of a precise gene expression profile, proteins production and different molecules deposition in the CCs intercellular space [145, 189, 196]. However, other relevant metabolic mechanisms occur in CCs. One of the most important is glycolysis, which is one of the main metabolic CCs process that is deeply influenced by the female gamete [197, 198]. The CCs glycolysis is reported to be essential for the gamete in term of nutritional needs. Thus, oocyte metabolizes glucose inefficiently. The CCs are able to transform glucose to pyruvate, which provides a glycolytic support for the oocyte during its growth and meiotic resumption in different mammalian species [199-201]

Cholesterol production is another metabolic pathway that takes place in CCs [202, 203]. CCs could synthesize cholesterol and transfer it to the oocyte. This metabolic activity is also driven by oocyte through BMP15 and GDF9 factors (Fig.7). Recently, Comiskey & Warner demonstrated that the cholesterol stored in the oocyte is essential not only for its maturation but also during the early embryonic developmental stages [204].

Steroidogenesis is another metabolic process guaranteed by CCs. Steroid hormones, mainly progesterone and estradiol, were reported to be produced in vitro by bovine CCs [205]. These steroids have a positive effect on the oocyte maturation and competence acquisition [206-208]. The oocyte is also able to prevent the luteinization both by stimulating estradiol production and at the same time by inhibiting progesterone production by cumulus cells [209, 210].

Amino acids availability is essentials for sustaining oocyte maturation and the oocyte is unable to use some of them even if present in the culture media. This is probably due to poor transport ability of the gamete [197, 211]. Conversely, specific amino acid transporters are overexpressed in CCs of antral follicles [144]. These allow the uptake of some selected amino acids such as L-histidine and L-alanine by CCs and their subsequent transport to the oocyte via GJC [211, 212].

Moreover, in order to support oocyte maturation and fertilization, the CCs are the site of action of several signaling pathways. For example, PKA has been the first identified kinase downstream the gonadotropins stimulation in mammalian CCs. This kinase is involved in ECM formation and stabilization as well as oocyte meiotic maturation [132, 213, 214] This pathway induces the

phosphorylation of some key factors such as p38MAPK, ERK1/2 and CREB in follicular cells [215, 216]. Additionally, the catalytic subunits of PKA could also move into the CCs' nucleus and activate specific transcription factors leading to the expression of several key genes such as EGF-like factors, HAS2, TNFAIP6 and CYP19A1 [177, 214, 216, 217].

Several works have widely demonstrated that cAMP has a fundamental role in the oocyte meiotic resumption regulation [193, 217., 218] Interestingly, cAMP is mainly produced by CCs. This cyclic nucleotide can enter into the oocyte via gap junctions. Once inside it arrests the meiotic resumption. The use of Cilostamide, a phosphodiesterase 3A (PDE3A) inhibitor, is able to maintains high endogenous levels of cAMP delaying meiotic resumption [101, 219]. After the gonadotropins surge, the meiosis resumption is associated with a progressive decrease of the cAMP concentration, mainly due to the GJC interruption. The induction as well as the inhibition of other phosphodiesterases such as PDE3A, PDE4B, PDE8 [148, 195, 217-220], and/or the block of cGMP entrance [221] also have profound effect in regulating this process and in mediating the signaling that induces meiotic resumption.

PKC and MAPK pathways are other relevant CCs signaling pathways that have a positive effect on oocyte maturation [220, 222]. The PKC pathway, mainly PLC/PIP2/DAG/PKC, is suggested to act in CCs upstream the MAPK cascades. This last pathway is necessary for the gonadotropin-induced meiotic resumption before the GVBD. It is also involved in microtubule organization and meiotic spindle formation [223] [224]. Several works demonstrated that the EGF-like factors trigger the PKC mediated induction oocyte maturation in different mammalian species [225, 226]. The MAPK induction of meiotic resumption in oocyte is suggested to act via MOS/MEK/ERK1/2 pathway [227]. Other oocyte-secreted factors, mainly the TGFp family, are crucial for the CCs differentiation, the support of oocyte maturation and the CCs expansion [161] [228]. These TGFp effects on CCs occurred mainly but non-exclusively through Smad 2/3 pathway [191, 229].

Keeping in mind all the aforesaid signaling pathways, it is obvious that CCs react to gonadotropins stimulation, oocyte and other intrafollicular factors (e.g. EGF-like factors) by triggering several different gene pathways. Despite the enormous complexity of such a type of regulation, these signaling cascades act harmoniously in order to properly support oocyte maturation, its subsequent fertilization and early embryo development.
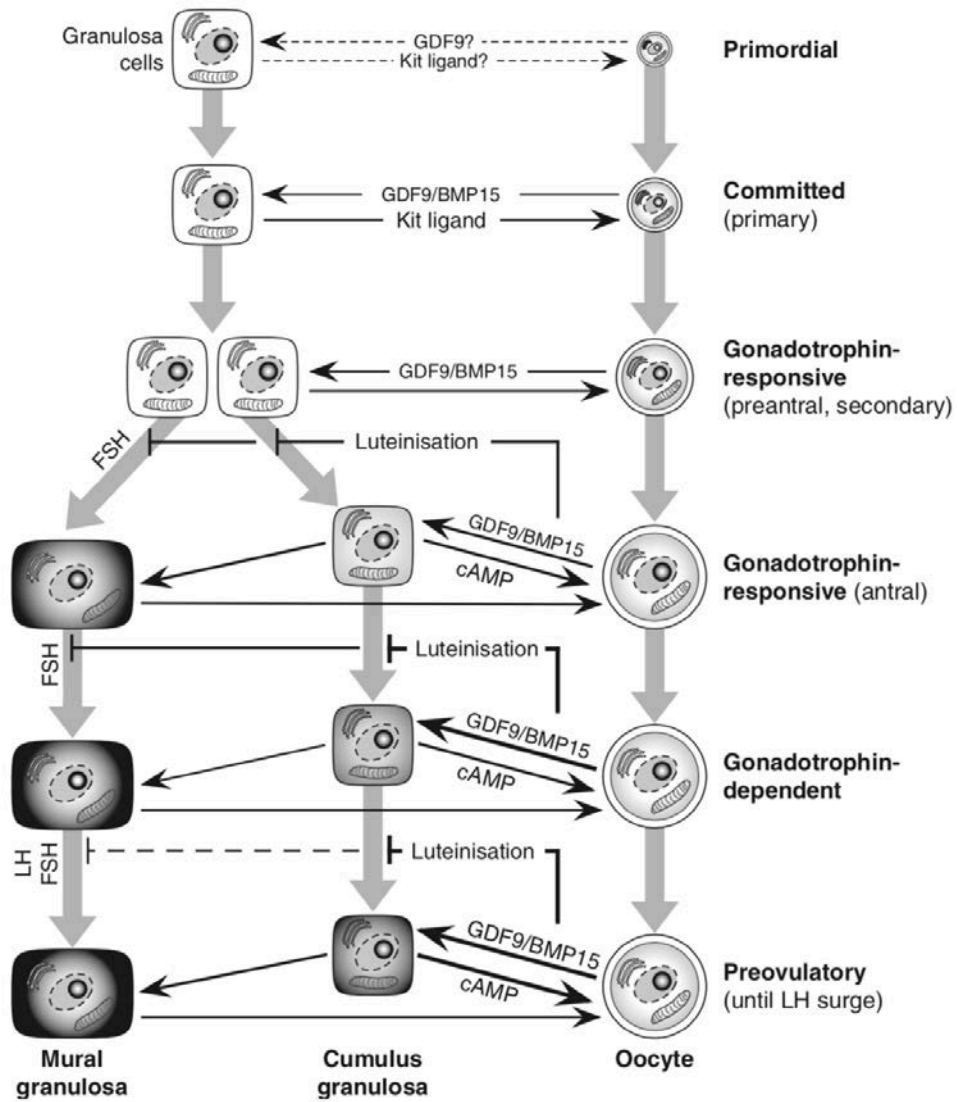
Fig. 7 A schematic illustration of the complex and highly integrated nature of folliculogenesis involving constant interactions between the oocyte and granulosa cells of developing follicles [63].

4.4 The importance of communications within the cumulus-oocyte complex (COC)

Several types of junctions exist between the plasma membranes of CCs and the female gamete. GJC, for example, play a pivotal role in small molecules trafficking. These junctional complexes increased in number and size in the rat preovulatory stages following FSH and/or estrogen actions. The inhibition of GJC in bovine COCs during maturation has a detrimental effect on oocyte developmental competence acquisition [123]. GJC consists in dimers of connexons. Each connexon is an oligomer formed by six connexins. Their formation starts with the passage of connexins through the Golgi apparatus, their oligomerization into hexameric connexons and their insertion into the plasmatic membrane. These hemichannels are kept closed until they attach to their complementary counterparts in the other side of the adjacent cell membrane [230, 231]. Connexin is the elementary unit of GJC. It is characterized by a transmembrane domain and by the ability to form functional channels. Many connexin isoforms arrange together in diverse combinations, thus affecting the channel selectivity. GJC are present at all the follicular stages in mammals. They are believed to be involved in the synchronization of cytoplasmic and nuclear maturation of the oocyte [232, 233]. The main connexins present in the follicle are Cx43 (GJA1), Cx 37 (GJA4) and Cx32 (GJB1) [142, 234]. Sutovsky has shown that cumulus- oocyte GJC are particularly rich in Cx43. Concerning communications between cumulus and oocyte, Luciano and collaborators documented a slight and constant decrease in GJC number during culture [193, 235]. GJC allow direct passage of small molecules less than 1 KDa of size, such as ions, cAMP, cGMP, inositol 1,4,5-triphosphate (IP3), nucleotides, amino acids, pyruvate, glucose and small peptides. They are reported to be involved in many signaling pathways and cellular functions like tissue-homeostasis maintenance, electrical and biochemical coupling between adjacent cells [236, 237]. A high number of genes code for different connexins, thus creating great diversity in terms of GJC sub-types [238]. Functional GJC is also fundamental in the oocyte competence acquisition in vitro. CCs co-culture with denuded oocytes didn't restore their developmental potential [123]. GJC permit also the passage of small interfering RNA (siRNA) up to 24 oligonucleotides [239]. Taken together, these findings highlight the need of additional studies to identify the different connexins patterns of expression both in CCs and oocyte during folliculogenesis, in order to better elucidate the communication flow between the two follicular compartments.

4.5 Cumulus cells contributions in oocyte maturation, ovulation and in early embryo development stages

While some oocyte-secreted factors are critical for CCs mucification, oocyte fails to reach its competence when its exchanges with CCs are interrupted [130, 131. During this process in vivo, the oocyte resumes meiosis following the LH surge and then arrests again in MII. As indicated before, proper oocyte nuclear and cytoplasmic maturations are essential to reach the developmental competence {Sirard, 2006 #1181]. Even if the meiotic resumption process is not completely understood, it is reported that CCs secrete a gonadotropin-dependent signal that promote meiosis resumption. This happens via the phosphatidylinositol 3-kinase (PI 3-kinase) and MAPK pathways, as well as GJC [240]. The activation of the MAPK / ERK 1/2 pathway in CCs is needed for the generation of a paracrine meiosis-inducing signal and CCs expansion [241]. The pivotal role high concentrations of cAMP in maintaining the meiosis arrest has been demonstrated by several authors (reviewed in[242]) The cAMP degradation is induced by phosphodiesterases (PDE) or by gonadotropins-dependent pathways including the EGF-like factors [243]. FSH was shown to increase the cAMP concentrations within the oocyte [49] and to overexpress the EGF-like factors in CCs [135, 146]. The GJC ensure continuous corona-radiata-oocyte exchanges during the maturation process [244]. When removed from the follicle, the oocyte resumes meiosis spontaneously. Taken together, these findings reveal the importance of the transcriptional and translational processes in the CCs. These two activities are able to produce and release some key factors that could be transferred thereafter to the oocyte. Once inside the gamete, these factors could trigger pathways involved in oocyte competence acquisition.

Since the oocyte nuclear status is easy to evaluate, it has been widely studied and used as a reference for the oocyte maturation progression [123, 221, 226, 243]. It is suggested that the meiotic arrest it is functional to permit the appropriate synchronization of cytoplasmic and nuclear maturation in the oocyte [232, 233]. On the contrary, cytoplasmic maturation remains a difficult process to be evaluated, and few useful criteria are available to describe it. Nevertheless, oocyte cytoplasmic maturation requires the metabolic and nutritive support of CCs [144] [202]. For example, CCs are involved in maintaining high levels of gluthatione (GSH) within the oocyte. This substance protects against oxidative stress, helps the male pronucleus decondensation and increases the oocyte developmental competence [245, 246]. CCs removal during bovine IVM, negatively affect fertilization as well as preimplantation embryonic development [247-249]. Furthermore, other ultrastructural rearrangements related to the cytoplasmic maturation such as mitochondrial

polarity and cortical granules migration were shown to be induced by the nitric oxide (NO) produced by CCs [250].

Ovulation is the process that allows the follicular rupture and the concomitant COC liberation to the fallopian tube. It is a pivotal event in the reproductive process that ensured two key events: the liberation of the female gamete and the luteinization of the remaining parts of the follicle. Whilst the first event is crucial for the fertilization, the second is critical for the correct pregnancy maintenance. Following the LH surge, final and rapid changes occurred including FF volume increase and CCs mucification. After CCs expansion, the COC acquired viscoelastic properties that ease its release from the follicle [251]. Impaired ECM structure or the KO of some related genes such as ADAMTS1 or TNFAIP6 negatively affect the ovulation process [252, 253]. There are several factors that act a key role in the ovulation process: firstly, the steroidogenic and proteases factors produced within the follicle and second, signals affecting the theca cell coming from blood. All these factors trigger CCs gene expression profile associated to an inflammatory-like response [254]. These findings suggested that CCs and the ECM around protect of the female gamete in an inflammatory and proapoptotic microenvironment during ovulation [255, 256]. Moreover, the ECM and particularly the HA was shown to prevent CCs apoptosis [257].

Prostaglandins (PGs) are also expressed in CCs and involved in the activation of the proteolytic process that leads to the rupture of the follicular wall by the activation of collegenases [258, 259]. For sure, additional studies are needed in order to gain supplementary information to treat ovulatory defects both in livestock and human species.

Because CCs are maintained in the vicinity of the oocyte during fertilization, the spermatozoa must cross in between CCs and their ECM before reaching the ZP. Intriguingly, CCs and ECM look to be more permissive to the good quality spermatozoa [260]. This selection may be mediated via ECM molecules like HA [261, 262]. CCs were also reported to secrete sperm attractants able to improve fertilization rates. This CCs- mediated attractive action is reinforced by chemotactic factors produced by the mature oocyte [263]. The progesterone was suggested as the suitable CCs chemoattractant [172]. Following the CCs penetration, the sperm binds to the ZP through the ZP3 protein. This ZP-sperm recognition induces the acrosomal exocytosis. [264, 265. The progesterone interactions with specific binding sites on the sperm membrane caused the intracellular Ca2+ increase and therefore the membranes' fusions and the release of the cortical granules avoiding polyspermy {Familiari, 2006 #1942, 266, 267]. Preventing harmful changes in the oocyte and ZP biochemical properties (e.g. zona hardening) was also considered as one of the main functions of

CCs during maturation and until fertilization [174].

Successful early embryo development is the consequence of appropriate achievement of all steps of maturation, ovulation and fertilization. Consequently, CCs are indispensable to the successful achievements of the early embryo development. Moreover, CCs expansion offers a suitable environment in the oocyte vicinity that is helpful for its cytoplasmic maturation which is correlated to the developmental competence. It was shown also that the degree of CCs expansion is correlated with the porcine developmental potential, and therefore suggested as predictor of early development competence [174, 268]. Taken together, all these findings support a fundamental role of CCs in the late stage of oocyte differentiation in determining the success of subsequent embryo development.

4.6 Role of CCs and gap junction mediated communications in the control of large-scale chromatin remodeling process and transcriptional silencing

The mechanisms involved in the control of large-scale chromatin configuration changes and transcriptional silencing that occur before meiotic resumption, are still poorly understood. Studies conducted in different animal species indicate that ovarian granulosa cells and their coupling with the oocytes through GJCs are implicated in such a regulation. For example, in the mouse, when GJC between the female gamete and cumulus cells are prevented, transcriptional silencing, normally occurring in wild type mice during oocyte growth, is impaired and chromatin remains decondensed thus not acquiring the typical SN configuration [232]. Moreover, if the oocytes are cultured in the absence of granulosa cells, as denuded oocytes, transcriptional silencing fails to occur [269].

The central role of GJC in the modulation of chromatin configuration and transcription has been confirmed also in the bovine model. Where, at the time of collection from early antral follicles, GV0 oocytes are characterize by a fully open state of GJC. Then, the percentage of oocytes with functionally open communications significantly decreases along with the increasement of chromatin condensation, from GV1 to GV3 pattern [107]. Furthermore, when GV0 oocytes are cultured *in vitro* with physiological concentration of FSH that ensures the maintenance of a patent bidirectional coupling, the chromatin gradually organizes into the GV1 configuration, thus acquiring the ability to mature and be fertilized in vitro [270].

On the contrary, in the absence of hormonal treatment, coupling is not sustained, and chromatin remains mainly in an uncondensed state. Strikingly, treatment with higher doses of FSH does not support functional coupling either, and it seems likely to force the oocyte to resume meiosis without an orderly remodeling of chromatin configuration. Thus, the apparent increased ability to resume meiosis is not accompanied by an equal increase of fertilization competence [270].

Other experiments using the bovine model, where low doses of FSH were used to sustain GJC functionality in COCs from early antral follicles, gave further insight into the mechanisms by which GJC may modulate changes in large-scale chromatin configuration and transcription. In this system, treatment with the uncoupler 1-heptanol induces sudden condensation of chromatin and a decrease in transcription. However, this effect is nullified by the addition of cilostamide to the culture medium [270]. This indicates that the functional status of GJC may affect both transcriptional activity and remodeling of large-scale chromatin configuration, potentially through cAMP-dependent mechanism(s). Cilostamide acts as a specific inhibitor of the PDE3, an enzyme-degrading cAMP [219, 248]. Besides the well-characterized mechanisms of action by which cAMP is known to regulate meiotic resumption [271, 272]. These works suggest that cAMP could be also involved in the regulation of transcription and in the large-scale chromatin remodeling during the final phase of oocyte growth and before the resumption of meiosis. To conclude, all these studies confirm the importance of maintaining a proper dialogue between the two compartments of the COCs in order to have a proper large-scale chromatin remodeling and to complete transcription during the late stage of differentiation [270].

4.7 CCs an additional "tool" to predict oocyte competence

From what has been described so far, it is clear that the cumulus cells accompany the oocyte development in the course of folliculogenesis through a metabolic activity that is stage-specific, contributing to the progressive and gradual differentiation of the female gamete thus determining its competence. Based on this, CCs become the ideal source of non-invasive approaches for predicting oocyte competence. While previous studies used the immature CCs morphology as an in vitro indicator of oocyte developmental potential [151, 268], an increasing number of studies is now focusing on CCs characteristic gene expression profile that intimately reflect the oocyte competence and may therefore be predictive of embryo development potential [152, 273]. In fact, a small biopsy of the cumulus oophorus could be easily collected before IVM, without perturbing oocyte viability, and assayed for expression of genes used as markers to predict the corresponding oocyte's quality.

In this context, several candidate genes expressed in CCs were suggested as potential markers of oocyte competence mainly in bovine and human [146, 273 7, 274]. Therefore, additional genomic more reliable markers could be added to the morphological criteria to accurately and non-invasively predict the oocyte developmental competence. Keeping in mind all the aforementioned CCs functions, genomic markers differentially expressed in CCs would represent a new powerful tool that will contribute in more accurate oocyte selection and therefore improved the outcome of the reproductive process both in livestock and human species.

4.8 CCs gene expression importance

CCs gene expression is an important process triggered by some of the various signaling pathways described in CCs. The inhibition of the transcription in the CCs impaired both oocyte maturation and fertilization [133, 134]. These findings suggested that CCs gene expression is essential to oocyte maturation and early development. Moreover, gene expression patterns in CCs were shown to be influenced by the oocyte-secreted paracrine factors mainly the TGF family [139, 198, 202]. The CCs gene expression profiles were studied in many mammalian species including mice [259 , 275], pig [276], cow [146] [149] and human [274] [273]. The analysis of these genome-wide studies has provided interesting molecular functions occurring in CCs [145, 146, 254]. Vigone et al., for example, confirmed that in murine model the developmental incompetence (NSN) or competence (SN) of antral oocytes can be predicted using transcript markers expressed by their surrounding CCs (i.e., *Has2, Ptx3, Tnfaip6, Ptgs2* and *Amh*) [275].

Despite the valuable contributions of these excellent studies, the CCs molecular dynamics and the precise molecular pathways needed to support oocyte competence are still poorly understood. In fact, gene expression patterns vary by switching from one follicular stage to the other, or between mammalian species. This may affect most of the CCs signaling and metabolic cascades and consequently their functions. Comparative biology studies are necessary to enlighten on the species similarities and differences in terms of follicular development and oocyte molecular maturation pathways. In order to rebuild the whole signaling and gene expression events that occurred in CCs and efficiently optimize IVP systems, additional studies that focus on time- and space-dependent molecular events are required.

SECTION 5: Assisted Reproductive Technologies

5.1 The Assisted Reproductive Technologies: focus on IVM

Assisted reproductive technologies (ARTs) are all the treatments and procedures that include the in vitro handling of oocytes, sperm or embryos for the purpose of establishing a pregnancy. In the last decades, the better understanding of the folliculogenesis process have opened new alternatives to achieve pregnancy. In addition to the widely use of ovarian stimulation, several technologies have been developed to face with human infertility and animal breeding. Of course, it necessitates sperm and oocyte collection, then their mixture to allow them to fertilize in vitro. The oocyte retrieval is achieved following hormonal stimulation and the fertilization occurs spontaneously in a Petri dish in the laboratory. The IVF protocols are under constant review in order to increase their efficiency, and therefore pregnancy outcomes. Following early embryo development in vitro, named also in vitro culture (IVC), the cleaved embryos are transferred to the uterus for implantation and embryo development. In some cases, mainly in bovine, porcine and equine species, immature oocytes can be harvested and matured in vitro. Some media are available for in vitro maturation (IVM) although the process is not completely efficient. The studies on livestock species have been of great value in this field. They offered available models where the media for the IVM, IVF and IVC technologies are optimized. Despite the advantages of human IVM to reduce the fertility drugs use, it is still a rudimentary strategy with poor clinical application.

As already mentioned above, in recent years, numerous IVM and pre-IVM systems based on the modulation of cAMP, have been suggested for stimulating oocyte maturation and embryonic developmental competence acquisition [277].

Several pharmacological and physiological agents have been used to modulate the oocyte cAMP content in order to temporally control the oocyte's meiotic resumption giving the oocyte the opportunity to acquire competences. For instance, cAMP concentration has been manipulated through the use of broad-spectrum such as IBMX or specific inhibitors of phosphodiesterases (PDEs) such as cilostamide, milrinone or Org9935, by activators of adenylate cyclase (forskolin, iAC), through cAMP analogs (dbcAMP) or by a combination of them. Several works have shown

that a delay of meiotic resumption has a beneficial effect on embryonic developmental competence. Specifically, the manipulation of intracellular cAMP concentration affects the functionality of GJCs between the oocyte and CCs. A decrease in cAMP determines the interruption of this fundamental crosstalk [101, 129, 193, 195. On the other hand, treatments that sustained the intracellular cAMP level prevented the loss of GJCs and increased oocyte developmental competence {Nogueira, 2006 #2395, 270, 278-285]. Also, the preservation of a correct cAMP concentration seems to be necessary to promote regular chromatin remodeling thus supporting oocyte differentiation [101, 270, 278, 282, 286] and an increase in oocyte quality [101, 270, 282, 287-290].

5.2 Implications of large-scale chromatin configurations in basic science and in ARTs

No doubt that the analysis of the functional and structural modifications that accompany large-scale chromatin configuration changes in the oocyte will have wide-ranging implications for understanding: the role of nuclear organization in meiosis, the events of nuclear reprogramming, and the spatio-temporal regulation of gene expression during oocyte and early embryo development. Moreover, experimental manipulation of large-scale chromatin configuration in vivo and in vitro will provide a tool to determine the key cellular pathways and oocyte-derived factors involved in genome-wide chromatin modifications. In this context, micromanipulation techniques, such as GV transfer [116, 291, 292], that allows the transplantation of an isolated GV from one oocyte to another, would deepen the knowledge of fundamental processes in oocyte biology. Using this technique, for instance, the nuclei of SN and NSN mouse antral oocytes were reciprocally exchanged and the meiotic and developmental competences of the reconstructed oocytes were assessed. Results of these experiments indicate that cytoplasmic factors are responsible for the oocyte's meiotic competence, while nuclear factors are responsible for the embryonic developmental competence [292].

Assessment of large-scale chromatin configurations has also large implication in assisted reproductive technologies (ART) in livestock and human species. It has been shown that different patterns of chromatin configuration are indicative of different metabolic properties; thus, they could represent a morphological marker to select a population of oocytes with different cultural needs. Several studies support the idea that treatments aimed to improve the developmental capability of immature oocytes can have a different effect with "pre-maturation culture" depending on the metabolic status of the oocyte at the moment of its removal from the follicle [278, 293, 294]. They

suggest that pre-maturation culture may be of greater benefit for growing oocytes, allowing them to achieve developmental competence [295]. This is confirmed also by morphological studies in bovine, which demonstrated that pharmacological pre-treatment can negatively affect oocyte belonging to medium antral follicles when compared with those isolated from smaller follicles [296]. Accordingly, findings in the mouse indicate that it is crucial to consider the transcriptional activity of the oocyte when attempting to maintain the female gamete in meiotic arrest *in vitro* for protracted periods. In fact, experimentally extending the interval between transcriptional inactivation and resumption of meiosis may be deleterious to subsequent embryonic development. In view of these considerations, success in attempting to improve the oocyte developmental capability in vitro may be dependent on the actual growth stage of the oocyte, when subjected to treatment. Surely, the possibility to predict large-scale chromatin configuration on the basis of morphological criteria of the oocyte or of the COC, as found in mouse and human [297, 298], would considerably improve the application of such cultural strategies.

It is of extreme importance noticing here that attempts to manipulate *in vitro* large-scale chromatin configuration must be performed cautiously. In fact, even though it is true that the chromatin configuration of an oocyte is indicative of its developmental capability at the time of its collection from the follicle, pharmacological treatments forcing chromatin abruptly into a high condensed state may not necessarily be beneficial to the oocyte [116]. Therefore, design of pre-maturative strategies must take into account that chromatin condensation and spatial reorganization should occur gradually, recapitulating at best the physiological process that normally occurs in vivo. For example, maintenance of a proper functional coupling between oocyte and cumulus seems to be crucial in sustaining a proper chromatin condensation in vitro [270]. Thus, if coupling is prematurely interrupted unexpected chromatin condensation can occur, thus preventing proper and gradual differentiation of large-scale chromatin configuration and function. In view of all given considerations, the knowledge of all the molecular mechanisms leading the correct oocyte chromatin remodeling process under physiological conditions will be of great value in order to increase the success of ART.

OBJECTIVES OF THE THESIS AND SIGNIFICANCE

The main goal of this thesis is to better understand and define the mechanisms and the key molecules involved in the production of good quality oocytes, knowing that the quality of the female gamete plays a pivotal role in ARTs successful outcome. The studies were conducted in porcine and bovine animal models. In both species, the progressive changes in large-scale chromatin configuration that characterize the oocyte differentiation process were used as a marker of oocyte differentiation and developmental potential acquisition.

In particular, the general idea was to utilize this marker as an indicator of the efficiency and efficacy of customized IVM protocols that allow to maximize the exploitation of the oocyte reservoir.

In the first part, we characterize the porcine oocyte GV chromatin configuration patterns. Then, we use this information to set up a pre-IVM protocol able to improve oocyte developmental competence.

In the second part, we studied in the bovine model the cumulus cells transcriptomic profiles based on the GV chromatin configuration as a marker of oocyte developmental competence. In these studies, the combined use of morphological parameters together with the analysis of the transcriptomic profiles of cumulus cells allowed us to validate an oocyte culture protocol that represents a proof of concept for the development of future IVM systems.

CHAPTER 2: The effect of cilostamide on gap junction communication dynamics, chromatin remodeling, and competence acquisition in pig oocytes following parthenogenetic activation and nuclear transfer

The effect of cilostamide on gap junction communication dynamics, chromatin remodeling, and competence acquisition in pig oocytes following parthenogenetic activation and nuclear transfer

Cecilia Dieci[1,†], Valentina Lodde[1,2,†], Federica Franciosi[2], Irina Lagutina[1], Irene Tessaro[2], Silvia Modina[2], David F. Albertini[3], Giovanna Lazzari[1,4], Cesare Galli[1,5] and Alberto M. Luciano[2]

[†]These two authors contributed equally to the paper and should be considered first coauthors

Running title: Chromatin remodeling and pig oocyte competence

Summary sentence: Cilostamide administration sustained functional coupling, progressive chromatin condensation and enhanced porcine oocyte developmental competence as reflected in higher blastocyst quality and improved SCNT efficiency.

Key Words: chromatin; cyclic adenosine monophosphate (cAMP); gamete biology; gap junctions; meiosis; oocyte; PDE3; embryonic development; parthenogenetic activation; SCNT.

Affiliations: [1]Avantea, Laboratory of Reproductive Technologies, 26100 Cremona, Italy; [2]Reproductive and Developmental Biology Laboratory, Department of Health, Animal Science and Food Safety, University of Milan, 20133 Milan, Italy; [3]Institute of Reproductive Health and Regenerative Medicine, Center for Reproductive Sciences, University of Kansas Medical Center, Kansas City, KS 66160, USA; [4]Fondazione Avantea, 26100 Cremona, Italy; [5]Dipartimento di Scienze Mediche Veterinarie, Università di Bologna, 40064 Bologna, Italy

Correspondence: Alberto M. Luciano, Dipartimento di Scienze Veterinarie per la Salute, la Produzione Animale e la Sicurezza Alimentare, Università degli Studi di Milano, Via Celoria, 10 - 20133 Milano, Italy Phone (+39) 02 50317969 - E-mail: alberto.luciano@unimi.it

Abstract

In the pig, the efficiency of *in vitro* embryo production and somatic cell nuclear transfer (SCNT) procedures remains limited. It has been suggested that prematuration treatments (pre-IVM) based on the prolongation of a patent bidirectional crosstalk between the oocyte and the cumulus cells through gap junction mediate communication (GJC), together with the maintenance of a proper level of cAMP, could improve the developmental capability of oocytes. The aim of this study was to assess: (i) dose dependent effects of cilostamide on nuclear maturation kinetics; (ii) the relationship between treatments on GJC functionality and large-scale chromatin configuration changes; (iii) and the impact of treatments on developmental competence acquisition after parthenogenic activation (PA) and SCNT. Accordingly, COC were collected from 3-6 mm antral follicles and cultured for 24 h in defined culture medium with or without 1 µM cilostamide. GJC functionality was assessed by Lucifer Yellow microinjection, while chromatin configuration was evaluated by fluorescence microscopy after nuclear staining. Cilostamide administration sustained functional coupling up to 24 h of culture and delayed meiotic resumption as only 25.6% of cilostamide-treated oocytes reached ProMI stage compared to the control (69.7%; *P<0.05)*. Moreover, progressive chromatin condensation was delayed before meiotic resumption based upon G2/M biomarker phosphoprotein epitope acquisition using immunolocalization. Importantly, cilostamide treatment under these conditions, improved oocyte developmental competence as reflected in higher blastocyst quality after both parthenogenetic activation and SCNT.

Introduction

In addition to its high agricultural value, the pig is an important domestic animal model for biomedical and reproductive research [1]. Pig organs are similar to those of humans in terms of size and physiology, providing a potential source for xenotransplantation [2]. Cloning by means of Somatic Cell Nuclear Transfer (SCNT) is the most used technique to generate genetically modified pigs for xenotransplantation and as models for studying various human diseases [3-6]. However, despite much progresses have been made in pig *in vitro* embryo production (IVP) and SCNT over the last decades, the efficiency of these techniques remains low and further improvements are still required [1, 4, 5, 7].

It is widely agreed that the low efficiencies of pig IVP and SCNT are at least in part due to a sub-optimal in vitro maturation (IVM) system that should ultimately produce mature oocytes able to support embryonic development. The challenge of oocyte IVM is firstly, to provide a milieu that reflects the naturally changing environment to which the oocyte is exposed and, secondly, to support the complex cellular changes taking place in the follicular cells and in the oocyte nuclear and cytoplasmic compartments.

One of the problems related to IVM is that oocytes spontaneously resume meiotic maturation when cumulus-oocyte complexes (COCs) are removed from the antral follicles [8] and thus bypass the so-called 'oocyte capacitation' that is in turn essential for the attainment of a full embryonic developmental competence [9]. Several studies have suggested that extending meiotic arrest in vitro by temporary blockage of spontaneous nuclear maturation, the so-called prematuration culture (PMC), might improve the synchronization between nuclear and cytoplasmic maturational status and ultimately the oocyte competence ([10-13], reviewed in [14])

Temporary blockage of spontaneous meiotic resumption can be achieved by preventing the intra-oocyte drop of cyclic adenosine monophosphate (cAMP) levels, that normally occurs after removal of the COC from the follicle, through the use of inhibitors of phosphodiesterases (PDEs), the enzymes that hydrolyze cAMP ([15, 16]. One of these compounds is cilostamide that specifically inhibits the type 3 PDE (PDE3), which is the major active cAMP-PDE in porcine oocytes [17]. While in some mammals PDE3 is a oocyte-specific enzyme [18], in the pig this PDE is also expressed in cumulus cells [19].

Interestingly, it has been shown that the use of cilostamide can prolong the functional coupling between oocytes and cumulus cells mediated by gap junctional communication (GJC) during in vitro culture of bovine, mouse and human oocytes [20-22]. This is important since bidirectional communications between oocyte and cumulus cells are essential to ensure a proper

oocyte differentiation and meiotic maturation. Furthermore, it has been recently shown in the bovine model that the maintenance of a proper functional coupling between oocyte and cumulus cells seems to be crucial in sustaining an orderly remodeling of large-scale chromatin configuration [22], that is in turn indicative of the oocyte differentiation and metabolic state [23-27] reviewed in [28, 29].

On the basis of these observations, this study aimed to test the utility of a prematuration treatment using cilostamide, by evaluating pig oocyte quality for various biotechnological applications including parthenogenesis and SCNT. With this objective in mind, we assessed: (i) dose dependent effects of cilostamide on the kinetics and the degree of nuclear maturation; (ii) the effect of the treatment on GJC functionality and on the process of large-scale chromatin configuration changes; (iii) the effect of the treatment on the developmental competence acquisition after parthenogenic activation and SCNT.

Materials and Methods

Cumulus-oocyte complexes Collection and Culture

All chemicals and reagents were purchased from Sigma Chemical Company, unless otherwise stated. Porcine ovaries were recovered at a local abattoir from pubertal females and transported to the laboratory at 30-33°C within 2 h. All the subsequent procedures were performed between 35°C and 38°C, unless differently specified. COCs were isolated from early antral follicles (EAF, diameter 0.5-2 mm) by dissecting individual follicles with a scalpel or from medium antral follicle (MAF, diameter 3-6 mm) by aspiration with a 19-gauge needle mounted on an vacuum pump (COOK-IVF, Brisbane QLD, Australia) with a pressure of -28 mm/Hg. Collection medium was TCM-199 supplemented with 20mM Hepes, 1790 IU/ml of heparin and 0.4% bovine serum albumin (BSA) fraction V (M199D). Where needed and according to the experimental design, COCs from MAF were collected in 500 μM 3-isobutyl-I-methylxantine (IBMX) supplemented medium, to avoid cAMP content drop during COC recovery [10, 12, 30]. COCs were examined under a stereomicroscope, and only those with intact, compact cumulus investments and finely granulated homogeneous ooplasm were used. The whole procedure was performed in approximately 30 min.

Groups of 25 to 30 COCs, isolated from MAF, were cultured, in four-well dishes (NUNC, VWR International, Italy) at 38.5°C under 5% CO_2 in humidified air, in 500 μl of defined IVM medium (dIVM) that was TCM199 supplemented with 0.4% BSA fatty acid free, 75 μg/ml kanamycin, 1 μl/ml ITS Media Supplement (insulin, transferrin and sodium selenite), 110 μg/ml sodium pyruvate, 75 μg/ml ascorbic acid, 100 μg/ml glutamine, 5 μg/ml myoinositol, 0.4 mM cystine, 0.6 mM cysteamine and 0.1 IU/ml of human recombinant FSH (r-hFSH, Gonal F, Serono S.p.a., Italy). According to the experimental design, dIVM medium was further supplemented with 0.1 or 1 μM cilostamide (Enzo Life Science, Farmingdale, NY, USA), a specific type 3 PDE inhibitor. Times of culture were different according to the experimental design and are specified for each experiment in the results section. In the experiments in which cilostamide dose response and reversibility were tested, oocytes were freed of cumulus cells, fixed in ethanol: acid acetic (3:1, v/v) for 48 h at room temperature and stained with Lacmoid to assess nuclear maturation status and precisely evaluate the presence of the nuclear envelope.

Analysis of Functional Status of GJ-mediated Communication Between Oocytes and Surrounding Cumulus Cells

Groups of 25-30 COCs were cultured for 0, 12, 18 and 24 h in dIVM medium in the absence or in the presence of 1 µM cilostamide. At each time interval, intercellular communications between oocytes and cumulus cells were assessed by Lucifer Yellow (LY) microinjection as previously described for bovine COCs [12]. Briefly, a 3% solution of LY in 5 mM of lithium chloride was pressure injected into the oocyte. A microinjection apparatus (Narishige Co. Ltd., Japan) was used to guide the holding and injecting micropipettes into a 50 µl drop of M199D supplemented with 5 % fetal calf serum (Gibco, Invitrogen s.r.l., Milan, Italy) and covered with mineral oil. Analysis of GJ functionality was performed after 10 min from the injection by the observation of LY spreading from the oocytes to the cumulus cells under fluorescence microscopy. COCs were classified as open, partially open or closed as previously described [12].

Assessment of Chromatin Configuration, Oocyte Diameter and Meiotic Progression

Changes of large-scale chromatin configuration were assessed at the time of collection and after different times of culture by Hoechst 33342 staining and fluorescence microscopy analysis. COCs were freed of cumulus cells by gentle pipetting in M199D. Denuded oocytes (DOs) were incubated for 10 min in the dark in M199D containing 1µg/ml Hoechst 33342 and transferred into a 5 µl drop of the same medium. Chromatin configuration was evaluated under an inverted fluorescence microscope (Olympus IX50, magnification 40X) and the DOs were classified according to the degree of chromatin mass condensation within the germinal vesicle according to [31, 32] for oocytes at the time of isolation from the follicles and after culture, respectively. In order to assess the relationship between chromatin configuration and the oocyte diameter at the time of collection, bright-field images of living DOs were taken by a digital camera (DS-5M; Nikon Corp.). Oocyte diameter was measured excluding the zona pellucida using NIH ImageJ 1.44 software [33] as previously described [25].

When chromatin configuration could not be assessed immediately after the culture period in living oocytes, DOs were, fixed in 500µl of 60% Methanol in Dulbecco's Phosphate Buffered Saline (DPBS) for at least 30 min at 4°C, stained with 1 µg/ml Hoechst 33342 and evaluated by florescence microscopy as previously described. Preliminary experiments showed that this fixation procedure did not alter large-scale chromatin configuration as previously reported in cow [28].

Parthenogenetic activation and somatic cell nuclear transfer

At the end of the culture period COCs were freed of their surrounding cumulus cell and washed twice in HEPES buffered synthetic oviduct fluid (H-SOF) [34]. The oocytes with first polar body extruded were selected and treated for parthenogenetic activation (PA) or for somatic cell nuclear transfer (SCNT) procedures.

Matured oocytes were activated as described previously [35]. Briefly, oocytes were washed in 0.3 M mannitol solution, containing 1 mM Ca^{2+} and activated by double DC-pulses of 1.2 kV/cm for 30 μsec applied in the same medium. After a brief wash in H-SOF, the oocytes were transferred into the chemically assisted activation medium, which was PZM-3 medium [36] supplemented with 5μg/ml cytochalasin B. After 4 h of incubation, parthenogenetic activated embryos were washed twice in H-SOF and transferred in 400 μl PZM3 in vitro culture (IVC) medium. Embryo cleavage and blastocyst development were observed at days 2 and 7, respectively.

In order to generate SCNT embryos, porcine adult fibroblasts were obtained through culture of minced tissue from ear or tail biopsies as previously described [35]. Briefly, fibroblasts were cultured in medium DMEM + TCM 199 (1:1) with 10% FCS in 5% CO_2 and 5% O_2 in humidified air at 38.5 °C. After the primary culture was established, they were either sub-cultured every 4–6 days or expanded and frozen in DMEM + TCM 199 (1:1) with 20% FCS and 10% DMSO and stored in liquid nitrogen. Donor cells were induced into quiescence by serum starvation (0.5% FCS) for 1–3 days prior to nuclear transfer. The cells were prepared by trypsinization 30 min before nuclear transfer then washed, pelleted by centrifugation and re-suspended in H-SOF supplemented with 10% FCS, to serve as nuclear donors. The zona pellucida of the matured oocytes was digested by 0.5% pronase solution for a few minutes. Zona-free oocytes were stained with Hoechst 33342 and subjected to 5 μg/ml cytochalasin B treatment. The enucleation of a de-zonated oocyte was performed with a blunt, non-bevelled pipette. In order to localize the metaphase plate oocytes were briefly exposed to UV light. Cytoplasts, were individually washed for few seconds in 300 μg/ml phytohemagglutinin P in PBS and then quickly dropped over a single donor cell [37]. After pairing donor cell and recipient cytoplasm, the couplets were subjected to electrofusion. After two 30 μsec direct current impulses of 1.2 Kv/cm, the construct were transferred to H-SOF medium supplemented with 10% FCS. After fusion, the reconstructed SCNT embryos were subjected to activation as previously described for parthenogenetic development. As for the PA embryos, the SCNT embryos were washed twice in H-SOF supplemented with 10% FCS and transferred in IVC

medium. In vitro culture was carried out under 5% CO_2 and 5% O_2 in humidified air at 38.5°. Embryos were positioned in a well of well (WOW) system [38]. The well was covered with 400 μl IVC-SOF [34]. Cleavage was assessed 48 h after activation whereas, the blastocyst rate (BL) was recorded on Days 7 (Day 0 was the day of activation). During embryo culture, half of the medium was renewed on Day 4 with fresh culture medium. On Day 7 the blastocysts were fixed in 60% Methanol in DPBS overnight at 4°C and stained with 1μg/ml Hoechst 33342 for cells number evaluation.

Immunofluorescence Staining

Indirect immunofluorescence was carried out to evaluate 1) chromatin condensation by monitoring phosphorylation of Histone H3 at Ser28 and 2) the patterns of mitosis-associated ser/thr phospho-proteins (MPM2) by using the monoclonal antibody MPM2. This antibody is known to detect epitopes of many relevant substrates for M-phase specific kinases and is a specific biomarker for the G2/M cell cycle transition [39-43].

Oocytes were simultaneously fixed and extracted in a microtubule-stabilizing buffer containing proteases and phosphatases inhibitors, as described elsewhere [40, 42, 43] and then incubated overnight with primary antibody at 4°C. The primary antibodies used were rabbit polyclonal anti-phospho-Histone H3 (Ser28) (diluition 1:100, Merk Millipore, Temecula, CA, USA) or mouse monoclonal anti-phospho-Ser/Thr-Pro antibody, MPM2 (dilution 1:100; Merk Milliopore, Temecula, CA, USA). After extensive washing in 0.1% Triton, 0.1% Tween and 1% BSA, oocytes were incubated for 1h at RT with conjugated secondary antibody that were:TRITC-conjugated AffiniPure Donkey Anti-Rabbit (diluition 1:100; Jackson ImmunoResearch Laboratories, INC., West Grove, PA, USA) or Alexa-Fluor-488-labeled donkey anti mouse (dilution 1:500; Invitrogen, Life Technologies, Carlsbad, CA, USA). Samples were extensively washed again and finally mounted on slides in the antifade medium Vecta Shield (Vector Laboratories) supplemented with 1 μg/ml DAPI. In each experiment negative controls were performed by omitting the primary antibodies and did not reveal any staining. Samples were analyzed on an epifluorescence microscope (Eclipse E600, Nikon Corp., Japan) equipped with a 40X objective and a digital camera (DS-Fi2, Nikon Corp., Japan). For the analysis of phosphorylation status of Histone H3 at Ser28, immune fluorescent staining were also conducted on paraformaldehyde fixed oocytes as described in [32].

Analysis of MPM2 staining was conducted by capturing images, using identical exposure times and gain settings, at the focal plain containing the GV chromatin and at the equatorial focal plane, in order to assess fluorescence intensity (FI) of the nucleus and cytoplasm respectively. Finally, mean FI of each GV was calculated using NIH ImageJ software. To determine the cytoplasmic FI, mean FI in 5 different areas of the cytoplasm was calculated using NIH ImageJ and averaged.

Statistical Analysis

All the experiments were repeated three to five times. Observations from all the experiments were pooled. Statistical analyses were performed using Prism GraphPad (GraphPad Software, San Diego, CA, USA). Differences in maturation, cleavage and blastocyst rates as well as differences in the percentages of COCs with open GCJ and in the percentage of oocytes with different chromatin configurations among the experimental groups were analyzed by Fisher's exact test. MPM2 fluorescence intensity, oocyte diameter and blastocyst cell number are expressed as means ±SE. In these cases, statistical significances were tested using one-way analysis of variance (ANOVA) followed by Tukey's Multiple comparison test or by student t-Test, when means of two groups were compared. Values of $P < 0.05$ were considered significant.

Results

Dose-response and reversibility of cilostamide treatment.

The first set of experiments aimed to determine the treatment that could prevent germinal vesicle breakdown (GVBD) in porcine oocytes under our experimental condition. COCs were cultured in dIVM medium (CTRL) or dIVM medium supplemented with 0.1 or 1 µM cilostamide for 24, 36 or 48h and oocyte nuclear maturation was assessed by lacmoid staining after acetic fixation. Oocytes were classified as GV, when the nuclear membrane was detectable and irrespectively on the chromatin organization within the nuclear envelope; intermediate when the chromosomes were arranged in pro-metaphase, metaphase I plate, anaphase I or telophase I; mature, when the chromosomes were arranged in a metaphase II plate with the first polar body extruded and degenerated, when none of the above classes could be recognised. As shown in Figure 1A, culture with 1 µM cilostamide for 24h was the most effective treatment in preventing the completion of meiosis I. Moreover, the effect of 1 µM cilostamide was reversible upon its withdrawal from the culture medium. In fact, when COCs were cultured in the presence of 1 µM cilostamide for 24 h and subsequently washed and cultured for additional 20 h in dIVM medium, the percentage of oocyte at intermediate and mature stages were equal to that obtained in the control group cultured for 44h in dIVM medium (Fig. 1B). Based on these results, treatment with 1 µM cilostamide for 24 h was adopted in all the following experiments.

Effect of cilostamide treatment on gap junction mediated communication between oocyte and surrounding cumulus cell

This set of experiments was designed to investigate the effect 1 µM cilostamide treatment on the persistence of a functional intercellular coupling between the oocyte and the surrounding cumulus cells. Gap junction-mediated communications (GJCs) functionality was assessed at the time of collection and after 12, 18, and 24 h of culture in dIVM medium supplemented with 0 (CTRL) or 1µM cilostamide. At the time of collection, the injection of LY in the oocytes resulted in an immediate spread of the dye into neighbouring corona radiata cells in 79.8% of COCs, whereas 5.1% and 15.2% of COCs showed a pattern of partially and completely closed communications, respectively (Fig. 2). As shown in Fig. 2.B, at 18 h of culture, we observed a substantial drop in GJCs functionality in the CTRL group. On the contrary, GJCs functionality was maintained up to 24 h of culture in cilostamide treated group. Importantly, when different times were compared, the

percentage of COCs with open GJCs in cilostamide treated group after 24 h of culture did not differ significantly to that observed at the time of collection (P=0.129).

Effect of cilostamide treatment on chromatin configuration remodeling and meiotic progression.

Before assessing the effect of cilostamide treatment on the process of chromatin configuration remodeling and meiotic progression, preliminary studies were conducted to identify discrete categories of prophase I arrested oocytes. To this aim we assessed chromatin configuration changes at the time of isolation from the follicles and compared our observations with the plethora of classifications present in the literature [31, 32, 44-48]. Chromatin configuration was assessed in living porcine oocytes soon after the isolation from early (EAF, 0.5-<2 mm in diameter) and middle antral follicles (MAF, 3-6 mm in diameter) by Hoechst 33342 staining and fluorescence microscopy analysis. Our observation confirmed to a large extent data from Bui et al. [32] and Hirao et al. [44]. As shown in Fig 3 A, the filamentous chromatin (FC) configuration was characterized by the presence of a diffuse filamentous pattern of chromatin distributed in the whole nuclear area. The stringy chromatin (SC) configuration was characterized by an increased level of condensation of the chromatin that became clearly thicker and organized into clumps. Within the SC class, a further distinction was based on the presence or absence of a ring of condensed chromatin around the nucleolus, thus the configuration in which clumped chromatin was distributed throughout the GV was designated as stringy chromatin distributed (SCd), whereas the configuration in which both clumped chromatin throughout the nucleoplasm and a rim of condensed chromatin surrounding the nucleolus were detected, was termed stringy chromatin with nucleolar rim (SCn). Finally, in the germinal vesicle I (GVI) configuration all the condensed chromatin mass was organized around the nucleolus as previously described also by Motlik and Fulka [31]. That the SCd and SCn configurations are intermediated state of chromatin condensation between the FC and the GVI configurations was confirmed by the oocyte diameter analysis, which showed that change of chromatin configuration from FC to GVI was accompanied by a significant increase of oocyte diameter (P<0.05, Fig 3 B). Mean diameter of FC oocytes from EAF and of SCn, SCd and GVI oocytes from MAF was 110.8±1.2, 118.4±0.8, 119.4±0.4 and 121.3±0.4 respectively. Moreover, as shown in Table 1, the distribution analysis of the above-described patterns in EAF and MAF showed that, at the time of collection the majority of oocytes isolated from EAF were characterized by a FC pattern. This configuration significantly decreased in oocytes isolated from MAF (P<0.05).

No differences were observed in the percentage of oocytes with SCd configuration between the two follicular classes, while the frequencies of SCn and GVI oocytes were significantly higher in MAF than in EAF. Few of the oocytes collected from MAF showed early sign of GVBD (GVII-GV IV stages; see below), as already reported [44].

After 18 h of culture in dIVM medium, we observed an increase of the oocytes that showed typical features of early GVBD (Table 2) as previously described by Motlik and Fulka [31] and oocytes were classified as GVII-IV stages accordingly (Fig. 4). Some of these oocytes were present also at the time of collection as previously reported [44]. In these oocytes signs of condensation and individualization of filamentous bivalents were detectable. Moreover, in some oocyte chromosomes were arranged in Pro-Metaphase I (Pro-MI) and Metaphase I (MI) plate (Fig. 4).

To further confirm that SC and GVII-IV configurations were different, and more precisely that GVII-IV are typical configurations that occur between removal of the COC from the follicle (i.e when spontaneous meiotic resumption occur) and GVBD, we conducted immunofluorescent staining of H3 Ser 28 and MPM2, at the time of collection and after 24h of culture, as these have been indicated as markers of meiotic progression [32, 39-43, 49]. In our conditions, H3 started to be phosphorylated at Pro-MI, while no differences were observed between SC, GVI and GVII-IV stages (Fig. 5). On the other hand, analysis of MPM2 staining revealed a progressive increase of signal intensity firstly in the nuclear and then in the cytoplasmic compartments from SC to Pro-MI stages (Fig 6). Importantly nuclear FI of GVII-GVIV oocytes was significantly higher than that of SC and GVI oocytes, confirming that GVII-GVIV configurations temporarily follow GVI stage (Fig. 6 C).

Having established the patterns of chromatin configuration changes before and during culture, we were finally able to evaluate the effect of cilostamide treatment on the process of chromatin configuration changes and meiotic progression. COCs were cultured for 18 and 24 h in dIVM medium supplemented with 0 (CTRL) or 1µM cilostamide. At the end of the culture periods, oocytes were freed of cumulus cells, stained with Hoechst 33342 and analyzed. As shown in Table 2, after 24h of culture, significantly less oocytes progressed to the ProMI-MI stages in the cilostamide treated group when compared to the CTRL group. Accordingly, the percentages of GVI and GVII-IV oocytes were significantly higher in cilostamide treated group indicating that meiotic resumption had been delayed by the treatment.

Effect of cilostamide treatment on embryonic developmental competence

In order to assess the effect of cilostamide treatment on the embryonic developmental competence of porcine oocytes, COCs were cultured for 44h in dIVM medium (CTRL) or for 24h in dIVM medium in the presence of 1μM cilostamide and then washed and cultured for additional 20 h in dIVM medium. After the culture period, matured oocytes were treated for parthenogenetic activation (PA) or somatic cell nuclear transfer (SCNT) procedures.

As shown in Table 3, cleavage rate after PA of cilostamide treated oocytes did not differ significantly from the CTRL group. Moreover, no differences were observed between treatments in the percentage of PA embryos that developed to the blastocyst stage after 7 days of culture. Interestingly however, the frequency of expanded blastocyst in cilostamide treated group was significantly higher when compared to the control group, whereas there was no significant effect of cilostamide treatment on PA blastocyst cell number.

As shown in Table 4, the cleavage and blastocyst rates, as well as the frequency of expanded blastocyst after SCNT treatment were similar in the control and cilostamide treated groups. However, the mean cell numbers per blastocyst was significantly higher in the cilostamide treated group when compared to the control group.

Discussion

The present study demonstrates that inhibition of PDE activity during COCs recovery by IBMX, and during the following 24 h of culture with cilostamide in defined serum-free medium, is able to delay meiotic resumption while prolonging functional coupling between oocytes and cumulus cells; importantly, these conditions improved the developmental capability of pig oocytes. The increased oocyte developmental competence is reflected in the enhancement of blastocyst quality based upon expansion capability after PA (cytoplasmic competence), and an increased cell number per blastocyst after SCNT, compared with control groups. The immediate implication of these findings is that improved quality of transferred embryos would materially enhance the overall efficiency of SCNT, which is currently low, with the average yield of live births per embryo transferred being no more than 1–5% [4, 6, 50-53]. This hypothesis is currently under investigations in our laboratories. Nevertheless, to the best of our knowledge, this is the first study reporting the use of cilostamide to improve pig SCNT efficiency.

Several cultural strategies have been proposed to improve oocyte quality in different mammals (for a review see [14, 54]). Many of these strategies, often referred to as 'pre-maturation culture', are based on the temporary blockage of oocyte spontaneous meiotic resumption, by modulating intra-oocyte cAMP content with different agents such as cAMP analogues or PDE inhibitors [12, 16, 20-22, 55-67]. Our results on the effect of the use of PDE inhibitors on meiotic resumption are largely supportive of previous data in pre-pubertal gilts in which cilostamide or other PDE3 inhibitors, such as milrinone, have been used [17, 67, 68]. Effects of cilostamide treatments on in vitro developmental potential have been tested in human [20, 21, 63], bovine [22, 64], ovine [65] and mouse [56, 62, 64, 69] with different outcomes depending on the species, the time of COC incubation with cilostamide, the combination with other agents and the experimental approach itself. In some cases, substantial differences exist among treatments that it is difficult to compare their efficacy. However, an important aspect that must be considered is the actual growth and differentiation stage of the immature oocytes subjected to the cilostamide-based treatment since oocytes with different metabolic properties may require different cultural conditions [29]. Moreover the source of the ovaries needs to be taken into account. In pigs, for examples many Authors use prepubertal gilts [17, 67, 68], while others, as well as in the present paper, pubertal animals are used as ovaries source.

In general, aim of the pre-maturation culture is to allow the oocytes to complete those processes that are interrupted once they are removed from the follicular environment [14, 29], i.e. the oocyte growth phase, for those oocytes collected from preantral or early antral follicles, and/or

the so called 'capacitation' process, that is the acquisition of the cytoplasmic machinery necessary to fully support preimplantation embryo development. These processes normally occur in fully grown oocytes when the follicle approach the preovulatory stage in vivo [9]. Therefore fully-grown oocytes at advanced stages of differentiation would not benefit from protracted period of in vitro culture [29, 70]. As a consequence, pre-maturation culture with cilostamide generally improves the yield (% of embryo obtained) of oocytes at early stages of their development [21, 22, 56, 62], while it increase the quality of the embryos obtained from oocytes at more advanced stages of their differentiation, collected from mid-sized antral follicles, without a significant increase of the embryo rate [20, 65, 71]. Accordingly, in the present study similar outcomes on the quality of SCNT embryos are reported. In fact, oocytes used in this study are to be considered at advanced stage of their development. This is demonstrated by the analysis of the chromatin configuration at the time of collection, which is a marker of the oocyte differentiation state [29]. It indeed revealed that this population of oocytes does not contain growing oocytes with filamentous chromatin configuration, while around 30% of the oocytes have already acquired the GVI configuration, in which the chromatin have reached its most compacted state before spontaneous meiotic resumption at the time of oocyte removal from the follicle [32] and this study). Therefore, this heterogeneity could account at least in part to the unchanged percentage of embryos obtained from treated oocytes when compared to the control groups. This supports original data in mouse where Authors tested the effect of PDE3 inhibitor Org 993 on the developmental competence of oocytes that were retrieved 24 h after gonadotropin injection, when the antral follicles were not yet fully developed. Importantly, the proportion of oocytes with condensed chromatin (SN configuration) was lower at 24h compared with 48 h after eCG priming and the arrest in vitro allowed the transition from uncondensed (NSN configuration) to SN configuration in the oocyte nucleus, which was associated to a significant increase of embryonic developmental competence [56].

Up to date, the only cilostamide-based treatment that substantially improved oocyte developmental outcomes, with a very high embryo yield is the 'Simulated physiological oocyte maturation', the so-called 'SPOM' system, proposed by R.B. Gilchrist's group in mouse and bovine [64]. In this system, COCs are incubated for 1–2 h with cAMP modulating agents (IBMX and the adenylate cyclase activator Forskolin) followed by an extended IVM phase containing FSH and cilostamide for the entire culture period. As indicated by the Authors, starting from the idea that specific PDE subtypes differentially exert their function within the somatic and the germ cell compartments in rodents [18] and bovine [15, 72], the SPOM is specifically designed to target initially both cumulus cell and oocytes PDEs, using the non-specific PDE inhibitor IBMX, and then the oocyte PDE only, by using the PDE3-specific inhibitor cilostamide [64]. On the contrary

porcine cumulus cells, also express PDE3 [19]. Therefore, our cultural approach uses a 'biphasic' system in which cilostamide is present only during the first 24 h of culture and where its concentration is reduced by 10-20 fold compared to the that used in bovine systems [22, 64] but able, at the same time, to delay meiotic resumption in a comparable manner than higher concentrations (20μM) used in previous works in pig [17, 68]. Importantly, cilostamide treatment in our system promotes the maintenance of a proper functional coupling between oocyte and cumulus cells up to 24h, confirming previous results in the bovine model [13, 22], which exerts in turn a positive effect on oocyte quality. We hypothesize that enhanced coupling during in vitro culture could stimulate the bidirectional transfer of essential molecules for the attainment of a full developmental competence. However, further studies are needed to understand the precise nature of these molecules.

Our previous studies in bovine suggest that the maintenance of a proper functional oocyte-cumulus cell coupling is essential for an orderly remodeling of chromatin during the G2/M cell cycle transition during in vitro culture [22, 29]. In fact, when bovine COCs from early antral follicles, in which chromatin is mostly decondensed (GV0, [25, 26]), are cultivated in vitro in a system that promote the maintenance of a patent bidirectional coupling, the chromatin gradually organizes into a configuration with a higher degree of condensation (GV1), thus acquiring the ability to mature and be fertilized in vitro [22]. In the present study, a direct relationship between the maintenance of GJC and the chromatin remodeling process before meiotic resumption could not be properly determined. More precisely, the synchronization in GVI configuration could not be directly verified. This is mainly due to the fact that meiosis is delayed by approximately 6 h, but not completely blocked. At 18 and 24h of culture, oocytes in both control and cilostamide groups, already present signs of meiotic resumption, being in GVII-GIV stages or having reached pro-MI stages. However, we could only speculate that at some point before the 18h of culture, most of the oocytes synchronize at GVI stage. On the other hand, since meiotic progression is delayed, chromatin/chromosomes rearrangements during the first 24h of culture are slowed down in the cilostamide group. We cannot exclude that this could account in part for the increased quality of these oocytes. This hypothesis remains to be rigorously tested though.

In this context, it is very important to point out that the present study confirms that GVII-GVIV configurations in pig are typical of oocytes that have already resumed meiosis, even though the nuclear envelope is still detectable and the chromatin is condensing into bivalents that will ultimately become fully-condensed metaphase chromosomes. It is worth noting that the expression "*GV stage*", commonly used by investigators to indicate the stage at which the oocyte is collected

from the ovarian follicle (or even the period when the GV is clearly detectable within the oocyte before GVBD occurs) should not to be confused with the phase of meiotic arrest, since meiotic resumption is initiated well ahead of the disappearance of the nuclear envelope [73]. Therefore, even though GVBD is the first grossly obvious manifestation of meiotic resumption, these two events should not to be considered equivalent [29]. That GVII-GVIV configurations represent early signs of meiotic resumption in pig is indicated by original experiments by Motlik and Fulka, who indeed proposed this classification [73]. In their work, using aceto-orcein staining, Authors describe GVII-GVIV as those configurations that characterize early stages of in vivo and in vitro maturation and that precedes the complete disappearance of the nuclear envelope [73]. This classification was further confirmed by Hirao et al. [44], who, studying oocytes collected from follicles of different diameters, introduced the SC configuration as the one preceding GVI stage. Finally immunofluorescence studies by Bui et al. [32] further confirm the above 'temporal' stages progression showing that the phosphorylation of histone H3-S28 is firstly detected in condensing chromosomes at the GVII–IV stage [32]. Since chromosome condensation begins at this point, the Authors suggest that H3-S28 phosphorylation might be one of the key events initiating meiotic chromosome condensation [32]. Because under our experimental conditions H3-S28 phosphorylation was not detected in GVII-GVIV oocytes we employed another G2/M cell cycle marker to test whether the chromatin configurations observed in GVII-GVIV stages are truly indicative of meiotic resumption. Therefore, SC and GVII-GVIV stages must be carefully evaluated to avoid misinterpretation of experimental data. Moreover, identification of additional unequivocal biomarkers will aid in discerning the events that are critical to establishing oocyte quality during IVM.

In conclusion, the present work demonstrates that delaying the timing of GJC interruption while slowing down early meiotic progression, have a long-acting effect on the developmental program of the oocyte. Our results contribute to our understanding of the mechanisms regulating oocyte maturation and the acquisition of developmental competence and offers intriguing tools for further studies.

Acknowledgements

References

1.	Prather RS, Hawley RJ, Carter DB, Lai L, Greenstein JL. Transgenic swine for biomedicine and agriculture. Theriogenology 2003; 59:115-123.

2.	Sachs DH, Galli C. Genetic manipulation in pigs. Curr Opin Organ Transplant 2009; 14:148-153.

3.	Aigner B, Renner S, Kessler B, Klymiuk N, Kurome M, Wunsch A, Wolf E. Transgenic pigs as models for translational biomedical research. J Mol Med (Berl) 2010; 88:653-664.

4.	Galli C, Lagutina I, Perota A, Colleoni S, Duchi R, Lucchini F, Lazzari G. Somatic cell nuclear transfer and transgenesis in large animals: current and future insights. Reprod Domest Anim 2012; 47 Suppl 3:2-11.

5.	Luo Y, Lin L, Bolund L, Jensen TG, Sorensen CB. Genetically modified pigs for biomedical research. J Inherit Metab Dis 2012; 35:695-713.

6.	Nagashima H, Matsunari H, Nakano K, Watanabe M, Umeyama K, Nagaya M. Advancing pig cloning technologies towards application in regenerative medicine. Reprod Domest Anim 2012; 47 Suppl 4:120-126.

7.	Niemann H, Lucas-Hahn A. Somatic cell nuclear transfer cloning: practical applications and current legislation. Reprod Domest Anim 2012; 47 Suppl 5:2-10.

8.	Pincus G, Enzmann EV. The Comparative Behavior of Mammalian Eggs in Vivo and in Vitro : I. The Activation of Ovarian Eggs. J Exp Med 1935; 62:665-675.

9.	Hyttel P, Fair T, Callesen H, Greve T. Oocyte growth, capacitation and final maturation in cattle. Theriogenology 1997; 47:23-32.

10.	Luciano AM, Pocar P, Milanesi E, Modina S, Rieger D, Lauria A, Gandolfi F. Effect of different levels of intracellular cAMP on the in vitro maturation of cattle oocytes and their subsequent development following in vitro fertilization. Mol Reprod Dev 1999; 54:86-91.

11.	Ponderato N, Crotti G, Turini P, Duchi R, Galli C, Lazzari G. Embryonic and foetal development of bovine oocytes treated with a combination of butyrolactone I and

roscovitine in an enriched medium prior to IVM and IVF. Mol Reprod Dev 2002; 62:513-518.

12.   Luciano AM, Modina S, Vassena R, Milanesi E, Lauria A, Gandolfi F. Role of intracellular cyclic adenosine 3',5'-monophosphate concentration and oocyte-cumulus cells communications on the acquisition of the developmental competence during in vitro maturation of bovine oocyte. Biol Reprod 2004; 70:465-472.

13.   Thomas RE, Armstrong DT, Gilchrist RB. Bovine cumulus cell-oocyte gap junctional communication during in vitro maturation in response to manipulation of cell-specific cyclic adenosine 3',5'-monophosophate levels. Biol Reprod 2004; 70:548-556.

14.   Gilchrist RB, Thompson JG. Oocyte maturation: emerging concepts and technologies to improve developmental potential in vitro. Theriogenology 2007; 67:6-15.

15.   Mayes MA, Sirard MA. Effect of type 3 and type 4 phosphodiesterase inhibitors on the maintenance of bovine oocytes in meiotic arrest. Biol Reprod 2002; 66:180-184.

16.   Lodde V, Franciosi F, Tessaro I, Modina SC, Luciano AM. Role of gap junction-mediated communications in regulating large-scale chromatin configuration remodeling and embryonic developmental competence acquisition in fully grown bovine oocyte. J Assist Reprod Genet 2013; doi:10.1007/s10815-013-0061-7.

17.   Sasseville M, Cote N, Guillemette C, Richard FJ. New insight into the role of phosphodiesterase 3A in porcine oocyte maturation. BMC Dev Biol 2006; 6:47, doi:10.1186/1471-213X-6-47

18.   Tsafriri A, Chun SY, Zhang R, Hsueh AJ, Conti M. Oocyte maturation involves compartmentalization and opposing changes of cAMP levels in follicular somatic and germ cells: studies using selective phosphodiesterase inhibitors. Dev Biol 1996; 178:393-402.

19.   Sasseville M, Cote N, Vigneault C, Guillemette C, Richard FJ. 3'5'-cyclic adenosine monophosphate-dependent up-regulation of phosphodiesterase type 3A in porcine cumulus cells. Endocrinology 2007; 148:1858-1867.

20. Shu YM, Zeng HT, Ren Z, Zhuang GL, Liang XY, Shen HW, Yao SZ, Ke PQ, Wang NN. Effects of cilostamide and forskolin on the meiotic resumption and embryonic development of immature human oocytes. Hum Reprod 2008; 23:504-513.

21. Vanhoutte L, Nogueira D, Dumortier F, De Sutter P. Assessment of a new in vitro maturation system for mouse and human cumulus-enclosed oocytes: three-dimensional prematuration culture in the presence of a phosphodiesterase 3-inhibitor. Hum Reprod 2009; 24:1946-1959.

22. Luciano AM, Franciosi F, Modina SC, Lodde V. Gap Junction-Mediated Communications Regulate Chromatin Remodeling During Bovine Oocyte Growth and Differentiation Through cAMP-Dependent Mechanism(s). Biol Reprod 2011; 85:1252-1259.

23. Zuccotti M, Rossi PG, Martinez A, Garagna S, Forabosco A, Redi CA. Meiotic and developmental competence of mouse antral oocytes. Biol Reprod 1998; 58:700-704.

24. Zuccotti M, Ponce RH, Boiani M, Guizzardi S, Govoni P, Scandroglio R, Garagna S, Redi CA. The analysis of chromatin organisation allows selection of mouse antral oocytes competent for development to blastocyst. Zygote 2002; 10:73-78.

25. Lodde V, Modina S, Galbusera C, Franciosi F, Luciano AM. Large-scale chromatin remodeling in germinal vesicle bovine oocytes: Interplay with gap junction functionality and developmental competence. Mol Reprod Dev 2007; 74:740-749.

26. Lodde V, Modina S, Maddox-Hyttel P, Franciosi F, Lauria A, Luciano AM. Oocyte morphology and transcriptional silencing in relation to chromatin remodeling during the final phases of bovine oocyte growth. Mol Reprod Dev 2008; 75:915-924.

27. Lodde V, Modina SC, Franciosi F, Zuccari E, Tessaro I, Luciano AM. Localization of DNA methyltransferase-1 during oocyte differentiation, in vitro maturation and early embryonic development in cow. Eur J Histochem 2009; 53(4):e24. doi:10.4081/ejh.2009.e24.

28. Luciano AM, Lodde V, Franciosi F, Tessaro I, Corbani D, Modina S. Large-scale chromatin morpho-functional changes during mammalian oocyte growth and differentiation. Eur J Histochem 2012; 56:e37.

29. Luciano AM, Lodde V. Changes of Large-Scale Chromatin Configuration During Mammalian Oocyte Differentiation. In: Coticchio G, Albertini DF, De Santis L (eds.), Oogenesis: Springer London; 2013: 93-108.

30. Aktas H, Wheeler MB, First NL, Leibfried-Rutledge ML. Maintenance of meiotic arrest by increasing [cAMP]i may have physiological relevance in bovine oocytes. J Reprod Fertil 1995; 105:237-245.

31. Motlik J, Fulka J. Breakdown of the germinal vesicle in pig oocytes in vivo and in vitro. J Exp Zool 1976; 198:155-162.

32. Bui HT, Van Thuan N, Kishigami S, Wakayama S, Hikichi T, Ohta H, Mizutani E, Yamaoka E, Wakayama T, Miyano T. Regulation of chromatin and chromosome morphology by histone H3 modifications in pig oocytes. Reproduction 2007; 133:371-382.

33. Abramoff MD, Magelhaes PJ. Image processing with ImageJ. Biophotonics International 2004; 11:36-42.

34. Tervit HR, Whittingham DG, Rowson LE. Successful culture in vitro of sheep and cattle ova. J Reprod Fertil 1972; 30:493-497.

35. Lagutina I, Lazzari G, Galli C. Birth of cloned pigs from zona-free nuclear transfer blastocysts developed in vitro before transfer. Cloning Stem Cells 2006; 8:283-293.

36. Yoshioka K, Suzuki C, Tanaka A, Anas IM, Iwamura S. Birth of piglets derived from porcine zygotes cultured in a chemically defined medium. Biol Reprod 2002; 66:112-119.

37. Vajta G, Lewis IM, Trounson AO, Purup S, Maddox-Hyttel P, Schmidt M, Pedersen HG, Greve T, Callesen H. Handmade somatic cell cloning in cattle: analysis of factors contributing to high efficiency in vitro. Biol Reprod 2003; 68:571-578.

38. Vajta G, Peura TT, Holm P, Paldi A, Greve T, Trounson AO, Callesen H. New method for culture of zona-included or zona-free embryos: the Well of the Well (WOW) system. Mol Reprod Dev 2000; 55:256-264.

39. Wickramasinghe D, Ebert KM, Albertini DF. Meiotic competence acquisition is associated with the appearance of M-phase characteristics in growing mouse oocytes. Dev Biol 1991; 143:162-172.

40.   Messinger SM, Albertini DF. Centrosome and microtubule dynamics during meiotic progression in the mouse oocyte. J Cell Sci 1991; 100 (Pt 2):289-298.

41.   Sanfins A, Lee GY, Plancha CE, Overstrom EW, Albertini DF. Distinctions in meiotic spindle structure and assembly during in vitro and in vivo maturation of mouse oocytes. Biol Reprod 2003; 69:2059-2067.

42.   McGinnis LK, Albertini DF, Kinsey WH. Localized activation of Src-family protein kinases in the mouse egg. Dev Biol 2007; 306:241-254.

43.   McGinnis LK, Albertini DF. Dynamics of protein phosphorylation during meiotic maturation. J Assist Reprod Genet 2010; 27:169-182.

44.   Hirao Y, Tsuji Y, Miyano T, Okano A, Miyake M, Kato S, Moor RM. Association between p34cdc2 levels and meiotic arrest in pig oocytes during early growth. Zygote 1995; 3:325-332.

45.   Nagai T, Ebihara M, Onishi A, Kubo M. Germinal vesicle stages in pig follicular oocytes collected by different methods. J Reprod Dev 1997; 43:339-343.

46.   Guthrie HD, Garrett WM. Changes in porcine oocyte germinal vesicle development as follicles approach preovulatory maturity. Theriogenology 2000; 54:389-399.

47.   Sun XS, Liu Y, Yue KZ, Ma SF, Tan JH. Changes in germinal vesicle (GV) chromatin configurations during growth and maturation of porcine oocytes. Mol Reprod Dev 2004; 69:228-234.

48.   Endo T, Naito K, Aoki F, Kume S, Tojo H. Changes in histone modifications during in vitro maturation of porcine oocytes. Mol Reprod Dev 2005; 71:123-128.

49.   Bui HT, Yamaoka E, Miyano T. Involvement of histone H3 (Ser10) phosphorylation in chromosome condensation without Cdc2 kinase and mitogen-activated protein kinase activation in pig oocytes. Biol Reprod 2004; 70:1843-1851.

50.   Kurome M, Hisatomi H, Matsumoto S, Tomii R, Ueno S, Hiruma K, Saito H, Nakamura K, Okumura K, Matsumoto M, Kaji Y, Endo F, et al. Production efficiency and telomere length of the cloned pigs following serial somatic cell nuclear transfer. J Reprod Dev 2008; 54:254-258.

51.   Matsunari H, Onodera M, Tada N, Mochizuki H, Karasawa S, Haruyama E, Nakayama N, Saito H, Ueno S, Kurome M, Miyawaki A, Nagashima H. Transgenic-cloned pigs systemically expressing red fluorescent protein, Kusabira-Orange. Cloning Stem Cells 2008; 10:313-323.

52.   Petersen B, Lucas-Hahn A, Oropeza M, Hornen N, Lemme E, Hassel P, Queisser AL, Niemann H. Development and validation of a highly efficient protocol of porcine somatic cloning using preovulatory embryo transfer in peripubertal gilts. Cloning Stem Cells 2008; 10:355-362.

53.   Zhao J, Ross JW, Hao Y, Spate LD, Walters EM, Samuel MS, Rieke A, Murphy CN, Prather RS. Significant improvement in cloning efficiency of an inbred miniature pig by histone deacetylase inhibitor treatment after somatic cell nuclear transfer. Biol Reprod 2009; 81:525-530.

54.   Bilodeau-Goeseels S. Bovine oocyte meiotic inhibition before in vitro maturation and its value to in vitro embryo production: does it improve developmental competence? Reprod Domest Anim 2012; 47:687-693.

55.   Guixue Z, Luciano AM, Coenen K, Gandolfi F, Sirard MA. The influence of cAMP before or during bovine oocyte maturation on embryonic developmental competence. Theriogenology 2001; 55:1733-1743.

56.   Nogueira D, Cortvrindt R, De Matos DG, Vanhoutte L, Smitz J. Effect of phosphodiesterase type 3 inhibitor on developmental competence of immature mouse oocytes in vitro. Biol Reprod 2003; 69:2045-2052.

57.   Nogueira D, Cortvrindt R, Everaerdt B, Smitz J. Effects of long-term in vitro exposure to phosphodiesterase type-3 inhibitors on follicle and oocyte development. Reproduction 2005; 130:177-186.

58.   Nogueira D, Ron-El R, Friedler S, Schachter M, Raziel A, Cortvrindt R, Smitz J. Meiotic arrest in vitro by phosphodiesterase 3-inhibitor enhances maturation capacity of human oocytes and allows subsequent embryonic development. Biol Reprod 2006; 74:177-184.

59.   Sa Barretto LS, Castro VS, Garcia JM, Mingoti GZ. Meiotic inhibition of bovine oocytes in medium supplemented with a serum replacer and hormones: effects on meiosis progression and developmental capacity. Zygote 2011; 19:107-116.

60.   Thomas RE, Thompson JG, Armstrong DT, Gilchrist RB. Effect of specific phosphodiesterase isoenzyme inhibitors during in vitro maturation of bovine oocytes on meiotic and developmental capacity. Biol Reprod 2004; 71:1142-1149.

61.   Vanhoutte L, Nogueira D, De Sutter P. Prematuration of human denuded oocytes in a three-dimensional co-culture system: effects on meiosis progression and developmental competence. Hum Reprod 2009; 24:658-669.

62.   Vanhoutte L, Nogueira D, Gerris J, Dhont M, De Sutter P. Effect of temporary nuclear arrest by phosphodiesterase 3-inhibitor on morphological and functional aspects of in vitro matured mouse oocytes. Mol Reprod Dev 2008; 75:1021-1030.

63.   Vanhoutte L, De Sutter P, Nogueira D, Gerris J, Dhont M, Van der Elst J. Nuclear and cytoplasmic maturation of in vitro matured human oocytes after temporary nuclear arrest by phosphodiesterase 3-inhibitor. Hum Reprod 2007; 22:1239-1246.

64.   Albuz FK, Sasseville M, Lane M, Armstrong DT, Thompson JG, Gilchrist RB. Simulated physiological oocyte maturation (SPOM): a novel in vitro maturation system that substantially improves embryo yield and pregnancy outcomes. Hum Reprod 2010; 25:2999-3011.

65.   Rose RD, Gilchrist RB, Kelly JM, Thompson JG, Sutton-McDowall ML. Regulation of sheep oocyte maturation using cAMP modulators. Theriogenology 2013; 79:142-148.

66.   Zeng HT, Ren Z, Guzman L, Wang X, Sutton-McDowall ML, Ritter LJ, De Vos M, Smitz J, Thompson JG, Gilchrist RB. Heparin and cAMP modulators interact during pre-in vitro maturation to affect mouse and human oocyte meiosis and developmental competence. Hum Reprod 2013; 28(6):1536-45. doi:10.1093/humrep/det086.

67.   Grupen CG, Fung M, Armstrong DT. Effects of milrinone and butyrolactone-I on porcine oocyte meiotic progression and developmental competence. Reprod Fertil Dev 2006; 18:309-317.

68.   Laforest MF, Pouliot E, Gueguen L, Richard FJ. Fundamental significance of specific phosphodiesterases in the control of spontaneous meiotic resumption in porcine oocytes. Mol Reprod Dev 2005; 70:361-372.

69.   Jee BC, Chen HY, Chian RC. Effect of a phosphodiesterase type 3 inhibitor in oocyte maturation medium on subsequent mouse embryo development. Fertil Steril 2009; 91:2037-2042.

70.   Nogueira D, Vanhoutte L. Use of phosphodiesterase type 3 inhibitor to improve IVM outcome: experimental set up matters. Fertil Steril 2009; 91:e3; author reply e4-5.

71.   Wu D, Cheung QC, Wen L, Li J. A growth-maturation system that enhances the meiotic and developmental competence of porcine oocytes isolated from small follicles. Biol Reprod 2006; 75:547-554.

72.   Thomas RE, Armstrong DT, Gilchrist RB. Differential effects of specific phosphodiesterase isoenzyme inhibitors on bovine oocyte meiotic maturation. Dev Biol 2002; 244:215-225.

73.   Motlik J, Crozet N, Fulka J. Meiotic competence in vitro of pig oocytes isolated from early antral follicles. J Reprod Fertil 1984; 72:323-328.

Tables

Table 1: Chromatin configurations distribution at the time of oocytes isolation from early and middle antral follicle

Follicle	N	FC (%)	SCd (%)	SCn (%)	GVI (%)	GVII-IV (%)	ProMI-MI (%)	Deg (%)
EAF	91	44 [a]	8	11 [a]	9 [a]	3	0	16
		(48.4)	(8.8)	(12.1)	(9.9)	(3.3)	(0.0)	(17.6)
MAF	245	9 [b]	23	87 [b]	71 [b]	20	0	35
		(3.7)	(9.4)	(35.5)	(29.0)	(8.2)	(0.0)	(14.3)

[a,b] different letters within columns indicate significant differences (Fisher's exact test, $P<0.05$)

Table 2: Effect of 1μM cilostamide treatment on chromatin configuration remodeling and meiotic progression

Treatment	N	FC (%)	SCd (%)	SCn (%)	GVI (%)	GVII-IV (%)	ProMI-MI (%)	Deg (%)
18 h CTRL	80	0 (0.0)	1 (1.3)	6 (7.5)	26 (32.5)	31 (38.8)	14 (17.5)	2 (2.5)
18 h CILO	82	0 (0.0)	5 (6.1)	14 (17.1)	26 (31.7)	24 (29.3)	8 (9.8)	5 (6.1)
24 h CTRL	89	0 (0.0)	5 (5.6)	1 (1.1)	8 [a] (9.0)	12[a] (13.5)	62 [a] (69.7)	1 (1.1)
24 h CILO	86	0 (0.0)	4 (4.7)	6 (7.0)	21 [b] (24.4)	29 [b] (33.7)	22 [b] (25.6)	4 (4.7)

[a,b] different letters within columns indicate significant differences (Fisher's exact test, $P<0.05$)

Table 3: Effect of 1µM cilostamide treatment on embryonic developmental competence after parthenogenetic activation

Treatment	N	Cleaved (%)	Blastocyst (%)	Expanded blastocyst of tot blastocyst (%)	Mean cell number per blastocyst ± SEM
CTRL		132	77	35 [a]	23 ± 1.21
	150	(88.0)	(51.3)	(45.5)	
CILO		120	59	38 [b]	26 ± 1.44
	142	(84.5)	(41.5)	(64.4)	

[a,b] different letters within columns indicate significant differences (Fisher's exact test, P<0.05)

Table 4: Effect of 1μM cilostamide treatment on embryonic developmental competence after somatic cell nuclear transfer

Treatment	N	Cleaved (%)	Blastocyst (%)	Expanded blastocyst of tot blastocyst (%)	Mean cell number per blastocyst ± SEM
CTRL		98	27	18	45 ± 3.35 [a]
	163	(60.1)	(16.6)	(66.7)	
CILO		84	25	21	58 ± 4.9 [b]
	161	(52.2)	(15.5)	(84.0)	

[a,b] different letters within columns indicate significant differences (Fisher's exact test, $P<0.05$)

Figure 1. **(A)** Dose-response effect of cilostamide on oocyte meiotic resumption. COCs were cultured in media supplemented with increasing concentrations of cilostamide (0, 0.1, 1 µM) for varying periods of time (24, 36 and 48h). A total of 960 oocytes were used in these experiments. Oocytes where judged intermediate when the chromosomes were arranged in pro-metaphase, metaphase I plate, anaphase I or telophase I; mature, when the chromosomes were arranged in a metaphase II plate with the first polar body extruded **(B)** Effect of the prematuration treatment on oocyte maturation status. COCs were incubated in the presence of 1µM cilostamide for 24h. The maturation status was assessed after culturing the COCs for further 20h in dIVM medium (see text). A total of 146 oocytes were used in these experiments. Data were analyzed by Fisher's exact test.

* indicates significant differences between classes (P<0.05).
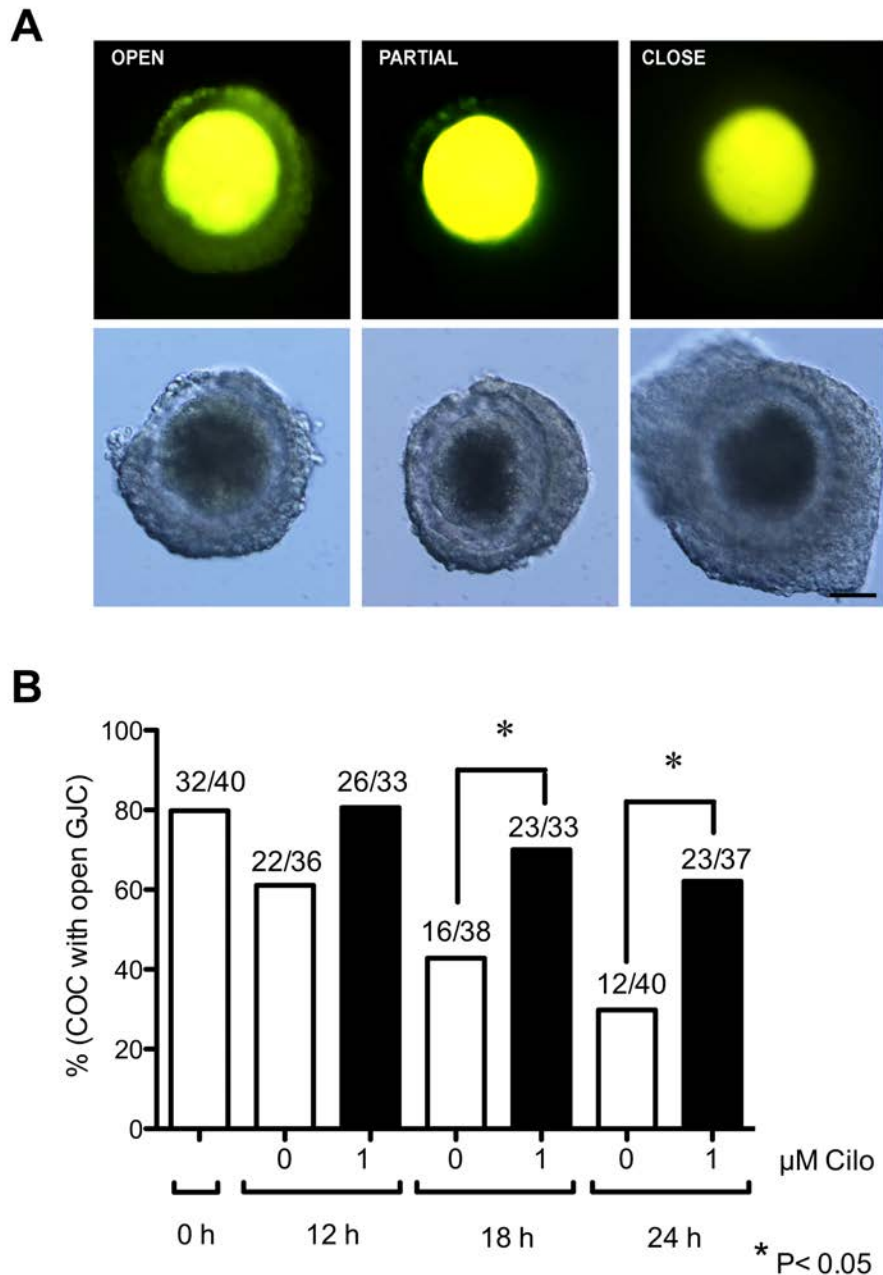
Figure 2. **(A)** Representative images showing the functional coupling between oocyte and cumulus cells after Lucifer Yellow dye injection (upper panel) and bright field images (lower panel). Gap junction communications were classified as Open, Partial or Close as previously described [12]. Scale bar: 50 μm. **(B)** The effect of cilostamide on open GJ mediated communication between the oocyte and cumulus cells after 0, 12, 18 and 24h IVM. A total of 257 oocytes were used in these experiments. Number of oocytes analyzed in each group is indicated. Data were analyzed by Fisher's exact test.

Figure 3. (A) Fluorescent images after Hoechst 33342 labeling of porcine oocytes at the time of collection with FC (a), SCd (b), SCn (c) and GVI (d) configuration. **(B)** GV chromatin configuration in relation to oocyte diameter at the time of collection. A total of 228 oocytes were used in these experiments. Number of oocytes analyzed in each group is indicated in the graph.

Mean diameter values, for each GV category, are expressed as means ± SE. Data were analyzed by ANOVA followed by Tukey's Multiple comparison test.

a, b, c indicate significant differences between groups (P<0.05).
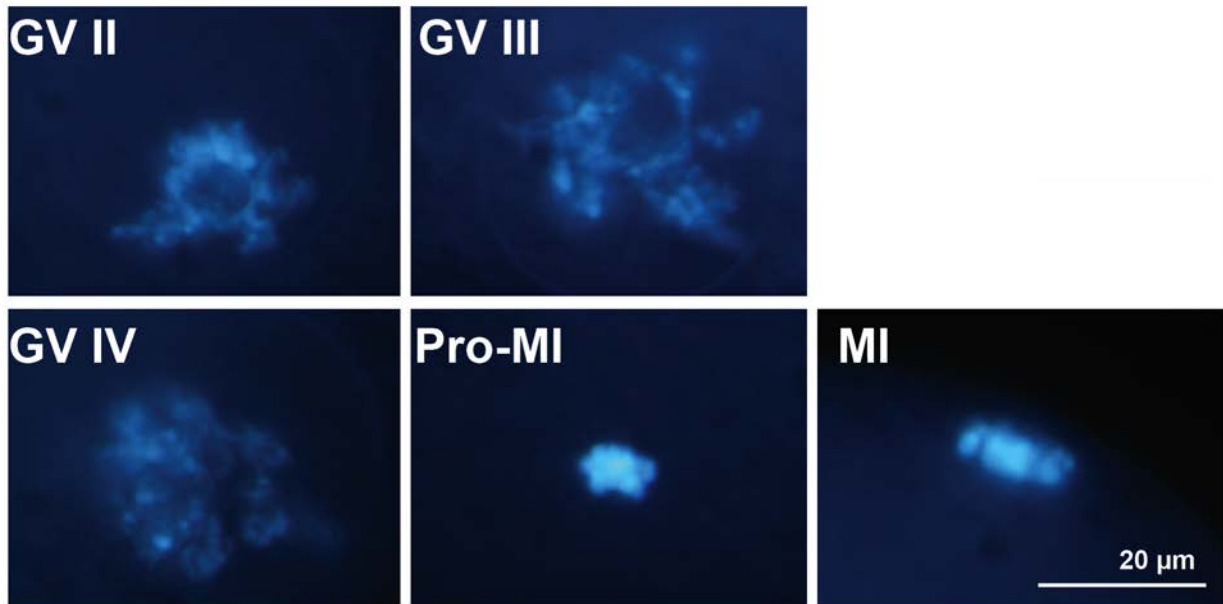
Figure 4. Representative fluorescent images after Hoechst 33342 labeling of porcine oocytes with GVII (e), GVIII (f) GVIV (g), ProMI (h) and MI (i) configurations after meiotic resumption.
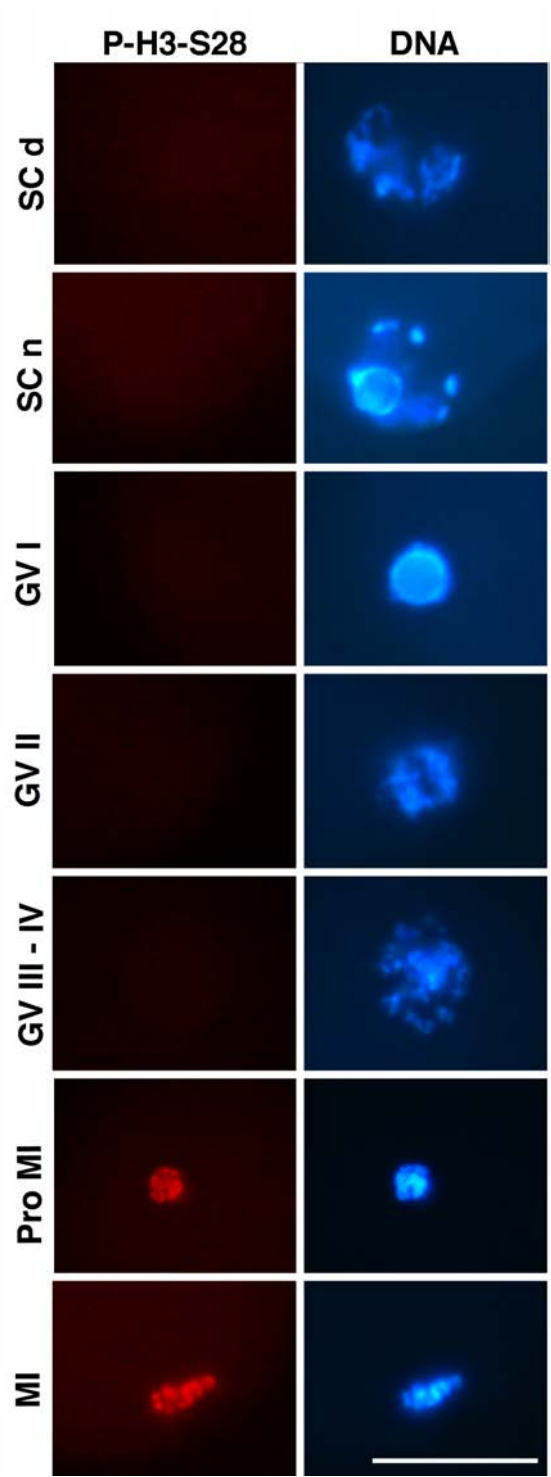
Figure 5. Representative images showing the status of histone H3-S28 (P-H3-S28) phosphorylation in porcine oocyte with different chromatin configurations and during early stages of meiotic maturation. Red P-H3-S28; Blue, DNA. Scale bar: 50 μm. No differences were observed in oocytes fixed either in paraformaldehyde or in microtubule-stabilizing fixative.
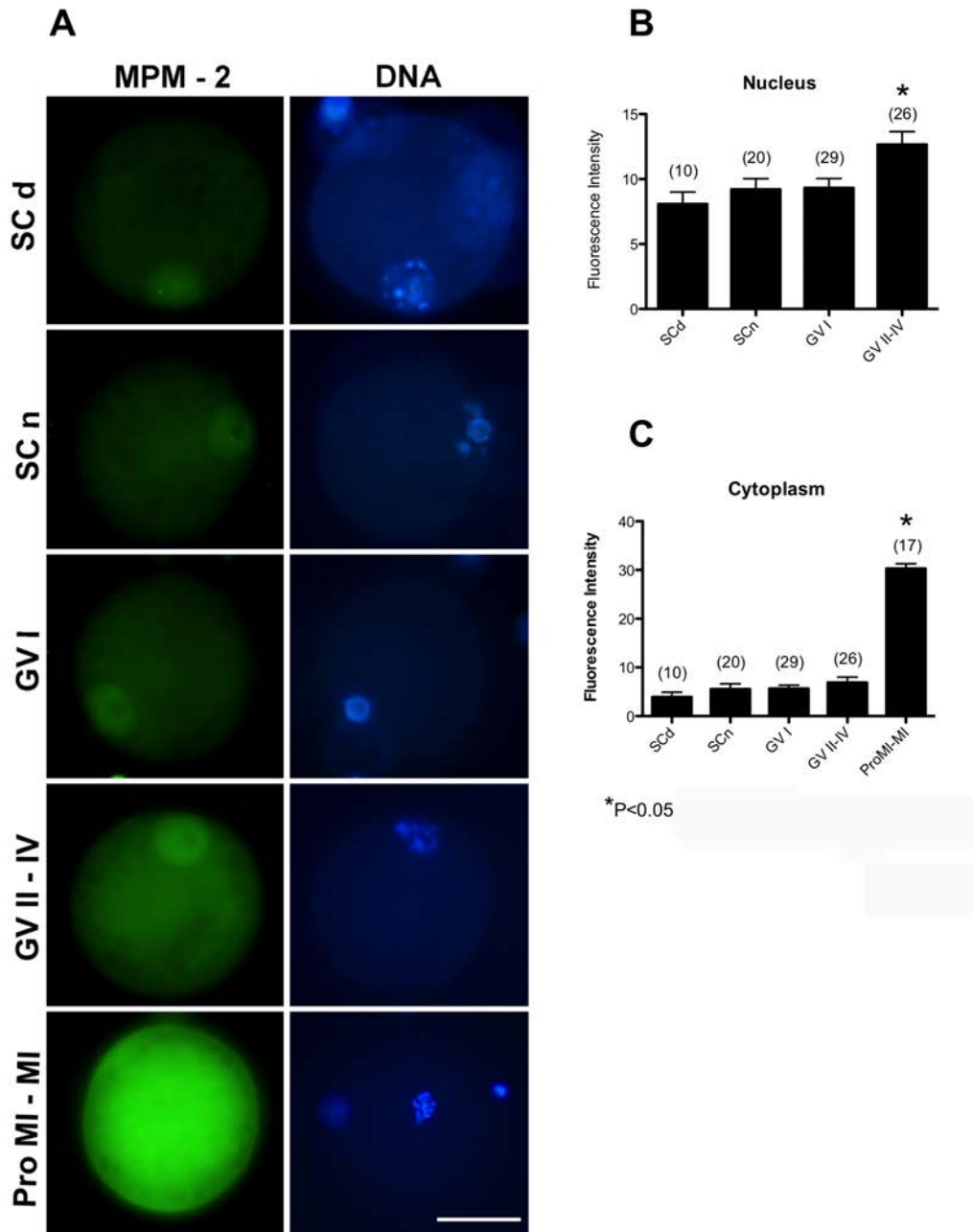
Figure 6. (A) Representative images showing the pattern of tyrosine phospho-proteins changes (MPM2 staining) in porcine oocyte with different chromatin configurations and during early stages of meiotic maturation. Green, MPM2; Blue, DNA. Scale bar: 50 µm. **(B, C)** Histograms indicate the fluorescence intensity of MPM2 signal within the nuclear **(B)** or cytoplasmic **(C)** area according to the chromatin configurations changes at the time of collection and during early stages of meiotic maturation. Values are expressed as means ± SE. Data were analyzed with ANOVA followed by Tukey's multiple comparison test. Number of oocytes analyzed in each group is indicated.

* indicates significant differences between classes (P<0.05).

CHAPTER 3: Differences in cumulus cell gene expression indicate the benefit of a pre-maturation step to improve in-vitro bovine embryo production

Differences in cumulus cell gene expression indicate the benefit of a pre-maturation step to improve in-vitro bovine embryo production

Cecilia Dieci[1][§], Valentina Lodde[1][§], Rémi Labreque[2], Isabelle Dufort[2], Irene Tessaro[1,3], Marc-André Sirard[2] and Alberto M. Luciano[1]

[1]Reproductive and Developmental Biology Laboratory, Department of Health, Animal Science and Food Safety, University of Milan, 20133 Milan, Italy; [2]Centre de Recherche en Biologie de la Reproduction, Département des Sciences Animales, Université Laval, Québec, QC, Canada.

[§]Contributed equally

Running Title: Cumulus cell gene expression and oocyte competence

Correspondence: Alberto M. Luciano, Dipartimento di Scienze Veterinarie per la Salute, la Produzione Animale e la Sicurezza Alimentare, Università degli Studi di Milano, Via Celoria, 10 - 20133 Milano, Italy - Phone (+39) 02 50317969 - alberto.luciano@unimi.it

[3]Present address: I.R.C.C.S. Istituto Ortopedico Galeazzi - Via R. Galeazzi, 4 – 20161 Milan (Italy).

Abstract

STUDY QUESTION: Does the gene expression profile of cumulus cells (CC) accompanying oocytes with different degrees of chromatin compaction within the germinal vesicle (GV) reflect the oocyte's quality and response in culture during in-vitro embryo production (IVP).

SUMMARY ANSWER: The transcriptomic profile of the cumulus cells is related to oocyte competence, setting the stage for the development of customized pre-maturation strategies to improve IVP.

WHAT IS KNOWN ALREADY: Oocytes complete the acquisition of their competence during antral follicle development. During this period, the chromatin configuration within the GV changes dynamically and is indicative of oocyte's developmental potential. The interactions between somatic and germ cells modulate chromatin morphology and function and are critical for acquisition of oocyte competence.

STUDY DESIGN, SIZE, DURATION: Bovine cumulus-oocyte complexes (COC) were isolated from 0.5-6 mm antral follicles. Surrounding CC were separated from the oocyte and classified as GV0, GV1, GV2 and GV3 according to the degree of the oocyte's chromatin compaction.

PARTICIPANTS/MATERIALS, SETTING, METHODS: RNA extracted from CC of each group was amplified and hybridized on a bovine embryo-specific 44K Agilent slide. The CC_GV1, CC_GV2 and CC_GV3 classes were each hybridized against the CC_GV0 class, representing an early oocyte differentiation stage with poor development competence. The data were normalizedand fold changes of the differentially expressed genes were determined. Microarray data were validated using quantitative RT-PCR on selected targets. Microarray data were further analyzed through: 1) between-group analysis (BGA), which classifies the samples according to their transcriptomic profiles; 2) cluster analysis according to the expression profile of each gene; and 3) Ingenuity Pathway Analysis (IPA) to study gene regulation patterns and predicted functions. Furthermore, CC ofeach GV group were cultured and apoptotic cells were assessed after 3 hrs by caspase analysis. Finally, based on the analysis of CC transcriptomic profiles and the relationship between morphological features of the COC and the oocyte chromatin configuration, a customized, stage-dependent oocyte pre-maturation (pre-IVM) system was used to improve oocyte developmental potential before IVM. For this, the blastocyst rate and quality were assessed after in-vitro maturation and fertilization of pre-matured oocytes.

MAIN RESULTS AND THE ROLE OF CHANCE: Overall, qRT-PCR results of a subset of five selected genes were consistent with the microarray data. Clustering analysis generated 16 clusters representing the main profiles of transcription modulation. Of the 5571 significantly differentially

expressed probes, the majority (25.49%) best fitted with cluster #6 (down regulation between CC_GV0 and CC_GV1 and stable low levels in successive groups). IPA identified the most relevant functions associated to each cluster. Genes included in cluster #1 were mostly related to biological processes such as "cell cycle" and "cell death and survival", while genes included in cluster #5 were mostly related to "gene expression". Interestingly, "lipid metabolism" was the most significant function identified in cluster # 6, #9 and #12. IPA of gene lists obtained from each contrast (i.e., CC_GV0 vs. CC_GV1; CC_GV0 vs. CC_GV2; CC_GV0 vs. CC_GV3) revealed that the main affected function in each contrast was "cell death and survival". Importantly, apoptosis was predicted to be inhibited in CC_GV1 and CC_GV2, but activated in CC_GV3. Caspase analysis indicated that a low percentage of CC_GV0 were prone to undergo apoptosis but apoptosis increased significantly in CC from oocytes with condensed chromatin, reaching a peak in CC_GV3 ($p<0.05$). Finally, the tailored oocyte pre-maturation strategy, based on morphological features of the COC and the oocyte chromatin configuration, demonstrated that pre-IVM improved the developmental capability of oocytes at early stages of differentiation (GV1-enriched COC) but was detrimental for oocytes at more advanced stages of development (GV3-enriched COC).

LARGE SCALE DATA: The data are available through the GEO series accession number GSE79886 (http://www.ncbi.nlm.nih.gov/geo/query/acc.cgi?acc=GSE79886).

LIMITATIONS, REASONS FOR CAUTION: This study was conducted with bovine samples. Whether or not the results are applicable to human oocytes requests further elucidation. Embryo transfer experiments are required to determine whether the improvement in blastocyst rates in the tailored system leads to increased live birth rates.

WIDER IMPLICATIONS OF THE FINDINGS: The identification of multiple non-invasive biomarkers predictive of oocyte quality can greatly strengthen the pre-IVM approach aimed to improve IVM outcomes. These results have potentially important implications in treating human infertility and in developing breeding schemes for domestic mammals.

Introduction

In-vitro embryo production (IVP) remains inefficient in both clinical applications of human reproduction and animal breeding. In particular, the development of suitable conditions for in-vitro oocyte maturation (IVM) that support high quality oocyte production is a major challenge in assisted reproductive technologies (Smitz *et al.* , 2011). In the bovine, although many attempts to increase the number of transferable embryos have been made in recent decades, the efficiency of IVP techniques, calculated as the proportion of immature oocytes aspirated from middle antral follicles (2-8 mm in diameter) that reach the blastocyst stage of embryonic development, is struggling to overcome a 35% threshold (Lonergan and Fair, 2008), unless very specific hormonal programming is used, that can double this rate (Blondin *et al.* , 2002, Landry *et al.* , 2016, Nivet *et al.* , 2012). In fact, oocytes retrieved from non-treated animals reveal heterogeneous cellular and molecular features as well as distinct embryonic developmental capabilities (Blondin and Sirard, 1995, Pavlok *et al.* , 1992). On the other hand, it is well known that oocytes enclosed in early antral follicles (less than 2 mm in diameter) have not yet acquired the competence to spontaneously resume meiosis once isolated from the follicular compartment (Blondin and Sirard, 1995, Pavlok *et al.*, 1992); thus they are generally not used in standard IVP protocols.

The diversity of oocyte competence is mainly due to the intrinsic heterogeneity of the cohort of follicles from which cumulus-oocyte complexes (COC), to be subjected to standard IVP procedures, are isolated (Merton *et al.* , 2003, Vassena *et al.* , 2003). In cows, as in humans, only one oocyte is released at each reproductive cycle while the remaining follicles undergo atresia (Gougeon, 1986, Lussier *et al.* , 1987). It is widely accepted that one of the main factors that impairs oocyte ability to become an embryo in vitro is the precocious meiotic resumption that occurs when oocytes are isolated from the follicles. This, indeed, interrupts the process of oocyte capacitation (Coticchio *et al.* , 2015, Gilchrist *et al.* , 2008, Hyttel *et al.* , 1997) and creates an asynchrony between the nuclear and the cytoplasmic events that are required for oocyte differentiation program before ovulation (Eppig *et al.* , 1994). In addition, a large proportion of these oocytes have already started an atretic process (Adams *et al.* , 2008, Gougeon, 1996, Monniaux *et al.* , 2014).

Oocyte quality heterogeneity is reflected in differences in the large-scale configuration of the chromatin enclosed in the germinal vesicle (GV) of immature oocytes (reviewed in (De La Fuente, 2006, Luciano *et al.* , 2014, Luciano and Lodde, 2013, Zuccotti *et al.* , 2005). In cows, oocytes isolated from early to middle antral follicles have four different patterns of chromatin configuration, from GV0 to GV3, which are characterized by progressive increases in chromatin

compaction (Lodde *et al.*, 2007), transcriptional silencing (Lodde *et al.*, 2008, Luciano *et al.*, 2011) and global DNA methylation (Lodde *et al.*, 2009). Notably, oocytes with a GV0 configuration (isolated from early antral follicles) display a very limited capability to resume meiosis, while virtually all of the GV1, GV2 and GV3 oocytes (isolated from mid-antral follicles) are capable of reaching the metaphase II (MII) stage in vitro, regardless their GV configuration (Lodde *et al.*, 2007). However, only a limited proportion of GV1 oocytes reach the blastocyst stage after IVF, while GV2 and GV3 oocytes have significantly higher embryonic developmental potentials (Lodde *et al.*, 2007). Thus, large-scale chromatin configuration is a marker of oocyte differentiation and competence.

It is clear that a better characterization of the molecular determinants of oocyte heterogeneity would be beneficial in understanding basic oocyte biology as well as in improving IVP efficiency. With this view, we have recently analyzed the transcriptomic profile of bovine oocytes with different chromatin configurations to identify changes in mRNA expression in the oocyte during the GV0 to GV3 transition (Labrecque *et al.*, 2015). The present study aimed to expand this knowledge by assessing the transcriptomic profile of cumulus cells (CC) isolated from oocytes with different chromatin configurations. In fact, proper assessment of the oocyte 'signature' cannot overlook features of the surrounding CC. It is well established that the CC play a fundamental role in the modulation of oocyte competence acquisition. During folliculogenesis, oocyte growth and differentiation rely upon the establishment of a microenvironment generated by bidirectional paracrine regulatory signals, and intercellular heterologous gap junction communications between oocytes and somatic cells are pivotal (Eppig, 2001, Gilchrist *et al.*, 2008, Matzuk *et al.*, 2002). Moreover, previous studies show that the tight association between oocyte and companion cumulus cells is required for the progressive suppression of transcriptional activity, chromatin remodeling and competence acquisition during the final phase of oocyte growth in mice (De La Fuente and Eppig, 2001), cows (Luciano *et al.*, 2011) and humans (Sanchez *et al.*, 2015).

Furthermore, based on the results of our microarray analysis, in a second part of this study, we hypothesize that each class of oocytes responds differently to the cultural environment during IVP. To test this hypothesis, and considering that it is technically not possible to identify the chromatin configuration without DNA staining after removal of CC, we first looked for possible morphological markers that could be related to the chromatin configuration of the corresponding oocyte, and used these criteria to select a population of COC enriched in GV1 oocytes (which are less competent compared to GV2 and GV3). Then, on the basis of the microarray results, we designed a culture system specifically formulated to fulfill the specific needs of the oocyte at a specific stage and to support in-vitro development. This system was used as proof-of-concept of an

in-vitro differentiation strategy, the so-called "pre-maturation" system, in order to improve oocyte developmental potential before IVM. This, in turn, confirmed the hypothesis that each class of oocytes responds differently to the cultural environment during IVP.

Materials and methods

All chemicals and reagents were purchased from Sigma-Aldrich, unless otherwise stated.

Cumulus oocytes complexes (COC) collection

Ovaries were recovered at the abattoir (INALCA Spa, Ospedaletto Lodigiano, LO, IT 2270M CE, Italy) from 4-8 years old Holstein dairy cows and COC were retrieved from early (0.5-2 mm) and middle antral follicles (2-8 mm) as previously described (Lodde *et al.*, 2007). All the COC collected were then washed in medium 199 (M199) supplemented with HEPES 20 mM, 1790 units/L Heparin and 0.4% of bovine serum albumin (HM199) and examined under a stereomicroscope. Only COC suitable for standard in-vitro embryo production procedures were used. Precisely only oocytes medium-brown in colour, with homogenous or finely granulated ooplasm and surrounded by five or more complete layers of CC were included in the study, (Luciano *et al.* , 2005). The same morphological selection criteria are commonly accepted by the scientific community and applied in the commercial settings worldwide (Gordon, 2003, Stringfellow and Givens, 2010).

Cumulus cells isolation

COC were individually vortexed (2 min, 35 Hz) in HM199 supplemented with 5% of calf serum (Gibco, Thermo Fisher Scientific) to isolate cumulus cells (CC). In order to assess the chromatin configuration of oocytes corresponding to each cumulus, the denuded oocytes (DO) were individually washed in HM199, stained in HM199 containing 1 μg/mL Hoechst 33342 for 5 min in the dark, and then transferred into a 5 μL drop of the same medium, overlaid with mineral oil, and observed under an inverted fluorescence microscope (Olympus IX50, Olympus, magnification 40x). Oocytes were classified according to the degree of chromatin compaction within the nuclear envelope as previously described (Lodde *et al.*, 2007): the GV0 stage is characterized by a diffuse filamentous pattern of chromatin in the whole nuclear area; the GV1 and GV2 configurations represent early and intermediate stages, respectively, of chromatin remodeling, a process starting with the appearance of few foci of condensation in GV1 oocytes and proceeding with the formation of distinct clumps of condensed chromatin in GV2 oocytes; the GV3 is the stage where the maximum level of condensation is reached with chromatin organized into a single clump.

For transcriptomic and gene expression analyses, CC isolated from each COC were individually collected in RNAse-free tubes, washed twice in cold PBS followed by centrifugation at 1000 rpm for 1 min at 4°C. After the removal of the supernatant, CC pellets (in the minimum volume of PBS possible) were snap-frozen in liquid nitrogen and stored at -80°C until RNA extraction. For the assessment of pan-caspase activity, CC were isolated following the same experimental procedure with the exception that they were removed by pipetting to avoid cell damage. Then, CC isolated from a single COC were transferred into culture medium and assayed as described below.

RNA extraction

Groups of CC isolated from 10 oocytes with the same chromatin configuration were pooled and processed for total RNA extraction. Total RNA was extracted and purified with the Pico-Pure RNA Isolation Kit (ARCTURUS® - Thermo Fisher Scientific) following the manufacturer's protocol, with minor modifications. Briefly, 10-30 µl of extraction buffer were added to each tube containing CC pellet from a single COC and incubated 30 minutes at 42 °C. Following incubation, extraction reaction mixtures from 10 tubes with CC isolated from oocytes bearing the same chromatin configuration were pooled and equal volumes of EtOH 70% were added to each tubes. Then, 250 µl of the RNA sample and EtOH mixture were loaded into the preconditioned purification columns and centrifuged for 2 minutes at 100 x g; this step was repeated until all the RNA/EtOH mixtures were loaded into the columns. Finally, the columns were centrifuged at 16000 x g for 30 seconds to remove the flow-through and bind RNA. Following these steps, the procedure was performed according manufactures instructions and including DNase treatment (Qiagen) on the purification columns. Four pools for each chromatin configuration (CC_GV0, CC_GV1, CC_GV2 and CC_GV3) were used for microarray analysis and an additional four pools for each chromatin configuration (from independent collections) were used for microarray validation by quantitative RT-PCR (qRT-PCR). Total RNA purity, integrity and concentration were evaluated using a 2100-Bioanalyzer (Agilent Technologies, Palo Alto, CA) with the RNA PicoLab Chip (Agilent Technologies). All extracted samples were of good quality with an RNA integrity number greater then 7.4.

RNA amplification, sample labeling and microarray hybridization

To generate enough material for the hybridization, RNA samples were linearly amplified according to the EmbryoGene pipeline. Antisense RNA (aRNA) was produced using the RiboAmp HS RNA amplification kit (Applied Biosystems, Thermo Fisher Scientific). After two amplification rounds of 6 hours each, the aRNA output was quantified using the NanoDrop ND-1000 (NanoDrop Technologies) (Gilbert *et al.*, 2009, Gilbert *et al.*, 2010). Then, for each sample, 4 μg of aRNA were labeled using the ULS Fluorescent Labeling Kit for Agilent arrays (with Cy3 and Cy5) (Kreatech Diagnostics, Amsterdam). The labeled product was then purified with the Pico-Pure RNA Isolation Kit. Labeling efficiency was measured using the Nano-Drop ND-1000. Samples from the four biological replicates, representing six different weeks of cumulus cells collection were hybridized on a custom bovine embryo specific Agilent 44K microarray slide (Robert *et al.*, 2011). The hybridizations were performed using a reference design, where cumulus cells isolated from oocytes bearing the GV1, GV2 or GV3 chromatin configuration were compared with CC isolated from GV0 oocytes (CC_GV0 vs. CC_GV1; CC_GV0 vs. CC_GV2; CC_GV0 vs. CC_GV3). Thus the reference group in the contrast is always represented by the CC_GV0 group. Overall, 12 hybridizations corresponding to the four biological replicates and three comparisons, were performed (Figure 1A). A total of 825 ng of each labeled sample (Cy3 and Cy5) were incubated in a solution containing 10X blocking agent and 25X fragmentation buffer in a volume of 55 μL at 60°C for 15 min and were put on ice immediately after. Then, 55 μl of 2X GEx Hybridization Buffer HI-RPM were added for a total volume of 110 μl. The hybridization mix (100 μl) was added onto the array and hybridization was performed at 60°C for 17 hours using an Agilent Hybridization chamber in a rotating oven. After washing and drying steps, the slides were scanned using the Tecan PowerScanner microarray scanner (Tecan Group Ltd, Männerdorf, Switzerland) and features were extracted using ArrayPro 6.4 Analyzer (Media Cybernetics, Bethesda, MD).

Microarray data analysis

Microarray data analysis was performed according to the EmbryoGENE pipeline. Intensities files were uploaded to ELMA software (EmbryoGENE LIMS Microarray Analysis, http://elma.embryogene.ca/), to run the quality control module.

To detect the presence or absence of the signal for each spot present on the slide, microarray datasets generated by ELMA were analyzed and an arbitrary cut-off corresponding to the mean intensity of the background level plus twice the Standard Deviation (SD) of the background was used. A Venn diagram was created using the online tool VENNY to show present and common probes between groups. Moreover, a between-group analysis (BGA) was performed to classify the samples according to their transcriptomic profiles (Culhane *et al.* , 2002).

To calculate the gene expression fold change for each contrast individually (CC_GV0 vs. CC_GV1; CC_GV0 vs. CC_GV2; CC_GV0 vs. CC_GV3) microarray datasets generated by ELMA were analyzed with the FlexArray microarray analysis software, Version 1.6.1 (Blazejczyk *et al.* , 2007). Briefly, raw data were subjected to a simple background subtraction, normalized within each array (Loess) and a Limma simple analysis was performed to obtain the fold change values. The reference group in the contrasts is represented by the CC_GV0 group.

In addition, datasets generated by ELMA were subjected to microarray analysis of variance (MAANOVA) that was conducted considering the four experimental groups and by using the CC_GV0 as reference group. Differences were considered statistically significant with a *P* value less than 0.05. After MANOVA analysis, probes were grouped in clusters according to their expression profile using the mFuzz Bioconductor package (Kumar and M, 2007).

Finally, the gene lists generated by our analysis were examined using Ingenuity Pathway Analysis (Ingenuity Systems, Mountain View, CA). All statistically significant genes (P-value <0.05) were uploaded to the application. The functional analysis identified the biological functions that were most significant to the molecules in the database.

cDNA preparation and quantitative RT-PCR

The validation of microarray results was performed by quantitative RT-PCR (qRT-PCR) using four independent biological replicates (each pool containing CC derived from 10 COC). For each sample, 1 ng of total RNA were reverse transcribed using the SuperScript First-Strand Synthesis for RT-PCR (Invitrogen - Thermo Fisher Scientific) with oligo-dT primers following the

manufacturer's recommendations. Primer sequences used for real time RT-PCR are provided in Supplemental Table 1. Primers were designed using the Primer3 online tool (http://primer3.ut.ee/) from sequences obtained using the UMD3.1 assembly of the bovine genome. Specificity of each primers pair was confirmed by electrophoresis analysis on a standard 2% agarose gel and sequencing analysis.

The PCR products were purified with the QIAquick PCR Purification kit (Qiagen), quantified using the Qbit 2.0 fluorometer and Qubit dsDNA HS Assay Kit (Invitrogen - Thermo Fisher Scientific). Serial dilutions of the PCR products (ranging from 2×10^{-4} to 2×10^{-8} ng/μL) were then used to create the standard curves for the evaluation of the amplification efficiencies. Quantitative real-time PCR was performed on an iQ5 (Bio-Rad) using SYBR incorporation. Each qPCR reaction, in a final volume of 20 μL, contained the cDNA corresponding to 1ng of RNA extracted, 0.1 μM of each primer and 1x SYBR mix (iTaq Universal SyBR Green Supermix, Bio-rad). The PCR conditions used for all genes were as follows: a denaturing step of 30 sec at 95°C, followed by 40 PCR cycles (95°C for 30 sec; 57°C for 1 min), a melting curve (55°C for 1 min and a step cycle starting at 55°C, up to 94,5°C). PCR specificity was confirmed by melting-curve analysis.

For each gene tested, four independent biological replicates were used. Analysis of gene expression stability over the four groups was performed using the GeNorm algorithm (Vandesompele *et al.*, 2002) through the Biogazelle's qBase+ software (Biogazelle, Zwijnaarde, Belgium). Beta actin (ACTB), glyceraldehyde-3-phosphate dehydrogenase (GAPDH) and hypoxanthine phosphoribosyl transferase 1 (HPRT1) were identified as the most stable genes among the different groups, with M-value <1.5, and thus used as reference genes. Complementary DNA quantification was performed with the iQ5 Optical System Software Version 2.0 (Bio-Rad) using the delta delta Ct method, where CC from GV0 was used as reference group.

Active caspase-positive cells analysis

Dispersed CC preparations (Luciano *et al.*, 2000) isolated from single oocytes with different chromatin configuration (CC_GV0, CC_GV1, CC_GV2 and CC_GV3) were collected as described above and processed through the CaspaTag™ Pan-Caspase In Situ Assay Kit (Merck Millipore, Billerica, MA, USA), a methodology based on Fluorochrome Inhibitors of Caspases (FLICA) to detect active caspase in cells undergoing apoptosis, following the manufacturer's specification sheet with slight modifications. Briefly, dispersed cumulus cells were plated in 4-well plate for 3 hours in TCM199 supplemented with 0.68 mM L-glutamine, 25 mM NaHCO$_3$, 0.2 mM

sodium pyruvate and 0.4% fatty acid free BSA at 38.5°C and 5% CO_2, to allow them to adhere to the plate. Subsequently, cells were cultured for one additional hour in the presence of a carboxyfluorescein-labeled inhibitor of caspases. After washings and fixation in 10% formaldehyde, cells were detached by gently pipetting and moved on a glass slide. When dried, cells were covered with the antifade medium Vecta Shield (Vector Laboratories, Burlingame, CA, USA) supplemented with 1 μg/ml 40,6-diamidino-2-phenylindole (DAPI) and analyzed under fluorescent microscopy (Nikon Eclipse E600). For each sample, 10/15 fields were randomly chosen and results were expressed as the number of active caspase-positive cells over the total number of cells observed.

Assessment of the relationship between COC features and oocyte chromatin configuration

In order to establish morphological criteria that would allow for the collection and /or selection of a population of COC enriched in one of the three GV chromatin configurations (GV1, GV2 or GV3), the relationship between the oocyte chromatin configuration and either 1) the size of the follicle from which the COC was isolated or 2) the morphology of the corresponding COC, were assessed.

With this aim, in a first set of experiments, follicle sizes were determined with a ruler by measuring their visible diameter on the surface of the ovary. COC were collected from 2-4 mm, 4-6 or >6 mm antral follicles. In the second set of experiments, COC were collected from 2-8 mm antral follicles. In any case, only COC suitable for standard IVP procedure were included in the study. After the first selection, COC were further divided in three groups on the basis of morphological characteristics previously described (Blondin and Sirard, 1995, Hazeleger *et al.* , 1995): Class 1, with homogeneous ooplasm and compact cumulus cells; Class 2, with minor granulation of the ooplasm with compact cumulus cells; Class 3, with highly granulated ooplasm and slight expansion of cumulus cells layers (Figure 6B) (Gordon, 2003, Stringfellow and Givens, 2010).

In both cases, COC were finally denuded, fixed in a methanol and Dulbecco's Phosphate-Buffered Saline (DPBS) solution (60:40), and stained with DAPI for the assessment of chromatin configuration under fluorescence microscopy as above described.

Glucose-6-phosphate dehydrogenase (G6PDH) activity determination by brilliant cresyl blue (BCB) staining

COC isolated from 2-8 mm antral follicles and selected as above described were separated into two groups based on the morphological criteria as Class 1 and Class 2/3 (Figure 6B). COC were then stained with BCB as previously described (Torner *et al.*, 2008), with slight modifications. Briefly, COC were incubated in 26 μM BCB diluted in DPBS with calcium and magnesium and supplemented with 0.4% of BSA for 90 min at 38.5 °C in humidified air atmosphere. After washing, CC were removed, and oocytes were examined under a stereomicroscope. Oocytes were classified as BCB negative (BCB-), when the oocyte showed a colourless cytoplasm, or BCB positive (BCB+) where oocytes showed different grades of blue/violet colour.

In-vitro pre-maturation (pre-IVM), IVM, IVF and embryo culture (IVC)

For in-vitro embryo production experiments, only COC from 2-8 mm middle antral follicles collected as above described were used. After isolation and selection, COC were divided based on the morphological criteria as Class 1, Class 2 and class 3 as above described. Groups of 20-30 COC belonging to Class 1, Class 2/3 or unsorted COC (a mix of Class1, Class 2 and Class 3, corresponding to the population of COC that is commonly used in standard IVP procedures) were subjected to standard IVP (IVM, IVF and IVC) with or without a pre-IVM culture step (Franciosi *et al.*, 2014). To avoid meiotic resumption before pre-IVM, COC were classified in HM199 supplemented with the non-selective PDE inhibitor 3-isobutyl-1-methyl-xanthine (IBMX) at the final concentration of 0.5 mM (Lodde *et al.*, 2013). Pre-IVM consisted of culture for 6 hours in M-199 added with 0.68 mM L-glutamine, 25 mM NaHCO$_3$, 0.4% BSA fatty acid free, 0.2 mM sodium pyruvate, 10^{-4} IU/ml of r-hFSH (Gonal-F, Serono, Rome, Italy) and 10 μM cilostamide in humidified air under 5% CO$_2$ at 38.5°C (Franciosi *et al.*, 2014).

For IVM, COC (immediately after collection or after 6h of pre-IVM) were cultured for 22 h in M-199 added with 0.68 mM L-glutamine, 25 mM NaHCO3, 0.4% BSA fatty acid free, 0.2 mM sodium pyruvate and 0.1 IU/ml of r-hFSH (Gonal-F, Merck Serono, Darmstadt, Germany) at 38.5°C in 5% CO$_2$ as described by Luciano et al. (Luciano *et al.*, 2005).

IVF and IVC were carried out as previously described (Luciano *et al.*, 2005). At the end of culture period (d+8), the blastocyst rate was assessed under a stereomicroscope. The embryos were then fixed in 60% methanol in DPBS and the cell nuclei were counted under a fluorescence microscope after staining with 0.5 mg/ml of propidium iodide (Luciano *et al.*, 2005).

Statistical analysis

Experiments were repeated at least three times. Data were analyzed by one-way ANOVA followed by Newman-Keuls Multiple Comparison test using Graph Pad Prism version 6.0h. Data are presented as mean ± SEM. P values <0.05 were considered statistically significant. For each experiment, the specific test used is indicated in the figure legend.

Results

Microarray results

To gain insights into transcriptomic profiles of CC associated to oocytes with different large-scale chromatin configurations, three microarray comparisons using the EmbryoGENE bovine microarray were performed. This microarray includes 42242 probes, of which 31138 represent reference genes, novel untranscribed regions, 3'-untranslated region variants and alternatively spliced exons (Robert *et al.*, 2011).

As shown in Figure 1A, the hybridizations were performed using a reference design, where the CC isolated GV1, GV2 or GV3 chromatin configuration where compared with CC from GV0 oocytes (CC_GV0 vs. CC_GV1; CC_GV0 vs. CC_GV2; CC_GV0 vs. CC_GV3; the reference group in the contrast is represented by the CC_GV0 group). Microarray data were deposited in the National Center for Biotechnology Information (NCBI)'s Gene Expression Omnibus (Edgar *et al.* , 2002), and are accessible through GEO series accession number GSE79886 (http://www.ncbi.nlm.nih.gov/geo/query/acc.cgi?acc=GSE79886).

Considering the threshold used to detect the presence/absence of the spots on the microarray slides, a total of 20155 probes were commonly expressed in all the four groups (Figure 1B), while 384, 1138, 949 and 827 were expressed only in CC_GV0, CC_GV1, CC_GV2 and CC_GV3 respectively. As shown in Figure 1C, the BGA revealed the global transcriptional differences among CC isolated from oocytes with different chromatin configurations. Considering the biological replicates (dots) within each group, the CC_GV0 and CC_GV1 groups displayed more variation (increased distance between the dots) compared to GV2 and GV3. Moreover, CC_GV0

and CC_GV3 groups were characterized by unique gene expression profiles, while some minimal overlapping existed between CC_GV1 and CC_GV2 groups.

The MAANOVA algorithm revealed that 5571 probes were significantly differentially expressed ($p<0.05$) between groups, of which 112, 127 and 204 presented a fold change difference more than ±2 in CC_GV0 vs. CC_GV1, CC_GV0 vs. CC_GV2 and CC_GV0 vs. CC_GV3 respectively (Table 1). Clustering analysis with the mFuzz Bioconductor package generated 16 clusters representing the main profiles of transcription modulation (Figure 2). Of the 5571 significantly differentially expressed probes, 25.49 % best fitted with cluster #6 profile (down regulation between CC_GV0 and CC_GV1 and relatively stable low levels in successive groups). Clusters #1 (constant decrease from CC_GV0 to CC_GV3), cluster #5 (constant increase from CC_GV0 to CC_GV3), cluster #9 (up regulation between CC_GV0 and CC_GV1 and relatively stable levels in successive groups) and cluster #12 (up regulation from CC_GV0 to CC_GV2 and relatively stable levels from CC_GV2 to CC_GV3) each included around 10% of the total probes, while the other clusters included low numbers of probes (Figure 2).

A subset of five genes was selected, according to their significant changes in the three comparisons after Flex Array analysis and their known biological functions, to validate the microarray results by qRT-PCR. The chosen genes were: Thrombospondine 1 (THBS1), Serpine 2, regulator of G-protein signaling 2 (RGS2), inhibin alpha (INHA) and solute carrier family 39, member 8 (SLC39A8, Supplemental Table 1). Overall, qRT-PCR results were consistent with the microarray data (Figure 3).

IPA-based functional analysis

Lists of genes that best fitted each of the main clusters (#1, #5, #6, #9 and #12) were submitted to IPA in order to identify the most relevant molecular and cellular functions associated to each cluster (Table 2). The genes included in cluster #1 were related to biological processes such as 'cell cycle' and 'cell death and survival', while genes included in cluster #5 were more related to molecular processes such as 'gene expression', 'RNA post transcriptional modification' and 'protein synthesis'. Interestingly, 'lipid metabolism' and 'small molecule biochemistry' were the most significant functions identified in clusters #6, #9 and #12.

Moreover, in order to gain insights into the molecular and cellular pathways that were likely affected in CC during oocyte chromatin compaction, gene lists obtained from each contrast

individually by Flexarray (CC_GV0 vs. CC_GV1; CC_GV0 vs. CC_GV2; CC_GV0 vs. CC_GV3) were uploaded to IPA and analyzed considering the fold change difference for each gene. Interestingly one of the main affected functions in each contrast was 'cell death and survival' (Table 3). Moreover, as shown in Figure 4, the number of apoptosis-related genes that were deregulated increased substantially from CC_GV0 vs. CC_GV1 to CC_GV0 vs. CC_GV3 contrasts. Importantly, IPA analysis revealed that apoptosis is predicted to be inhibited in CC_GV1 and CC_GV2, while it is activated in CC_GV3 (Figure 4, gene lists shown in Figure 4 are provided as Supplemental Table 2).

Active caspase-positive cells analysis

In order to validate the in-silico functional prediction (generated by IPA) that CC_GV3 are more prone to apoptosis, we analyzed the susceptibility of CC isolated from oocytes with different chromatin configuration to undergo apoptosis.

It has been shown that apoptotic cell death of granulosa cells is the molecular mechanism underlying follicle atresia (Jolly *et al.* , 1994). A previous study demonstrated that the dissociation of both mural granulosa cells and cumulus cells triggers apoptosis in both cell subsets (Luciano *et al.*, 2000). Therefore we used CC dissociation as a 'stress test' in order to assess whether chromatin compaction (from GV0 to GV3) was associated to an increased tendency of the oocyte's associated CC to undergo apoptosis. CC isolated from single oocytes with different chromatin configurations (CC_GV0, CC_GV1, CC_GV2 and CC_GV3) were isolated and in-vitro cultured for 3 h and then assayed for pan-caspase activity. As shown in Figure 5, the percentage of caspase positive cells was significantly lower in CC from GV0 oocytes, whereas it increased in CC from GV1 and GV2 oocytes, reaching the highest value in CC from GV3 oocytes, as predicted by IPA.

Relationship between COC features and oocyte chromatin configuration

The findings that CC isolated from oocytes with different chromatin configuration differ in their transcriptomic profiles and in their susceptibility to undergo apoptosis, lead us to hypothesis that COC isolated from middle antral follicles bearing oocytes with different chromatin configurations (GV1, GV2 or GV3) could respond differently to specific in-vitro cultural conditions.

To test this hypothesis, and considering that it is technically not possible to directly identify the chromatin configuration without DNA staining after CC removal, we first looked for possible morphological markers that could be related to the chromatin configuration of the corresponding oocyte, and that therefore could be used to isolate a population of COC from middle antral follicle enriched in one of the GV stages (GV1, GV2 or GV3). Precisely, we considered the possible relationship between chromatin configuration and 1) the size of the follicle and 2) the morphology of the COC, using morphological criteria commonly accepted by the scientific community and clearly recognizable under a stereomicroscope. These studies revealed a relationship between the oocyte chromatin configuration and the morphology of the COC but not with the size of the follicle from which they originate (Figure 6). In fact, oocytes with GV1, GV2 and GV3 chromatin configuration were equally distributed in follicle of 2-4, 4-6 and > 6 mm in diameter (Figure 6A). On the other hand, as shown in Figure 6B, when isolated and additionally sub-grouped into three classes based on their morphology (Blondin and Sirard, 1995), Class 1 COC (with homogeneous ooplasm and compact cumulus cells) was the only one in which oocytes with GV1 chromatin configuration could be found, while oocytes with GV1 chromatin configuration were almost absent in Class 2 and 3 COC (minor granulation of the ooplasm with compact cumulus cells, or highly granulated ooplasm and/or few outer layers cumulus cells showing expansion in Class 2 and 3 respectively),

Furthermore, BCB staining of Class 1, 2 and 3 COC indicated that Class 1 COC are in an earlier stage of differentiation when compared with Class 2 and 3 COC, giving additional (indirect) confirmation that chromatin compaction is associated with oocyte (and accompanying CC) differentiation. Indeed, as shown in Figure 6C, the percentage of BCB-negative oocytes was significantly higher in Class 1 than Class 2/3 COC (P<0.05).

Effect of pre-IVM treatment on oocyte developmental competence

Having established that Class 1 and Class 2/3 COC differ in the relative percentage of oocytes with different chromatin configuration, and that Class 1 was the only class enriched with GV1 oocytes, we tested the hypothesis that these classes respond differently to specific in-vitro cultural conditions.

As shown in Figure 7, when subjected to standard IVP procedures (within a regular IVM protocol), Class 1 COC showed a limited embryonic developmental competence (Figure 7). Indeed after 7 days of culture both the blastocyst rate and mean blastocyst cell number per embryo were

significantly lower in Class 1 COC when compared to the Class 2/3 groups ($p<0.05$). As expected, the group composed of the mix of Class 1, 2 and 3 COC, which correspond to the unsorted group of COC commonly used in IVP protocols, showed intermediate values between Class 1 and Class 2/3 COC. On the other hand, pre-IVM treatment increased significantly the developmental capability (blastocyst rate and mean blastocyst cell number per embryo) of Class 1 COC and had no effect on the mixed group, while it reduced the developmental competence of Class 2/3 COC.

Discussion

The present work provides the first comprehensive transcriptome analysis of bovine CC associated with oocytes with a specific large-scale chromatin configuration. This is particularly relevant as chromatin configuration is indicative of the state of oocyte differentiation in the antral follicle before dominance emergence in naturally cycling animals (Lodde *et al.*, 2007, Lodde *et al.*, 2008, Lodde *et al.*, 2009). Transcriptomic data analysis confirmed the hypothesis that features of the cumulus oophorus investment change along with oocyte chromatin compaction. Interestingly, results of the BGA analysis, that gives information on the overall transcriptomic profile of each biological sample, are in accordance with the global change in distribution of transcriptomic data obtained from oocytes with different chromatin configurations (compare Figure 1C of the present study and Figure 2 in Labrecque et al., 2015 (Labrecque *et al.*, 2015)). Collectively these data, and in particular the relative distance between each group, effectively confirms that global transcriptional differences exist among oocytes with different chromatin configurations as well as in their surrounding CC. Thus, the transcriptome of the whole cumulus-oocyte complex changes along with the increase in chromatin compaction.

According to our previous morphological and functional studies, the present clustering analysis of microarray data revealed that major changes in terms of CC transcripts differences occur during the GV0-to-GV1 transition (Figure 2). Indeed, the cluster profiles # 6 and 9 (down or up regulation between CC_GV0 and CC_GV1 and relatively stable low levels in successive groups) collect about 36% of the differentially expressed probes. Interestingly, in-silico functional analysis through IPA of the subsets of genes that best fitted with these two profiles, revealed a major change of CC transcripts involved in lipid metabolism during the GV0-to-GV1 transition. Recent works showed that the lipid content in CC reflect the quality of the female gamete (Auclair *et al.* , 2013, Montani *et al.* , 2012) both in human (Matorras *et al.* , 1998) and in bovine (Kim *et al.* , 2001). It has been also recently reported that CC are able to protect the oocyte by storing elevated levels of free fatty acids from follicular fluid (Aardema *et al.* , 2013). In addition, studies in mice revealed that oocytes are deficient in cholesterol production and require CC to provide products of the cholesterol biosynthesis pathway, and suggest that oocytes promote cholesterol biosynthesis in CC through oocyte derived paracrine factors, probably to compensate for their deficiency (Su *et al.* , 2008). Altogether these data sustain the general idea that defective lipid metabolism inside the COC may be in part responsible for the lower meiotic and developmental competence of the oocyte. In this view, we can speculate that CC acquire the "competence" of metabolizing lipids during the GV0-GV1 transition, which occurs during the early-to-middle stage of follicle development, and

that the inability of GV0 oocytes to mature and develop into an embryo might be, at least in part, from an inappropriate capacity of the surrounding CC to metabolize lipids. Nevertheless, this hypothesis remains to be confirmed experimentally.

Gene expression profiles in CC have attracted great interest in the last years. In fact, a small biopsy of the cumulus oophorus could be easily collected before IVM, without perturbing oocyte viability, and assayed for expression of genes used as markers to predict the corresponding oocyte's quality. With this view, the present study confirms several previously reported markers associated with poor or high embryonic developmental potential in cattle, such as GATM or MAN1A1 (Bunel *et al.* , 2015, Bunel *et al.* , 2014). Notably, a similar approach has been conducted in the primed mouse model by comparing the transcriptomic profiles of CC isolated from antral oocytes with a non-surrounded nucleolus configuration (NSN, less compacted chromatin) and surrounded nucleolus configuration (SN, more compacted chromatin) (Vigone *et al.* , 2013, Zuccotti *et al.* , 1995). Compared to the present study in the cow, Vigone et al found a relatively low number of differentially expressed genes with fold changes higher than 2. The difference of the animal model of course could explain this difference. Moreover, we cannot exclude that taking advantages of the gradual chromatin remodeling by considering two intermediate stages of compaction (GV1 and GV2) between the two extremes (GV0 and GV3) allowed the identification of a higher number of differentially expressed genes. It may be possible indeed that mouse oocytes with intermediated configurations (Bonnet-Garnier *et al.* , 2012, Bouniol-Baly *et al.* , 1999), which are generally grouped together with one of the two extremes may limit the capacity for revealing certain differences. On the other hand, we found correspondence with some of the genes identified by Vigone et al., such as Has2, which is up regulated in bovine CC_GV3 and mouse SN oocytes when compared to GV0 and NSN oocytes respectively. This sets the stage for further comparative studies between the mouse and the bovine models.

Importantly, besides the assessment and confirmation of genes with known function in the reproductive system, our analysis provides multiple new biomarkers that are potentially involved in oocyte competence acquisition. For example, our data indicate that SLC39A8 is one of the genes whose expression constantly increases in CC during the GV0-to-GV3 transition. SLC39A8, also known as ZIP8, encodes for a member of the SLC39 family of solute-carrier genes, which shows structural characteristics of zinc transporters (Wang *et al.* , 2012). Recently, it has been shown that the oocyte zinc content exerts important roles in oocyte function in mice, especially during meiotic maturation and fertilization (Bernhardt *et al.* , 2011, Bernhardt *et al.* , 2012, Kim *et al.* , 2011, Kim *et al.* , 2010, Kong *et al.* , 2012, Tian and Diaz, 2012). Moreover, Lisle et al. suggested that CC regulate the amount of free-Zinc in the oocyte during maturation (Lisle *et al.* , 2013). Interestingly,

findings in mice show that acute dietary zinc deficiency during preconception (i.e. restricted to 3-5 days before ovulation) disrupts oocyte chromatin methylation and alters transcriptional regulation of repetitive elements, which is associated with severe defects of pre- and post-implantation embryonic development as well as of placental development (Tian *et al.* , 2014, Tian and Diaz, 2013). This is important since the period in which the mice were fed with a zinc deficiency diet in these studies, corresponds to the final oocyte growth phase, when chromatin remodeling occurs (Albertini, 1992, Bonnet-Garnier *et al.*, 2012, Bouniol-Baly *et al.*, 1999, De La Fuente *et al.* , 2004, Debey *et al.* , 1993, Zuccotti *et al.*, 1995). These data clearly indicate that zinc plays important roles also before meiotic resumption and our data might set the stage for further investigation on the role of SLC39A8 as a possible player acting in the somatic compartment and involved in the control of oocyte zinc content, which is in turn important for the establishment of the oocyte epigenetic signature. Interestingly, in the mouse model the zinc transporter SLC39A10 was found to be up regulated in CC from SN oocytes, when compared to NSN oocytes (Vigone *et al.*, 2013).

Importantly, besides the identification of single gene's function, the present dataset gives the opportunity to find pathways and mechanisms that are set in place in the somatic compartment that ultimately affect oocyte quality. This has paramount implications in the development of oocyte culture systems specifically formulated to fulfill the specific needs of the oocyte at a specific stage and support their in vitro development. For example, in-silico analysis of differentially expressed genes in the three contrasts through IPA, revealed that apoptosis is predicted to be inhibited in CC of GV1 and of GV2 (even if at a lower extent) while it is predicted to be activated in CC of oocytes with the highest degree of chromatin compaction (GV3). Among the apoptosis-related genes identified by IPA, angiopoietin 2 (ANGPT2) was the most up regulated gene in CC_GV3 when compared to CC_GV0. ANGPT2 is an antagonist of the angiogenic factor ANGPT1 that signals through the endothelial cell–specific Tie2 receptor tyrosine kinase. ANGPT2 disrupts the vascular remodeling ability of ANGPT1 and may induce endothelial cell apoptosis (Maisonpierre *et al.* , 1997). In the cyclic ovary, ANGPT1, ANGPT2, Tie1 and Tie2, play important roles in the modulation of vascular growth and regression (Goede *et al.* , 1998, Hazzard *et al.* , 1999, Wulff *et al.* , 2001a, Wulff *et al.* , 2000, Wulff *et al.* , 2001b) and studies in cow revealed a function of this system in the remodeling of the vascular network specifically in the ovarian follicle (Hayashi *et al.* , 2003, Hayashi *et al.* , 2004). Strikingly, ANGPT2 was found to be up-regulated in early atretic follicles (Girard *et al.* , 2015, Hayashi *et al.*, 2003), thus supporting our finding that CC_GV3 are more prone to apoptosis.

These in-silico predictions are experimentally confirmed by the fact that the CC's susceptibility to apoptosis increases with oocyte's chromatin compaction. Moreover these data are

in agreement with previous findings indicating that functional gap-junction mediated communication between the oocyte and the surrounding CC is impaired in COC enclosing a GV3 oocyte and with signs of early cellular degeneration observed in GV3 oocytes at the ultrastructure level (Lodde *et al.*, 2007, Lodde *et al.*, 2008). On the other hand, the present findings support the general idea that COC enclosing a GV1 oocyte are in an earlier stage of oocyte differentiation. In fact, Class 1 COC, which was originally characterized as the one with no morphological signs of degeneration and lower developmental competence (Blondin and Sirard, 1995, Hazeleger *et al.*, 1995) and whose oocytes were found to be in an earlier stage of differentiation as assessed by BCB staining (present study), was the only class enriched in GV1 oocytes.

On the basis of our findings, we designed a tailored culture system, which confirmed that the success of in-vitro cultural strategies aimed at improving oocyte developmental capability is 'stage dependent', i.e. mainly due to the characteristic of the COC that are subjected to the procedure. Indeed we demonstrated that standard IVM conditions are inappropriate to support pre-implantation embryonic development of GV1 enriched Class 1 COC, while their developmental competence is positively affected by a 6 h period of inhibition of meiotic resumption through cAMP modulators. On the contrary, the same treatment negatively affected Class 1 and 2 COC developmental competence, which is consistent with the findings that these classes only contain GV2 and GV3 oocytes. This in turn confirms earlier studies in which prolonged Pre-IVM (24h) increased GV0 meiotic and developmental competencies (Luciano *et al.*, 2011). These data are consistent with one of the concepts beyond pre-maturation strategies (Franciosi *et al.*, 2014, Gilchrist, 2011, Gilchrist *et al.* , 2016, Sirard, 2011, Smitz *et al.*, 2011) i.e. the prolongation of GJ-mediated communication between the somatic and germinal compartments is expected to be more effective in COC with a functional oocyte-CC coupling (as in GV0 and GV1 (Lodde *et al.*, 2007)).

An important finding of the present work is that, in naturally cycling animals, COC selection based on follicle size does not allow isolation of a homogeneous population in terms of chromatin configuration. This implies that at each follicular wave, GV1-to-GV2 transition, which marks the acquisition of a high embryonic developmental potential, occurs at almost any size as the growth of the follicle slows down before dominant follicle emergence and concomitantly with decline in the FSH level (Adams *et al.*, 2008, Forde *et al.* , 2011). After the highest FSH level is attained in the preovulatory peak, the atretic events would start and GV2-to-GV3 transition eventually occurs. The timing of such a sequence would fit the preparation of the oocyte for ovulation or atresia, which requires chromatin compaction in both cases. This further confirms a previously postulated hypothesis that "GV3 oocytes represent that proportion of gametes, which have reached a high developmental capability during follicular growth, and that, at the time of collection, were

undergoing early events of atresia" (Lodde et al., 2007, Lodde et al., 2008). These concepts are summarized in a tentative model illustrated in Figure 8 which relates well with an average competence of 33% and early atresia improving developmental potential (Blondin and Sirard, 1995). If each follicle would contain a GV2 stage oocyte at its plateau phase and such status would be permissive for further development, it would explain the extraordinary stable blastocyst rate observed with bovine IVM since 1995. The growing follicles would be mainly GV1, the plateau phase would be (low FSH) GV2 and the early atretic would be GV3 with respectively low, high and medium developmental competence.

In conclusion, our data support the idea that the synchrony between nuclear, cytoplasmic and molecular events is finely tuned during the final phase of oocyte growth. Our results also demonstrate the necessity of a deep knowledge of the biological process occurring in cumulus cells during the final growth of the oocyte for the refinement of customized culture systems, which should consider the metabolic requirements of the heterogeneous population of oocytes that are submitted to IVM. This is mandatory to significantly improve assisted reproductive technologies. Very recently a high similarity in the process of chromatin remodeling occurring in bovine and human immature oocytes, that reflects a high cellular and molecular heterogeneity in human oocytes, have been reported (Sanchez *et al.*, 2015). Thus the present work may have important consequences for human IVM in which the results are still suboptimal compared to conventional IVF (Coticchio *et al.* , 2012). In addition to avoiding the primary adverse effects caused by ovarian stimulation, further improvements in IVM effectiveness and efficiency may help broaden the use of IVM for fertility preservation and in infertile patients.

Authors' Roles

All authors contributed substantially to this manuscript. AML, VL and MAS designed the study; CD, VL, RL, ID, IT and AML executed experiments; CD, RL, VL, AML and MAS analyzed the data; VL, CD and AML wrote the manuscript. All authors revised and approved the final manuscript.

Conflict of Interest

None declared.

Reference List

Aardema H, Lolicato F, van de Lest CH, Brouwers JF, Vaandrager AB, van Tol HT, Roelen BA, Vos PL, Helms JB, Gadella BM. Bovine cumulus cells protect maturing oocytes from increased fatty acid levels by massive intracellular lipid storage. *Biol Reprod* 2013;**88**: 164.

Adams GP, Jaiswal R, Singh J, Malhi P. Progress in understanding ovarian follicular dynamics in cattle. *Theriogenology* 2008;**69**: 72-80.

Albertini DF. Cytoplasmic microtubular dynamics and chromatin organization during mammalian oogenesis and oocyte maturation. *Mutat Res* 1992;**296**: 57-68.

Auclair S, Uzbekov R, Elis S, Sanchez L, Kireev I, Lardic L, Dalbies-Tran R, Uzbekova S. Absence of cumulus cells during in vitro maturation affects lipid metabolism in bovine oocytes. *Am J Physiol Endocrinol Metab* 2013;**304**: E599-613.

Bernhardt ML, Kim AM, O'Halloran TV, Woodruff TK. Zinc requirement during meiosis I-meiosis II transition in mouse oocytes is independent of the MOS-MAPK pathway. *Biol Reprod* 2011;**84**: 526-536.

Bernhardt ML, Kong BY, Kim AM, O'Halloran TV, Woodruff TK. A zinc-dependent mechanism regulates meiotic progression in mammalian oocytes. *Biol Reprod* 2012;**86**: 114.

Blazejczyk M, Miron M, Nadon R. FlexArray: A statistical data analysis software for gene expression microarrays. *Genome Quebec, Montreal, Canada* 2007.

Blondin P, Bousquet D, Twagiramungu H, Barnes F, Sirard MA. Manipulation of follicular development to produce developmentally competent bovine oocytes. *Biol Reprod* 2002;**66**: 38-43.

Blondin P, Sirard MA. Oocyte and follicular morphology as determining characteristics for developmental competence in bovine oocytes. *Mol Reprod Dev* 1995;**41**: 54-62.

Bonnet-Garnier A, Feuerstein P, Chebrout M, Fleurot R, Jan HU, Debey P, Beaujean N. Genome organization and epigenetic marks in mouse germinal vesicle oocytes. *Int J Dev Biol* 2012;**56**: 877-887.

Bouniol-Baly C, Hamraoui L, Guibert J, Beaujean N, Szollosi MS, Debey P. Differential transcriptional activity associated with chromatin configuration in fully grown mouse germinal vesicle oocytes. *Biol Reprod* 1999;**60**: 580-587.

Bunel A, Jorssen EP, Merckx E, Leroy JL, Bols PE, Sirard MA. Individual bovine in vitro embryo production and cumulus cell transcriptomic analysis to distinguish cumulus-oocyte complexes with high or low developmental potential. *Theriogenology* 2015;**83**: 228-237.

Bunel A, Nivet AL, Blondin P, Vigneault C, Richard FJ, Sirard MA. Cumulus cell gene expression associated with pre-ovulatory acquisition of developmental competence in bovine oocytes. *Reprod Fertil Dev* 2014;**26**: 855-865.

Coticchio G, Dal Canto M, Mignini Renzini M, Guglielmo MC, Brambillasca F, Turchi D, Novara PV, Fadini R. Oocyte maturation: gamete-somatic cells interactions, meiotic resumption, cytoskeletal dynamics and cytoplasmic reorganization. *Hum Reprod Update* 2015;**21**: 427-454.

Coticchio G, Dal-Canto M, Guglielmo MC, Mignini-Renzini M, Fadini R. Human oocyte maturation in vitro. *Int J Dev Biol* 2012;**56**: 909-918.

Culhane AC, Perriere G, Considine EC, Cotter TG, Higgins DG. Between-group analysis of microarray data. *Bioinformatics* 2002;**18**: 1600-1608.

De La Fuente R. Chromatin modifications in the germinal vesicle (GV) of mammalian oocytes. *Dev Biol* 2006;**292**: 1-12.

De La Fuente R, Eppig JJ. Transcriptional activity of the mouse oocyte genome: companion granulosa cells modulate transcription and chromatin remodeling. *Dev Biol* 2001;**229**: 224-236.

De La Fuente R, Viveiros MM, Burns KH, Adashi EY, Matzuk MM, Eppig JJ. Major chromatin remodeling in the germinal vesicle (GV) of mammalian oocytes is dispensable for global transcriptional silencing but required for centromeric heterochromatin function. *Dev Biol* 2004;**275**: 447-458.

Debey P, Szollosi MS, Szollosi D, Vautier D, Girousse A, Besombes D. Competent mouse oocytes isolated from antral follicles exhibit different chromatin organization and follow different maturation dynamics. *Mol Reprod Dev* 1993;**36**: 59-74.

Edgar R, Domrachev M, Lash AE. Gene Expression Omnibus: NCBI gene expression and hybridization array data repository. *Nucleic Acids Res* 2002;**30**: 207-210.

Eppig JJ. Oocyte control of ovarian follicular development and function in mammals. *Reproduction* 2001;**122**: 829-838.

Eppig JJ, Schultz RM, O'Brien M, Chesnel F. Relationship between the developmental programs controlling nuclear and cytoplasmic maturation of mouse oocytes. *Dev Biol* 1994;**164**: 1-9.

Forde N, Beltman ME, Lonergan P, Diskin M, Roche JF, Crowe MA. Oestrous cycles in Bos taurus cattle. *Anim Reprod Sci* 2011;**124**: 163-169.

Franciosi F, Coticchio G, Lodde V, Tessaro I, Modina SC, Fadini R, Dal Canto M, Renzini MM, Albertini DF, Luciano AM. Natriuretic peptide precursor C delays meiotic resumption and sustains gap junction-mediated communication in bovine cumulus-enclosed oocytes. *Biol Reprod* 2014;**91**: 61.

Gilbert I, Scantland S, Dufort I, Gordynska O, Labbe A, Sirard MA, Robert C. Real-time monitoring of aRNA production during T7 amplification to prevent the loss of sample representation during microarray hybridization sample preparation. *Nucleic Acids Res* 2009;**37**: e65.

Gilbert I, Scantland S, Sylvestre EL, Dufort I, Sirard MA, Robert C. Providing a stable methodological basis for comparing transcript abundance of developing embryos using microarrays. *Mol Hum Reprod* 2010;**16**: 601-616.

Gilchrist RB. Recent insights into oocyte-follicle cell interactions provide opportunities for the development of new approaches to in vitro maturation. *Reprod Fertil Dev* 2011;**23**: 23-31.

Gilchrist RB, Lane M, Thompson JG. Oocyte-secreted factors: regulators of cumulus cell function and oocyte quality. *Hum Reprod Update* 2008;**14**: 159-177.

Gilchrist RB, Luciano AM, Richani D, Zeng HT, Wang X, Sugimura S, Smitz J, Richard FJ, Thompson JG. Oocyte maturation and quality: role of cyclic nucleotides. *Reproduction* 2016;**doi:** http://dx.doi.org/10.1530/REP-15-0606.

Girard A, Dufort I, Douville G, Sirard MA. Global gene expression in granulosa cells of growing, plateau and atretic dominant follicles in cattle. *Reprod Biol Endocrinol* 2015;**13**: 17.

Goede V, Schmidt T, Kimmina S, Kozian D, Augustin HG. Analysis of blood vessel maturation processes during cyclic ovarian angiogenesis. *Lab Invest* 1998;**78**: 1385-1394.

Gordon I. *Laboratory production of cattle embryos, 2nd Ed.*, 2003. CABI Publishing, Cambridge MA (USA).

Gougeon A. Dynamics of follicular growth in the human: a model from preliminary results. *Hum Reprod* 1986;**1**: 81-87.

Gougeon A. Regulation of ovarian follicular development in primates: facts and hypotheses. *Endocr Rev* 1996;**17**: 121-155.

Hayashi KG, Acosta TJ, Tetsuka M, Berisha B, Matsui M, Schams D, Ohtani M, Miyamoto A. Involvement of angiopoietin-tie system in bovine follicular development and atresia: messenger RNA expression in theca interna and effect on steroid secretion. *Biol Reprod* 2003;**69**: 2078-2084.

Hayashi KG, Berisha B, Matsui M, Schams D, Miyamoto A. Expression of mRNA for the angiopoietin-tie system in granulosa cells during follicular development in cows. *J Reprod Dev* 2004;**50**: 477-480.

Hazeleger NL, Hill DJ, Stubbing RB, Walton JS. Relationship of morphology and follicular fluid environment of bovine oocytes to their developmental potential in vitro. *Theriogenology* 1995;**43**: 509-522.

Hazzard TM, Molskness TA, Chaffin CL, Stouffer RL. Vascular endothelial growth factor (VEGF) and angiopoietin regulation by gonadotrophin and steroids in macaque granulosa cells during the peri-ovulatory interval. *Mol Hum Reprod* 1999;**5**: 1115-1121.

Hyttel P, Fair T, Callesen H, Greve T. Oocyte growth, capacitation and final maturation in cattle. *Theriogenology* 1997;**47**: 23-32.

Jolly PD, Tisdall DJ, Heath DA, Lun S, McNatty KP. Apoptosis in bovine granulosa cells in relation to steroid synthesis, cyclic adenosine 3',5'-monophosphate response to follicle-stimulating hormone and luteinizing hormone, and follicular atresia. *Biol Reprod* 1994;**51**: 934-944.

Kim AM, Bernhardt ML, Kong BY, Ahn RW, Vogt S, Woodruff TK, O'Halloran TV. Zinc sparks are triggered by fertilization and facilitate cell cycle resumption in mammalian eggs. *ACS Chem Biol* 2011;**6**: 716-723.

Kim AM, Vogt S, O'Halloran TV, Woodruff TK. Zinc availability regulates exit from meiosis in maturing mammalian oocytes. *Nat Chem Biol* 2010;**6**: 674-681.

Kim JY, Kinoshita M, Ohnishi M, Fukui Y. Lipid and fatty acid analysis of fresh and frozen-thawed immature and in vitro matured bovine oocytes. *Reproduction* 2001;**122**: 131-138.

Kong BY, Bernhardt ML, Kim AM, O'Halloran TV, Woodruff TK. Zinc maintains prophase I arrest in mouse oocytes through regulation of the MOS-MAPK pathway. *Biol Reprod* 2012;**87**: 11, 11-12.

Kumar L, M EF. Mfuzz: a software package for soft clustering of microarray data. *Bioinformation* 2007;**2**: 5-7.

Labrecque R, Lodde V, Dieci C, Tessaro I, Luciano AM, Sirard MA. Chromatin remodelling and histone mRNA accumulation in bovine germinal vesicle oocytes. *Mol Reprod Dev* 2015;**82**: 450-462.

Landry DA, Bellefleur AM, Labrecque R, Grand FX, Vigneault C, Blondin P, Sirard MA. Effect of cow age on the in vitro developmental competence of oocytes obtained following FSH stimulation/coasting treatments. *Theriogenology* 2016.

Lisle RS, Anthony K, Randall MA, Diaz FJ. Oocyte-cumulus cell interactions regulate free intracellular zinc in mouse oocytes. *Reproduction* 2013;**145**: 381-390.

Lodde V, Franciosi F, Tessaro I, Modina SC, Luciano AM. Role of gap junction-mediated communications in regulating large-scale chromatin configuration remodeling and embryonic developmental competence acquisition in fully grown bovine oocyte. *J Assist Reprod Genet* 2013;**30**: 1219-1226.

Lodde V, Modina S, Galbusera C, Franciosi F, Luciano AM. Large-scale chromatin remodeling in germinal vesicle bovine oocytes: interplay with gap junction functionality and developmental competence. *Mol Reprod Dev* 2007;**74**: 740-749.

Lodde V, Modina S, Maddox-Hyttel P, Franciosi F, Lauria A, Luciano AM. Oocyte morphology and transcriptional silencing in relation to chromatin remodeling during the final phases of bovine oocyte growth. *Mol Reprod Dev* 2008;**75**: 915-924.

Lodde V, Modina SC, Franciosi F, Zuccari E, Tessaro I, Luciano AM. Localization of DNA methyltransferase-1 during oocyte differentiation, in vitro maturation and early embryonic development in cow. *Eur J Histochem* 2009;**53**: e24.

Lonergan P, Fair T. In vitro-produced bovine embryos: dealing with the warts. *Theriogenology* 2008;**69**: 17-22.

Luciano AM, Franciosi F, Dieci C, Lodde V. Changes in large-scale chromatin structure and function during oogenesis: a journey in company with follicular cells. *Anim Reprod Sci* 2014;**149**: 3-10.

Luciano AM, Franciosi F, Modina SC, Lodde V. Gap junction-mediated communications regulate chromatin remodeling during bovine oocyte growth and differentiation through cAMP-dependent mechanism(s). *Biol Reprod* 2011;**85**: 1252-1259.

Luciano AM, Lodde V. Changes of Large-Scale Chromatin Configuration During Mammalian Oocyte Differentiation. In Coticchio G, Albertini DF, De Santis L (eds) Oogenesis. 2013. Springer London, pp. 93-108.

Luciano AM, Lodde V, Beretta MS, Colleoni S, Lauria A, Modina S. Developmental capability of denuded bovine oocyte in a co-culture system with intact cumulus-oocyte complexes: role of cumulus cells, cyclic adenosine 3',5'-monophosphate, and glutathione. *Mol Reprod Dev* 2005;**71**: 389-397.

Luciano AM, Modina S, Gandolfi F, Lauria A, Armstrong DT. Effect of cell-to-cell contact on in vitro deoxyribonucleic acid synthesis and apoptosis responses of bovine granulosa cells to insulin-like growth factor-I and epidermal growth factor. *Biol Reprod* 2000;**63**: 1580-1585.

Lussier JG, Matton P, Dufour JJ. Growth rates of follicles in the ovary of the cow. *J Reprod Fertil* 1987;**81**: 301-307.

Maisonpierre PC, Suri C, Jones PF, Bartunkova S, Wiegand SJ, Radziejewski C, Compton D, McClain J, Aldrich TH, Papadopoulos N et al. Angiopoietin-2, a natural antagonist for Tie2 that disrupts in vivo angiogenesis. *Science* 1997;**277**: 55-60.

Matorras R, Ruiz JI, Mendoza R, Ruiz N, Sanjurjo P, Rodriguez-Escudero FJ. Fatty acid composition of fertilization-failed human oocytes. *Hum Reprod* 1998;**13**: 2227-2230.

Matzuk MM, Burns KH, Viveiros MM, Eppig JJ. Intercellular communication in the mammalian ovary: oocytes carry the conversation. *Science* 2002;**296**: 2178-2180.

Merton JS, de Roos AP, Mullaart E, de Ruigh L, Kaal L, Vos PL, Dieleman SJ. Factors affecting oocyte quality and quantity in commercial application of embryo technologies in the cattle breeding industry. *Theriogenology* 2003;**59**: 651-674.

Monniaux D, Clement F, Dalbies-Tran R, Estienne A, Fabre S, Mansanet C, Monget P. The ovarian reserve of primordial follicles and the dynamic reserve of antral growing follicles: what is the link? *Biol Reprod* 2014;**90**: 85.

Montani DA, Cordeiro FB, Regiani T, Victorino AB, Pilau EJ, Gozzo FC, Ferreira CR, Fraietta R, Lo Turco EG. The follicular microenviroment as a predictor of pregnancy: MALDI-TOF MS lipid profile in cumulus cells. *J Assist Reprod Genet* 2012;**29**: 1289-1297.

Nivet AL, Bunel A, Labrecque R, Belanger J, Vigneault C, Blondin P, Sirard MA. FSH withdrawal improves developmental competence of oocytes in the bovine model. *Reproduction* 2012;**143**: 165-171.

Pavlok A, Lucas-Hahn A, Niemann H. Fertilization and developmental competence of bovine oocytes derived from different categories of antral follicles. *Mol Reprod Dev* 1992;**31**: 63-67.

Robert C, Nieminen J, Dufort I, Gagne D, Grant JR, Cagnone G, Plourde D, Nivet AL, Fournier E, Paquet E et al. Combining resources to obtain a comprehensive survey of the bovine embryo transcriptome through deep sequencing and microarrays. *Mol Reprod Dev* 2011;**78**: 651-664.

Sanchez F, Romero S, De Vos M, Verheyen G, Smitz J. Human cumulus-enclosed germinal vesicle oocytes from early antral follicles reveal heterogeneous cellular and molecular features associated with in vitro maturation capacity. *Hum Reprod* 2015;**30**: 1396-1409.

Sirard MA. Follicle environment and quality of in vitro matured oocytes. *J Assist Reprod Genet* 2011;**28**: 483-488.

Smitz JE, Thompson JG, Gilchrist RB. The promise of in vitro maturation in assisted reproduction and fertility preservation. *Semin Reprod Med* 2011;**29**: 24-37.

Stringfellow D, A., Givens MD. *Manual of the International Embryo Transfer Society: a procedural guide and general information for the use of embryo transfer technology emphasizing sanitary procedures, 4th Ed.*, 2010. Savoy, IL (USA).

Su YQ, Sugiura K, Wigglesworth K, O'Brien MJ, Affourtit JP, Pangas SA, Matzuk MM, Eppig JJ. Oocyte regulation of metabolic cooperativity between mouse cumulus cells and oocytes: BMP15 and GDF9 control cholesterol biosynthesis in cumulus cells. *Development* 2008;**135**: 111-121.

Tian X, Anthony K, Neuberger T, Diaz FJ. Preconception zinc deficiency disrupts postimplantation fetal and placental development in mice. *Biol Reprod* 2014;**90**: 83.

Tian X, Diaz FJ. Zinc depletion causes multiple defects in ovarian function during the periovulatory period in mice. *Endocrinology* 2012;**153**: 873-886.

Tian X, Diaz FJ. Acute dietary zinc deficiency before conception compromises oocyte epigenetic programming and disrupts embryonic development. *Dev Biol* 2013;**376**: 51-61.

Torner H, Ghanem N, Ambros C, Holker M, Tomek W, Phatsara C, Alm H, Sirard MA, Kanitz W, Schellander K et al. Molecular and subcellular characterisation of oocytes screened for their developmental competence based on glucose-6-phosphate dehydrogenase activity. *Reproduction* 2008;**135**: 197-212.

Vandesompele J, De Preter K, Pattyn F, Poppe B, Van Roy N, De Paepe A, Speleman F. Accurate normalization of real-time quantitative RT-PCR data by geometric averaging of multiple internal control genes. *Genome Biol* 2002;**3**: RESEARCH0034.

Vassena R, Mapletoft RJ, Allodi S, Singh J, Adams GP. Morphology and developmental competence of bovine oocytes relative to follicular status. *Theriogenology* 2003;**60**: 923-932.

Vigone G, Merico V, Prigione A, Mulas F, Sacchi L, Gabetta M, Bellazzi R, Redi CA, Mazzini G, Adjaye J et al. Transcriptome based identification of mouse cumulus cell markers that predict the developmental competence of their enclosed antral oocytes. *BMC Genomics* 2013;**14**: 380.

Wang CY, Jenkitkasemwong S, Duarte S, Sparkman BK, Shawki A, Mackenzie B, Knutson MD. ZIP8 is an iron and zinc transporter whose cell-surface expression is up-regulated by cellular iron loading. *J Biol Chem* 2012;**287**: 34032-34043.

Wulff C, Wiegand SJ, Saunders PT, Scobie GA, Fraser HM. Angiogenesis during follicular development in the primate and its inhibition by treatment with truncated Flt-1-Fc (vascular endothelial growth factor Trap(A40)). *Endocrinology* 2001a;**142**: 3244-3254.

Wulff C, Wilson H, Largue P, Duncan WC, Armstrong DG, Fraser HM. Angiogenesis in the human corpus luteum: localization and changes in angiopoietins, tie-2, and vascular endothelial growth factor messenger ribonucleic acid. *J Clin Endocrinol Metab* 2000;**85**: 4302-4309.

Wulff C, Wilson H, Rudge JS, Wiegand SJ, Lunn SF, Fraser HM. Luteal angiogenesis: prevention and intervention by treatment with vascular endothelial growth factor trap(A40). *J Clin Endocrinol Metab* 2001b;**86**: 3377-3386.

Zuccotti M, Garagna S, Merico V, Monti M, Alberto Redi C. Chromatin organisation and nuclear architecture in growing mouse oocytes. *Mol Cell Endocrinol* 2005;**234**: 11-17.

Zuccotti M, Piccinelli A, Giorgi Rossi P, Garagna S, Redi CA. Chromatin organization during mouse oocyte growth. *Mol Reprod Dev* 1995;**41**: 479-485.
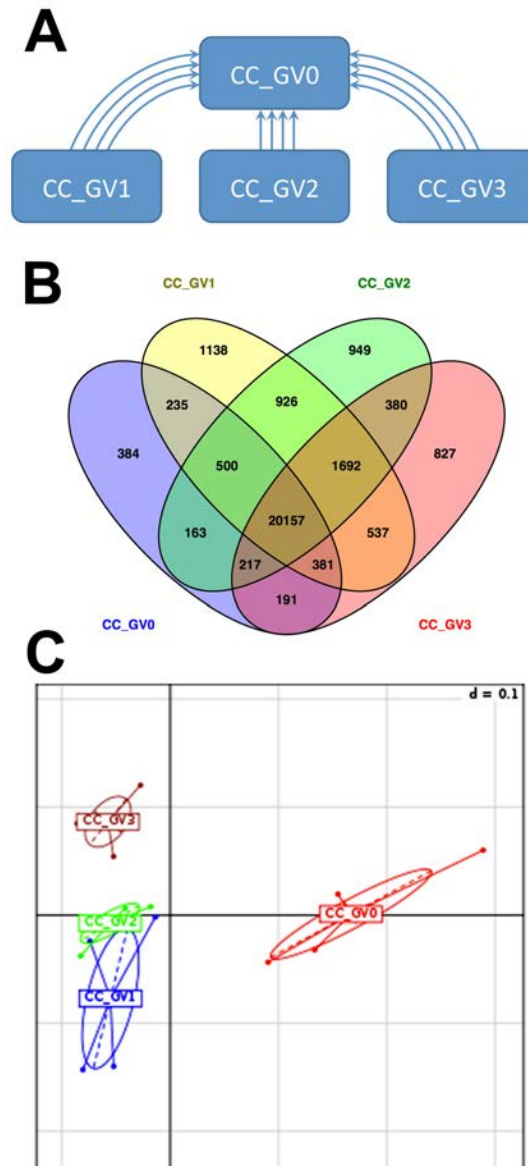
Figure 1: Microarray analysis of cumulus cells isolated from oocytes with different large-scale chromatin configuration.

A: Experimental design. Cumulus cells (CC) associated with oocytes with GV0, GV1, GV2 and GV3 chromatin configuration were isolated and subjected to microarray analysis. The hybridizations were performed using a reference design, where cumulus cells isolated from oocytes with GV1, GV2 and GV3 chromatin configuration where compared with CC isolated from GV0 oocytes (CC_GV0 vs. CC_GV1; CC_GV0 vs. CC_GV2; CC_GV0 vs. CC_GV3). In each contrast, the CC_GV0 group represents the reference group. Overall, twelve hybridizations corresponding to the four biological replicates and three comparisons were performed.

B: Venn's diagram showing commonly expressed probes in the four experimental groups. Diagram was generated using the online tool VENNY 2.0 (*Oliveros, J.C. (2007-2015) Venny. An interactive tool for comparing lists with Venn's diagrams.* http://bioinfogp.cnb.csic.es/tools/venny/index.html), in which the lists of expressed probes in each group were uploaded.

C: Between group analysis (BGA) of the cumulus cells microarray data, in which the samples are classified according to their transcriptomic profile (Culhane *et al.*, 2002) using the online tool available within the EmbryoGENE LIMS and Microarray Analysis (ELMA) pipeline. The plot illustrates the global distribution of transcriptome data (expressed probes) from the four experimental groups (cumulus cells from GV0, GV1, GV2 or GV3 oocytes) and the four biological replicates (dots in each group). The relative distance between each group indicates the global transcriptional differences among cumulus cells isolated from oocytes with different chromatin configurations.
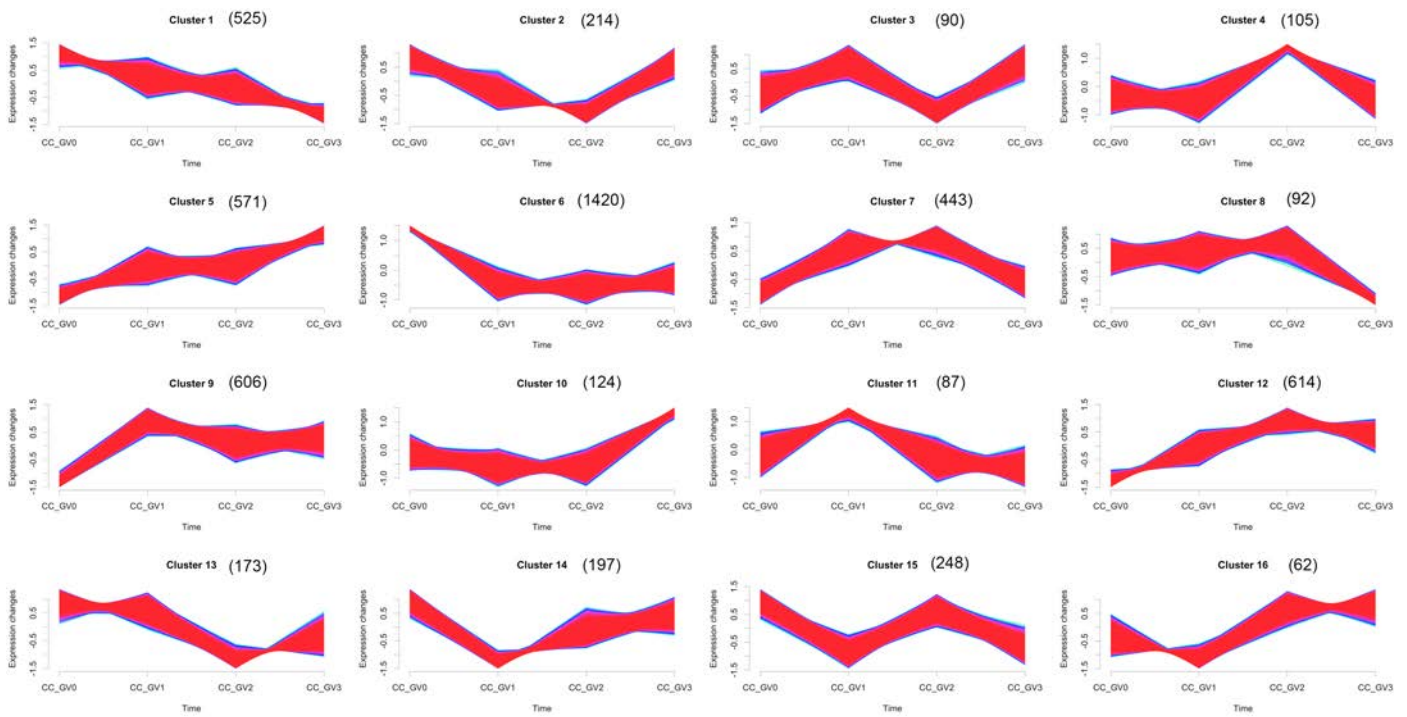
Figure 2: Clusters analysis.

Graphs represent the 16 clusters generated by the mFuzz clustering analysis (Kumar and M, 2007). For each cluster the number of statistically significant probes that best fit to each profile is indicated between brackets. Note: cluster #6 is the one with the higher number of best fit probes.
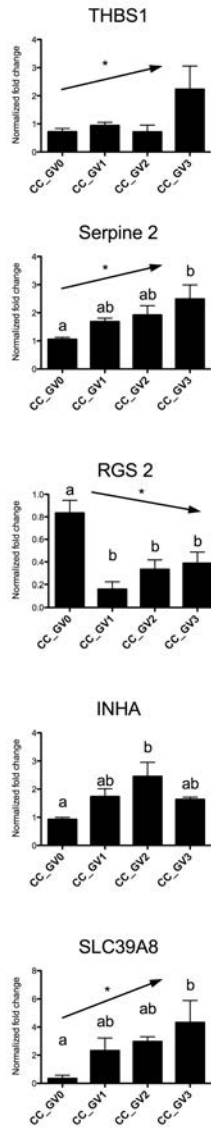
Figure 3: Quantitative reverse-transcriptase-PCR (qRT-PCR) validation of the microarray results.

Validation of microarray data by means of qRT-PCR. Graphs indicate relative expression levels of selected genes in cumulus cells isolated from oocytes with GV0, GV1, GV2 or GV3 chromatin configuration; expression levels for each gene were normalized using ACTB, GAPDH and HPRT1 as reference genes. Relative fold changes were calculated using the delta-delta Ct method using CC_GV0 as reference group. Data were analyzed by one-way ANOVA followed by Newman-Keuls multiple comparison test and are expressed as means ± SEM. Different superscripts indicate significant differences between groups ($p < 0.05$). Where applicable, test for linear trend was also conducted (*, $p < 00.5$)

Note: the selected genes, with accession number, primer sequences, annealing temperature and product size are as in Supplemental Table 1.
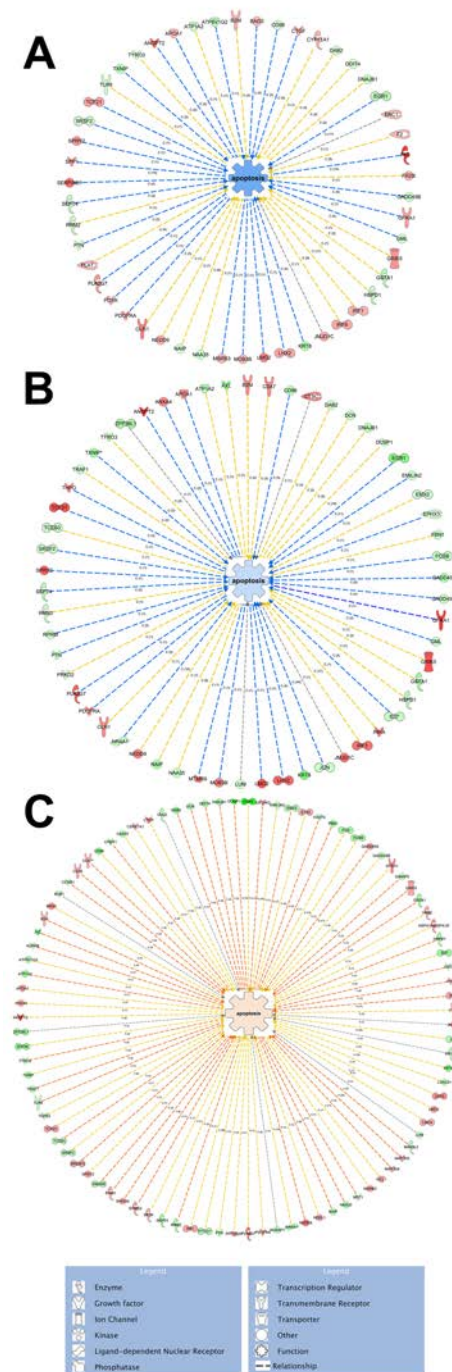
Figure 4: Functional analysis

IPA generated diagrams representing deregulated apoptosis-related genes (p<0.05; fold change higher than ±2) in CC_GV0 vs. CC_GV1 (A), CC_GV0 vs. CC_GV2 (B) and CC_GV0 vs.

CC_GV3. Note that apoptosis is predicted to be inhibited (blue) in CC_GV1 and CC_GV2, while it is activated (orange) in CC_GV3. Gene lists are provided in Supplemental Table 2; genes in red are up-regulated; genes in green are down-regulated.
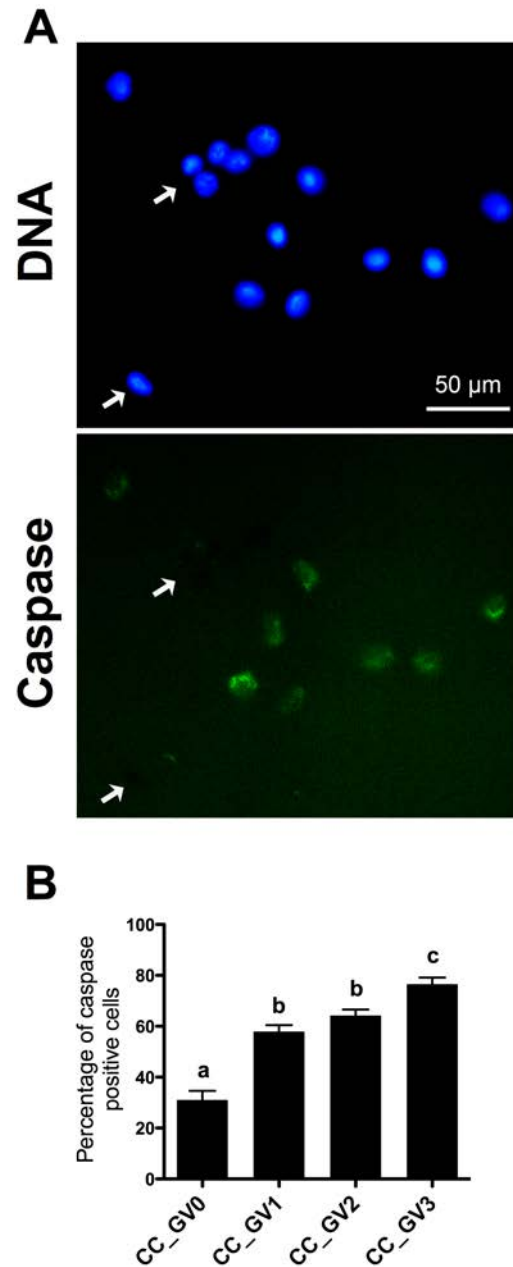
Figure 5: Assessment of caspase activity in cells isolated from oocytes with different chromatin configuration

CC associated to oocytes with GV0, GV1, GV2 and GV3 chromatin configuration were isolated and assayed for Caspase activity after 3 h of culture using the CaspaTag™ Pan-Caspase In Situ Assay Kit. **A)** Representative pictures show active caspase in cells undergoing apoptosis and

negative (arrows) cells. **B)** Graph shows the percentage of caspase-active cells in each GV category; data from three independent experiments were analyzed by one-way ANOVA followed by Newman-Keuls multiple comparison test; data are expressed as means ± SEM; a,b,c: different superscripts indicate significant differences between groups ($p < 0.05$).

Figure 6: Relationship between large-scale chromatin configuration, follicle size, COC morphology and oocyte glucose-6-phosphate dehydrogenase (G6PDH) activity

A) COC were collected from follicles of different diameter and chromatin configuration were assessed after cumulus cells removal. Graphs show the frequency of GV1, GV2 and GV3 chromatin configurations in each follicle size category. A total of 277 oocytes (167, 52 and 52 from small, medium and large antral follicle respectively), were used in this study in three independent experiments. Data were analyzed by one-way ANOVA. **B)** After collection, COC were separated according to morphological criteria as shown in the representative pictures (Class 1: homogeneous ooplasm and absence of expansion of outer layer cumulus cells; Class 2: minor granulation of the ooplasm and/or beginning of expansion of outer layer cumulus cells; Class 3: highly granulated ooplasm and few cumulus cells layers showing expansion). After classification, cumulus cells were removed and the chromatin configuration was assessed. Graphs show the frequency of GV1, GV2 and GV3 chromatin configurations in each class. A total of 300 oocytes (101 Class 1, 119 Class 2 and 80 Class 3) were used in this study in three independent experiments. Data were analyzed by one-way ANOVA followed by Newman-Keuls multiple comparison test; a,b, different letters indicate significant differences, $p<0.05$). **C)** After collection, COC were separated into Class 1 and Class 2/3 on the basis of their morphology and subjected to Brilliant Cresyl Blue staining (BCB). After removal of cumulus cells, oocytes were classified as BCB+ or BCB- as shown in the representative picture. Graph shows the percentage of BCB+ and BCB- oocytes in Class 1 and 2/3 COC. A total of 337 COC were analyzed (126 Class 1 and 211 of Class 2/3) in nine independent experiments. Data were analyzed by one way ANOVA followed by Newman-Keuls multiple comparison test; data are expressed as means ± SEM; a, b, c, d different letters indicate significant differences ($p<0.05$).

A

Blastocyst rate on total oocytes (d+8)

B

Blastocyst cell number (d+8)

Figure 7: Effect of pre-maturation treatment on COC with different morphology

After collection, COC were separated into Class 1 and Class 2/3 on the basis of their morphology and in-vitro matured with or without the Pre-IVM treatment. Then oocytes were in-vitro fertilized and in-vitro cultured for 8 days. Groups of unsorted COC (mix of Class 1/2/3) were subjected to the same experimental procedure and were used as controls. Graphs show the effect of the pre-IVM treatment on the blastocyst rate (**A**) and mean cell number per blastocyst (**B**). A total of 947 oocytes were analyzed in this study (292 mixed oocytes, 321 Class 1 and 334 Class 2/3) in six independent experiments. Data were analyzed by one way ANOVA followed by Newman-Keuls multiple comparison test; data are expressed as means ± SEM; a, b, different letters indicates significant differences ($p<0.05$).

Figure 8: Chromatin remodeling during follicular development: a model.

The figure shows chromatin remodeling, as it would occur during the bovine estrous cycle. Follicles with white oocytes are non-atretic, while follicles with pink oocytes are early atretic and those with purple oocytes are atretic. The growing follicles would be mainly GV1, the plateau phase would be mainly GV2 and the early atretic would be GV 3. Adapted from Merton et al., 2003 (Merton *et al.*, 2003).

GENERAL DISCUSSION AND FUTURE PERSPECTIVES

The quality of the oocytes is pivotal for ART successful outcome. Moreover, it is widely accepted that the maturation of the oocyte represents the first key limiting step of the IVP process. For these reasons, during the course of this PhD program, we deepened previous works conducted at the Reproductive and Developmental Biology Laboratory (RedBioLab) that suggest that the maintenance of a proper functional oocyte-cumulus cell coupling is one of the crucial factors for female gamete developmental competence acquisition.

In the first part, the studies on GV chromatin configuration of porcine oocyte soon after their isolation from the follicle demonstrated that the large-scale chromatin configuration is indicative of the state of oocyte differentiation also in a species different from mice and cows. Secondly, we demonstrate that maintenance an appropriate level of cAMP through the inhibition of PDE activity during COCs recovery and during the following 24 h of culture with cilostamide, delay meiotic resumption while prolonging functional coupling between oocytes and CCs. These conditions improved the embryonic developmental capability of porcine oocytes after PA and SCNT. The future perspective of these findings is that improved quality of transferred embryos would materially enhance the overall efficiency of SCNT, which is currently still low, with the average yield of live births per embryo transferred being not higher than 5% [6, 299].

In the second part, we provided the first comprehensive transcriptome analysis of bovine CCs associated with oocytes with a specific large-scale chromatin configuration. In this case, the general idea is that CCs could reflect oocyte quality. Thus, we utilized CCs as a possible source of non-invasive biomarker(s) of oocyte health status and final differentiation. Ideally, these markers could be useful to select good quality oocyte and to identify specific oocyte cultural needs. Importantly, on the basis of our findings, we designed a tailored culture system, which confirm that the success of in-vitro cultural strategies, aim at improving oocyte developmental capability, is 'stage dependent', i.e. mainly due to the characteristic of the COC that are subjected to the procedure. Interestingly, we collaborated also to the analysis of the transcriptomic profile of bovine oocytes with different chromatin configurations to identify changes in mRNA expression in the oocyte during the GV0 to GV3 transition [300]. Both these studies clearly demonstrated that oocyte

characterized by a specific chromatin configuration present also a peculiar transcriptomic profile both considering the oocyte itself or its surrounding CCs.

Indeed, we demonstrate that standard IVM conditions are inappropriate to support pre-implantation embryonic development of GV1 enriched Class 1 COC, while their developmental competence is positively affected by a 6 h period of inhibition of meiotic resumption through cAMP modulators. On the contrary, the same treatment negatively affected Class 2 and 3 COC developmental competence, which is consistent with the findings that these classes only contain GV2 and GV3 oocytes. These data are coherent with one of the concepts beyond pre-IVM strategies [141, 277, 287, 301, 302] i.e. the prolongation of GJC between the somatic and germinal compartments is expected to be more effective in COC with a functional oocyte-CC coupling as in less-differentiated GV0 and GV1 oocytes [107] while is detrimental in GV3 oocyte. This further confirms the postulated hypothesis that GV3 oocytes represent those gametes that have reached a high developmental capability during follicular growth, and that, at the time of collection, were undergoing early events of atresia [107].

From all the above observations, we hypothesize that the poor success of the IVP could be mainly due to the intrinsic heterogeneity of the oocyte population that are normally subjected to IVM and to the lack of dedicated in vitro approaches to finalize the oocyte differentiation process.

In the past years, these concepts have led to the design of several in vitro approaches that take into account the need for the oocyte to complete its differentiation. Many of these strategies, often referred to as "pre-IVM culture systems" (as already mentioned in chapter I), are based on the possibility to block or delay spontaneous meiotic resumption of the oocyte, after its removal from the follicle, by modulating the cAMP oocyte content [277]. Although, several pre-IVM approaches have been developed since 1980'[101, 129, 193, 195, 270, 278-286] the ultimate results show only a slight improvement in oocyte developmental competence. Often, rather than increasing the number of blastocysts obtained, only an improvement in the parameters related to embryo quality was observed. For instance, blastocysts with higher number of cells or embryo with better developmental kinetics. In worst cases, results showed no significant improvement over the current standard IVP system [303-305].

In general, notwithstanding the meiotic arrest method used, little to no improvement has been observed when oocytes were cultured in bulk, regardless their follicular origin. In our works, we demonstrate that the high heterogeneity of the population of COCs subjected to in vitro pre-IVM protocols is one of the cause for its limited success rate. In most of the cases, indeed, studies on in

vitro pre-IVM efficiency have been conducted on ovaries obtained from slaughtered animals, thus contain all types and sizes of antral follicles. This type of approach doesn't take into account the stage of differentiation of each female gamete and its cultural specific needs.

As indicated before, for characterizing population of female gamete with different needs we used oocyte large-scale chromatin configuration as morphological indicator of oocyte competence knowing that chromatin remodeling is associated with oocyte growth and it changes during follicular antral development [107, 118, 270, 306]. Moreover, we demonstrate that the changes in chromatin configuration also accompany significant changes in the transcriptome signature in the oocyte [300] and in the corresponding cumulus cells [153] suggesting that it also reflects phases of follicle development [307].

In conclusion, our findings indicated that in order to improve IVP process it is necessary to select a more homogeneous oocyte population that must be treated considering specific oocyte cultural needs, designing customized pre-IVM culture system. At the same time, this type of approaches could be associated with in vivo stimulation strategy to synchronize the growth of ovarian follicles in the donor in order to obtain oocytes specifically suitable for pre-IVM/IVM protocols.

REFERENCES OF INTRODUCTION AND GENERAL DISCUSSION

1.   Dobson, H., et al., *The high-producing dairy cow and its reproductive performance.* Reprod Domest Anim, 2007. **42 Suppl 2**: p. 17-23.

2.   Lonergan, P., et al., *Embryo development in dairy cattle.* Theriogenology, 2016. **86**(1): p. 270-7.

3.   Royal, M., G.E. Mann, and A.P. Flint, *Strategies for reversing the trend towards subfertility in dairy cattle.* Vet J, 2000. **160**(1): p. 53-60.

4.   Smitz, J.E., J.G. Thompson, and R.B. Gilchrist, *The promise of in vitro maturation in assisted reproduction and fertility preservation.* Semin Reprod Med, 2011. **29**(1): p. 24-37.

5.   Prather, R.S., et al., *Transgenic swine for biomedicine and agriculture.* Theriogenology, 2003. **59**(1): p. 115-23.

6.   Galli, C., et al., *Somatic cell nuclear transfer and transgenesis in large animals: current and future insights.* Reprod Domest Anim, 2012. **47 Suppl 3**: p. 2-11.

7.   Menezo, Y.J. and F. Herubel, *Mouse and bovine models for human IVF.* Reprod Biomed Online, 2002. **4**(2): p. 170-5.

8.   Sarty, G.E., G.P. Adams, and R.A. Pierson, *Three-dimensional magnetic resonance imaging for the study of ovarian function in a bovine in vitro model.* J Reprod Fertil, 2000. **119**(1): p. 69-75.

9.   Pesce, M.W., X.;Wolgemuth, D.J.; Scholer, H. , *Differential expression of the Oct-4 transcription factor during mouse germ cell differentiation.* Mech Dev 1998. **71**: p. 89-98

10.   McLaughlin, E.A. and S.C. McIver, *Awakening the oocyte: controlling primordial follicle development.* Reproduction, 2009. **137**(1): p. 1-11.

11.   Skinner, M.K., *Regulation of primordial follicle assembly and development.* Hum Reprod Update, 2005. **11**(5): p. 461-71.

12.   Makabe, S. and P.M. Motta, *Migration of human germ cells and their relationship with the developing ovary: ultrastructural aspects.* Prog Clin Biol Res, 1989. **296**: p. 41-54.

13.   Pereda, J. and P.M. Motta, *A unique fibrillar coat on the surface of migrating human primordial germ cells.* Arch Histol Cytol, 1991. **54**(4): p. 419-25.

14.   Byskov, A.G., *Differentiation of mammalian embryonic gonad.* Physiol Rev, 1986. **66**(1): p. 71-117.

15.   Pinkerton, J.H., et al., *Development of the human ovary--a study using histochemical technics.* Obstet Gynecol, 1961. **18**: p. 152-81.

16.   Motta, P.M., et al., *Morphodynamics of the follicular-luteal complex during early ovarian development and reproductive life.* Int Rev Cytol, 2003. **223**: p. 177-288.

17.   Pereda, J., T. Zorn, and M. Soto-Suazo, *Migration of human and mouse primordial germ cells and colonization of the developing ovary: an ultrastructural and cytochemical study.* Microsc Res Tech, 2006. **69**(6): p. 386-95.

18.   Nakatsuji, N. and S. Chuma, *Differentiation of mouse primordial germ cells into female or male germ cells.* Int J Dev Biol, 2001. **45**(3): p. 541-8.

19.   Voronina, E. and G.M. Wessel, *The regulation of oocyte maturation.* Curr Top Dev Biol, 2003. **58**: p. 53-110.

20.   Driancourt, M.A., *Regulation of ovarian follicular dynamics in farm animals. Implications for manipulation of reproduction.* Theriogenology, 2001. **55**(6): p. 1211-39.

21.   van den Hurk, R. and J. Zhao, *Formation of mammalian oocytes and their growth, differentiation and maturation within ovarian follicles.* Theriogenology, 2005. **63**(6): p. 1717-51.

22.   Fair, T., et al., *Oocyte ultrastructure in bovine primordial to early tertiary follicles.* Anat Embryol (Berl), 1997. **195**(4): p. 327-36.

23.   Braw-Tal, R. and S. Yossefi, *Studies in vivo and in vitro on the initiation of follicle growth in the bovine ovary.* J Reprod Fertil, 1997. **109**(1): p. 165-71.

24.   Johnson, M.L., et al., *Expression of gap junctional proteins connexin 43, 32, and 26 throughout follicular development and atresia in cows.* Endocrine, 1999. **10**(1): p. 43-51.

25.   Maheshwari, A. and P.A. Fowler, *Primordial follicular assembly in humans--revisited.* Zygote, 2008. **16**(4): p. 285-96.

26.   Luciano, A.L., V., *Changes of Large-Scale Chromatin Configuration During Mammalian Oocyte Differentiation, in Oogenesis.* 2013. **Oogenesis**: p. 93-108

27.   Picton, H.M., *Activation of follicle development: the primordial follicle.* Theriogenology, 2001. **55**(6): p. 1193-210.

28.   Hyttel, P., *Electron Microscopy of Mammalian Oocyte Development, Maturation and Fertilization. .* , 2011. Oocyte Maturation and Fertilization: a Long History for a Short Event: p. 1-37.

29.   Knight, P.G. and C. Glister, *TGF-beta superfamily members and ovarian follicle development.* Reproduction, 2006. **132**(2): p. 191-206.

30.   Magoffin, D.A., *Ovarian theca cell.* Int J Biochem Cell Biol, 2005. **37**(7): p. 1344-9.

31.   Picton, H., D. Briggs, and R. Gosden, *The molecular basis of oocyte growth and development.* Mol Cell Endocrinol, 1998. **145**(1-2): p. 27-37.

32.   Reese, W.O., 2004. Duke's Physiology of Domestic Animals. 12th Edition. 12 ed. Cornell University Press.

33.   Rodgers, R.J. and H.F. Irving-Rodgers, *Formation of the ovarian follicular antrum and follicular fluid.* Biol Reprod, 2010. **82**(6): p. 1021-9.

34.   Fair, T., P. Hyttel, and T. Greve, *Bovine oocyte diameter in relation to maturational competence and transcriptional activity.* Mol Reprod Dev, 1995. **42**(4): p. 437-42.

35.   Fair, T., et al., *Nucleus ultrastructure and transcriptional activity of bovine oocytes in preantral and early antral follicles.* Mol Reprod Dev, 1997. **46**(2): p. 208-15.

36.   Abel, M.H., et al., *The effect of a null mutation in the follicle-stimulating hormone receptor gene on mouse reproduction.* Endocrinology, 2000. **141**(5): p. 1795-803.

37.   Russe, I., *Oogenesis in cattle and sheep.* Bibl Anat, 1983. **24**: p. 77-92.

38.   Celik, H.A., et al., *Number of follicular waves and their effect on pregnancy rate in the cow.* Reprod Domest Anim, 2005. **40**(2): p. 87-92.

39.   Li, R. and D.F. Albertini, *The road to maturation: somatic cell interaction and self-organization of the mammalian oocyte.* Nat Rev Mol Cell Biol, 2013. **14**(3): p. 141-52.

40.   Sirois, J. and J.E. Fortune, *Ovarian follicular dynamics during the estrous cycle in heifers monitored by real-time ultrasonography.* Biol Reprod, 1988. **39**(2): p. 308-17.

41.   Ginther, O.J., et al., *Selection of the dominant follicle in cattle.* Biol Reprod, 1996. **55**(6): p. 1187-94.

42.   Roche, J.F., *Control and regulation of folliculogenesis--a symposium in perspective.* Rev Reprod, 1996. **1**(1): p. 19-27.

43.   Gordon, I., 1994. Laboratory production of cattle embryos. Biotehcnology in agriculture 11 Edited by I Gordon. CAB INTERNATIONAL Wallingford UK

44.   Baker, J., et al., *Effects of an Igf1 gene null mutation on mouse reproduction.* Mol Endocrinol, 1996. **10**(7): p. 903-18.

45.   Monget, P., et al., *Regulation of ovarian folliculogenesis by IGF and BMP system in domestic animals.* Domest Anim Endocrinol, 2002. **23**(1-2): p. 139-54.

46.   Erickson, G.F., *Follicle Growth and Development.* 2018.

47.   Soede, N.M., P. Langendijk, and B. Kemp, *Reproductive cycles in pigs.* Anim Reprod Sci, 2011. **124**(3-4): p. 251-8.

48.   Adams, G.P., *Comparative patterns of follicle development and selection in ruminants.* J Reprod Fertil Suppl, 1999. **54**: p. 17-32.

49.   Webb, R.J., et al., *Follicle-stimulating hormone induces a gap junction-dependent dynamic change in [cAMP] and protein kinase a in mammalian oocytes.* Dev Biol, 2002. **246**(2): p. 441-54.

50.   Turzillo, A.M. and J.E. Fortune, *Suppression of the secondary FSH surge with bovine follicular fluid is associated with delayed ovarian follicular development in heifers.* J Reprod Fertil, 1990. **89**(2): p. 643-53.

51.   Adams, G.P., A.C. Evans, and N.C. Rawlings, *Follicular waves and circulating gonadotrophins in 8-month-old prepubertal heifers.* J Reprod Fertil, 1994. **100**(1): p. 27-33.

52.   Fortune, J.E., *Ovarian follicular growth and development in mammals.* Biol Reprod, 1994. **50**(2): p. 225-32.

53.   Kubisch, H.M., M.A. Larson, and D.O. Kiesling, *Control of interferon-tau secretion by in vitro-derived bovine blastocysts during extended culture and outgrowth formation.* Mol Reprod Dev, 2001. **58**(4): p. 390-7.

54.   Chuan, S., et al., *Hyperglycosylated human chorionic gonadotropin as an early predictor of pregnancy outcomes after in vitro fertilization.* Fertil Steril, 2014. **101**(2): p. 392-8.

55.   Irving-Rodgers, H.F., et al., *Atresia revisited: two basic patterns of atresia of bovine antral follicles.* Reproduction, 2001. **122**(5): p. 761-75.

56.   Matzuk, M.M., *Eggs in the balance.* Nat Genet, 2001. **28**(4): p. 300-1.

57.   Takai, Y., et al., *Caspase-12 compensates for lack of caspase-2 and caspase-3 in female germ cells.* Apoptosis, 2007. **12**(4): p. 791-800.

58.   Coticchio, G.A., D.F.; De Santis,L., 2013. Oogenesis. Edited by Giovanni Coticchio, David F Albertini, and Lucia De Santis. London: Springer London.

59.   Lund, S.A., et al., *Mitogenic and antioxidant mechanisms of estradiol action in preovulatory ovine follicles: relevance to luteal function.* Biol Reprod, 1999. **61**(2): p. 388-92.

60.   Nivet, A.L., et al., *Changes in granulosa cells' gene expression associated with increased oocyte competence in bovine.* Reproduction, 2013. **145**(6): p. 555-65.

61.   Girard, A., et al., *Global gene expression in granulosa cells of growing, plateau and atretic dominant follicles in cattle.* Reprod Biol Endocrinol, 2015. **13**: p. 17.

62.   Jolly, P.D., et al., *Apoptosis in bovine granulosa cells in relation to steroid synthesis, cyclic adenosine 3',5'-monophosphate response to follicle-stimulating hormone and luteinizing hormone, and follicular atresia.* Biol Reprod, 1994. **51**(5): p. 934-44.

63.   Scaramuzzi, R.J., et al., *Regulation of folliculogenesis and the determination of ovulation rate in ruminants.* Reprod Fertil Dev, 2011. **23**(3): p. 444-67.

64. Baerwald, A.R., G.P. Adams, and R.A. Pierson, *Characterization of ovarian follicular wave dynamics in women.* Biol Reprod, 2003. **69**(3): p. 1023-31.

65. Dixon, S.N. and K.L. Russell, *Radioimmunoassay of the anabolic agent zeranol. II. Zeranol concentrations in urine of sheep and cattle implanted with zeranol (Ralgro).* J Vet Pharmacol Ther, 1983. **6**(3): p. 173-9.

66. Gosden, R. and B. Lee, *Portrait of an oocyte: our obscure origin.* J Clin Invest, 2010. **120**(4): p. 973-83.

67. Buccione, R., A.C. Schroeder, and J.J. Eppig, *Interactions between somatic cells and germ cells throughout mammalian oogenesis.* Biol Reprod, 1990. **43**(4): p. 543-7.

68. Eppig, J.J., *The relationship between cumulus cell-oocyte coupling, oocyte meiotic maturation, and cumulus expansion.* Dev Biol, 1982. **89**(1): p. 268-72.

69. Byskov, A.G., *Control of meiosis. A summary.* Arch Anat Microsc Morphol Exp, 1985. **74**(1): p. 17-8.

70. Campagna, C., et al., *Effect of an environmentally relevant metabolized organochlorine mixture on porcine cumulus-oocyte complexes.* Reprod Toxicol, 2007. **23**(2): p. 145-52.

71. Sirard, M.A., S. Desrosier, and M. Assidi, *In vivo and in vitro effects of FSH on oocyte maturation and developmental competence.* Theriogenology, 2007. **68 Suppl 1**: p. S71-6.

72. Hyttel, P.F., T.; Callesen, H.; Grève, T. , *Oocyte growth, capacitation and final maturation in cattle.* Theriogenology, 1997: p. 23-32

73. Hyttel, P., et al., *Ultrastructure of in-vitro oocyte maturation in cattle.* J Reprod Fertil, 1986. **78**(2): p. 615-25.

74. Isaji, M., et al., *The localization of LAP2beta in bovine oocytes after in vitro activation and fertilization.* Zygote, 2004. **12**(1): p. 81-93.

75. Liu, H., J.M. Kim, and F. Aoki, *Regulation of histone H3 lysine 9 methylation in oocytes and early pre-implantation embryos.* Development, 2004. **131**(10): p. 2269-80.

76. Tremblay, K., et al., *Expression of cyclin B1 messenger RNA isoforms and initiation of cytoplasmic polyadenylation in the bovine oocyte.* Biol Reprod, 2005. **72**(4): p. 1037-44.

77. Arnt, J. and J. Hyttel, *Behavioural differentiation between effects elicited at dopamine D-1 and D-2 receptors in rats.* Clin Neuropharmacol, 1986. **9 Suppl 4**: p. 17-9.

78. Fair, T., P. Hyttel, and T. Greve, *Bovine oocyte diameter in relation to maturational competence and transcriptional activity.* Molecular reproduction and development, 1995. **42**(4): p. 437-42.

79. Sun, Q.Y., *Cellular and molecular mechanisms leading to cortical reaction and polyspermy block in mammalian eggs.* Microsc Res Tech, 2003. **61**(4): p. 342-8.

80. Conti, M. and F. Franciosi, *Acquisition of oocyte competence to develop as an embryo: integrated nuclear and cytoplasmic events.* Hum Reprod Update, 2018.

81. Sirard, M.A., et al., *Contribution of the oocyte to embryo quality.* Theriogenology, 2006. **65**(1): p. 126-36.

82. Sirard, M.A., et al., *Timing of nuclear progression and protein synthesis necessary for meiotic maturation of bovine oocytes.* Biol Reprod, 1989. **40**(6): p. 1257-63.

83. Barnes, F.L. and N.L. First, *Embryonic transcription in in vitro cultured bovine embryos.* Mol Reprod Dev, 1991. **29**(2): p. 117-23.

84. Kastrop, P.M., et al., *Protein synthesis and phosphorylation patterns of bovine oocytes maturing in vivo.* Mol Reprod Dev, 1991. **29**(3): p. 271-5.

85. Levesque, J.T. and M.A. Sirard, *Resumption of meiosis is initiated by the accumulation of cyclin B in bovine oocytes.* Biol Reprod, 1996. **55**(6): p. 1427-36.

86. Henrion, G., et al., *Differential regulation of the translation and the stability of two maternal transcripts in preimplantation rabbit embryos.* Mol Reprod Dev, 2000. **56**(1): p. 12-25.

87. Tomek, W., H. Torner, and W. Kanitz, *Comparative analysis of protein synthesis, transcription and cytoplasmic polyadenylation of mRNA during maturation of bovine oocytes in vitro.* Reprod Domest Anim, 2002. **37**(2): p. 86-91.

88. de Loos, F., et al., *Heterologous cell contacts and metabolic coupling in bovine cumulus oocyte complexes.* Mol Reprod Dev, 1991. **28**(3): p. 255-9.

89. Kalous, J., et al., *PKB/AKT is involved in resumption of meiosis in mouse oocytes.* Biol Cell, 2006. **98**(2): p. 111-23.

90. Coffer, P.J., J. Jin, and J.R. Woodgett, *Protein kinase B (c-Akt): a multifunctional mediator of phosphatidylinositol 3-kinase activation.* Biochem J, 1998. **335 (Pt 1)**: p. 1-13.

91. Cetica, P.D., et al., *Effect of lactate dehydrogenase activity and isoenzyme localization in bovine oocytes and utilization of oxidative substrates on in vitro maturation.* Theriogenology, 1999. **51**(3): p. 541-50.

92. Krisher, R.L. and B.D. Bavister, *Enhanced glycolysis after maturation of bovine oocytes in vitro is associated with increased developmental competence.* Mol Reprod Dev, 1999. **53**(1): p. 19-26.

93. Parfenov, V., et al., *Human antral follicles: oocyte nucleus and the karyosphere formation (electron microscopic and autoradiographic data).* Gamete Res, 1989. **22**(2): p. 219-31.

94. Mattson, B.A. and D.F. Albertini, *Oogenesis: chromatin and microtubule dynamics during meiotic prophase.* Mol Reprod Dev, 1990. **25**(4): p. 374-83.

95. Wickramasinghe, D., K.M. Ebert, and D.F. Albertini, *Meiotic competence acquisition is associated with the appearance of M-phase characteristics in growing mouse oocytes.* Dev Biol, 1991. **143**(1): p. 162-72.

96. Debey, P., et al., *Competent mouse oocytes isolated from antral follicles exhibit different chromatin organization and follow different maturation dynamics.* Mol Reprod Dev, 1993. **36**(1): p. 59-74.

97. Zuccotti, M., et al., *Chromatin organization during mouse oocyte growth.* Mol Reprod Dev, 1995. **41**(4): p. 479-85.

98. Bouniol-Baly, C., et al., *Differential transcriptional activity associated with chromatin configuration in fully grown mouse germinal vesicle oocytes.* Biol Reprod, 1999. **60**(3): p. 580-7.

99. Schramm, R.D., et al., *Chromatin configurations and meiotic competence of oocytes are related to follicular diameter in nonstimulated rhesus monkeys.* Biol Reprod, 1993. **48**(2): p. 349-56.

100. Bui, H.T., et al., *Regulation of chromatin and chromosome morphology by histone H3 modifications in pig oocytes.* Reproduction, 2007. **133**(2): p. 371-82.

101. Dieci, C., et al., *The effect of cilostamide on gap junction communication dynamics, chromatin remodeling, and competence acquisition in pig oocytes following parthenogenetic activation and nuclear transfer.* Biol Reprod, 2013. **89**(3): p. 68.

102. Combelles, C.M., D.F. Albertini, and C. Racowsky, *Distinct microtubule and chromatin characteristics of human oocytes after failed in-vivo and in-vitro meiotic maturation.* Hum Reprod, 2003. **18**(10): p. 2124-30.

103. Miyara, F., et al., *Chromatin configuration and transcriptional control in human and mouse oocytes.* Mol Reprod Dev, 2003. **64**(4): p. 458-70.

104. Hinrichs, K., et al., *In vitro maturation of horse oocytes: characterization of chromatin configuration using fluorescence microscopy.* Biol Reprod, 1993. **48**(2): p. 363-70.

105. Franciosi, F., et al., *Changes in histone H4 acetylation during in vivo versus in vitro maturation of equine oocytes.* Mol Hum Reprod, 2012. **18**(5): p. 243-52.

106. Chohan, K.R. and A.G. Hunter, *Meiotic competence of bovine fetal oocytes following in vitro maturation.* Anim Reprod Sci, 2003. **76**(1-2): p. 43-51.

107. Lodde, V., et al., *Large-scale chromatin remodeling in germinal vesicle bovine oocytes: interplay with gap junction functionality and developmental competence.* Mol Reprod Dev, 2007. **74**(6): p. 740-9.

108. Liu, Y., et al., *Germinal vesicle chromatin configurations of bovine oocytes.* Microsc Res Tech, 2006. **69**(10): p. 799-807.

109. Sui, H.S., et al., *Configurations of germinal vesicle (GV) chromatin in the goat differ from those of other species.* Mol Reprod Dev, 2005. **71**(2): p. 227-36.

110. Russo, V., et al., *Modifications in chromatin morphology and organization during sheep oogenesis.* Microsc Res Tech, 2007. **70**(8): p. 733-44.

111. Wang, H.L., et al., *Dynamic changes of germinal vesicle chromatin configuration and transcriptional activity during maturation of rabbit follicles.* Fertil Steril, 2009. **91**(4 Suppl): p. 1589-94.

112. Yousaf, M.R. and K.R. Chohan, *Nuclear morphology, diameter and meiotic competence of buffalo oocytes relative to follicle size.* Reprod Fertil Dev, 2003. **15**(4): p. 223-9.

113. Lee, H.S., et al., *Germinal vesicle chromatin configuration and meiotic competence is related to the oocyte source in canine.* Anim Reprod Sci, 2008. **103**(3-4): p. 336-47.

114. Reynaud, K., et al., *Follicle population, cumulus mucification, and oocyte chromatin configuration during the periovulatory period in the female dog.* Theriogenology, 2009. **72**(8): p. 1120-31.

115. Sun, X., et al., *Chromatin configurations in the ferret germinal vesicle that reflect developmental competence for in vitro maturation.* Reprod Domest Anim, 2009. **44**(2): p. 320-5.

116. Comizzoli, P., B.S. Pukazhenthi, and D.E. Wildt, *The competence of germinal vesicle oocytes is unrelated to nuclear chromatin configuration and strictly depends on cytoplasmic quantity and quality in the cat model.* Hum Reprod, 2011. **26**(8): p. 2165-77.

117. Hinrichs, K., *The equine oocyte: factors affecting meiotic and developmental competence.* Mol Reprod Dev, 2010. **77**(8): p. 651-61.

118. Lodde, V., et al., *Oocyte morphology and transcriptional silencing in relation to chromatin remodeling during the final phases of bovine oocyte growth.* Mol Reprod Dev, 2008. **75**(5): p. 915-24.

119. Hinrichs, K. and A.L. Schmidt, *Meiotic competence in horse oocytes: interactions among chromatin configuration, follicle size, cumulus morphology, and season.* Biol Reprod, 2000. **62**(5): p. 1402-8.

120. Fuhrer, F., et al., *Maturation competence and chromatin behaviour in growing and fully grown cattle oocytes.* Zentralbl Veterinarmed A, 1989. **36**(4): p. 285-91.

121. Zuccotti, M., et al., *Meiotic and developmental competence of mouse antral oocytes.* Biol Reprod, 1998. **58**(3): p. 700-4.

122. Zuccotti, M., et al., *The analysis of chromatin organisation allows selection of mouse antral oocytes competent for development to blastocyst.* Zygote, 2002. **10**(1): p. 73-8.

123. Luciano, A.M., et al., *Developmental capability of denuded bovine oocyte in a co-culture system with intact cumulus-oocyte complexes: role of cumulus cells, cyclic adenosine 3',5'-monophosphate, and glutathione.* Mol Reprod Dev, 2005. **71**(3): p. 389-97.

124. Motlik, J. and J. Fulka, *Breakdown of the germinal vesicle in pig oocytes in vivo and in vitro.* J Exp Zool, 1976. **198**(2): p. 155-62.

125. Motlik, J., N. Crozet, and J. Fulka, *Meiotic competence in vitro of pig oocytes isolated from early antral follicles.* J Reprod Fertil, 1984. **72**(2): p. 323-8.

126. Hirao, Y., et al., *Association between p34cdc2 levels and meiotic arrest in pig oocytes during early growth.* Zygote, 1995. **3**(4): p. 325-32.

127. Biggs, M.J., et al., *Regulation of implant surface cell adhesion: characterization and quantification of S-phase primary osteoblast adhesions on biomimetic nanoscale substrates.* J Orthop Res, 2007. **25**(2): p. 273-82.

128. Bonnet-Garnier, A., et al., *Genome organization and epigenetic marks in mouse germinal vesicle oocytes.* Int J Dev Biol, 2012. **56**(10-12): p. 877-87.

129. Modina, S., et al., *Oocyte developmental competence after in vitro maturation depends on the persistence of cumulus-oocyte comunications which are linked to the intracellular concentration of cAMP.* Italian journal of anatomy and embryology = Archivio italiano di anatomia ed embriologia, 2001. **106**(2 Suppl 2): p. 241-8.

130. Matzuk, M.M., et al., *Intercellular communication in the mammalian ovary: oocytes carry the conversation.* Science, 2002. **296**(5576): p. 2178-80.

131. Sutton, M.L., R.B. Gilchrist, and J.G. Thompson, *Effects of in-vivo and in-vitro environments on the metabolism of the cumulus-oocyte complex and its influence on oocyte developmental capacity.* Hum Reprod Update, 2003. **9**(1): p. 35-48.

132. Ali, A. and M.A. Sirard, *Protein kinases influence bovine oocyte competence during short-term treatment with recombinant human follicle stimulating hormone.* Reproduction, 2005. **130**(3): p. 303-10.

133. Motlik, J., et al., *RNA and protein synthesis requirements for the resumption of meiosis in rabbit oocytes: the role of cumulus cells.* Reprod Nutr Dev, 1989. **29**(5): p. 601-9.

134. Tatemoto, H. and T. Terada, *Time-dependent effects of cycloheximide and alpha-amanitin on meiotic resumption and progression in bovine follicular oocytes.* Theriogenology, 1995. **43**(6): p. 1107-13.

135. Park, J.Y., et al., *EGF-like growth factors as mediators of LH action in the ovulatory follicle.* Science, 2004. **303**(5658): p. 682-4.

136. Eppig, J.J., *Oocyte control of ovarian follicular development and function in mammals.* Reproduction, 2001. **122**(6): p. 829-38.

137. Gilchrist, R.B., L.J. Ritter, and D.T. Armstrong, *Oocyte-somatic cell interactions during follicle development in mammals.* Anim Reprod Sci, 2004. **82-83**: p. 431-46.

138. Su, Y.Q., et al., *Synergistic roles of BMP15 and GDF9 in the development and function of the oocyte-cumulus cell complex in mice: genetic evidence for an oocyte-granulosa cell regulatory loop.* Dev Biol, 2004. **276**(1): p. 64-73.

139. Gilchrist, R.B., M. Lane, and J.G. Thompson, *Oocyte-secreted factors: regulators of cumulus cell function and oocyte quality.* Hum Reprod Update, 2008. **14**(2): p. 159-77.

140. Hickey, T.E., et al., *Androgens augment the mitogenic effects of oocyte-secreted factors and growth differentiation factor 9 on porcine granulosa cells.* Biol Reprod, 2005. **73**(4): p. 825-32.

141. Gilchrist, R.B., *Recent insights into oocyte-follicle cell interactions provide opportunities for the development of new approaches to in vitro maturation.* Reprod Fertil Dev, 2011. **23**(1): p. 23-31.

142. Sutovsky, P., et al., *Dynamic changes of gap junctions and cytoskeleton during in vitro culture of cattle oocyte cumulus complexes.* Biol Reprod, 1993. **49**(6): p. 1277-87.

143. Goldberg, G.S., A.P. Moreno, and P.D. Lampe, *Gap junctions between cells expressing connexin 43 or 32 show inverse permselectivity to adenosine and ATP.* J Biol Chem, 2002. **277**(39): p. 36725-30.

144. Eppig, J.J., et al., *Mouse oocytes regulate metabolic cooperativity between granulosa cells and oocytes: amino acid transport.* Biol Reprod, 2005. **73**(2): p. 351-7.

145. Feuerstein, P., et al., *Gene expression in human cumulus cells: one approach to oocyte competence.* Hum Reprod, 2007. **22**(12): p. 3069-77.

146. Assidi, M., et al., *Identification of potential markers of oocyte competence expressed in bovine cumulus cells matured with follicle-stimulating hormone and/or phorbol myristate acetate in vitro.* Biol Reprod, 2008. **79**(2): p. 209-22.

147. Hamel, M., et al., *Identification of differentially expressed markers in human follicular cells associated with competent oocytes.* Hum Reprod, 2008. **23**(5): p. 1118-27.

148. Sasseville, M., et al., *Characterization of novel phosphodiesterases in the bovine ovarian follicle.* Biol Reprod, 2009. **81**(2): p. 415-25.

149. Tesfaye, D., et al., *Gene expression profile of cumulus cells derived from cumulus-oocyte complexes matured either in vivo or in vitro.* Reprod Fertil Dev, 2009. **21**(3): p. 451-61.

150. Huang, Z. and D. Wells, *The human oocyte and cumulus cells relationship: new insights from the cumulus cell transcriptome.* Mol Hum Reprod, 2010. **16**(10): p. 715-25.

151. Blondin, P. and M.A. Sirard, *Oocyte and follicular morphology as determining characteristics for developmental competence in bovine oocytes.* Mol Reprod Dev, 1995. **41**(1): p. 54-62.

152. Assou, S., et al., *Human cumulus cells as biomarkers for embryo and pregnancy outcomes.* Mol Hum Reprod, 2010. **16**(8): p. 531-8.

153. Dieci, C., et al., *Differences in cumulus cell gene expression indicate the benefit of a pre-maturation step to improve in-vitro bovine embryo production.* Mol Hum Reprod, 2016. **22**(12): p. 882-897.

154. Sawyer, H.R., et al., *Formation of ovarian follicles during fetal development in sheep.* Biol Reprod, 2002. **66**(4): p. 1134-50.

155. Byskov, A.G.N., M. , *Ontogeny of the mammalian ovary.* 2003. Biology and Pathology of the Oocyte: Its Role in Fertility and Reproductive: p. 13-28.

156. Moore, G.P., et al., *RNA synthesis in the mouse oocyte.* J Cell Biol, 1974. **60**(2): p. 416-22.

157. Robert, C., et al., *Presence of LH receptor mRNA in granulosa cells as a potential marker of oocyte developmental competence and characterization of the bovine splicing isoforms.* Reproduction, 2003. **125**(3): p. 437-46.

158. Shimada, M., et al., *Luteinizing hormone receptor formation in cumulus cells surrounding porcine oocytes and its role during meiotic maturation of porcine oocytes.* Biol Reprod, 2003. **68**(4): p. 1142-9.

159. Fu, M., et al., *Luteinizing hormone receptors expression in cumulus cells closely related to mouse oocyte meiotic maturation.* Front Biosci, 2007. **12**: p. 1804-13.

160. Meduri, G., et al., *New functional zonation in the ovary as shown by immunohistochemistry of luteinizing hormone receptor.* Endocrinology, 1992. **131**(1): p. 366-73.

161. Pangas, S.A. and M.M. Matzuk, *The art and artifact of GDF9 activity: cumulus expansion and the cumulus expansion-enabling factor.* Biol Reprod, 2005. **73**(4): p. 582-5.

162. Albertini, D.F., et al., *Cellular basis for paracrine regulation of ovarian follicle development.* Reproduction, 2001. **121**(5): p. 647-53.

163. Diaz, F.J., K. Wigglesworth, and J.J. Eppig, *Oocytes are required for the preantral granulosa cell to cumulus cell transition in mice.* Dev Biol, 2007. **305**(1): p. 300-11.

164. Ingman, W.V., P.C. Owens, and D.T. Armstrong, *Differential regulation by FSH and IGF-I of extracellular matrix IGFBP-5 in bovine granulosa cells: effect of association with the oocyte.* Mol Cell Endocrinol, 2000. **164**(1-2): p. 53-8.

165. Li, R., et al., *Oocyte-secreted factor(s) determine functional differences between bovine mural granulosa cells and cumulus cells.* Biol Reprod, 2000. **63**(3): p. 839-45.

166. Salustri, A., *Paracrine actions of oocytes in the mouse pre-ovulatory follicle.* Int J Dev Biol, 2000. **44**(6): p. 591-7.

167. Cittadini, G., Jr., R. Conzi, and G. Motta, *[Spiral computed tomography in the diagnosis and staging of bronchopulmonary carcinoma].* Chir Ital, 1995. **47**(3): p. 13-7.

168. Peng, X.R., et al., *Localization of luteinizing hormone receptor messenger ribonucleic acid expression in ovarian cell types during follicle development and ovulation.* Endocrinology, 1991. **129**(6): p. 3200-7.

169. Eppig, J.J., et al., *Murine oocytes suppress expression of luteinizing hormone receptor messenger ribonucleic acid by granulosa cells.* Biol Reprod, 1997. **56**(4): p. 976-84.

170. Shimada, M. and T. Terada, *FSH and LH induce progesterone production and progesterone receptor synthesis in cumulus cells: a requirement for meiotic resumption in porcine oocytes.* Mol Hum Reprod, 2002. **8**(7): p. 612-8.

171. Shimada, M., et al., *Paracrine and autocrine regulation of epidermal growth factor-like factors in cumulus oocyte complexes and granulosa cells: key roles for prostaglandin synthase 2 and progesterone receptor.* Mol Endocrinol, 2006. **20**(6): p. 1352-65.

172. Guidobaldi, H.A., et al., *Progesterone from the cumulus cells is the sperm chemoattractant secreted by the rabbit oocyte cumulus complex.* PLoS One, 2008. **3**(8): p. e3040.

173. Erickson, G.F. and S. Shimasaki, *The role of the oocyte in folliculogenesis.* Trends Endocrinol Metab, 2000. **11**(5): p. 193-8.

174. Tanghe, S., et al., *Minireview: Functions of the cumulus oophorus during oocyte maturation, ovulation, and fertilization.* Mol Reprod Dev, 2002. **61**(3): p. 414-24.

175. Yokoo, M. and E. Sato, *Cumulus-oocyte complex interactions during oocyte maturation.* Int Rev Cytol, 2004. **235**: p. 251-91.

176. Eppig, J.J., et al., *Oocyte control of granulosa cell development: how and why.* Hum Reprod, 1997. **12**(11 Suppl): p. 127-32.

177. Tirone, E., et al., *Hyaluronan synthesis by mouse cumulus cells is regulated by interactions between follicle-stimulating hormone (or epidermal growth factor) and a soluble oocyte factor (or transforming growth factor beta1).* J Biol Chem, 1997. **272**(8): p. 4787-94.

178. Mattioli, M. and B. Barboni, *Signal transduction mechanism for LH in the cumulus-oocyte complex.* Mol Cell Endocrinol, 2000. **161**(1-2): p. 19-23.

179. Ashkenazi, H., et al., *Epidermal growth factor family members: endogenous mediators of the ovulatory response.* Endocrinology, 2005. **146**(1): p. 77-84.

180. Liu, Z., et al., *Interleukin-6: an autocrine regulator of the mouse cumulus cell-oocyte complex expansion process.* Endocrinology, 2009. **150**(7): p. 3360-8.

181. Salustri, A., M. Yanagishita, and V.C. Hascall, *Synthesis and accumulation of hyaluronic acid and proteoglycans in the mouse cumulus cell-oocyte complex during follicle-stimulating hormone-induced mucification.* J Biol Chem, 1989. **264**(23): p. 13840-7.

182. Carrette, O., et al., *TSG-6 is concentrated in the extracellular matrix of mouse cumulus oocyte complexes through hyaluronan and inter-alpha-inhibitor binding.* Biol Reprod, 2001. **65**(1): p. 301-8.

183. Knudson, W., et al., *CD44-anchored hyaluronan-rich pericellular matrices: an ultrastructural and biochemical analysis.* Exp Cell Res, 1996. **228**(2): p. 216-28.

184. Lesley, J., et al., *TSG-6 modulates the interaction between hyaluronan and cell surface CD44.* J Biol Chem, 2004. **279**(24): p. 25745-54.

185. Bottazzi, B., et al., *The long pentraxin PTX3 as a link among innate immunity, inflammation, and female fertility.* J Leukoc Biol, 2006. **79**(5): p. 909-12.

186. Diaz, F.J., K. Sugiura, and J.J. Eppig, *Regulation of Pcsk6 expression during the preantral to antral follicle transition in mice: opposing roles of FSH and oocytes.* Biol Reprod, 2008. **78**(1): p. 176-83.

187. Richards, J.S., *Genetics of ovulation.* Semin Reprod Med, 2007. **25**(4): p. 235-42.

188. Elvin, J.A., et al., *Paracrine actions of growth differentiation factor-9 in the mammalian ovary.* Mol Endocrinol, 1999. **13**(6): p. 1035-48.

189. Zhuo, L. and K. Kimata, *Cumulus oophorus extracellular matrix: its construction and regulation.* Cell Struct Funct, 2001. **26**(4): p. 189-96.

190. Richards, F.J., *Regulation of meiotic maturation.* J Anim Sci, 2007. **85**: p. E4-6.

191. Edson, M.A., A.K. Nagaraja, and M.M. Matzuk, *The mammalian ovary from genesis to revelation.* Endocr Rev, 2009. **30**(6): p. 624-712.

192. Modina, S., et al., *Oocyte developmental competence after in vitro maturation depends on the persistence of cumulus-oocyte comunications which are linked to the intracellular concentration of cAMP.* Ital J Anat Embryol, 2001. **106**(2 Suppl 2): p. 241-8.

193. Luciano, A.M., et al., *Role of intracellular cyclic adenosine 3',5'-monophosphate concentration and oocyte-cumulus cells communications on the acquisition of the*

developmental competence during in vitro maturation of bovine oocyte. Biol Reprod, 2004. **70**(2): p. 465-72.

194. Colleoni, S., A.M. Luciano, and F. Gandolfi, *Cumulus-oocyte communications in the horse: role of the breeding season and of the maturation medium.* Reprod Domest Anim, 2004. **39**(2): p. 70-5.

195. Thomas, R.E., D.T. Armstrong, and R.B. Gilchrist, *Bovine cumulus cell-oocyte gap junctional communication during in vitro maturation in response to manipulation of cell-specific cyclic adenosine 3',5'-monophosophate levels.* Biol Reprod, 2004. **70**(3): p. 548-56.

196. Memili, E., et al., *Bovine germinal vesicle oocyte and cumulus cell proteomics.* Reproduction, 2007. **133**(6): p. 1107-20.

197. Sugiura, K., F.L. Pendola, and J.J. Eppig, *Oocyte control of metabolic cooperativity between oocytes and companion granulosa cells: energy metabolism.* Dev Biol, 2005. **279**(1): p. 20-30.

198. Sugiura, K., et al., *Oocyte-derived BMP15 and FGFs cooperate to promote glycolysis in cumulus cells.* Development, 2007. **134**(14): p. 2593-603.

199. Leese, H.J. and A.M. Barton, *Production of pyruvate by isolated mouse cumulus cells.* J Exp Zool, 1985. **234**(2): p. 231-6.

200. Mayes, M.A., et al., *Adenosine 5'-monophosphate kinase-activated protein kinase (PRKA) activators delay meiotic resumption in porcine oocytes.* Biol Reprod, 2007. **76**(4): p. 589-97.

201. Thompson, J.G., M. Lane, and R.B. Gilchrist, *Metabolism of the bovine cumulus-oocyte complex and influence on subsequent developmental competence.* Soc Reprod Fertil Suppl, 2007. **64**: p. 179-90.

202. Su, Y.Q., et al., *Oocyte regulation of metabolic cooperativity between mouse cumulus cells and oocytes: BMP15 and GDF9 control cholesterol biosynthesis in cumulus cells.* Development, 2008. **135**(1): p. 111-21.

203. Perret, B.P., et al., *Lipoprotein and phospholipid distribution in human follicular fluids.* Fertil Steril, 1985. **43**(3): p. 405-9.

204. Comiskey, M. and C.M. Warner, *Spatio-temporal localization of membrane lipid rafts in mouse oocytes and cleaving preimplantation embryos.* Dev Biol, 2007. **303**(2): p. 727-39.

205. Mingoti, G.Z., J.M. Garcia, and A.A. Rosa-e-Silva, *Steroidogenesis in cumulus cells of bovine cumulus-oocyte-complexes matured in vitro with BSA and different concentrations of steroids.* Anim Reprod Sci, 2002. **69**(3-4): p. 175-86.

206.   Tesarik, J. and C. Mendoza, *Nongenomic effects of 17 beta-estradiol on maturing human oocytes: relationship to oocyte developmental potential.* J Clin Endocrinol Metab, 1995. **80**(4): p. 1438-43.

207.   Ali, A. and M.A. Sirard, *The effects of 17beta-estradiol and protein supplement on the response to purified and recombinant follicle stimulating hormone in bovine oocytes.* Zygote, 2002. **10**(1): p. 65-71.

208.   Li, Q., L.J. McKenzie, and M.M. Matzuk, *Revisiting oocyte-somatic cell interactions: in search of novel intrafollicular predictors and regulators of oocyte developmental competence.* Mol Hum Reprod, 2008. **14**(12): p. 673-8.

209.   Vanderhyden, B.C., J.N. Cohen, and P. Morley, *Mouse oocytes regulate granulosa cell steroidogenesis.* Endocrinology, 1993. **133**(1): p. 423-6.

210.   Lucidi, P., et al., *Cumulus cells steroidogenesis is influenced by the degree of oocyte maturation.* Reprod Biol Endocrinol, 2003. **1**: p. 45.

211.   Colonna, R., et al., *Amino acid transport systems in growing mouse oocytes.* Cell Biol Int Rep, 1983. **7**(12): p. 1007-15.

212.   Haghighat, N. and L.J. Van Winkle, *Developmental change in follicular cell-enhanced amino acid uptake into mouse oocytes that depends on intact gap junctions and transport system Gly.* J Exp Zool, 1990. **253**(1): p. 71-82.

213.   Bornslaeger, E.A., P. Mattei, and R.M. Schultz, *Involvement of cAMP-dependent protein kinase and protein phosphorylation in regulation of mouse oocyte maturation.* Dev Biol, 1986. **114**(2): p. 453-62.

214.   Yamashita, Y., M. Hishinuma, and M. Shimada, *Activation of PKA, p38 MAPK and ERK1/2 by gonadotropins in cumulus cells is critical for induction of EGF-like factor and TACE/ADAM17 gene expression during in vitro maturation of porcine COCs.* J Ovarian Res, 2009. **2**: p. 20.

215.   Richards, J.S., *New signaling pathways for hormones and cyclic adenosine 3',5'-monophosphate action in endocrine cells.* Mol Endocrinol, 2001. **15**(2): p. 209-18.

216.   Ning, G., et al., *3',5'-cyclic adenosine monophosphate response element binding protein up-regulated cytochrome P450 lanosterol 14alpha-demethylase expression involved in follicle-stimulating hormone-induced mouse oocyte maturation.* Mol Endocrinol, 2008. **22**(7): p. 1682-94.

217.   Zhang, M., H. Ouyang, and G. Xia, *The signal pathway of gonadotrophins-induced mammalian oocyte meiotic resumption.* Mol Hum Reprod, 2009. **15**(7): p. 399-409.

218. Conti, M., *Specificity of the cyclic adenosine 3',5'-monophosphate signal in granulosa cell function.* Biol Reprod, 2002. **67**(6): p. 1653-61.

219. Conti, M., et al., *Role of cyclic nucleotide signaling in oocyte maturation.* Mol Cell Endocrinol, 2002. **187**(1-2): p. 153-9.

220. Sela-Abramovich, S., et al., *Mitogen-activated protein kinase mediates luteinizing hormone-induced breakdown of communication and oocyte maturation in rat ovarian follicles.* Endocrinology, 2005. **146**(3): p. 1236-44.

221. Vaccari, S., et al., *Cyclic GMP signaling is involved in the luteinizing hormone-dependent meiotic maturation of mouse oocytes.* Biol Reprod, 2009. **81**(3): p. 595-604.

222. Su, Y.Q., et al., *Protein kinase C and intracellular calcium are involved in follicle-stimulating hormone-mediated meiotic resumption of cumulus cell-enclosed porcine oocytes in hypoxanthine-supplemented medium.* Mol Reprod Dev, 1999. **53**(1): p. 51-8.

223. Fan, H.Y., et al., *Protein kinase C and mitogen-activated protein kinase cascade in mouse cumulus cells: cross talk and effect on meiotic resumption of oocyte.* Biol Reprod, 2004. **70**(4): p. 1178-87.

224. Fan, H.Y., et al., *MAPK3/1 (ERK1/2) in ovarian granulosa cells are essential for female fertility.* Science, 2009. **324**(5929): p. 938-41.

225. Downs, S.M. and J. Chen, *EGF-like peptides mediate FSH-induced maturation of cumulus cell-enclosed mouse oocytes.* Mol Reprod Dev, 2008. **75**(1): p. 105-14.

226. Mehlmann, L.M., *Stops and starts in mammalian oocytes: recent advances in understanding the regulation of meiotic arrest and oocyte maturation.* Reproduction, 2005. **130**(6): p. 791-9.

227. Liang, C.G., et al., *Cyclic adenosine 3',5'-monophosphate-dependent activation of mitogen-activated protein kinase in cumulus cells is essential for germinal vesicle breakdown of porcine cumulus-enclosed oocytes.* Endocrinology, 2005. **146**(10): p. 4437-44.

228. Hussein, T.S., J.G. Thompson, and R.B. Gilchrist, *Oocyte-secreted factors enhance oocyte developmental competence.* Dev Biol, 2006. **296**(2): p. 514-21.

229. Diaz, F.J., K. Wigglesworth, and J.J. Eppig, *Oocytes determine cumulus cell lineage in mouse ovarian follicles.* J Cell Sci, 2007. **120**(Pt 8): p. 1330-40.

230. Szollosi, D., *On the role of gap junctions between follicle cells and oocyte in the mammalian ovarian follicle.* Res Commun Chem Pathol Pharmacol, 1978. **10**(2): p. 3-4.

231. Musil, L.S. and D.A. Goodenough, *Multisubunit assembly of an integral plasma membrane channel protein, gap junction connexin43, occurs after exit from the ER.* Cell, 1993. **74**(6): p. 1065-77.

232. Carabatsos, M.J., et al., *Oocyte-granulosa cell heterologous gap junctions are required for the coordination of nuclear and cytoplasmic meiotic competence.* Dev Biol, 2000. **226**(2): p. 167-79.

233. Vozzi, C., et al., *Involvement of connexin 43 in meiotic maturation of bovine oocytes.* Reproduction, 2001. **122**(4): p. 619-28.

234. Juneja, S.C., et al., *Defects in the germ line and gonads of mice lacking connexin43.* Biol Reprod, 1999. **60**(5): p. 1263-70.

235. Luciano, A.M., et al., *Effect of different levels of intracellular cAMP on the in vitro maturation of cattle oocytes and their subsequent development following in vitro fertilization.* Mol Reprod Dev, 1999. **54**(1): p. 86-91.

236. Schwarzmann, G., et al., *Diameter of the cell-to-cell junctional membrane channels as probed with neutral molecules.* Science, 1981. **213**(4507): p. 551-3.

237. Mese, G., G. Richard, and T.W. White, *Gap junctions: basic structure and function.* J Invest Dermatol, 2007. **127**(11): p. 2516-24.

238. Kumar, N.M. and N.B. Gilula, *The gap junction communication channel.* Cell, 1996. **84**(3): p. 381-8.

239. Valiunas, V., et al., *Connexin-specific cell-to-cell transfer of short interfering RNA by gap junctions.* J Physiol, 2005. **568**(Pt 2): p. 459-68.

240. Shimada, M. and T. Terada, *Phosphatidylinositol 3-kinase in cumulus cells and oocytes is responsible for activation of oocyte mitogen-activated protein kinase during meiotic progression beyond the meiosis I stage in pigs.* Biol Reprod, 2001. **64**(4): p. 1106-14.

241. Su, Y.Q., et al., *Oocyte-dependent activation of mitogen-activated protein kinase (ERK1/2) in cumulus cells is required for the maturation of the mouse oocyte-cumulus cell complex.* Dev Biol, 2003. **263**(1): p. 126-38.

242. Gilchrist, R.B., et al., *Oocyte maturation and quality: role of cyclic nucleotides.* Reproduction, 2016. **152**(5): p. R143-57.

243. Richard, F.J., *Regulation of meiotic maturation.* J Anim Sci, 2007. **85**(13 Suppl): p. E4-6.

244. Isobe, N. and T. Terada, *Effect of the factor inhibiting germinal vesicle breakdown on the disruption of gap junctions and cumulus expansion of pig cumulus-oocyte complexes cultured in vitro.* Reproduction, 2001. **121**(2): p. 249-57.

245. Yoshida, M., *Role of glutathione in the maturation and fertilization of pig oocytes in vitro.* Mol Reprod Dev, 1993. **35**(1): p. 76-81.

246. Basso, K., et al., *Integrated biochemical and computational approach identifies BCL6 direct target genes controlling multiple pathways in normal germinal center B cells.* Blood, 2010. **115**(5): p. 975-84.

247. Zhang, L., et al., *Cumulus cell function during bovine oocyte maturation, fertilization, and embryo development in vitro.* Mol Reprod Dev, 1995. **40**(3): p. 338-44.

248. Sasseville, M., et al., *Regulation of gap junctions in porcine cumulus-oocyte complexes: contributions of granulosa cell contact, gonadotropins, and lipid rafts.* Mol Endocrinol, 2009. **23**(5): p. 700-10.

249. Yamazaki, Y., T. Wakayama, and R. Yanagimachi, *Contribution of cumulus cells and serum to the maturation of oocyte cytoplasm as revealed by intracytoplasmic sperm injection (ICSI).* Zygote, 2001. **9**(4): p. 277-82.

250. Matta, S.G., et al., *Effect of inhibition of synthesis of inducible nitric oxide synthase-derived nitric oxide by aminoguanidine on the in vitro maturation of oocyte-cumulus complexes of cattle.* Anim Reprod Sci, 2009. **111**(2-4): p. 189-201.

251. Russell, D.L. and A. Salustri, *Extracellular matrix of the cumulus-oocyte complex.* Semin Reprod Med, 2006. **24**(4): p. 217-27.

252. Fulop, C., et al., *Impaired cumulus mucification and female sterility in tumor necrosis factor-induced protein-6 deficient mice.* Development, 2003. **130**(10): p. 2253-61.

253. Mittaz, L., et al., *Adamts-1 is essential for the development and function of the urogenital system.* Biol Reprod, 2004. **70**(4): p. 1096-105.

254. Russell, D.L. and R.L. Robker, *Molecular mechanisms of ovulation: co-ordination through the cumulus complex.* Hum Reprod Update, 2007. **13**(3): p. 289-312.

255. Espey, L.L., *Current status of the hypothesis that mammalian ovulation is comparable to an inflammatory reaction.* Biol Reprod, 1994. **50**(2): p. 233-8.

256. Richards, J.S., *Ovulation: new factors that prepare the oocyte for fertilization.* Mol Cell Endocrinol, 2005. **234**(1-2): p. 75-9.

257. Saito, H., et al., *Hyaluronan in follicular fluids and fertilization of oocytes.* Fertil Steril, 2000. **74**(6): p. 1148-52.

258. Robker, R.L., et al., *Ovulation: a multi-gene, multi-step process.* Steroids, 2000. **65**(10-11): p. 559-70.

259. Hernandez-Gonzalez, I., et al., *Gene expression profiles of cumulus cell oocyte complexes during ovulation reveal cumulus cells express neuronal and immune-related genes: does this expand their role in the ovulation process?* Mol Endocrinol, 2006. **20**(6): p. 1300-21.

260. Hong, S.J., et al., *Cumulus cells and their extracellular matrix affect the quality of the spermatozoa penetrating the cumulus mass.* Fertil Steril, 2009. **92**(3): p. 971-8.

261. Bains, R., et al., *Hyaluronic acid increases motility/intracellular CA2+ concentration in human sperm in vitro.* Arch Androl, 2001. **47**(2): p. 119-25.

262. Chiu, P.C., et al., *Cumulus oophorus-associated glycodelin-C displaces sperm-bound glycodelin-A and -F and stimulates spermatozoa-zona pellucida binding.* J Biol Chem, 2007. **282**(8): p. 5378-88.

263. Sun, F., et al., *Human sperm chemotaxis: both the oocyte and its surrounding cumulus cells secrete sperm chemoattractants.* Hum Reprod, 2005. **20**(3): p. 761-7.

264. Wassarman, P.M., *Contribution of mouse egg zona pellucida glycoproteins to gamete recognition during fertilization.* J Cell Physiol, 2005. **204**(2): p. 388-91.

265. Ni, Y., et al., *Acrosome reaction induced by recombinant human zona pellucida 3 peptides rhuZP3a22 approximately 176 and rhuZP3b177 approximately 348 and their mechanism.* J Androl, 2007. **28**(3): p. 381-8.

266. Familiari, G., et al., *Three-dimensional structure of the zona pellucida at ovulation.* Microsc Res Tech, 2006. **69**(6): p. 415-26.

267. Wassarman, P.M. and E.S. Litscher, *Mammalian fertilization: the egg's multifunctional zona pellucida.* Int J Dev Biol, 2008. **52**(5-6): p. 665-76.

268. Qian, Y., et al., *Predictive value of the area of expanded cumulus mass on development of porcine oocytes matured and fertilized in vitro.* J Reprod Dev, 2003. **49**(2): p. 167-74.

269. De La Fuente, R. and J.J. Eppig, *Transcriptional activity of the mouse oocyte genome: companion granulosa cells modulate transcription and chromatin remodeling.* Dev Biol, 2001. **229**(1): p. 224-36.

270. Luciano, A.M., et al., *Gap junction-mediated communications regulate chromatin remodeling during bovine oocyte growth and differentiation through cAMP-dependent mechanism(s).* Biol Reprod, 2011. **85**(6): p. 1252-9.

271. Downs, S.M., *Regulation of the G2/M transition in rodent oocytes.* Mol Reprod Dev, 2010. **77**(7): p. 566-85.

272. Bilodeau-Goeseels, S., *Cows are not mice: the role of cyclic AMP, phosphodiesterases, and adenosine monophosphate-activated protein kinase in the maintenance of meiotic arrest in bovine oocytes.* Mol Reprod Dev, 2011. **78**(10-11): p. 734-43.

273. Assou, S., et al., *A non-invasive test for assessing embryo potential by gene expression profiles of human cumulus cells: a proof of concept study.* Mol Hum Reprod, 2008. **14**(12): p. 711-9.

274. McKenzie, L.J., et al., *Human cumulus granulosa cell gene expression: a predictor of fertilization and embryo selection in women undergoing IVF.* Hum Reprod, 2004. **19**(12): p. 2869-74.

275. Vigone, G., et al., *Transcriptome based identification of mouse cumulus cell markers that predict the developmental competence of their enclosed antral oocytes.* BMC Genomics, 2013. **14**: p. 380.

276. Kawashima, I., et al., *Sequential exposure of porcine cumulus cells to FSH and/or LH is critical for appropriate expression of steroidogenic and ovulation-related genes that impact oocyte maturation in vivo and in vitro.* Reproduction, 2008. **136**(1): p. 9-21.

277. Benson, P.E., et al., *Development of the Malocclusion Impact Questionnaire (MIQ) to measure the oral health-related quality of life of young people with malocclusion: part 2 - cross-sectional validation.* J Orthod, 2016. **43**(1): p. 14-23.

278. Nogueira, D., et al., *Meiotic arrest in vitro by phosphodiesterase 3-inhibitor enhances maturation capacity of human oocytes and allows subsequent embryonic development.* Biol Reprod, 2006. **74**(1): p. 177-84.

279. Ozawa, M., et al., *Comparison between effects of 3-isobutyl-1-methylxanthine and FSH on gap junctional communication, LH-receptor expression, and meiotic maturation of cumulus-oocyte complexes in pigs.* Mol Reprod Dev, 2008. **75**(5): p. 857-66.

280. Shu, Y.M., et al., *Effects of cilostamide and forskolin on the meiotic resumption and embryonic development of immature human oocytes.* Hum Reprod, 2008. **23**(3): p. 504-13.

281. Albuz, F.K., et al., *Simulated physiological oocyte maturation (SPOM): a novel in vitro maturation system that substantially improves embryo yield and pregnancy outcomes.* Hum Reprod, 2010. **25**(12): p. 2999-3011.

282. Lodde, V., et al., *Role of gap junction-mediated communications in regulating large-scale chromatin configuration remodeling and embryonic developmental competence acquisition in fully grown bovine oocyte.* J Assist Reprod Genet, 2013. **30**(9): p. 1219-26.

283. Rose, R.D., et al., *Regulation of sheep oocyte maturation using cAMP modulators.* Theriogenology, 2013. **79**(1): p. 142-8.

284. Zeng, H.T., et al., *Heparin and cAMP modulators interact during pre-in vitro maturation to affect mouse and human oocyte meiosis and developmental competence.* Hum Reprod, 2013. **28**(6): p. 1536-45.

285. Richani, D., et al., *Pre-maturation with cAMP modulators in conjunction with EGF-like peptides during in vitro maturation enhances mouse oocyte developmental competence.* Mol Reprod Dev, 2014. **81**(5): p. 422-35.

286. Sanchez, F., et al., *Human cumulus-enclosed germinal vesicle oocytes from early antral follicles reveal heterogeneous cellular and molecular features associated with in vitro maturation capacity.* Hum Reprod, 2015. **30**(6): p. 1396-409.

287. Franciosi, F., et al., *Natriuretic peptide precursor C delays meiotic resumption and sustains gap junction-mediated communication in bovine cumulus-enclosed oocytes.* Biol Reprod, 2014. **91**(3): p. 61.

288. Azari-Dolatabad, N., et al., *Effects of cilostamide and/or forskolin on the meiotic resumption and development competence of growing ovine oocytes selected by brilliant cresyl blue staining.* Theriogenology, 2016. **85**(8): p. 1483-90.

289. Park, B., et al., *Cilostamide and forskolin treatment during pre-IVM improves preimplantation development of cloned embryos by influencing meiotic progression and gap junction communication in pigs.* Theriogenology, 2016. **86**(3): p. 757-65.

290. Soares, A.C.S., et al., *Steroid hormones interact with natriuretic peptide C to delay nuclear maturation, to maintain oocyte-cumulus communication and to improve the quality of in vitro-produced embryos in cattle.* Reprod Fertil Dev, 2017. **29**(11): p. 2217-2224.

291. Franciosi, F., et al., *Developmental competence of gametes reconstructed by germinal vesicle transplantation from fresh and cryopreserved bovine oocytes.* Fertil Steril, 2010. **93**(1): p. 229-38.

292. Inoue, A., et al., *Contribution of the oocyte nucleus and cytoplasm to the determination of meiotic and developmental competence in mice.* Hum Reprod, 2008. **23**(6): p. 1377-84.

293. Vanhoutte, L., D. Nogueira, and P. De Sutter, *Prematuration of human denuded oocytes in a three-dimensional co-culture system: effects on meiosis progression and developmental competence.* Hum Reprod, 2009. **24**(3): p. 658-69.

294. Vanhoutte, L., et al., *Effect of temporary nuclear arrest by phosphodiesterase 3-inhibitor on morphological and functional aspects of in vitro matured mouse oocytes.* Mol Reprod Dev, 2008. **75**(6): p. 1021-30.

295. Pavlok, A., et al., *Culture of bovine oocytes from small antral follicles in meiosis-inhibiting medium with butyrolactone I: RNA synthesis, nucleolar morphology and meiotic competence.* Anim Reprod Sci, 2000. **64**(1-2): p. 1-11.

296. Fair, T., et al., *Maintenance of meiotic arrest in bovine oocytes in vitro using butyrolactone I: effects on oocyte ultrastructure and nucleolus function.* Mol Reprod Dev, 2002. **62**(3): p. 375-86.

297. Inoue, A., et al., *The perivitelline space-forming capacity of mouse oocytes is associated with meiotic competence.* J Reprod Dev, 2007. **53**(5): p. 1043-52.

298.   Escrich, L., et al., *Morphologic indicators predict the stage of chromatin condensation of human germinal vesicle oocytes recovered from stimulated cycles.* Fertil Steril, 2010. **93**(8): p. 2557-64.

299.   Nagashima, H., et al., *Advancing pig cloning technologies towards application in regenerative medicine.* Reprod Domest Anim, 2012. **47 Suppl 4**: p. 120-6.

300.   Labrecque, R., et al., *Chromatin remodelling and histone m RNA accumulation in bovine germinal vesicle oocytes.* Mol Reprod Dev, 2015. **82**(6): p. 450-62.

301.   Sirard, M.A., *Follicle environment and quality of in vitro matured oocytes.* J Assist Reprod Genet, 2011. **28**(6): p. 483-8.

302.   Adriaenssens, T., et al., *The cumulus cell gene expression profile of oocytes with different nuclear maturity and potential for blastocyst formation.* J Assist Reprod Genet, 2011. **28**(1): p. 31-40.

303.   Gharibi, S., et al., *Effect of phosphodiesterase type 3 inhibitor on nuclear maturation and in vitro development of ovine oocytes.* Theriogenology, 2013. **80**(4): p. 302-12.

304.   Guimaraes, A.L., et al., *Evaluation of the simulated physiological oocyte maturation system for improving bovine in vitro embryo production.* Theriogenology, 2015. **83**(1): p. 52-7.

305.   Diogenes, M.N., et al., *Effect of prematuration and maturation with fibroblast growth factor 10 (FGF10) on in vitro development of bovine oocytes.* Theriogenology, 2017. **102**: p. 190-198.

306.   De La Fuente, R., *Chromatin modifications in the germinal vesicle (GV) of mammalian oocytes.* Dev Biol, 2006. **292**(1): p. 1-12.

307.   Luciano, A.M. and M.A. Sirard, *Successful in vitro maturation of oocytes: a matter of follicular differentiation.* Biol Reprod, 2018. **98**(2): p. 162-169.

APPENDIX: PUBLISHED FULL PAPERS, LIST OF PUBLICATIONS AND COMMUNICATIONS

Full Papers

1. **Dieci C**, Lodde V, Franciosi F, Lagutina I, Tessaro I, Modina SC, Albertini DF, Lazzari G, Galli C and Luciano AM. The effect of cilostamide on gap junction communication dynamics, chromatin remodeling, and competence acquisition in pig oocytes following parthenogenetic activation and nuclear transfer. Biol Reprod 2013, 89, 278-279

2. Luciano AM, Franciosi F, **Dieci C** and Lodde V. Changes in large-scale chromatin structure and function during oogenesis: A journey in company with follicular cells. Animal Reproduction Science 2014, DOI: 10.1016/j.anireprosci.2014.06.026

3. Luciano AM, Franciosi F, **Dieci C**, Tessaro I, Terzaghi L, Modina SC and Lodde V. Large-scale chromatin structure and function changes during oogenesis: the interplay between oocyte and companion cumulus cells. Anim Reprod 2014; 11:141-149.

4. Labrecque R; Lodde V; **Dieci C**; Tessaro I; Luciano AM; Sirard MA. Chromatin remodeling and histones mRNA accumulation in bovine germinal vesicle oocyte. Mol Reprod Dev 2015 Jun;82(6):450-62.

5. **Dieci C**, Lodde V, Labrecque R, Dufort I, Tessaro I, Sirard MA, Luciano AM. Differences in cumulus cell gene expression indicate the benefit of a pre-maturation step to improve in-vitro bovine embryo production. Mol Hum Reprod 2016; 22:882-897.

6. Luciano AM, Franciosi F, Barros GR, **Dieci C**, Lodde V. The variable success of in vitro maturation: can we do better? Anim Reprod 2018; (Under revision).

7. Lodde V, Franciosi F, Dall'Acqua PC, Barros GR, **Dieci C**, Robert C, Sirard MA, Luciano AM. The zinc sink: role in oocyte growth and embryonic developmental competence acquisition (Manuscript in preparation) 2018.

Abstracts & Communications

1. **Dieci** C, Lodde V, Dufort I, Sirard MA, Luciano AM. Transcriptomic analysis of bovine cumulus cells investment of oocytes at different stage of differentiation based on the degree of their chromatin configuration: preliminary study. In: *46th Annual Meeting of the Society for the Study of Reproduction*. Montreal, Quebec (Canada). 2013 Biology of Reproduction.

2. Lodde V, Colleoni N, Franciosi F, **Dieci** C, Tessaro I, Corbani D, Lazzari G, Modina SC, Galli C, Luciano AM. Intercellular coupling and chromatin configuration state in horse oocyte–cumulus cell complexes of different origins. In: *Proceedings of the 39th Annual Conference of the International Embryo Transfer Society*. Hannover, Germany. Reproduction Fertility and Development, 2013, 25, 241-241.

3. Lodde V, Colleoni S, Franciosi F, **Dieci** C, Tessaro I, Corbani D, Corlazzoli F, Lazzari G, Modina SC, Galli C, Luciano AM. Effect of cilostamide treatment on the intercellular coupling, meiotic and embryonic developmental competence in horse oocyte-cumulus cells complexes of different origins. In: *46th Annual Meeting of the Society for the Study of Reproduction*. Montreal, Quebec (Canada). 2013, Biology of Reproduction.

4. Galli C, Colleoni S, Turini P, Crotti E, **Dieci** C, Lodde V, Luciano AM, Lazzari G. Holding equine oocytes at room temperature for 18 hours prior to in vitro maturation maintains their developmental competence. In: *XIth International Symposium on Equine Reproduction*. Hamilton, New Zealand. 2014, Journal of Equine Veterinary Science, 34, 174-175

5. **Dieci C**, Labrecque R, Lodde V, Tessaro I, Baruffini V, Lodi G, Modina SC, Sirard MA and Luciano AM. Morphological markers to select populations of oocytes with different cultural needs for dedicated pre-maturation systems. In: *Word Congress of Reproductive Biology* 2014, Edinburgh, Scotland. Conference proceedings of Reproduction.

6. Labrecque R Lodde V **Dieci C,** Tessaro I Luciano AM and Sirard MA. Chromatin remodelling and histones mRNA accumulation in bovine germinal vesicle oocyte. In: *Word Congress of Reproductive Biology* 2014, Edinburgh, Scotland. Conference proceedings of Reproduction.

7. Luciano AM, **Dieci C**, Labrecque R, Dufort I, Tessaro I, Sirard MA, Lodde V. Transcriptomic analysis of bovine cumulus cells investment of oocytes at different stage of differentiation based on the degree of their chromatin configuration. In: *48th Annual Meeting of the Society for the Study of Reproduction 18-22 June 2015, San Juan, Puerto Rico, USA*

8. Milan, 30 September 2016, Seminar Redbiolab Meeting - Oral communication "Molecular determinants in the acquisition of oocyte developmental competence in mammals: interplay between cumulus cells and oocyte chromatin remodeling"

9. **Dieci C**, Lodde V, Labrecque R, Tessaro I, Sirard MA, Luciano AM. Morphological markers to select populations of oocytes with different cultural needs for dedicated pre-maturation protocols. In: HAF (ed.) *Proceedings of Veterinary and Animal Science Days* 2017, 6th-8th June, Milan, Italy, vol. IV. Milan, Italy: International Journal of Health, Animal Science and Food Safety; 2017.

10. Barros GR, Lodde V, **Dieci C**, Franciosi F, Luciano AM. Study on the effects of zinc supplementation during in vitro embryo production technologies in cattle. In: HAF (ed.) *Proceedings of Veterinary and Animal Science* Days 2018, 6th-8th June, Milan, Italy, vol. IV. Milan, Italy: International Journal of Health, Animal Science and Food Safety; 2018.

The Effect of Cilostamide on Gap Junction Communication Dynamics, Chromatin Remodeling, and Competence Acquisition in Pig Oocytes Following Parthenogenetic Activation and Nuclear Transfer[1]

Cecilia Dieci,[3,4] Valentina Lodde,[3,4,5] Federica Franciosi,[5] Irina Lagutina,[4] Irene Tessaro,[5] Silvia C. Modina,[5] David F. Albertini,[6] Giovanna Lazzari,[4,7] Cesare Galli,[4,8] and Alberto M. Luciano[2,5]

[4]*Avantea, Laboratory of Reproductive Technologies, Cremona, Italy*
[5]*Reproductive and Developmental Biology Laboratory, Department of Health, Animal Science and Food Safety, University of Milan, Milan, Italy*
[6]*Institute of Reproductive Health and Regenerative Medicine, Center for Reproductive Sciences, University of Kansas Medical Center, Kansas City, Kansas*
[7]*Fondazione Avantea, Cremona, Italy*
[8]*Dipartimento di Scienze Mediche Veterinarie, Università di Bologna, Bologna, Italy*

ABSTRACT

In the pig, the efficiency of in vitro embryo production and somatic cell nuclear transfer (SCNT) procedures remains limited. It has been suggested that prematuration treatments (pre-IVM) based on the prolongation of a patent, bidirectional crosstalk between the oocyte and the cumulus cells through gap junction mediate communication (GJC), with the maintenance of a proper level of cAMP, could improve the developmental capability of oocytes. The aim of this study was to assess: 1) dose-dependent effects of cilostamide on nuclear maturation kinetics, 2) the relationship between treatments on GJC functionality and large-scale chromatin configuration changes, and 3) the impact of treatments on developmental competence acquisition after parthenogenetic activation (PA) and SCNT. Accordingly, cumulus-oocyte complexes were collected from 3- to 6-mm antral follicles and cultured for 24 h in defined culture medium with or without 1 μM cilostamide. GJC functionality was assessed by Lucifer yellow microinjection, while chromatin configuration was evaluated by fluorescence microscopy after nuclear staining. Cilostamide administration sustained functional coupling for up to 24 h of culture and delayed meiotic resumption, as only 25.6% of cilostamide-treated oocytes reached the pro-metaphase I stage compared to the control (69.7%; $P < 0.05$). Moreover, progressive chromatin condensation was delayed before meiotic resumption based upon G2/M biomarker phosphoprotein epitope acquisition using immunolocalization. Importantly, cilostamide treatment under these conditions improved oocyte developmental competence, as reflected in higher blastocyst quality after both parthenogenetic activation and SCNT.

INTRODUCTION

In addition to its high agricultural value, the pig is an important domestic animal model for biomedical and reproductive research [1]. Pig organs are similar to those of humans in terms of size and physiology, providing a potential source for xenotransplantation [2]. Cloning by means of somatic cell nuclear transfer (SCNT) is the technique used most often to generate genetically modified pigs for xenotransplantation and as models for studying various human diseases [3–6]. However, despite much progress having been made in pig in vitro embryo production (IVP) and SCNT over the last decades, the efficiency of these techniques remains low and further improvements are still required [1, 4, 5, 7].

It is widely agreed that the low efficiencies of pig IVP and SCNT are at least in part due to a suboptimal in vitro maturation (IVM) system that should ultimately produce mature oocytes able to support embryonic development. The challenge of oocyte IVM is, first, to provide a milieu that reflects the naturally changing environment to which the oocyte is exposed and, second, to support the complex cellular changes taking place in the follicular cells and in the oocyte nuclear and cytoplasmic compartments.

One of the problems related to IVM is that oocytes spontaneously resume meiotic maturation when cumulus-oocyte complexes (COCs) are removed from the antral follicles [8] and thus bypass the so-called ''oocyte capacitation'' that is, in turn, essential for the attainment of a full embryonic developmental competence [9]. Several studies have suggested that extending meiotic arrest in vitro by temporary blockage of spontaneous nuclear maturation, the so-called prematuration culture (PMC), might improve the synchronization between nuclear and cytoplasmic maturational status and ultimately the oocyte competence [10–13] (reviewed in Ref. 14).

Temporary blockage of spontaneous meiotic resumption can be achieved by preventing the intraoocyte drop of cAMP levels, which normally occurs after removal of the COC from the follicle, through the use of inhibitors of phosphodiesterases

(PDEs), the enzymes that hydrolyze cAMP [15, 16]. One of these compounds is cilostamide, which specifically inhibits the type 3 PDE (PDE3), which is the major active cAMP-PDE in porcine oocytes [17]. While, in some mammals, PDE3 is an oocyte-specific enzyme [18], in the pig this PDE is also expressed in cumulus cells [19].

Interestingly, it has been shown that the use of cilostamide can prolong the functional coupling between oocytes and cumulus cells mediated by gap junction-mediated communication (GJC) during in vitro culture (IVC) of bovine, mouse, and human oocytes [20–22]. This is important, since bidirectional communications between oocyte and cumulus cells are essential to ensure a proper oocyte differentiation and meiotic maturation. Furthermore, it has been recently shown in the bovine model that the maintenance of a proper functional coupling between oocyte and cumulus cells seems to be crucial in sustaining an orderly remodeling of large-scale chromatin configuration [22], which is, in turn, indicative of the oocyte differentiation and metabolic state [23–27] (reviewed in Refs. 28, 29).

On the basis of these observations, this study aimed to test the utility of a prematuration treatment using cilostamide by evaluating pig oocyte quality for various biotechnological applications, including parthenogenesis and SCNT. With this objective in mind, we assessed: 1) dose-dependent effects of cilostamide on the kinetics and the degree of nuclear maturation, 2) the effect of the treatment on GJC functionality and on the process of large-scale chromatin configuration changes, and 3) the effect of the treatment on developmental competence acquisition after parthenogenetic activation (PA) and SCNT.

MATERIALS AND METHODS

COC Collection and Culture

All chemicals and reagents were purchased from Sigma Chemical Company, unless otherwise stated. Porcine ovaries were recovered at a local abattoir from pubertal females and transported to the laboratory at 30–33°C within 2 h. All the subsequent procedures were performed between 35°C and 38°C, unless otherwise specified. COCs were isolated from early antral follicles (EAFs; diameter 0.5–2 mm) by dissecting individual follicles with a scalpel, or from medium antral follicles (MAFs; diameter 3–6 mm) by aspiration with a 19-gauge needle mounted on an vacuum pump (Cook-IVF, Brisbane, QLD, Australia) with a pressure of −28 mm Hg. Collection medium was TCM199 supplemented with 20 mM Hepes, 1790 IU/ml of heparin, and 0.4% bovine serum albumin (BSA) fraction V (M199D). Where needed and according to the experimental design, COCs from MAFs were collected in 500 μM 3-isobutyl-I-methylxantine (IBMX) supplemented medium to avoid cAMP content drop during COC recovery [10, 12, 30]. COCs were examined under a stereomicroscope, and only those with intact, compact cumulus investments and finely granulated homogeneous ooplasm were used. The whole procedure was performed in approximately 30 min.

Groups of 25–30 COCs isolated from MAFs were cultured in four-well dishes (NUNC; VWR International, Italy) at 38.5°C under 5% CO_2 in humidified air, in 500 μl of defined IVM medium (dIVM), which was TCM199 supplemented with fatty acid-free 0.4% BSA, 75 μg/ml kanamycin, 1 μl/ml ITS media supplement (insulin, transferrin, and sodium selenite), 110 μg/ml sodium pyruvate, 75 μg/ml ascorbic acid, 100 μg/ml glutamine, 5 μg/ml myoinositol, 0.4 mM cystine, 0.6 mM cysteamine, and 0.1 IU/ml of human recombinant FSH (r-hFSH; Gonal F; Serono S.p.a., Italy). According to the experimental design, dIVM medium was further supplemented with 0.1 or 1 μM cilostamide (Enzo Life Science, Farmingdale, NY), a specific type 3 PDE inhibitor. Times of culture were different according to the experimental design and are specified for each experiment in the *Results* section. In the experiments in which cilostamide dose-response and reversibility were tested, oocytes were freed of cumulus cells, fixed in ethanol:acetic acid (3:1, v/v) for 48 h at room temperature, and stained with Lacmoid to assess nuclear maturation status and precisely evaluate the presence of the nuclear envelope.

Analysis of Functional Status of GJ-Mediated Communication Between Oocytes and Surrounding Cumulus Cells

Groups of 25–30 COCs were cultured for 0, 12, 18, and 24 h in dIVM medium in the absence or presence of 1 μM cilostamide. At each time point, intercellular communications between oocytes and cumulus cells were assessed by Lucifer yellow (LY) microinjection, as previously described for bovine COCs [12]. Briefly, a 3% solution of LY in 5 mM lithium chloride was pressure injected into the oocyte. A microinjection apparatus (Narishige Co. Ltd., Japan) was used to guide the holding and injecting micropipettes into a 50-μl drop of M199D supplemented with 5 % fetal calf serum (FCS; Gibco, Invitrogen s.r.l., Milan, Italy) and covered with mineral oil. Analysis of GJ functionality was performed 10 min after the injection by the observation of LY spreading from the oocytes to the cumulus cells under fluorescence microscopy. COCs were classified as open, partially open, or closed, as previously described [12].

Assessment of Chromatin Configuration, Oocyte Diameter, and Meiotic Progression

Changes of large-scale chromatin configuration were assessed at the time of collection and after different times of culture by Hoechst 33 342 staining and fluorescence microscopy analysis. COCs were freed of cumulus cells by gentle pipetting in M199D. Denuded oocytes (DOs) were incubated for 10 min in the dark in M199D containing 1 μg/ml Hoechst 33 342 and transferred into a 5-μl drop of the same medium. Chromatin configuration was evaluated under an inverted fluorescence microscope (Olympus IX50, magnification 40×) and the DOs classified according to the degree of chromatin mass condensation within the germinal vesicle (GV), as previously described [31, 32], for oocytes at the time of isolation from the follicles and after culture, respectively. In order to assess the relationship between chromatin configuration and the oocyte diameter at the time of collection, bright-field images of living DOs were taken by a digital camera (DS-5M; Nikon Corp.). Oocyte diameter was measured excluding the zona pellucida using NIH ImageJ 1.44 software [33], as previously described [25].

When chromatin configuration could not be assessed immediately after the culture period in living oocytes, DOs were, fixed in 500 μl of 60% methanol in Dulbecco PBS (DPBS) for at least 30 min at 4°C, stained with 1 μg/ml Hoechst 33 342, and evaluated by florescence microscopy as previously described. Preliminary experiments showed that this fixation procedure did not alter large-scale chromatin configuration as previously reported in cow [28].

PA and SCNT

At the end of the culture period, COCs were freed of their surrounding cumulus cells and washed twice in Hepes-buffered synthetic oviduct fluid (H-SOF) [34]. The oocytes with the first polar body extruded were selected and treated for PA or for SCNT procedures.

Matured oocytes were activated as described previously [35]. Briefly, oocytes were washed in 0.3 M mannitol solution, containing 1 mM Ca^{2+} and activated by double direct current pulses of 1.2 kV/cm for 30 μsec applied in the same medium. After a brief wash in H-SOF, the oocytes were transferred into the chemically assisted activation medium, which was PZM-3 medium [36] supplemented with 5 μg/ml cytochalasin B. After 4 h of incubation, PA embryos were washed twice in H-SOF and transferred to 400 μl PZM3 IVC medium. Embryo cleavage and blastocyst development were observed at Days 2 and 7, respectively.

In order to generate SCNT embryos, porcine adult fibroblasts were obtained through culture of minced tissue from ear or tail biopsies, as previously described [35]. Briefly, fibroblasts were cultured in medium Dulbecco modified Eagle medium (DMEM) + TCM199 (1:1) with 10% FCS in 5% CO_2 and 5% O_2 in humidified air at 38.5°C. After the primary culture was established, they were either subcultured every 4–6 days or expanded and frozen in DMEM + TCM199 (1:1) with 20% FCS and 10% dimethyl sulfoxide and stored in liquid nitrogen. Donor cells were induced to quiescence by serum starvation (0.5% FCS) for 1–3 days prior to nuclear transfer. The cells were prepared by trypsinization 30 min before nuclear transfer and then washed, pelleted by centrifugation, and resuspended in H-SOF supplemented with 10% FCS, to serve as nuclear donors. The zona pellucida of the matured oocytes was digested by 0.5% pronase solution for a few minutes. Zona-free oocytes were stained with Hoechst 33 342 and subjected to 5 μg/ml cytochalasin B treatment. The enucleation of a dezonated oocyte was performed with a blunt, nonbeveled pipette. In order to localize the metaphase plate, oocytes were briefly exposed to ultraviolet light. Cytoplasts were individually washed for few seconds in 300 μg/ml phytohemagglutinin P in PBS and then quickly dropped over a single

donor cell [37]. After pairing donor cell and recipient cytoplasm, the couplets were subjected to electrofusion. After two 30-μsec direct current impulses of 1.2 Kv/cm, the constructs were transferred to H-SOF medium supplemented with 10% FCS. After fusion, the reconstructed SCNT embryos were subjected to activation as previously described for parthenogenetic development. As for the PA embryos, the SCNT embryos were washed twice in H-SOF supplemented with 10% FCS and transferred in IVC medium. IVC was carried out under 5% CO_2 and 5% O_2 in humidified air at 38.5°. Embryos were positioned in a well of well system [38]. The well was covered with 400 μl IVC-SOF [34]. Cleavage was assessed 48 h after activation, whereas the blastocyst rate (BL) was recorded on Day 7 (Day 0 was the day of activation). During embryo culture, half of the medium was renewed on Day 4 with fresh culture medium. On Day 7, the blastocysts were fixed in 60% methanol in DPBS overnight at 4°C and stained with 1 μg/ml Hoechst 33 342 for cell number evaluation.

Immunofluorescence Staining

Indirect immunofluorescence was carried out to evaluate 1) chromatin condensation by monitoring phosphorylation of histone H3 at Ser28 (HE-S28) and 2) the patterns of mitosis-associated ser/thr phospho-proteins (MPM2) by using the monoclonal antibody MPM2. This antibody is known to detect epitopes of many relevant substrates for M-phase-specific kinases and is a specific biomarker for the G2/M cell cycle transition [39–43].

Oocytes were simultaneously fixed and extracted in a microtubule-stabilizing buffer containing proteases and phosphatases inhibitors, as described elsewhere [40, 42, 43] and then incubated overnight with primary antibody at 4°C. The primary antibodies used were rabbit polyclonal anti-phospho-histone H3 (Ser28; dilution, 1:100; Merk Millipore, Temecula, CA) or mouse monoclonal anti-phospho-Ser/Thr-Pro antibody, MPM2 (dilution 1:100; Merck Millipore). After extensive washing in 0.1% Triton, 0.1% Tween, and 1% BSA, oocytes were incubated for 1 h at room temperature with conjugated secondary antibodies that were TRITC-conjugated AffiniPure Donkey Anti-Rabbit (diliution 1:100; Jackson ImmunoResearch Laboratories, Inc., West Grove, PA) or AlexaFluor-488-labeled donkey anti-mouse (dilution 1:500; Invitrogen, Life Technologies, Carlsbad, CA). Samples were extensively washed again and finally mounted on slides in the antifade medium, Vecta Shield (Vector Laboratories) supplemented with 1 μg/ml 4′,6-diamidino-2-phenylindole. In each experiment, negative controls were performed by omitting the primary antibodies, and did not reveal any staining. Samples were analyzed on an epifluorescence microscope (Eclipse E600; Nikon Corp., Japan) equipped with a 40× objective and a digital camera (DS-Fi2; Nikon Corp., Japan). For the analysis of phosphorylation status of histone H3-S28, immune fluorescent staining was also conducted on paraformaldehyde-fixed oocytes, as previously described [32].

Analysis of MPM2 staining was conducted by capturing images, using identical exposure times and gain settings, at the focal plane containing the GV chromatin and at the equatorial focal plane, in order to assess fluorescence intensity (FI) of the nucleus and cytoplasm respectively. Finally, mean FI of each GV was calculated using NIH ImageJ software. To determine the cytoplasmic FI, mean FI in five different areas of the cytoplasm was calculated using NIH ImageJ and averaged.

Statistical Analysis

All the experiments were repeated three to five times. Observations from all the experiments were pooled. Statistical analyses were performed using GraphPad Prism (GraphPad Software, San Diego, CA). Differences in maturation, cleavage, and BLs, as well as differences in the percentages of COCs with open GCJ and of oocytes with different chromatin configurations among the experimental groups, were analyzed by Fisher exact test. FI of MPM2, oocyte diameter, and blastocyst cell number are expressed as means ± SE. In these cases, statistical significance was tested using one-way ANOVA followed by Tukey multiple comparison test or by the Student t-test when means of two groups were compared. Values of $P < 0.05$ were considered significant.

RESULTS

Dose-Response and Reversibility of Cilostamide Treatment

The first set of experiments aimed at determining the treatment that could prevent GV breakdown (GVBD) in porcine oocytes under our experimental condition. COCs were cultured in dIVM medium (control) or dIVM medium supplemented with 0.1 or 1 μM cilostamide for 24, 36, or 48
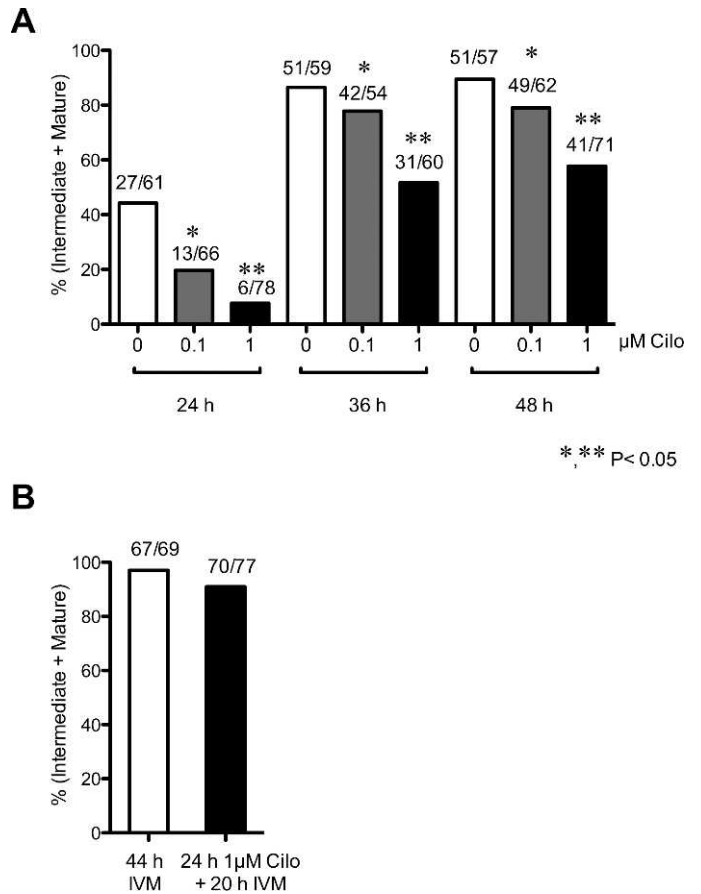
FIG. 1. **A**) Dose-response effect of cilostamide on oocyte meiotic resumption. COCs were cultured in media supplemented with increasing concentrations of cilostamide (0, 0.1, and 1 μM) for varying periods of time (24, 36, and 48 h). A total of 960 oocytes were used in these experiments. Oocytes where judged to be: intermediate when the chromosomes were arranged in prometaphase, metaphase I plate, anaphase I, or telophase I; and mature when the chromosomes were arranged in a metaphase II plate with the first polar body extruded. **B**) Effect of the prematuration treatment on oocyte maturation status. COCs were incubated in the presence of 1 μM cilostamide for 24 h. The maturation status was assessed after culturing the COCs for a further 20 h in dIVM medium (see main text). A total of 146 oocytes were used in these experiments. Data were analyzed by Fisher exact test. Asterisks (single and double) indicate significant differences between classes ($P < 0.05$).

h, and oocyte nuclear maturation was assessed by lacmoid staining after acetic fixation. Oocytes were classified as: GV when the nuclear membrane was detectable independently of the chromatin organization within the nuclear envelope; intermediate when the chromosomes were arranged in prometaphase, metaphase I plate, anaphase I, or telophase I; and mature when the chromosomes were arranged in a metaphase II plate with the first polar body extruded and degenerated (Deg), when none of the above classes could be recognized. As shown in Figure 1A, culture with 1 μM cilostamide for 24 h was the most effective treatment in preventing the completion of meiosis I. Moreover, the effect of 1 μM cilostamide was reversible upon its withdrawal from the culture medium. In fact, when COCs were cultured in the presence of 1 μM cilostamide for 24 h and subsequently washed and cultured for an additional 20 h in dIVM medium, the percentages of oocytes at intermediate and mature stages were equal to that obtained in the control group cultured for 44 h in dIVM medium (Fig. 1B). Based on these results, treatment

A

B

FIG. 2. **A**) Representative images showing the functional coupling between oocyte and cumulus cells after LY dye injection (upper panel) and bright-field images (lower panel). Gap junction communications were classified as open, partial, or closed as previously described [12]. Scale b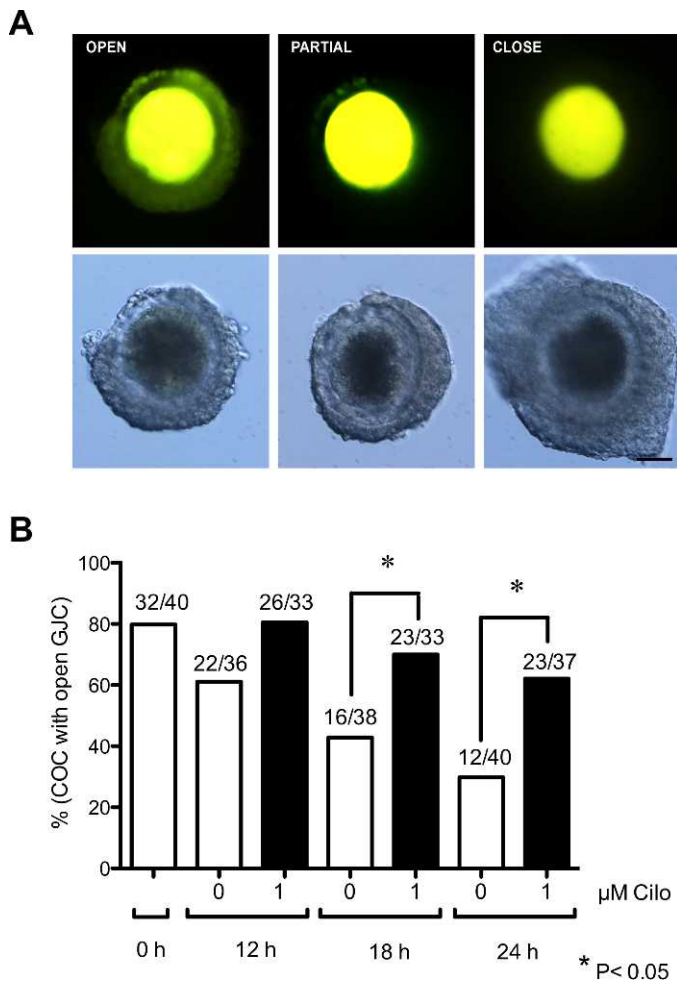ar = 50 μm. **B**) The effect of cilostamide on open GJC between the oocyte and cumulus cells after 0-, 12-, 18-, and 24-h IVM. A total of 257 oocytes were used in these experiments. The number of oocytes analyzed in each group is indicated. Data were analyzed by Fisher exact test. Asterisk indicates significant differences between classes ($P < 0.05$).

with 1 μM cilostamide for 24 h was adopted in all the following experiments.

Effect of Cilostamide Treatment on GJC Between Oocytes and Surrounding Cumulus Cells

This set of experiments was designed to investigate the effect 1 μM cilostamide treatment on the persistence of a functional intercellular coupling between the oocyte and the surrounding cumulus cells. GJCs functionality was assessed at the time of collection and after 12, 18, and 24 h of culture in dIVM medium supplemented with 0 (control) or 1 μM

cilostamide. At the time of collection, the injection of LY in the oocytes resulted in an immediate spread of the dye into neighboring corona radiata cells in 79.8% of COCs, whereas 5.1% and 15.2% of COCs showed a pattern of partially and completely closed communications, respectively (Fig. 2). As shown in Figure 2B, at 18 h of culture, we observed a substantial drop in GJC functionality in the control group. In contrast, GJCs functionality was maintained for up to 24 h of culture in the cilostamide-treated group. Importantly, when different times were compared, the percentage of COCs with open GJCs in the cilostamide-treated group after 24 h of culture did not differ significantly to that observed at the time of collection ($P = 0.129$).

Effect of Cilostamide Treatment on Chromatin Configuration Remodeling and Meiotic Progression

Before assessing the effect of cilostamide treatment on the process of chromatin configuration remodeling and meiotic progression, preliminary studies were conducted to identify discrete categories of prophase I arrested oocytes. To this end, we assessed chromatin configuration changes at the time of isolation from the follicles and compared our observations with the plethora of classifications present in the literature [31, 32, 44–48]. Chromatin configuration was assessed in living porcine oocytes soon after the isolation from EAFs (0.5 to <2 mm in diameter) and MAFs (3–6 mm in diameter) by Hoechst 33 342 staining and fluorescence microscopy analysis. Our observation confirmed, to a large extent, data from Bui et al. [32] and Hirao et al. [44]. As shown in Figure 3A, the filamentous chromatin (FC) configuration was characterized by the presence of a diffuse filamentous pattern of chromatin distributed in the whole nuclear area. The stringy chromatin (SC) configuration was characterized by an increased level of condensation of the chromatin that became clearly thicker and organized into clumps. Within the SC class, a further distinction was based on the presence or absence of a ring of condensed chromatin around the nucleolus, thus the configuration in which clumped chromatin was distributed throughout the GV was designated as SC distributed (SCd), whereas the configuration in which both clumped chromatin throughout the nucleoplasm and a rim of condensed chromatin surrounding the nucleolus were detected was termed SC with nucleolar rim (SCn). Finally, in the GVI configuration, all the condensed chromatin mass was organized around the nucleolus, as previously described by Motlik and Fulka [31]. That the SCd and SCn configurations are intermediated states of chromatin condensation between the FC and GVI configurations was confirmed by the oocyte diameter analysis, which showed that change of chromatin configuration from FC to GVI was accompanied by a significant increase of oocyte diameter ($P < 0.05$; Fig. 3B). Mean diameter of FC oocytes from EAF and of SCn, SCd, and GVI oocytes from MAF was 110.8 ± 1.2, 118.4 ± 0.8, 119.4 ± 0.4, and 121.3 ± 0.4 μm, respectively. Moreover, as shown in Table 1, the distribution analysis of the above-described patterns in EAFs and MAFs showed that, at the time of collection, the majority of oocytes isolated from

TABLE 1. Chromatin configuration distribution at the time of oocyte isolation from early and medium antral follicles.

Follicle	N	FC (%)	SCd (%)	SCn (%)	GVI (%)	GVII–GVIV (%)	Pro-MI–MI (%)	Deg (%)*
EAF	91	44 (48.4)[a]	8 (8.8)	11 (12.1)[a]	9 (9.9)[a]	3 (3.3)	0 (0.0)	16 (17.6)
MAF	245	9 (3.7)[b]	23 (9.4)	87 (35.5)[b]	71 (29.0)[b]	20 (8.2)	0 (0.0)	35 (14.3)

[a,b] Different letters within columns indicate significant differences (Fisher exact test, $P < 0.05$).
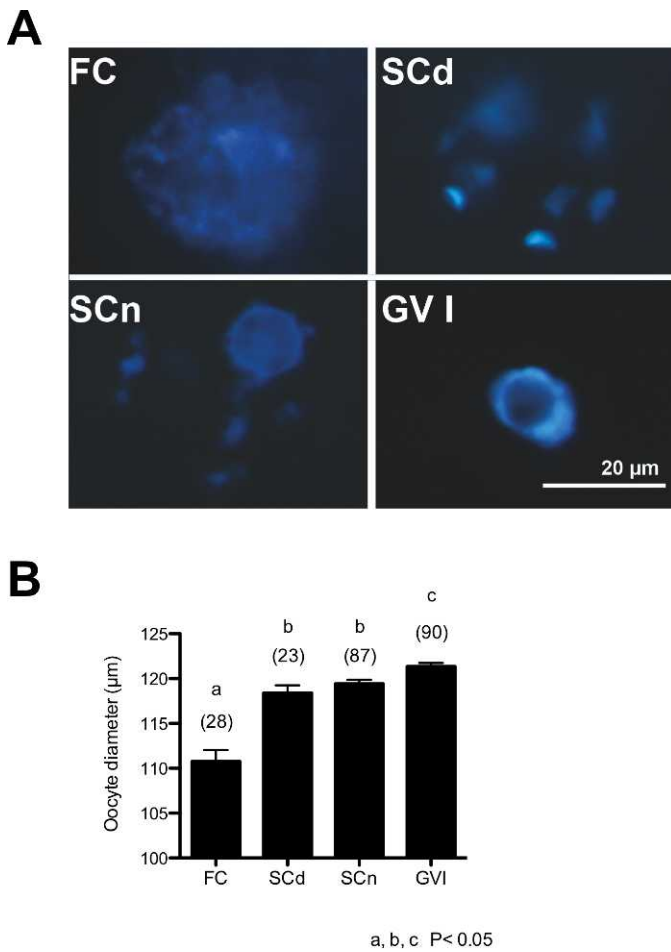* Deg, degenerated.

Article 68

FIG. 3.   **A**) Fluorescent images after Hoechst 33 342 labeling of porcine oocytes at the time of collection with FC (a), SCd (b), SCn (c), and GVI (d) configuration. **B**) GV chromatin configuration in relation to oocyte diameter at the time of collection. A total of 228 oocytes were used in these experiments. Number of oocytes analyzed in each group is indicated in the graph. Mean diameter values, for each GV category, are expressed as means ± SE. Data were analyzed by ANOVA followed by the Tukey multiple comparison test. Superscript letters indicate significant differences between groups ($P < 0.05$).

EAFs were characterized by an FC pattern. This configuration significantly decreased in oocytes isolated from MAFs ($P < 0.05$). No differences were observed in the percentage of oocytes with the SCd configuration between the two follicular classes, while the frequencies of SCn and GVI oocytes were significantly higher in MAFs than in EAFs. Few of the oocytes collected from MAFs showed early signs of GVBD (GVII–GVIV stages; see below), as already reported [44].

After 18 h of culture in dIVM medium, we observed an increase of the oocytes that showed typical features of early GVBD (Table 2), as previously described by Motlik and Fulka

[31], and oocytes were classified as GVII–IV stages accordingly (Fig. 4). Some of these oocytes were also present at the time of collection, as previously reported [44]. In these oocytes, signs of condensation and individualization of filamentous bivalents were detectable. Moreover, in some oocytes, chromosomes were arranged in pro-metaphase I (pro-MI) and metaphase I (MI) plate (Fig. 4).

To further confirm that SC and GVII–GVIV configurations were different, and more precisely that GVII–GVIV are typical configurations that occur between removal of the COC from the follicle (i.e., when spontaneous meiotic resumption occurs) and GVBD, we conducted immunofluorescent staining of H3-S28 and MPM2 at the time of collection and after 24 h of culture, as these have been indicated as markers of meiotic progression [32, 39–43, 49]. Under our conditions, H3 started to be phosphorylated at pro-MI, while no differences were observed between SC, GVI, and GVII–GVIV stages (Fig. 5). On the other hand, analysis of MPM2 staining revealed a progressive increase of signal intensity, first in the nuclear and then in the cytoplasmic compartments from SC to pro-MI stages (Fig. 6). Importantly, nuclear FI of GVII–GVIV oocytes was significantly higher than that of SC and GVI oocytes, confirming that GVII–GVIV configurations temporarily follow the GVI stage (Fig. 6C).

Having established the patterns of chromatin configuration changes before and during culture, we were finally able to evaluate the effect of cilostamide treatment on the process of chromatin configuration changes and meiotic progression. COCs were cultured for 18 and 24 h in dIVM medium supplemented with 0 (control) or 1 μM cilostamide. At the end of the culture periods, oocytes were freed of cumulus cells, stained with Hoechst 33 342, and analyzed. As shown in Table 2, after 24 h of culture, significantly fewer oocytes progressed to the pro-MI–MI stages in the cilostamide-treated group when compared to the control group. Accordingly, the percentages of GVI and GVII–GVIV oocytes were significantly higher in the cilostamide-treated group, indicating that meiotic resumption had been delayed by the treatment.

Effect of Cilostamide Treatment on Embryonic Developmental Competence

In order to assess the effect of cilostamide treatment on the embryonic developmental competence of porcine oocytes, COCs were cultured for 44 h in dIVM medium (control) or for 24 h in dIVM medium in the presence of 1 μM cilostamide, and then washed and cultured for an additional 20 h in dIVM medium. After the culture period, matured oocytes were treated for PA or SCNT procedures.

As shown in Table 3, cleavage rate after PA of cilostamide-treated oocytes did not differ significantly from the control group. Moreover, no differences were observed between treatments in the percentage of PA embryos that developed to the blastocyst stage after 7 days of culture. Interestingly however, the frequency of expanded blastocyst in the

TABLE 2.   Effect of 1 μM cilostamide treatment on chromatin configuration remodeling and meiotic progression.*

Treatment	N	FC (%)	SCd (%)	SCn (%)	GVI (%)	GVII–GVIV (%)	Pro-MI–MI (%)	Deg (%)
18 h CTRL	80	0 (0.0)	1 (1.3)	6 (7.5)	26 (32.5)	31 (38.8)	14 (17.5)	2 (2.5)
18 h CILO	82	0 (0.0)	5 (6.1)	14 (17.1)	26 (31.7)	24 (29.3)	8 (9.8)	5 (6.1)
24 h CTRL	89	0 (0.0)	5 (5.6)	1 (1.1)	8 (9.0)[a]	12[a] (13.5)	62 (69.7)[a]	1 (1.1)
24 h CILO	86	0 (0.0)	4 (4.7)	6 (7.0)	21 (24.4)[b]	29[b] (33.7)	22 (25.6)[b]	4 (4.7)

[a,b] Different letters within columns indicate significant differences (Fisher exact test, $P < 0.05$).
* CILO, cilostamide; CTRL, control; Deg, degenerated.

5   Article 68
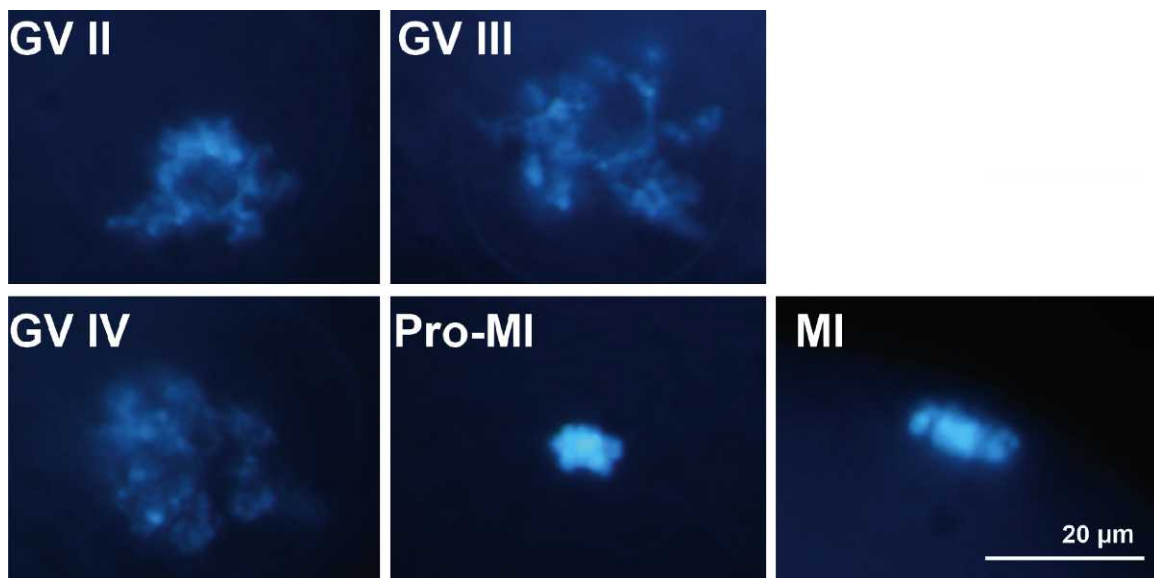
FIG. 4. Representative fluorescent images after Hoechst 33 342 labeling of porcine oocytes with GVII, GVIII, GVIV, pro-MI, and MI configurations after meiotic resumption.

cilostamide-treated group was significantly higher when compared to the control group, whereas there was no significant effect of cilostamide treatment on PA blastocyst cell number.

As shown in Table 4, the cleavage and BLs, as well as the frequency of expanded blastocyst after SCNT treatment, were similar in the control and cilostamide-treated groups. However, the mean cell numbers per blastocyst were significantly higher in the cilostamide-treated group when compared to the control group.

DISCUSSION

The present study demonstrates that inhibition of PDE activity during COC recovery by IBMX, and during the following 24 h of culture with cilostamide in defined serum-free medium, is able to delay meiotic resumption while prolonging functional coupling between oocytes and cumulus cells; importantly, these conditions improved the developmental capability of pig oocytes. The increased oocyte developmental competence is reflected in the enhancement of blastocyst quality based upon expansion capability after PA (cytoplasmic competence), and an increased cell number per blastocyst after SCNT, compared with control groups. The immediate implication of these findings is that improved quality of transferred embryos would materially enhance the overall efficiency of SCNT, which is currently low, with the average yield of live births per embryo transferred being no more than 1%–5% [4, 6, 50–53]. This hypothesis is currently under investigation in our laboratories. Nevertheless, to the best of our knowledge, this is the first study reporting the use of cilostamide to improve pig SCNT efficiency.

Several cultural strategies have been proposed to improve oocyte quality in different mammals (for a review see Refs. 14, 54). Many of these strategies, often referred to as "prematuration culture," are based on the temporary blockage of oocyte spontaneous meiotic resumption by modulating intraoocyte cAMP content with different agents, such as cAMP analogs or PDE inhibitors [12, 16, 20–22, 55–67]. Our results on the effect of the use of PDE inhibitors on meiotic resumption are largely supportive of previous data in prepubertal gilts in which cilostamide or other PDE3 inhibitors, such as milrinone, have been used [17, 67, 68]. Effects of cilostamide treatments on in vitro developmental potential have been tested in human [20, 21, 63], cow [22, 64], sheep [65], and mouse [56, 62, 64, 69], with different outcomes depending on the species, the time of COC incubation with cilostamide, the combination with other

TABLE 3. Effect of 1 μM cilostamide treatment on embryonic developmental competence after parthenogenetic activation.*

Treatment	N	Cleaved (%)	Blastocyst (%)	Expanded blastocyst of total blastocyst (%)	Mean cell number per blastocyst ± SEM
CTRL	150	132 (88.0)	77 (51.3)	35 (45.5)[a]	23 ± 1.21
CILO	142	120 (84.5)	59 (41.5)	38 (64.4)[b]	26 ± 1.44

[a,b] Different letters within columns indicate significant differences (Fisher exact test, $P < 0.05$)
* CILO, cilostamide; CTRL, control.

TABLE 4. Effect of 1 μM cilostamide treatment on embryonic developmental competence after somatic cell nuclear transfer.*

Treatment	N	Cleaved (%)	Blastocyst (%)	Expanded blastocyst of total blastocyst (%)	Mean cell number per blastocyst ± SEM
CTRL	163	98 (60.1)	27 (16.6)	18 (66.7)	45 ± 3.35[a]
CILO	161	84 (52.2)	25 (15.5)	21 (84.0)	58 ± 4.9[b]

[a,b] Different letters within columns indicate significant differences (Fisher exact test, $P < 0.05$).
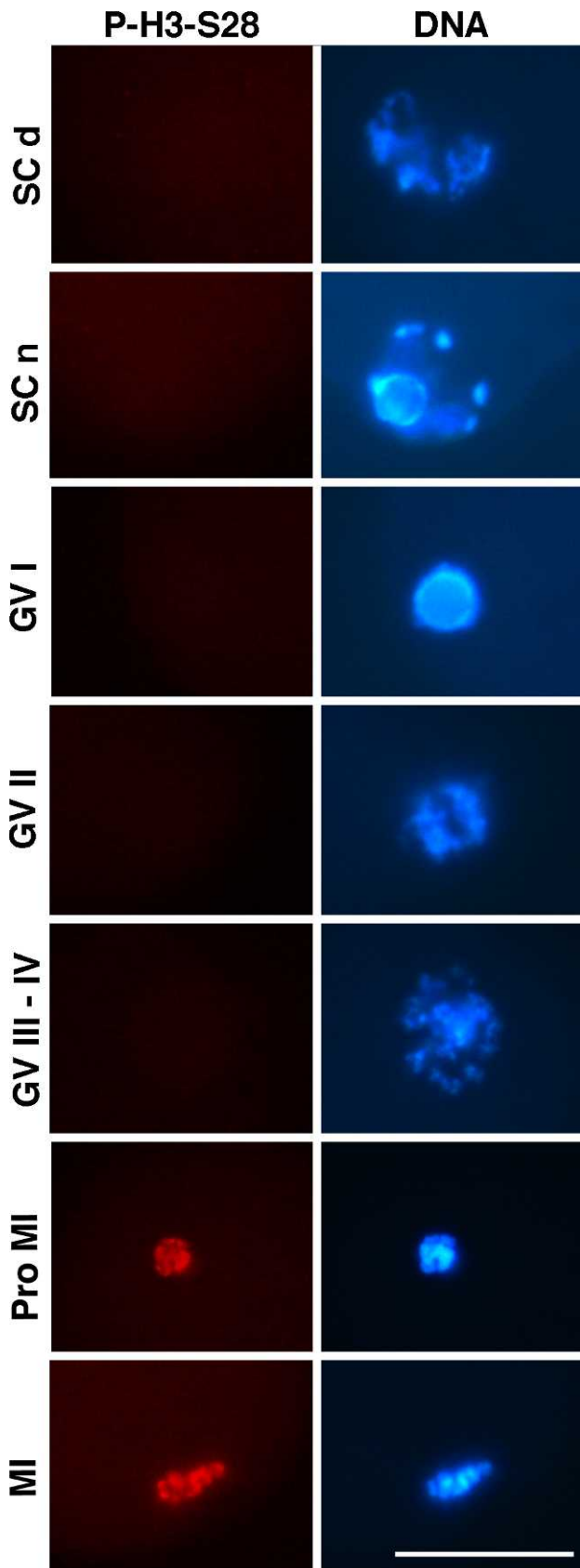* CILO, cilostamide; CTRL, control.

FIG. 5. Representative images showing the status of histone H3-S28 phosphorylation (P-H3-S28) in porcine oocyte with different chromatin configurations and during early stages of meiotic maturation. Red, P-H3-S28; blue, DNA. Scale bar = 50 μm. No differences were observed in oocytes fixed either in paraformaldehyde or in microtubule-stabilizing fixative.

agents, and the experimental approach itself. In some cases, substantial differences exist among treatments, making it difficult to compare their efficacies. However, an important aspect that must be considered is the actual growth and differentiation stage of the immature oocytes subjected to the cilostamide-based treatment, since oocytes with different metabolic properties may require different cultural conditions [29]. Moreover the source of the ovaries needs to be taken into account. In pigs, for examples, many studies have used prepubertal gilts [17, 67, 68], while others, including the present study, have used pubertal animals as the source of ovaries.

In general, the aim of the PMC is to allow the oocytes to complete those processes that are interrupted once they are removed from the follicular environment [14, 29] (i.e., the oocyte growth phase, for those oocytes collected from preantral or EAFs, and/or the so called ''capacitation'' process, that is the acquisition of the cytoplasmic machinery necessary to fully support preimplantation embryo development). These processes normally occur in fully grown oocytes when the follicles approach the preovulatory stage in vivo [9]. Therefore, fully grown oocytes at advanced stages of differentiation would not benefit from a protracted period of IVC [29, 70]. As a consequence, PMC with cilostamide generally improves the yield (% of embryo obtained) of oocytes at early stages of their development [21, 22, 56, 62], while it increases the quality of the embryos obtained from oocytes at more advanced stages of their differentiation, collected from midsized antral follicles, without a significant increase in the embryo rate [20, 65, 71]. Accordingly, in the present study, similar outcomes on the quality of SCNT embryos are reported. In fact, oocytes used in this study are to be considered to have been at advanced stages of development. This is demonstrated by the analysis of the chromatin configuration at the time of collection, which is a marker of the oocyte differentiation state [29]. It indeed revealed that this population of oocytes did not contain growing oocytes with the FC configuration, while around 30% of the oocytes had already acquired the GVI configuration, in which the chromatin has reached its most compacted state before spontaneous meiotic resumption at the time of oocyte removal from the follicle (see Ref. 32 and the present study). Therefore, this heterogeneity could account at least in part for the unchanged percentage of embryos obtained from treated oocytes when compared to the control groups. This supports the original data in mice where the authors tested the effect of PDE3 inhibitor Org 9935 on the developmental competence of oocytes that were retrieved 24 h after gonadotropin injection, when the antral follicles were not yet fully developed. Importantly, the proportion of oocytes with condensed chromatin (SN configuration) was lower at 24 h compared with 48 h after eCG priming, and the arrest in vitro allowed the transition from uncondensed (NSN configuration) to SN configuration in the oocyte nucleus, which was associated with a significant increase in embryonic developmental competence [56].

To date, the only cilostamide-based treatment that substantially improved oocyte developmental outcomes, with a very high embryo yield, is the ''simulated physiological oocyte maturation,'' the so-called ''SPOM'' system, proposed by R.B. Gilchrist's group in mouse and cow [64]. In this system, COCs are incubated for 1–2 h with cAMP modulating agents (IBMX and the adenylate cyclase activator Forskolin), followed by an extended IVM phase containing FSH and cilostamide for the entire culture period. As indicated by the authors, starting from the idea that specific PDE subtypes differentially exert their function within the somatic and the germ cell compartments in
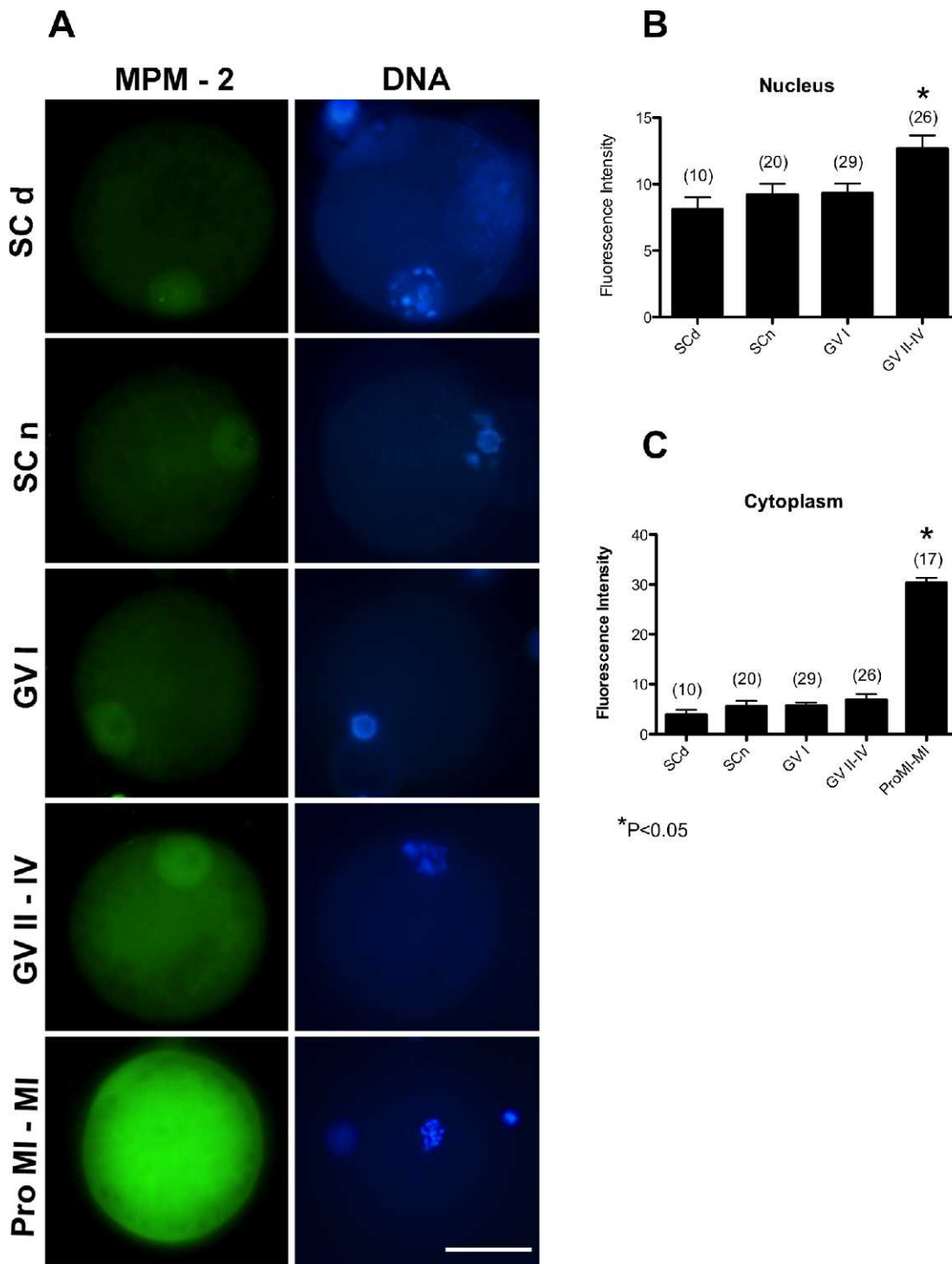
FIG. 6. **A)** Representative images showing the pattern of tyrosine phospho-protein changes (MPM2 staining) in porcine oocyte with different chromatin configurations and during early stages of meiotic maturation. Green, MPM2; blue, DNA. Scale bar = 50 μm. **B** and **C**) Histograms indicate the FI of MPM2 signal within the nuclear (**B**) or cytoplasmic (**C**) area according to the chromatin configuration changes at the time of collection and during early stages of meiotic maturation. Values are expressed as means ± SE. Data were analyzed with ANOVA followed by the Tukey multiple comparison test. Number of oocytes analyzed in each group is indicated. Asterisk indicates significant differences between classes ($P < 0.05$).

rodents [18] and cow [15, 72], the SPOM is specifically designed to target initially both cumulus cell and oocyte PDEs, by using the nonspecific PDE inhibitor IBMX, and then the oocyte PDE only, by using the PDE3-specific inhibitor cilostamide [64]. On the contrary pigs express PDE3 also in the cumulus cells [19]. Therefore, our cultural approach uses a

''biphasic'' system in which cilostamide is present only during the first 24 h of culture, and where its concentration is reduced by 10–20 fold compared to the that used in bovine systems [22, 64], but that is able, at the same time, to delay meiotic resumption at the same extent obtained with higher concentrations (20 μM) used in previous works in pig [17, 68].

Importantly, cilostamide treatment in our system promotes the maintenance of a proper functional coupling between oocyte and cumulus cells up to 24 h, confirming previous results in the bovine model [13, 22], which exerts, in turn, a positive effect on oocyte quality. We hypothesize that enhanced coupling during IVC could stimulate the bidirectional transfer of essential molecules for the attainment of full developmental competence. However, further studies are needed to understand the precise nature of these molecules.

Our previous studies in cows suggest that the maintenance of a proper functional oocyte-cumulus cell coupling is essential for an orderly remodeling of chromatin during the G2/M cell cycle transition during IVC [22, 29]. In fact, when bovine COCs from EAFs, in which chromatin is mostly decondensed (GV0; [25, 26]), are cultivated in vitro in a system that promotes the maintenance of a patent bidirectional coupling, the chromatin gradually organizes into a configuration with a higher degree of condensation (GV1), thus acquiring the ability to mature and be fertilized in vitro [22]. In the present study, a direct relationship between the maintenance of GJC and the chromatin remodeling process before meiotic resumption could not be properly determined. More precisely, the synchronization in GVI configuration could not be directly verified. This is mainly due to the fact that meiosis is delayed by approximately 6 h, but not completely blocked. At 18 and 24 h of culture, oocytes in both control and cilostamide groups already presented signs of meiotic resumption, being in GVII–GVIV stages or having reached pro-MI stages. However, we could only speculate that, at some point before the 18th h of culture, most of the oocytes synchronize at the GVI stage. On the other hand, since meiotic progression is delayed, chromatin/chromosome rearrangements during the first 24 h of culture are slowed down in the cilostamide group. We cannot exclude that this could account, in part, for the increased quality of these oocytes. However, this hypothesis remains to be rigorously tested.

In this context, it is very important to point out that the present study confirms that GVII–GVIV configurations in pig are typical of oocytes that have already resumed meiosis, even though the nuclear envelope is still detectable and the chromatin is condensing into bivalents that will ultimately become fully condensed metaphase chromosomes. It is worth noting that the expression ''GV stage,'' commonly used by investigators to indicate the stage at which the oocyte is collected from the ovarian follicle (or even the period when the GV is clearly detectable within the oocyte before GVBD occurs), should not to be confused with the phase of meiotic arrest, since meiotic resumption is initiated well ahead of the disappearance of the nuclear envelope [73]. Therefore, even though GVBD is the first grossly obvious manifestation of meiotic resumption, these two events should not to be considered equivalent [29]. That GVII–GVIV configurations represent early signs of meiotic resumption in pig is indicated by original experiments by Motlik and Fulka, who indeed proposed this classification [73]. In their work, using aceto-orcein staining, the authors describe GVII–GVIV as those configurations that characterize early stages of in vivo maturation and IVM, and that precede the complete disappearance of the nuclear envelope [73]. This classification was further confirmed by Hirao et al. [44], who, studying oocytes collected from follicles of different diameters, introduced the SC configuration as the one preceding the GVI stage. Finally immunofluorescence studies by Bui et al. [32] further confirm the above ''temporal'' stage progression showing that the phosphorylation of histone H3-S28 is first detected in condensing chromosomes at the GVII–GVIV stages [32].

Since chromosome condensation begins at this point, the authors suggest that H3-S28 phosphorylation might be one of the key events initiating meiotic chromosome condensation [32]. Because, under our experimental conditions, H3-S28 phosphorylation was not detected in GVII–GVIV oocytes, we employed another G2/M cell cycle marker to test whether the chromatin configurations observed in GVII–GVIV stages are truly indicative of meiotic resumption. Therefore, SC and GVII–GVIV stages must be carefully evaluated to avoid misinterpretation of experimental data. Moreover, identification of additional unequivocal biomarkers will aid in discerning the events that are critical to establishing oocyte quality during IVM.

In conclusion, the present work demonstrates that delaying the timing of GJC interruption while slowing down early meiotic progression has a long-acting effect on the developmental program of the oocyte. Our results contribute to our understanding of the mechanisms regulating oocyte maturation and the acquisition of developmental competence, and offer intriguing tools for further studies.

REFERENCES

1. Prather RS, Hawley RJ, Carter DB, Lai L, Greenstein JL. Transgenic swine for biomedicine and agriculture. Theriogenology 2003; 59:115–123.
2. Sachs DH, Galli C. Genetic manipulation in pigs. Curr Opin Organ Transplant 2009; 14:148–153.
3. Aigner B, Renner S, Kessler B, Klymiuk N, Kurome M, Wunsch A, Wolf E. Transgenic pigs as models for translational biomedical research. J Mol Med (Berl) 2010; 88:653–664.
4. Galli C, Lagutina I, Perota A, Colleoni S, Duchi R, Lucchini F, Lazzari G. Somatic cell nuclear transfer and transgenesis in large animals: current and future insights. Reprod Domest Anim 2012; 47(suppl 3):2–11.
5. Luo Y, Lin L, Bolund L, Jensen TG, Sorensen CB. Genetically modified pigs for biomedical research. J Inherit Metab Dis 2012; 35:695–713.
6. Nagashima H, Matsunari H, Nakano K, Watanabe M, Umeyama K, Nagaya M. Advancing pig cloning technologies towards application in regenerative medicine. Reprod Domest Anim 2012; 47(suppl 4):120–126.
7. Niemann H, Lucas-Hahn A. Somatic cell nuclear transfer cloning: practical applications and current legislation. Reprod Domest Anim 2012; 47(suppl 5):2–10.
8. Pincus G, Enzmann EV. The comparative behavior of mammalian eggs in vivo and in vitro: I. The activation of ovarian eggs. J Exp Med 1935; 62:665–675.
9. Hyttel P, Fair T, Callesen H, Greve T. Oocyte growth, capacitation and final maturation in cattle. Theriogenology 1997; 47:23–32.
10. Luciano AM, Pocar P, Milanesi E, Modina S, Rieger D, Lauria A, Gandolfi F. Effect of different levels of intracellular cAMP on the in vitro maturation of cattle oocytes and their subsequent development following in vitro fertilization. Mol Reprod Dev 1999; 54:86–91.
11. Ponderato N, Crotti G, Turini P, Duchi R, Galli C, Lazzari G. Embryonic and foetal development of bovine oocytes treated with a combination of butyrolactone I and roscovitine in an enriched medium prior to IVM and IVF. Mol Reprod Dev 2002; 62:513–518.
12. Luciano AM, Modina S, Vassena R, Milanesi E, Lauria A, Gandolfi F. Role of intracellular cyclic adenosine 3′,5′-monophosphate concentration and oocyte-cumulus cells communications on the acquisition of the developmental competence during in vitro maturation of bovine oocyte. Biol Reprod 2004; 70:465–472.
13. Thomas RE, Armstrong DT, Gilchrist RB. Bovine cumulus cell-oocyte gap junctional communication during in vitro maturation in response to manipulation of cell-specific cyclic adenosine 3′,5′-monophosphate levels. Biol Reprod 2004; 70:548–556.
14. Gilchrist RB, Thompson JG. Oocyte maturation: emerging concepts and technologies to improve developmental potential in vitro. Theriogenology 2007; 67:6–15.
15. Mayes MA, Sirard MA. Effect of type 3 and type 4 phosphodiesterase

inhibitors on the maintenance of bovine oocytes in meiotic arrest. Biol Reprod 2002; 66:180–184.

16. Lodde V, Franciosi F, Tessaro I, Modina SC, Luciano AM. Role of gap junction-mediated communications in regulating large-scale chromatin configuration remodeling and embryonic developmental competence acquisition in fully grown bovine oocyte. J Assist Reprod Genet; (in press). Published online ahead of print 24 July 2013; DOI:10.1007/s10815-013-0061-7.

17. Sasseville M, Cote N, Guillemette C, Richard FJ. New insight into the role of phosphodiesterase 3A in porcine oocyte maturation. BMC Dev Biol 2006; 6:47.

18. Tsafriri A, Chun SY, Zhang R, Hsueh AJ, Conti M. Oocyte maturation involves compartmentalization and opposing changes of cAMP levels in follicular somatic and germ cells: studies using selective phosphodiesterase inhibitors. Dev Biol 1996; 178:393–402.

19. Sasseville M, Cote N, Vigneault C, Guillemette C, Richard FJ. 3′5′-cyclic adenosine monophosphate-dependent up-regulation of phosphodiesterase type 3A in porcine cumulus cells. Endocrinology 2007; 148:1858–1867.

20. Shu YM, Zeng HT, Ren Z, Zhuang GL, Liang XY, Shen HW, Yao SZ, Ke PQ, Wang NN. Effects of cilostamide and forskolin on the meiotic resumption and embryonic development of immature human oocytes. Hum Reprod 2008; 23:504–513.

21. Vanhoutte L, Nogueira D, Dumortier F, De Sutter P. Assessment of a new in vitro maturation system for mouse and human cumulus-enclosed oocytes: three-dimensional premature culture in the presence of a phosphodiesterase 3-inhibitor. Hum Reprod 2009; 24:1946–1959.

22. Luciano AM, Franciosi F, Modina SC, Lodde V. Gap junction-mediated communications regulate chromatin remodeling during bovine oocyte growth and differentiation through cAMP-dependent mechanism(s). Biol Reprod 2011; 85:1252–1259.

23. Zuccotti M, Rossi PG, Martinez A, Garagna S, Forabosco A, Redi CA. Meiotic and developmental competence of mouse antral oocytes. Biol Reprod 1998; 58:700–704.

24. Zuccotti M, Ponce RH, Boiani M, Guizzardi S, Govoni P, Scandroglio R, Garagna S, Redi CA. The analysis of chromatin organisation allows selection of mouse antral oocytes competent for development to blastocyst. Zygote 2002; 10:73–78.

25. Lodde V, Modina S, Galbusera C, Franciosi F, Luciano AM. Large-scale chromatin remodeling in germinal vesicle bovine oocytes: interplay with gap junction functionality and developmental competence. Mol Reprod Dev 2007; 74:740–749.

26. Lodde V, Modina S, Maddox-Hyttel P, Franciosi F, Lauria A, Luciano AM. Oocyte morphology and transcriptional silencing in relation to chromatin remodeling during the final phases of bovine oocyte growth. Mol Reprod Dev 2008; 75:915–924.

27. Lodde V, Modina SC, Franciosi F, Zuccari E, Tessaro I, Luciano AM. Localization of DNA methyltransferase-1 during oocyte differentiation, in vitro maturation and early embryonic development in cow. Eur J Histochem 2009; 53(4):e24.

28. Luciano AM, Lodde V, Franciosi F, Tessaro I, Corbani D, Modina S. Large-scale chromatin morpho-functional changes during mammalian oocyte growth and differentiation. Eur J Histochem 2012; 56:e37.

29. Luciano AM, Lodde V. Changes of large-scale chromatin configuration during mammalian oocyte differentiation. In: Coticchio G, Albertini DF, De Santis L (eds.), Oogenesis. London: Springer; 2013:93–108.

30. Aktas H, Wheeler MB, First NL, Leibfried-Rutledge ML. Maintenance of meiotic arrest by increasing [cAMP]i may have physiological relevance in bovine oocytes. J Reprod Fertil 1995; 105:237–245.

31. Motlik J, Fulka J. Breakdown of the germinal vesicle in pig oocytes in vivo and in vitro. J Exp Zool 1976; 198:155–162.

32. Bui HT, Van Thuan N, Kishigami S, Wakayama S, Hikichi T, Ohta H, Mizutani E, Yamaoka E, Wakayama T, Miyano T. Regulation of chromatin and chromosome morphology by histone H3 modifications in pig oocytes. Reproduction 2007; 133:371–382.

33. Abramoff MD, Magelhaes PJ. Image processing with ImageJ. Biophotonics Int 2004; 11:36–42.

34. Tervit HR, Whittingham DG, Rowson LE. Successful culture in vitro of sheep and cattle ova. J Reprod Fertil 1972; 30:493–497.

35. Lagutina I, Lazzari G, Galli C. Birth of cloned pigs from zona-free nuclear transfer blastocysts developed in vitro before transfer. Cloning Stem Cells 2006; 8:283–293.

36. Yoshioka K, Suzuki C, Tanaka A, Anas IM, Iwamura S. Birth of piglets derived from porcine zygotes cultured in a chemically defined medium. Biol Reprod 2002; 66:112–119.

37. Vajta G, Lewis IM, Trounson AO, Purup S, Maddox-Hyttel P, Schmidt M, Pedersen HG, Greve T, Callesen H. Handmade somatic cell cloning in

38. cattle: analysis of factors contributing to high efficiency in vitro. Biol Reprod 2003; 68:571–578.

38. Vajta G, Peura TT, Holm P, Paldi A, Greve T, Trounson AO, Callesen H. New method for culture of zona-included or zona-free embryos: the Well of the Well (WOW) system. Mol Reprod Dev 2000; 55:256–264.

39. Wickramasinghe D, Ebert KM, Albertini DF. Meiotic competence acquisition is associated with the appearance of M-phase characteristics in growing mouse oocytes. Dev Biol 1991; 143:162–172.

40. Messinger SM, Albertini DF. Centrosome and microtubule dynamics during meiotic progression in the mouse oocyte. J Cell Sci 1991; 100(pt 2):289–298.

41. Sanfins A, Lee GY, Plancha CE, Overstrom EW, Albertini DF. Distinctions in meiotic spindle structure and assembly during in vitro and in vivo maturation of mouse oocytes. Biol Reprod 2003; 69:2059–2067.

42. McGinnis LK, Albertini DF, Kinsey WH. Localized activation of Src-family protein kinases in the mouse egg. Dev Biol 2007; 306:241–254.

43. McGinnis LK, Albertini DF. Dynamics of protein phosphorylation during meiotic maturation. J Assist Reprod Genet 2010; 27:169–182.

44. Hirao Y, Tsuji Y, Miyano T, Okano A, Miyake M, Kato S, Moor RM. Association between p34cdc2 levels and meiotic arrest in pig oocytes during early growth. Zygote 1995; 3:325–332.

45. Nagai T, Ebihara M, Onishi A, Kubo M. Germinal vesicle stages in pig follicular oocytes collected by different methods. J Reprod Dev 1997; 43:339–343.

46. Guthrie HD, Garrett WM. Changes in porcine oocyte germinal vesicle development as follicles approach preovulatory maturity. Theriogenology 2000; 54:389–399.

47. Sun XS, Liu Y, Yue KZ, Ma SF, Tan JH. Changes in germinal vesicle (GV) chromatin configurations during growth and maturation of porcine oocytes. Mol Reprod Dev 2004; 69:228–234.

48. Endo T, Naito K, Aoki F, Kume S, Tojo H. Changes in histone modifications during in vitro maturation of porcine oocytes. Mol Reprod Dev 2005; 71:123–128.

49. Bui HT, Yamaoka E, Miyano T. Involvement of histone H3 (Ser10) phosphorylation in chromosome condensation without Cdc2 kinase and mitogen-activated protein kinase activation in pig oocytes. Biol Reprod 2004; 70:1843–1851.

50. Kurome M, Hisatomi H, Matsumoto S, Tomii R, Ueno S, Hiruma K, Saito H, Nakamura K, Okumura K, Matsumoto M, Kaji Y, Endo F, et al. Production efficiency and telomere length of the cloned pigs following serial somatic cell nuclear transfer. J Reprod Dev 2008; 54:254–258.

51. Matsunari H, Onodera M, Tada N, Mochizuki H, Karasawa S, Haruyama E, Nakayama N, Saito H, Ueno S, Kurome M, Miyawaki A, Nagashima H. Transgenic-cloned pigs systemically expressing red fluorescent protein, Kusabira-Orange. Cloning Stem Cells 2008; 10:313–323.

52. Petersen B, Lucas-Hahn A, Oropeza M, Hornen N, Lemme E, Hassel P, Queisser AL, Niemann H. Development and validation of a highly efficient protocol of porcine somatic cloning using preovulatory embryo transfer in peripubertal gilts. Cloning Stem Cells 2008; 10:355–362.

53. Zhao J, Ross JW, Hao Y, Spate LD, Walters EM, Samuel MS, Rieke A, Murphy CN, Prather RS. Significant improvement in cloning efficiency of an inbred miniature pig by histone deacetylase inhibitor treatment after somatic cell nuclear transfer. Biol Reprod 2009; 81:525–530.

54. Bilodeau-Goeseels S. Bovine oocyte meiotic inhibition before in vitro maturation and its value to in vitro embryo production: does it improve developmental competence? Reprod Domest Anim 2012; 47:687–693.

55. Guixue Z, Luciano AM, Coenen K, Gandolfi F, Sirard MA. The influence of cAMP before or during bovine oocyte maturation on embryonic developmental competence. Theriogenology 2001; 55:1733–1743.

56. Nogueira D, Cortvrindt R, De Matos DG, Vanhoutte L, Smitz J. Effect of phosphodiesterase type 3 inhibitor on developmental competence of immature mouse oocytes in vitro. Biol Reprod 2003; 69:2045–2052.

57. Nogueira D, Cortvrindt R, Everaerdt B, Smitz J. Effects of long-term in vitro exposure to phosphodiesterase type-3 inhibitors on follicle and oocyte development. Reproduction 2005; 130:177–186.

58. Nogueira D, Ron-El R, Friedler S, Schachter M, Raziel A, Cortvrindt R, Smitz J. Meiotic arrest in vitro by phosphodiesterase 3-inhibitor enhances maturation capacity of human oocytes and allows subsequent embryonic development. Biol Reprod 2006; 74:177–184.

59. Sa Barretto LS, Castro VS, Garcia JM, Mingoti GZ. Meiotic inhibition of bovine oocytes in medium supplemented with a serum replacer and hormones: effects on meiosis progression and developmental capacity. Zygote 2011; 19:107–116.

60. Thomas RE, Thompson JG, Armstrong DT, Gilchrist RB. Effect of specific phosphodiesterase isoenzyme inhibitors during in vitro maturation

of bovine oocytes on meiotic and developmental capacity. Biol Reprod 2004; 71:1142–1149.

61. Vanhoutte L, Nogueira D, De Sutter P. Prematuration of human denuded oocytes in a three-dimensional co-culture system: effects on meiosis progression and developmental competence. Hum Reprod 2009; 24: 658–669.

62. Vanhoutte L, Nogueira D, Gerris J, Dhont M, De Sutter P. Effect of temporary nuclear arrest by phosphodiesterase 3-inhibitor on morphological and functional aspects of in vitro matured mouse oocytes. Mol Reprod Dev 2008; 75:1021–1030.

63. Vanhoutte L, De Sutter P, Nogueira D, Gerris J, Dhont M, Van der Elst J. Nuclear and cytoplasmic maturation of in vitro matured human oocytes after temporary nuclear arrest by phosphodiesterase 3-inhibitor. Hum Reprod 2007; 22:1239–1246.

64. Albuz FK, Sasseville M, Lane M, Armstrong DT, Thompson JG, Gilchrist RB. Simulated physiological oocyte maturation (SPOM): a novel in vitro maturation system that substantially improves embryo yield and pregnancy outcomes. Hum Reprod 2010; 25:2999–3011.

65. Rose RD, Gilchrist RB, Kelly JM, Thompson JG, Sutton-McDowall ML. Regulation of sheep oocyte maturation using cAMP modulators. Theriogenology 2013; 79:142–148.

66. Zeng HT, Ren Z, Guzman L, Wang X, Sutton-McDowall ML, Ritter LJ, De Vos M, Smitz J, Thompson JG, Gilchrist RB. Heparin and cAMP modulators interact during pre-in vitro maturation to affect mouse and human oocyte meiosis and developmental competence. Hum Reprod 2013; 28(6):1536–1545.

67. Grupen CG, Fung M, Armstrong DT. Effects of milrinone and butyrolactone-I on porcine oocyte meiotic progression and developmental competence. Reprod Fertil Dev 2006; 18:309–317.

68. Laforest MF, Pouliot E, Gueguen L, Richard FJ. Fundamental significance of specific phosphodiesterases in the control of spontaneous meiotic resumption in porcine oocytes. Mol Reprod Dev 2005; 70:361–372.

69. Jee BC, Chen HY, Chian RC. Effect of a phosphodiesterase type 3 inhibitor in oocyte maturation medium on subsequent mouse embryo development. Fertil Steril 2009; 91:2037–2042.

70. Nogueira D, Vanhoutte L. Use of phosphodiesterase type 3 inhibitor to improve IVM outcome: experimental set up matters. Fertil Steril 2009; 91:e3 (author reply e4–e5).

71. Wu D, Cheung QC, Wen L, Li J. A growth-maturation system that enhances the meiotic and developmental competence of porcine oocytes isolated from small follicles. Biol Reprod 2006; 75:547–554.

72. Thomas RE, Armstrong DT, Gilchrist RB. Differential effects of specific phosphodiesterase isoenzyme inhibitors on bovine oocyte meiotic maturation. Dev Biol 2002; 244:215–225.

73. Motlik J, Crozet N, Fulka J. Meiotic competence in vitro of pig oocytes isolated from early antral follicles. J Reprod Fertil 1984; 72:323–328.

Chromatin Remodelling and Histone mRNA Accumulation in Bovine Germinal Vesicle Oocytes

R. LABRECQUE,[1] V. LODDE,[2] C. DIECI,[2] I. TESSARO,[2] A. M. LUCIANO[2], AND M. A. SIRARD[1,3]*

[1] Département des Sciences Animales, Centre de Recherche en Biologie de la Reproduction, Université Laval, Québec, Québec, Canada

[2] Reproductive and Developmental Biology Laboratory, Department of Health, Animal Sciences and Food Safety, University of Milan, Milan, Italy

[3] Department of Animal Sciences, Laval University, Québec, Québec, Canada

SUMMARY

Major remodelling of the chromatin enclosed within the germinal vesicle occurs towards the end of oocyte growth in mammals, but the mechanisms involved in this process are not completely understood. In bovine, four distinct stages of chromatin compaction—ranging from a diffused state (GV0) to a fully compacted configuration (GV3)—are linked to the gradual acquisition of developmental potential. To better understand the molecular events and to identify mRNA modulations occurring in the oocyte during the GV0-to-GV3 transition, transcriptomic analysis was performed with the EmbryoGENE microarray platform. The mRNA abundance of several genes decreased as chromatin compaction increased, which correlates with progressive transcriptional silencing that is characteristic of the end of oocyte growth. On the other hand, the abundance of some transcripts increased during the same period, particularly several histone gene transcripts from the H2A, H2B, H3, H4, and linker H1 family. In silico analysis predicted RNA-protein interactions between specific histone transcripts and the bovine stem-loop binding protein 2 (SLBP2), which helps regulate the translation of histone mRNA during oogenesis. These results suggest that some histone-encoding transcripts are actively stored, possibly to sustain the needs of the embryo before genome activation. This dataset offers a unique opportunity to survey which histone mRNAs are needed to complete chromatin compaction during oocyte maturation and which are stockpiled for the first three cell cycles following fertilization.

INTRODUCTION

The germinal-vesicle (GV) oocyte harbours various chromatin configurations during its growth. A diffuse chromatin pattern, frequently termed non-surrounded nucleus (NSN) due to the absence of a compacted ring of chromatin around the nucleolus, can be observed in the mouse oocyte with various DNA staining methods and microscopy techniques; in contrast, the presence of a distinctive ring characterizes the surrounded-nucleolus (SN) configuration (Mattson and Albertini, 1990). Chromatin remodelling has

Abbreviations: GV[BD], germinal vesicle [breakdown]; MAANOVA, microarray analysis of variance; [N]SN, [non-] surrounded nucleus; SLBP, stem-loop binding protein

been observed in oocytes of all mammalian species studied to date, although the patterns vary among species. For example, while the formation of a well-defined ring of chromatin around the nucleolus is a common feature in several species, other configurations have been reported in bovine and equine species, where chromatin is condensed into a single clump that often encapsulates the nucleolus (Lodde et al., 2007; Lodde et al., 2008; Hinrichs, 2010; Franciosi et al., 2012). Species-specific chromatin configurations also appear to correlate with the ability of an immature oocyte to reach the metaphase-II stage and to develop into an embryo (for review see Tan et al. (2009); Luciano and Lodde, (2013).

Different groups have identified progressive states of chromatin compaction in bovine oocytes (Fuhrer et al., 1989; Chohan and Hunter, 2003; Liu et al., 2006). In 2007, Lodde and colleagues proposed a unified classification system consisting of four discrete and progressive stages of chromatin condensation in growing and full-grown bovine oocytes: The chromatin configuration of GV0 stage is characterized by a diffuse, filamentous pattern in the whole nuclear area. GV1 also presents with a diffuse filamentous pattern, but a few foci of condensed chromatin are visible in the nucleus. The GV2 stage contains more chromatin condensation and includes distinct clumps or strands. Finally, GV3 is characterized by the presence of a single clump of compacted chromatin within the nuclear envelope (Lodde et al., 2007). The progressive chromatin compaction in bovine oocytes was later correlated with the sequential acquisition of meiotic and developmental potential (Lodde et al., 2007), progressive transcriptional silencing (Lodde et al., 2008; Luciano et al., 2011), as well as a global increase in DNA methylation (Lodde et al., 2009).

During oocyte growth, a period of intense transcriptional activity is followed by a substantial decrease in RNA synthesis—which in bovine occurs once the oocyte reaches 110 μm in diameter (Fair et al., 1995). Experimental evidence indicates that the complete arrest of transcription occurs only at meiotic resumption since RNA synthesis, although at a very low level, is still detectable 1 hr before germinal vesicle breakdown (GVBD) in the bovine oocyte (Hunter and Moor, 1987). Similar results were reported in the mouse oocyte, where transcription is still detectable between the end of oocyte growth and GVBD (Rodman and Bachvarova, 1976) and transcriptional activity ceases completely only at the time of GVBD (Wassarman and Letourneau, 1976).

Transcriptional activity of the oocyte relates back to the chromatin configuration of the GV. In the mouse, NSN oocytes with a diffused chromatin configuration are still transcriptionally active, whereas SN oocytes with a compacted chromatin do not show any signs of transcriptional activity from RNA polymerase I or II, as assessed by immunofluorescence detection of bromouridine into nascent RNAs (Bouniol-Baly et al., 1999; De La Fuente and Eppig, 2001). Labelling with a radioactive precursor followed by autoradiography revealed intense RNA synthesis activity in bovine GV0 oocytes, while GV1 and GV2 displayed a progressive decrease of transcription, and GV3

was associated with a global repression of transcriptional activity (Lodde et al., 2008). Although chromatin remodelling and transcriptional repression occur simultaneously, data suggest that they are controlled by different mechanisms (De La Fuente et al., 2004). For example, nucleoplasmin 2 (Npm2)-knockout mouse oocytes were unable to transition from the NSN to the SN configuration, even though the repression of transcriptional activity was still observed in pre-ovulatory oocytes (De La Fuente et al., 2004). This suggests that changes in transcriptional machinery instead of chromatin configuration may be responsible for the decrease in transcription (Pan et al., 2005); indeed, reduced expression of transcription factors such as SP1 (Sp1 transcription factor) and TBP (TATA-box binding protein) was observed towards the end of mouse oocyte growth (Worrad et al., 1994).

The accumulation of transcripts that are potentially important for the development of the early embryo is believed to occur mostly during the last phases of oocyte growth. Various transcriptome analysis tools have been used to study this phase in bovine, mouse, and human oocytes to gain a better understanding of the which genes are needed for early development (reviewed in Labrecque and Sirard, 2014). In the mouse, a chromatin-configuration model was used to better understand the molecular changes occurring in the oocyte during the rapid transition from less-condensed to more-compacted stages—e.g. the transcriptomes of NSN and SN immature (Monti et al., 2013) and mature oocytes (Zuccotti et al., 2008) were compared using microarray technologies. The entire transcriptome was more recently interrogated through an RNAseq experiment in which NSN and SN immature mouse oocytes were compared (Ma et al., 2013). Even though all of these studies detected a number of differences in the transcription of several genes that are potentially important for developmental competence, no studies have examined the transcriptome of oocytes in which chromatin condenses gradually.

The aim of our study was to take advantage of the gradual chromatin remodelling process characterized in bovine oocytes (Lodde et al., 2007) to obtain a more refined view of the transcriptome of these oocytes based on their chromatin configuration. These results will help us understand the molecular changes occurring in the oocyte during chromatin remodelling as well as how these changes influence the acquisition of developmental potential.

RESULTS

Microarray Results

The transcriptome of bovine GV-stage oocytes, grouped according to their chromatin configuration (Fig 1), was interrogated by microarray in order to better understand the molecular changes occurring during the chromatin remodelling process. Microarray data were deposited in the National Center for Biotechnology Information (NCBI)'s Gene Expression Omnibus, and are accessible through GEO series accession number GSE48376. After considering the threshold used to detect the presence/absence of
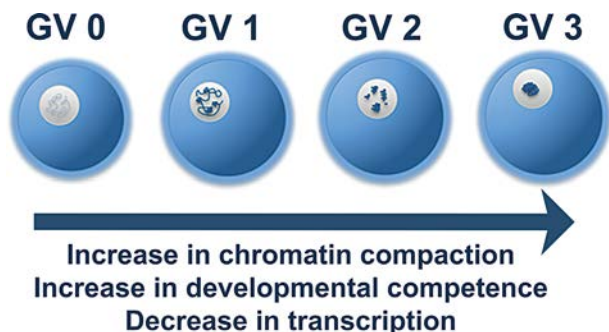
Figure 1. Representation of large-scale chromatin configuration changes in bovine oocytes. Oocytes were classified into four stages based on their chromatin configuration, as assessed with a fluorescence microscope. The GV0 stage is characterized by a diffuse filamentous pattern of chromatin in the whole nuclear area. The GV1 and GV2 configurations represent early and intermediate stages, respectively, of chromatin remodelling, which starts with the appearance of few foci of condensation in GV1 oocytes and proceeds with the formation of distinct clumps of condensed chromatin in GV2 oocytes. The GV3 stage contains the maximum level of condensation, with chromatin organized into a single clump. Modified from Luciano and Lodde (2013). Original fluorescent microscopy images can be found elsewhere (Lodde et al., 2007; Lodde et al., 2008; Lodde et al., 2009; Luciano et al., 2011; Luciano et al., 2012).

probes on the microarray slide, a total of 14,733 probes were detected among the four groups. A between-group analysis (Fig 2) showed that all of the biological replicates (dots) of a group clustered together, even though the GV1 and GV2 groups displayed more variation (increased distance between the dots) compared to GV0 and GV3. The relative distance between each group effectively confirmed that global transcriptional differences exist among the different chromatin configurations.

Microarray analysis of variance (MAANOVA) analysis revealed that 2,792 probes were significantly different ($P < 0.01$) between the chromatin configuration stages. In the first three comparisons (GV0 vs GV1; GV0 vs GV2; and GV0 vs GV3), between 264 and 325 probes had a fold-change difference of more than two (Table 1). The number of probes with a negative fold change across the different comparisons was higher than those with a positive fold change (less than 20% of the probes had a positive fold change (> 2)). Comparison of GV2 vs GV3 revealed 61 significantly different probes, with 51 probes increasing at the GV3 stage (fold change > 2) and only 10 probes decreasing (fold change < -2).

Clustering analysis was performed using all the probes from our microarray analysis to group the probes according to their profile across the different chromatin configurations. Sixteen clusters, representing the main profiles of transcript modulation, were generated (Fig S1 and Table S1). Considering only the 2,792 probes for which the differences were significant between groups, five clusters out of the 16 (♯12, ♯11, ♯8, ♯5, and ♯6) included significantly more probes (Fig 3). In particular, cluster ♯12 included more than 45% of the statistically significant probes; its profile illustrated an

important decrease in transcript abundance between GV0 and GV1, with relatively stable levels in successive chromatin configuration states.

A high proportion of the probes that presented an increased level as the chromatin became more compacted (clusters ♯11, ♯8, and ♯5) were related to histone genes. The microarray platform used in this study included a total of 160 histone-related probes, of which 104 are present in the oocyte. Thirty histone-related probes presented a significantly increased mRNA level as the chromatin became more compacted (MAANOVA, $P < 0.01$) (Table 2). Interestingly, the majority (29/30) of these probes were related to the canonical histones (H2A, H2B, H3, H4, and linker H1). Only one variant was identified (*H3.3*, also known as *H3F3C*), and its fold changes across the various comparisons were small.

Functional Analysis

Functional enrichment analyses were performed with DAVID Bioinformatics resources to gain a better overview of the differences found in the oocyte during chromatin condensation. Gene lists from each of the main clusters or from individual comparisons (fold-change cut-off > 1.5) were submitted to DAVID. The genes included in cluster ♯12 (main decrease between GV0 and GV1) were related to various biological processes such as catabolic process,
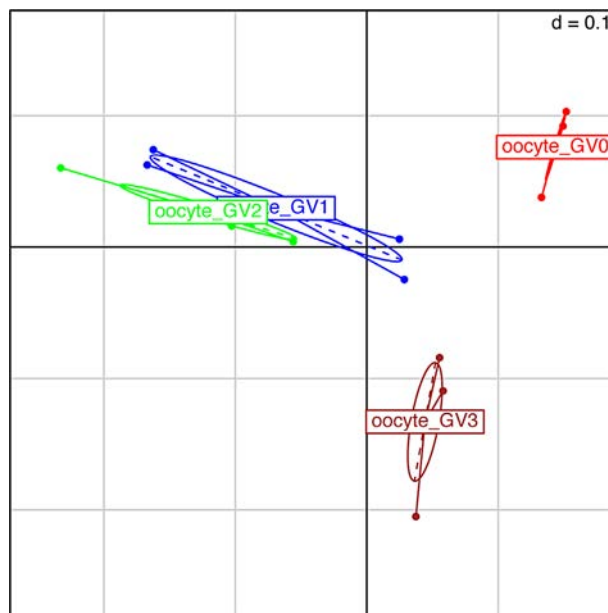
Figure 2. Between-group analysis of the oocyte microarray data. Red, GV0; Blue, GV1; Green, GV2; and Brown, GV3. The plot illustrates the global distribution of transcriptome data from the biological samples (four chromatin configurations) and the four biological replicates (dots in each group). The samples are separated along the axes; the samples that are the most responsible for separation of the groups are those with the highest (or lowest) coordinates along these axes (Culhane et al., 2002).

	fold change > 2 total	fold change >2	fold change < −2
GV0 vs GV1	264	48	216
GV0 vs GV2	325	62	263
GV0 vs GV3	302	44	258

transcription, regulation of apoptosis, and cell proliferation. Genes included in cluster ♯11 (increase at GV1-GV2 followed by a decrease) or cluster ♯8 (increase until GV2) were related to protein transport and protein localization in addition to transcription. Cluster ♯5 (increase at the beginning of chromatin condensation) included genes related to nucleosome assembly, chromatin organization, and DNA packaging (Table S2). Similar results were obtained when gene lists from individual comparisons were used: Transcription was the main molecular function affected in the GV0 vs GV1 and GV0 vs GV2 pairings. In the GV0 vs GV2 pair, however, the process of protein−DNA complex assembly was also significantly affected. Chromosome organization, protein−DNA complex assembly, DNA packaging, and transcription were the main functions affected in the GV0-to-

GV3 comparison. The GV2-to-GV3 comparison revealed that translation and transcriptional regulation were significantly affected.

Quantitative Reverse-Transcriptase PCR Validation of Microarray Results

The microarray results were validated using quantitative reverse-transcriptase PCR for a subset of ten genes (*HIST1H1A, HIST1H1E, H2B, HIST1H3A, HIST1H4I, AEBP2, PIWIL3, PTCH1, CBX3,* and *TMPO*) that represent the main gene expression profiles identified. These results were consistent with the microarray data. Considering the general particularities of canonical histone transcripts (e.g., the absence of poly-A tail; see Discussion), reverse transcription was performed either with oligo (dT) or random primers. Higher mRNA abundance was observed in random-primed cDNA preparations compared to the oligo (dT)-primed reactions, as shown by a lower cycle-threshold value obtained during qPCR experiments (data not shown), for all but one (*HIST1H3A*) of the histone transcripts assessed. Therefore, quantification was performed with random-primed cDNA for these histone genes, whereas quantifications of the other genes were based on oligo (dT)-primed cDNA. The quantities of eight transcripts
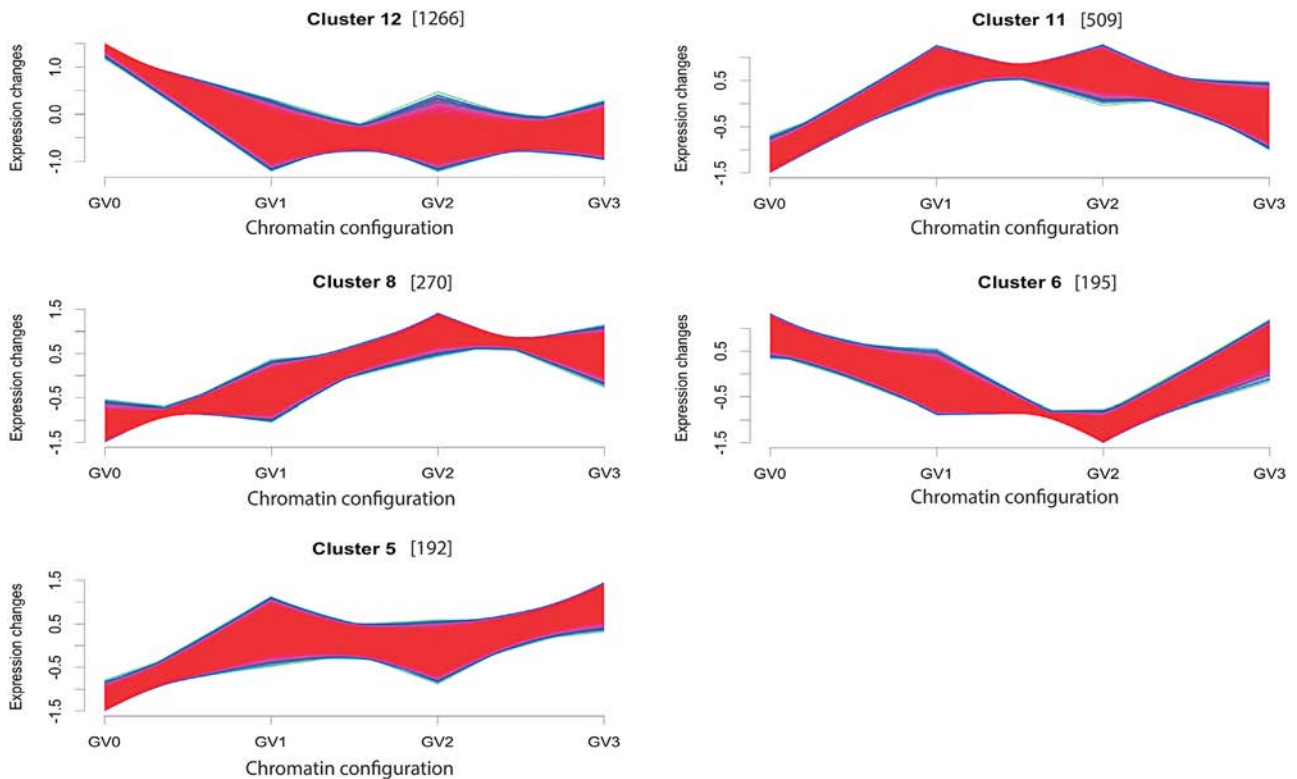
Figure 3. Main clusters identified from Mfuzz clustering analysis (Kumar and Futschik, 2007). The number of statistically significant probes specific to these profiles is displayed for each cluster. Cluster ♯12 included more than 45% of the statistically significant genes with a lower mRNA level between GV0 and GV1 that remains relatively stable thereafter. The other clusters illustrate the transcripts with an increase followed by a decrease profile (♯11), a constant increase until GV2 (♯8), a decrease followed by an increase at GV2 (♯6), and an increase at GV1 (♯5).

TABLE 2. Number of Histone-Related Probes

Histone family	Number of probes on the embryogene microarray platform	Number of probes detected in the oocyte	Number of probes presenting a statistically significant differences (MAANOVA, $P < 0.01$)
H1	9	6	5
H2A	15	10	4
H2B	68	33	7
H3	14	13	9
H4	16	12	4
H2A variant	12	10	0
H2B variant	3	0	0
H3 variant	12	10	1
H1 variant	11	10	0

The number of probes detected in the oocyte corresponds to the probes with signal intensity above the cut-off level of 7.4. The complete list of histone variants is described by Kamakaka and Biggins (2005). H2A variants include H2AFB2, H2AFJ, H2AFV, H2AFX, H2AFY, H2AFY2, H2AFZ, and H2A testis specific. H2B variants include H2B testis variant. H3 variants include H3.3. CENPA and H1 variants include H1F0, H1FNT, H1FX, and H1foo.

(*HIST1H1A*, *HIST1H1E*, *H2B*, *HIST1H3A*, *PIWIL3*, *AEBP2*, *PTCH1*, and *CBX3*) were significantly different between chromatin configuration stages ($P < 0.05$). The abundance of one transcript (*HIST1H4I*, $P = 0.10$) tended to differ, whereas another (*TMPO*, $P = 0.17$) was not significantly different between stages (Fig 4).

In Silico Protein-RNA Interactions

The catRAPID-omics web server was used to calculate the propensity for interaction between the bovine stem-loop binding protein 2 (SLBP2) and histone transcripts (Table 3) in order to evaluate the potential for a mRNA storage mechanism in bovine oocytes, similar to what was previously described in the Xenopus oocyte (Wang et al., 1999). To validate this approach, the prediction analysis was performed with the human and mouse SLBP protein sequences, which are known to interact with histone transcripts (Whitfield et al., 2004; Townley-Tilson et al., 2006), against their respective transcriptomes; as expected, high interaction scores were also reported for these positive-control histone mRNA (Table S3). The high in silico interaction scores for several bovine protein-RNA pairs indicated that SLBP2 could bind histone mRNA. For example, high interaction scores were obtained for canonical histones such as *H3*, and *H2B*, while some histone variants (*H2B testis-specific*, *H1FOO*, and *H1FX*) had low interaction scores.

DISCUSSION

This study provided comprehensive transcriptome analysis of the bovine oocyte based on gradual chromatin condensation. The four distinct and progressive stages of chromatin configuration described by Lodde et al. (2007) offered a unique opportunity to characterize the molecular changes occurring in the oocyte during this major remodelling process. Compared to similar studies conducted in the mouse (Zuccotti et al., 2008; Ma et al., 2013; Monti et al., 2013), the data described herein have the important advantage of examining transcriptional changes that occur gradually over four stages rather than comparing only two distinct phenotypes (NSN vs SN murine oocytes).

Even if there is a significant increase in the diameter of the oocyte between the GV0, GV1-GV2, and GV3 stages, as described (Lodde et al., 2007), the amount of total RNA extracted from pooled oocytes representing each stage was not significantly different (data not shown). This is consistent with reports that a mouse oocyte at 65% of its final volume has accumulated 95% of the total amount of RNA present in the full-grown oocyte (Sternlicht and Schultz, 1981). The intense transcriptional activity observed in growing oocyte (GV0, with a diameter of 108 μm (Lodde et al., 2008; Luciano et al., 2011)) illustrates the high turnover rates necessary to ensure oocyte growth. In contrast, some RNAs are translated into protein during the final growth phase of oogenesis, which may also account for the stable amounts of RNA observed. These data together suggest no global increase in the amount of RNA in oocytes from larger follicles compared to oocytes from early antral follicles (GV0). This is further supported by the observation that the number of probes detected on the microarray slides was constant across the different chromatin configurations, in accordance with our previous studies using bovine oocytes (Labrecque et al., 2013; Labrecque et al., 2014).

Considering that GV0 oocytes are more transcriptionally active than their GV3 counterparts, as shown by H[3]-uridine incorporation and autoradiography (Lodde et al., 2008), the high number of genes for which mRNA abundance decreased as the chromatin became more compacted is not surprising. Our data did, however, indicate that despite the global repression of transcription and the highly compacted chromatin, the abundance of a subset of mRNAs increased in oocytes. This implies that a low level of transcription is still possible in bovine oocytes with compacted chromatin. A

similar observation was made during mouse spermatogenesis, in which mature spermatids harboring a very high degree of chromatin compaction still exhibit active expression of several important genes (Li et al., 2014). The microarray comparison between GV2 and GV3 oocytes also effectively point in that direction. Even with compacted chromatin, the abundance of 51 transcripts increased at

GV3 with a fold change >2, suggesting that some active transcription was occurring in these oocytes; in contrast, the abundance of only ten transcripts decreased between GV2 and GV3. Functional analysis of the transcripts with an increased or decreased abundance in the GV2 vs GV3 microarray comparison highlighted important biological processes, namely translation and transcriptional
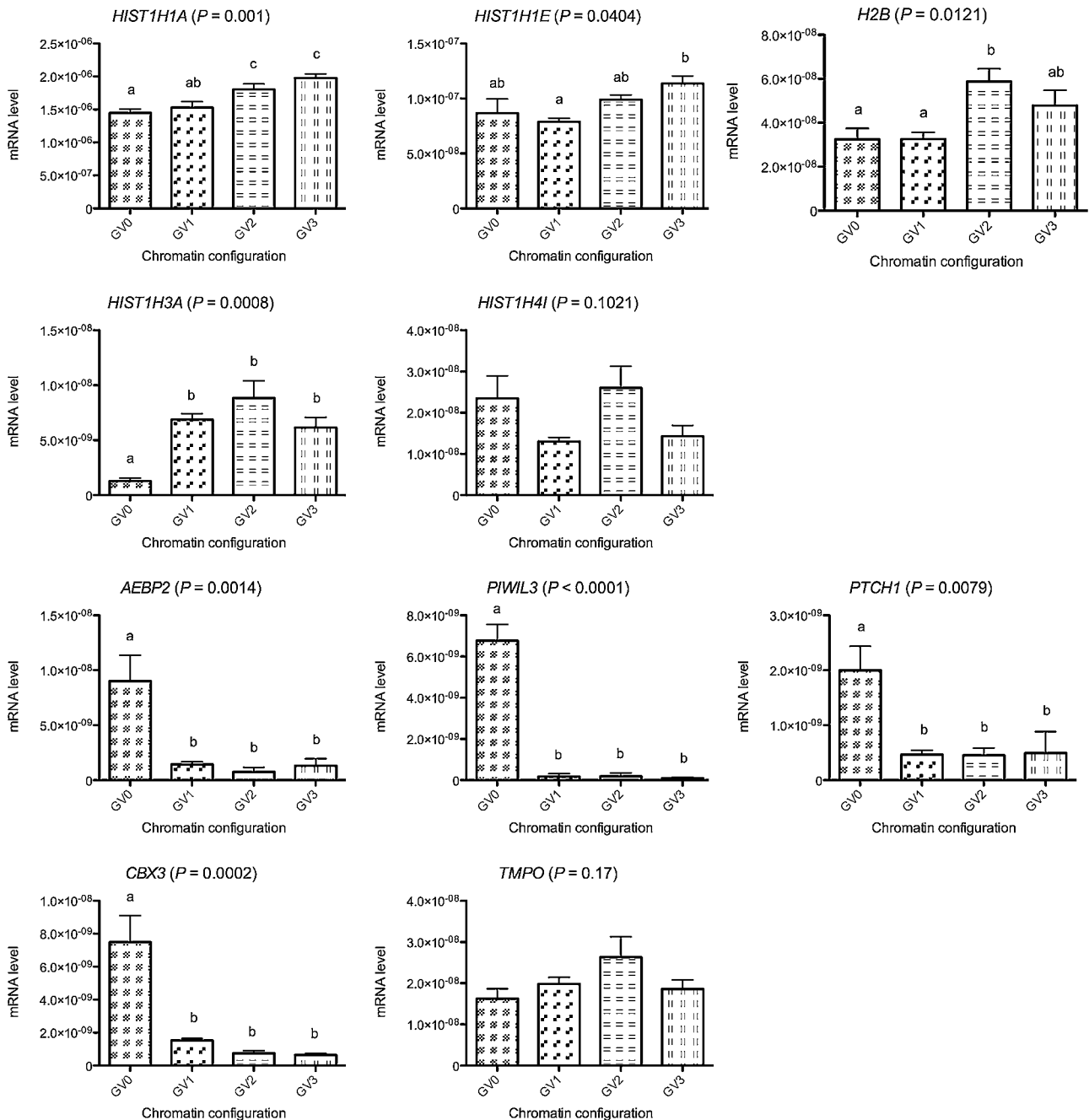

Figure 4. Quantitative reverse-transcriptase-PCR validation of the microarray results. Messenger RNA quantification data are presented as mean ± standard error. Different superscripts represent significant differences ($P < 0.05$) using one-way ANOVA followed by a Newman–Keuls post-test.

TABLE 3. List of Possible Protein-RNA Interactions Calculated with CatRAPIDomics

Protein ID/transcript ID	Interaction strength	Discriminative power	Score
bSLBP2/HIST1H3a-like_XM_005223798.1	0.92	0.87	1.90
bSLBP2/HIST1H3a-like_XM_005196649.1	0.87	0.66	1.85
bSLBP2/H2AFJ_NM_001078089.2	1.00	1.00	1.37
bSLBP2/H2AFV_NM_001038197.1	0.99	0.99	1.05
bSLBP2/H2AFZ_X1_XM_005207694.1	0.99	0.98	1.03
bSLBP2/H2AFZ_X2_XM_005207695.1	0.99	0.98	1.02
bSLBP2/H2AFY2_NM_001076086.1	0.98	0.97	0.98
bSLBP2/H4-like_germinal_NM_001145871.2	0.97	0.95	0.94
bSLBP2/H1FOO_X1_XM_005223064.1	0.95	0.93	0.93
bSLBP2/H2AFZ_NM_174809.2	0.95	0.92	0.92
bSLBP2/H2AFY_X4_XM_005209379.1	0.94	0.90	0.91
bSLBP2/H2B_1/2-like_XM_002699769.2	0.93	0.90	0.91
bSLBP2/H2B_1/2-like_XM_003585165.2	0.93	0.90	0.91
bSLBP2/H2AFY_X3_XM_005209378.1	0.95	0.89	0.91
bSLBP2/H2B_type_1-like_XM_582268.5	0.89	0.81	0.89
bSLBP2/H2AFY_X1_XM_005209376.1	0.95	0.80	0.89
bSLBP2/H2AFY_X2_XM_005209377.1	0.81	0.79	0.88
bSLBP2/H2AFJ_X1_XM_005206990.1	0.81	0.76	0.87
bSLBP2/H1FNT_XM_869593.6	0.77	0.71	0.86
bSLBP2/H2AFY_NM_001046340.1	0.72	0.71	0.86
bSLBP2/H1F0_NM_001076487.1	0.73	0.69	0.86
bSLBP2/H2B_5-like_XM_002684861.1	0.73	0.69	0.86
bSLBP2/H1FX_XM_002697143.3	0.64	0.57	0.84
bSLBP2/H2bd-like_XM_002693561.1	0.69	0.50	0.83
bSLBP2/H2A-Bbd_NM_001075905.2	0.41	0.42	0.82
bSLBP2/H2B_7-like_XM_002699905.1	0.34	0.35	0.81
bSLBP2/H2B_7-like_XM_002707268.1	0.57	0.35	0.81
bSLBP2/H1FOO_X2_XM_005223065.1	0.34	0.33	0.81
bSLBP2/H2ai-like_XM_005223728.1	0.31	0.28	0.80
bSLBP2/H2A-like_XM_002683953.1	0.20	0.22	0.78
bSLBP2/H2B_5-like_XM_866181.3	0.12	0.20	0.78
bSLBP2/H2AFX_NM_001079780.2	0.34	0.17	0.77
bSLBP2/H2AFY_X5_XM_005209380.1	0.07	0.14	0.76
bSLBP2/H1FOO_NM_001035372.1	0.08	0.14	0.74
bSLBP2/H2B_7-like_XM_005196102.1	0.17	0.10	0.68
bSLBP2/H2B_7-like_XM_005201133.1	0.17	0.10	0.68
bSLBP2/H2B_testis-specific-like_XM_002699853.1	0	0	0,64

Interactions with a discriminative-power value above 75% (bold) represent high-confidence predictions, while those values above 50% are likely to take place.bSLPB2, bovine SLBP2 (NP_001268838.1).

regulation. Indeed, several members of the eukaryotic translation initiation factor (*EIF3G, EIF3I, EIF5A*) and of several ribosomal proteins (*RPL18, RPL28, RPL29*) effectively increased in GV3 oocytes, whereas the mRNA level for several other genes involved in transcriptional regulation decreased following chromatin compaction. Consistent with the previous model proposed for mouse oocytes (Worrad et al., 1994; Pan et al., 2005), a decrease in the expression of specific members of the transcriptional machinery could explain the transcriptional arrest observed towards the end of oogenesis in the bovine.

The mRNA level of *CBX3* (chromobox homolog 3), also known as *HP1gamma* (heterochromatin protein 1 homolog gamma), and *AEBP2*, a member of the Polycomb repressive complex 2 (PRC2), decreased considerably (by microarray and quantitative PCR) once chromatin started to condense. *CBX3* plays important roles involving transcription to nuclear organization (Lomberk et al., 2006), while *AEBP2* is involved in transcriptional repression (Cao and Zhang, 2004; Kim et al., 2009). In both cases, it is possible that the observed depletion of mRNA is associated with

translation. Consistent with this hypothesis, CBX3 protein was detected in mouse GV-stage oocytes (Wang et al., 2010; Pfeiffer et al., 2011) and AEBP2 was detected in the polysomal-mRNA population of mouse GV-stage oocytes (Potireddy et al., 2006).

Patched 1 (*PTCH1*), a member of the sonic hedgehog (SHH) signalling pathway, decreased once chromatin started to condense. The GLI transcription factor family was also reported to be involved in the regulation of SHH signalling (Bai et al., 2002); indeed, a recent study established an interesting link between PTCH1 and GLI2 regarding transcriptional regulation in mouse embryonic stem cells (Li et al., 2013). *PIWIL3* encodes a member of the PIWI subfamily of Argonaute proteins, which play an important role in RNA-mediated gene silencing through translational regulation during spermatogenesis (Grivna et al., 2006), although a role for this family of proteins is also emerging in the female germ cell, given the detection of *PIWIL2* during the early stages of mouse oocyte development (Aravin et al., 2008). Together, the abundance of *PTCH1* and *PIWIL3* transcripts in oocytes with a diffuse

pattern of chromatin compaction, followed by an important decrease once the chromatin started to condense, represents the type of dynamic regulation required to ensure chromatin remodelling and transcriptional silencing. Thymopoietin (*TMPO*), also known as lamina-associated protein 2 (*LAP2*), is involved in the organization of the nuclear envelope (Gerace and Huber, 2012). In contrast to the above transcripts, our microarray data revealed an increased mRNA abundance for this gene when chromatin compaction was nearly complete, although quantitative PCR validation did not reach a statistically significant level.

Many of the mRNAs that increased as chromatin became more compacted were related to histone genes. The number of histone transcripts detected in our study was higher than in previous studies in which oocytes bearing different chromatin configurations were compared. Monti et al. (2013), for example, reported a higher abundance of *His3h2bb*, *His1h2ab*, and *His1h4j* mRNA in SN mouse oocytes by microarray analysis while Ma et al. (2013) observed increased *His1h2bc* and *His1h4h* mRNA levels in SN oocytes by RNAseq.

The observation of such a high proportion of histone genes in our bovine data is both surprising and interesting due to the nature of the procedure used to amplify the RNA (T7-based technique). It is generally assumed that T7 RNA amplification targets transcripts bearing a poly-A tail, since the T7 RNA polymerase promoter is coupled to oligo(dT) whose length is between 15−24 deoxythymidines in most commercial T7-based RNA amplification kits (Kerkhoven et al., 2008); conversely, the length of the poly-A tail at the 3′ end of the targeted transcripts is currently unknown. Canonical histone mRNAs, however, represent the principal class of transcripts without a poly-A tail (Marzluff et al., 2008) —although the presence of a short poly-A tail after the stem loop has long been known for Xenopus oocytes (Ballantine and Woodland, 1985). This short poly-A tail in frog oocytes is approximately 6−10 adenine residues long, and is located after the stem-loop sequence at the 3' end of histone mRNAs (Sanchez and Marzluff, 2004). Given that the minimal length that an oligo(dT) coupled to the T7 promoter is able to target falls between 5 and 10 adenine residues (Graindorge et al., 2006), even short poly-A tails of histone transcript can be targeted for priming. Indeed, results from our laboratory previously revealed that some histone mRNAs could effectively be polyadenylated in bovine oocytes—including *H1FOO* (McGraw et al., 2006), H3 variants (*H3F3A*, *H3F3B*), and even some replication-dependant histones such as *HIST1H2BN* (Gohin et al., 2014). Similar results were also reported for the H2B-histone family in various cell lines (Kari et al., 2013). A recent study, where the poly-A tail length was assessed genome-wide through a novel approach—poly-A tail length profiling by sequencing (PAL-seq)—in various human and mouse cell lines, also observed the polyadenylation of several canonical histone mRNAs (Subtelny et al., 2014). Interestingly, the production of polyadenylated transcripts from canonical histone genes was also reported during chicken (Challoner et al., 1989) and mouse

spermatogenesis (Li et al., 2014), concurrent with their involvement in chromatin remodelling.

Pre-mRNA processing and translation of canonical histones are mainly controlled by stem-loop binding protein (SLBP) (reviewed by Dominski and Marzluff, (1999)). Studies in *Xenopus laevis* revealed the existence of an additional SLBP protein, xSLBP2, which is present exclusively in the oocyte. SLBP2 lacks histone pre-mRNA processing functions, instead binding to histone mRNA in immature oocytes to inhibit their translation. SLBP2 is degraded throughout oocyte maturation, which makes histone mRNAs available for processing by SLBP1 in preparation for their translation (Wang et al., 1999). In addition to SLBP2, the short poly-A tail at the 3′ end of histone mRNAs plays a role in their translational repression —at least in frog oocytes (Sanchez and Marzluff, 2004). Importantly, a mammalian SLBP2 ortholog was recently identified in bovine oocytes (Thelie et al., 2012), suggesting that histone mRNAs may also be stored in the bovine oocyte/early embryo in a manner analogous to that used in Xenopus. SLBP2 protein is detectable in bovine oocytes, and is also gradually degraded (RNA and protein) towards the morula stage (Thelie et al., 2012). The constant presence of SLBP2 during the transcriptionally silent period could ensure that an optimal supply of histone mRNA is protected from early translation or degradation, and remains available to be used when needed.

Protein-RNA interactions, assessed in silico by catRAPID omics, strongly suggest that some histone mRNAs could be stored in the bovine oocyte through associations with SLBP2. This in silico approach was previously validated by the accurate prediction of interactions between various histone transcripts and human and mouse SLBP proteins, using immunoprecipitation experiments in both species (Whitfield et al., 2004; Townley−Tilson et al., 2006). The high interaction scores obtained for specific canonical bovine histones (*H3* and *H2B*) suggest that the SLBP2-dependent protection of mRNA provides an optimal supply of histone transcripts for the first three embryonic cell cycles. On the other hand, low scores were obtained for other bovine histone variants —such as the H2B testis variant, *H1FX*, *H1F0*, and *H1FNT* —suggesting that their accumulation in the oocyte is unlikely, which is in agreement with the absence of these specific transcripts in the oocyte. Interestingly, out of three possible *H1FOO* transcripts, two had low interaction scores, implying that the high-scoring variant was actively being stored for later use. As *H1FOO* is an oocyte-specific mRNA that will be progressively degraded in the period between fertilization and embryonic genome activation (McGraw et al., 2006), it could be hypothesized that the specific transcript variant (*H1FOO_X1*) bound to SLBP2 is translated during early cleavage to ensure a constant supply of histones during that period. Of course, further experiments are required to test this hypothesis.

The gradual chromatin remodelling process that occurs in the bovine GV oocyte allowed us to identify dynamic modulations in mRNA content through transcriptome analysis. By comparing the four distinct and progressive stages

of chromatin compaction, the establishment of the transcriptional repressive context was clearly observed from the decline in transcript abundance associated with increasing chromatin compaction. Transcripts that significantly accumulated over the same period encoded several histones. This massive storage event is likely made possible by the association of these mRNAs with bovine SLBP2, in a manner similar to that utilized by Xenopus oocytes, and resulted in an optimal supply of histone transcripts for use during the first embryonic cell cycles.

MATERIALS AND METHODS

All chemicals were obtained from Sigma−Aldrich (St. Louis, MO), unless otherwise stated.

Oocyte Recovery

Bovine ovaries (Holstein dairy cows) were obtained from a local abattoir and transported to the laboratory within 2 hr in a saline solution (9 g/L NaCl) maintained at 26°C. Cumulus-oocytes complexes (COCs) were aspirated from follicles 2−6 mm in diameter with a 16-gauge needle mounted on an COOK-IVF aspiration pump (Brisbane, QLD, Australia) using a vacuum pressure of −28 mm/Hg. Following aspiration, small pieces of ovarian cortex were removed and examined under a dissecting microscope, and COCs were isolated from early antral follicles 0.5−<2 mm in diameter by rupturing the follicle wall with a scalpel. All the COCs collected were washed in medium 199 (M199) supplemented with HEPES (20 mM), heparin (1790 units/L), and 0.4% of bovine serum albumin (HM199). Only COCs suitable for in vitro embryo production procedures—with finely granulated ooplasm and five or more layers of compacted cumulus cells—were used.

Chromatin-configuration assessment was performed as previously described (Lodde et al., 2007). Briefly, COCs were mechanically denuded by vortexing (2 min, 35 Hz) in HM199 supplemented with 5% calf serum (Gibco, Invitrogen, Milan, Italy). Denuded oocytes were washed twice in HM199, stained in HM199 containing 1 μg/mL Hoechst 33342 for 5 min in the dark, and then individually transferred to a 5 μL drop of the same medium overlaid with mineral oil. Chromatin configuration was evaluated under an inverted fluorescence microscope (Olympus IX, magnification 40x); oocytes were exposed to ultraviolet light for no more than 3 sec. The oocytes were collected and visualized individually under the microscope; the presence of a single cumulus cell would have been evident under ultraviolet light. Therefore, all efforts were taken to ensure the complete removal of all cumulus cells. Individual oocytes were classified according to the degree of chromatin compaction by the same evaluator in order to reduce variation over the course of this study. Following chromatin evaluation, oocytes were washed twice in a phosphate-buffered saline (PBS)−

0.1% polyvinyl alcohol (PVA) solution; once in PBS; collected in groups of ten in a minimal volume of PBS; snap-frozen in liquid nitrogen; and stored at −80°C until RNA extraction.

RNA Extraction and Amplification

Total RNA was extracted from four pools of ten oocytes for each configuration stage (GV0, GV1, GV2, and GV3) with the Pico-Pure RNA Isolation Kit (Applied Biosystems, Carlsbad, CA) following the manufacturer's protocol and including an on-column DNase I treatment (Qiagen, Mississauga, ON, Canada). Total RNA integrity and concentration were evaluated using a 2100-Bioanalyzer (Agilent Technologies, Palo Alto, CA) with the RNA PicoLab Chip (Agilent Technologies). RNA samples were linearly amplified using a T7 RNA polymerase amplification approach (T7-IVT) to generate enough material for hybridization. Antisense RNA (aRNA) was produced using the RiboAmp HS RNA amplification kit (Applied Biosystems). After two amplification rounds of 6 hr each, the aRNA output was quantified using a NanoDrop ND-1000 (NanoDrop Technologies, Wilmington, DE).

Sample Labelling and Microarray Hybridization

For each sample, 2 μg of aRNA were labelled using the ULS Fluorescent Labelling Kit for Agilent arrays (Cy3−Cy5) (Kreatech Diagnostics, Amsterdam, Netherlands). The labelled product was then purified with the Pico-Pure RNA Isolation Kit. Labelling efficiency was measured using the Nano-Drop ND-1,000. Samples from the four biological replicates, representing six different weeks of oocyte collection, were hybridized on a custom bovine Agilent 44K microarray slide (Robert et al., 2011). The hybridizations were performed using a reference design, where oocytes bearing the GV0 chromatin configuration were compared with the other three groups (GV0 vs GV1; GV0 vs GV2; GV0 vs GV3). An additional microarray comparison was performed between GV2 and GV3 oocytes. Overall, 16 hybridizations were performed using a dye-swap set-up. A total of 825 ng of each labelled sample (Cy3 and Cy5) were incubated in a solution containing 2X blocking agent and 5X fragmentation buffer in a volume of 55 μL at 60°C for 15 min, and were put on ice immediately after. 55 μL of 2X GEx Hybridization Buffer HI-RPM were then added for a total volume of 110 μL. The hybridization mix (100 μL) was added onto the array, and hybridization was performed at 65°C for 17 hr using an Agilent Hybridization chamber in a rotating oven. Following hybridization, chambers were disassembled and slides were washed with Gene Expression Wash Buffer one containing 0.005% Triton X-102 for 3 min at room temperature, and then transferred to Gene Expression Wash Buffer two containing 0.005% Triton X-102 for 3 min at 42°C. Final washes with acetonitrile for 10 sec at room temperature and with Stabilization and Drying Solution (Agilent) for 30 sec at room temperature were performed before air-drying the slides. The slides were scanned using the Tecan PowerScanner microarray

scanner (Tecan Group Ltd, Männerdorf, Switzerland) and features were extracted using ArrayPro 6.4 (Media Cybernetics, Bethesda, MD).

Microarray Data Analysis

Intensities files were uploaded to ELMA (EmbryoGENE LIMS Microarray Analysis, http://elma.embryogene.ca/) to run the quality-control module. Microarray datasets were then analysed with the FlexArray microarray analysis software, Version 1.6.1 (Blazejczyk et al., 2007). Briefly, raw data were subjected to a simple background subtraction, Loess within array, and Quantile between-array normalizations. The MAANOVA algorithm was applied to accommodate the four chromatin configurations, using the GV0 group as a reference. A Limma simple analysis was performed to obtain the fold change for each contrast individually. Differences were considered statistically significant with a P value less than 0.01. To detect the presence or absence of signal for each spot present on the slide, an arbitrary cut-off level of 7.4 (log2) was used, which corresponds to the mean intensity of the background level plus twice the standard deviation of the background. A between-group analysis was performed to classify the samples according to their transcriptomic profile (Culhane et al., 2002). Genes were then grouped in clusters according to their profile with the mFuzz Bioconductor package (Kumar and Futschik, 2007). DAVID bioinformatics resources were also used to perform functional-enrichment analysis of specific gene lists (Huang et al., 2009b; Huang et al., 2009a).

cDNA Preparation and Quantitative Reverse-Transcriptase PCR

To confirm the results of microarray analysis, quantitative reverse-transcriptase PCR (q-RT-PCR) was performed with four independent biological replicates (pools of 10 oocytes). Total RNA was extracted and reverse transcribed in duplicate using q-Script Flex cDNA Synthesis Kit (Quanta Biosciences, Gaithersburg, MD), either with oligo(dT) or random primers, following the manufacturer's recommendations. The primers used for q-RT-PCR are listed in Table 4 and were designed using the IDT Primer-Quest tool (http://www.idtdna.com/Scitools/Applications/Primerquest/) from sequences obtained using the UMD3.1 assembly of the bovine genome and results from our microarray analysis. To confirm the specificity of each pair of primers, electrophoresis on a standard 1.2% agarose gel was performed for each amplified fragment. The PCR product was purified with the QIAquick PCR Purification kit (Qiagen), quantified using the Nano-Drop ND-1,000, and sequenced. The products were then used to create the standard curve for quantification experiments, with dilutions ranging from 2×10^{-4} to 2×10^{-8} ng/μL. q-RT-PCR was performed on a LightCycler 480 (Roche Diagnostics, Laval, QC, Canada) using SYBR incorporation. Each q-RT-PCR reaction contained the cDNA corresponding to 1/40 of an oocyte, 0.25 mM of each primer, and 1X SYBR mix in a final volume of 20 μL (LightCycler 480 SYBR Green I Master, Roche Diagnostics). The PCR conditions used for all genes were as follows: a denaturing step of 10 min at 95°C followed by 50 PCR cycles (denaturing, 95°C for 1 sec; annealing, based on the primer temperature [Table 4] for 5 sec; extension, 72°C for 5 sec); a melting curve (94°C for 5 sec, 72°C for 30 sec, and a step cycle starting at 72°C up to 94°C at 0.2°C /sec); and a final holding step at 4°C. Complementary DNA quantification was performed with the LightCycler 480 Software Version 1.5 (Roche Diagnostics) by comparison with the standard curve. PCR specificity was confirmed by melting-curve analysis.

Statistical Analysis of q-RT-PCR Results

Four independent biological replicates were used for each gene tested. Analysis of gene-expression stability over the four groups was performed using the geNorm algorithm (Vandesompele et al., 2002) through the Biogazelle's qBase+ software (Biogazelle, Zwijnaarde, Belgium). *ACTB*, *B2M*, and *YWHAZ* were identified as the most stable reference genes among the different

TABLE 4. Primers Used for Quantitative Reverse-Transcriptase PCR Validations

Gene symbol	GenBank accession number	Forward primer	Reverse primer	Annealing temp. (°C)	Product size (bp)
HIST1H1A	XM_005196651.1	5'-GTTGACAAAGAAGTCCTCTAAG	5'-CTTGGTTACCTTCACTTTGG	59	124
HIST1H1E	XM_870179.4	5'-CAGCTAAGAAGCCGAAGAAG	5'-TTTGGCGGTCTTTGGTTTAG	60	215
H2B	XM_870344.3	5'-AGAAGAAGGATGGGAAGAAG	5'-ATATCGTTGACGAAGGAGTT	59	142
HIST1H3A	XM_005196648.1	5'-TCAAGACCGACTTGCGTTTC	5'-ACAGGTTGGTGTCCTCAAAG	62	96
HIST1H4I	XM_005223796.1	5'-AACATCCAGGGTATTACCAA	5'-CATAGATGAGGCCAGAAATAC	58	82
PIWIL3	XM_867297.4	5'-GATAGCTGTACCATCATCAG	5'-CCACTCCATTTAGAAGTATAGG	57	156
AEBP2	NM_001083485.2	5'-AATTACGGGAGGCTTTATTC	5'-ACCATTCCAGAATGTCTTAC	57	121
PTCH1	XM_005210407.1	5'-GGAATGGGTTTGTGTCATTTC	5'-CACTCATGTCTCAGCAAAGT	60	178
CBX3	NM_001101198.1	5'-AGTCTCTGTGCTGTATTTAG	5'-GTAGGTCAAGCGTAGATTAG	57	152
TMPO	NM_001098005.1	5'-GGCTAGCTATAAGGCTATAA	5'-CAAATGGAATCTAAGACTGG	56	152
ACTB	NM_173979	5'-ATCGTCCACCGCAAATGCTTCT	5'-GCCATGCCAATCTCATCTCGTT	59	102
B2M	NM_173893.3	5'-AGACACCCACCAGAAGATGG	5'-GGGGTTGTTCCAAAGTAACG	54	234
YWHAZ	NM_174814.2	5'-CCAGTCACAGCAAGCATACC	5'-CTTCAGCTTCGTCTCCTTGG	55	286

GV-stage oocyte groups. One-way ANOVA followed by a Newman−Keuls post-test was performed using GraphPad Prism version 5.0. Differences were considered to be statistically significant at the 95% confidence level ($P < 0.05$). Data are presented as mean $\pm$ standard error.

Histones mRNA Analysis

The catRAPID-omics web server (http://s.tartaglialab.com/page/catrapid_omics_group) was used to identify histone mRNAs potentially bound to SLBP2, which is known to play a role in the regulation of histone mRNA translation during Xenopus oogenesis (Wang et al., 1999). This in silico analysis tool estimates the binding propensity between a protein-RNA pair (Agostini et al., 2013). The interaction is calculated for each pair based on the physicochemical properties of the amino acids and the nucleotide sequence. The interaction strength is computed using a reference list of 100 random proteins and 100 random RNA sequences with the same length as those under investigation. The Discriminative Power is a statistical measure to evaluate the Interaction Propensity, and represents the confidence of the prediction. The Discriminative Power ranges from 0% (unpredictability) to 100% (predictability); values above 50% indicate that the interaction is likely to take place while values above 75% represent high-confidence predictions. The global score is then calculated based on three individual values: the catRAPID normalized propensity, the presence of RNA binding domains, and the presence of known RNA-binding motifs. A custom library was generated using the bovine histone mRNA sequences retrieved from National Center for Biotechnology Information (NCBI) (http://www.ncbi.nlm.nih.gov/nuccore/). SLBP sequences were retrieved from Uniprot (http://www.uniprot.org/). Additional analyses were performed with the sequences of human (hSLBP, NP_006518.1) and mouse SLBP (mSLBP, NP_001276653.1), where each protein sequence was analysed against its respective transcriptome.

ACKNOWLEDGMENTS

REFERENCES

Agostini F, Zanzoni A, Klus P, Marchese D, Cirillo D, Tartaglia GG. 2013. CatRAPID omics: A web server for large-scale prediction of protein-RNA interactions. Bioinformatics 29:2928−2930.

Aravin AA, Sachidanandam R, Bourc'his D, Schaefer C, Pezic D, Toth KF, Bestor T, Hannon GJ. 2008. A piRNA pathway primed by individual transposons is linked to de novo DNA methylation in mice. Mol Cell 31:785−799.

Bai CB, Auerbach W, Lee JS, Stephen D, Joyner AL. 2002. Gli2, but not Gli1, is required for initial Shh signaling and ectopic activation of the Shh pathway. Development 129:4753−4761.

Ballantine JE, Woodland HR. 1985. Polyadenylation of histone mRNA in Xenopus oocytes and embryos. FEBS Lett 180:224−228.

Blazejczyk M, Miron M, Nadon R. 2007. FlexArray: A statistical data analysis software for gene expression microarrays. Montréal, Canada: Genome Quebec.

Bouniol-Baly C, Hamraoui L, Guibert J, Beaujean N, Szollosi MS, Debey P. 1999. Differential transcriptional activity associated with chromatin configuration in fully grown mouse germinal vesicle oocytes. Biol Reprod 60:580−587.

Cao R, Zhang Y. 2004. SUZ12 is required for both the histone methyltransferase activity and the silencing function of the EED-EZH2 complex. Mol Cell 15:57−67.

Challoner PB, Moss SB, Groudine M. 1989. Expression of replication-dependent histone genes in avian spermatids involves an alternate pathway of mRNA 3'-end formation. Mol Cell Biol 9:902−913.

Chohan KR, Hunter AG. 2003. Meiotic competence of bovine fetal oocytes following in vitro maturation. Anim Reprod Sci 76:43−51.

Culhane AC, Perriere G, Considine EC, Cotter TG, Higgins DG. 2002. Between-group analysis of microarray data. Bioinformatics 18:1600−1608.

De La Fuente R, Eppig JJ. 2001. Transcriptional activity of the mouse oocyte genome: Companion granulosa cells modulate transcription and chromatin remodeling. Dev Biol 229:224−236.

De La Fuente R, Viveiros MM, Burns KH, Adashi EY, Matzuk MM, Eppig JJ. 2004. Major chromatin remodeling in the germinal vesicle (GV) of mammalian oocytes is dispensable for global transcriptional silencing but required for centromeric heterochromatin function. Dev Biol 275:447−458.

Dominski Z, Marzluff WF. 1999. Formation of the 3' end of histone mRNA. Gene 239:1−14.

Fair T, Hyttel P, Greve T. 1995. Bovine oocyte diameter in relation to maturational competence and transcriptional activity. Mol Reprod Dev 42:437−442.

Franciosi F, Lodde V, Goudet G, Duchamp G, Deleuze S, Douet C, Tessaro I, Luciano AM. 2012. Changes in histone H4 acetylation during in vivo versus in vitro maturation of equine oocytes. Mol Hum Reprod 18:243−252.

Fuhrer F, Mayr B, Schellander K, Kalat M, Schleger W. 1989. Maturation competence and chromatin behaviour in growing and fully grown cattle oocytes. Zentralbl Veterinarmed A 36:285−291.

Gerace L, Huber MD. 2012. Nuclear lamina at the crossroads of the cytoplasm and nucleus. J Struct Biol 177:24−31.

Gohin M, Fournier E, Dufort I, Sirard MA. 2014. Discovery, identification and sequence analysis of RNAs selected for very short

or long poly A tail in immature bovine oocytes. Mol Hum Reprod 20:127−138.

Graindorge A, Thuret R, Pollet N, Osborne HB, Audic Y. 2006. Identification of post-transcriptionally regulated Xenopus tropicalis maternal mRNAs by microarray. Nucleic Acids Res 34:986−995.

Grivna ST, Pyhtila B, Lin H. 2006. MIWI associates with translational machinery and PIWI-interacting RNAs (piRNAs) in regulating spermatogenesis. Proc Natl Acad Sci U S A 103:13415−13420.

Hinrichs K. 2010. The equine oocyte: Factors affecting meiotic and developmental competence. Mol Reprod Dev 77:651−661.

Huang DW, Sherman BT, Lempicki RA. 2009a. Systematic and integrative analysis of large gene lists using DAVID bioinformatics resources. Nat Protoc 4:44−57.

Huang DW, Sherman BT, Lempicki RA. 2009b. Bioinformatics enrichment tools: paths toward the comprehensive functional analysis of large gene lists. Nucleic Acids Res 37:1−13.

Hunter AG, Moor RM. 1987. Stage-dependent effects of inhibiting ribonucleic acids and protein synthesis on meiotic maturation of bovine oocytes in vitro. J Dairy Sci 70:1646−1651.

Kari V, Karpiuk O, Tieg B, Kriegs M, Dikomey E, Krebber H, Begus-Nahrmann Y, Johnsen SA. 2013. A subset of histone H2B genes produces polyadenylated mRNAs under a variety of cellular conditions. PLoS ONE 8:e63745.

Kerkhoven RM, Sie D, Nieuwland M, Heimerikx M, De Ronde J, Brugman W, Velds A. 2008. The T7-primer is a source of experimental bias and introduces variability between microarray platforms. PLoS ONE 3:e1980.

Kim H, Kang K, Kim J. 2009. AEBP2 as a potential targeting protein for Polycomb Repression Complex P RC2. Nucleic Acids Res 37:2940−2950.

Kumar L, Futschik ME. 2007. Mfuzz: A software package for soft clustering of microarray data. Bioinformation 2:5−7.

Labrecque R, Sirard MA. 2014. The study of mammalian oocyte competence by transcriptome analysis: progress and challenges. Mol Hum Reprod 20:103−116.

Labrecque R, Vigneault C, Blondin P, Sirard MA. 2013. Gene Expression Analysis of Bovine Oocytes With High Developmental Competence Obtained From FSH-Stimulated Animals. Mol Reprod Dev 80:428−440.

Labrecque R, Vigneault C, Blondin P, Sirard MA. 2014. Gene expression analysis of bovine oocytes at optimal coasting time combined with GnRH antagonist during the no-FSH period. Theriogenology 81:1092−1100.

Li W, Wu J, Kim SY, Zhao M, Hearn SA, Zhang MQ, Meistrich ML, Mills AA. 2014. Chd5 orchestrates chromatin remodelling during sperm development. Nat Commun 5:3812.

Li Y, Drnevich J, Akraiko T, Band M, Li D, Wang F, Matoba R, Tanaka TS. 2013. Gene expression profiling reveals the heterogeneous transcriptional activity of Oct3/4 and its possible interaction with Gli2 in mouse embryonic stem cells. Genomics 102:456−467.

Liu Y, Sui HS, Wang HL, Yuan JH, Luo MJ, Xia P, Tan JH. 2006. Germinal vesicle chromatin configurations of bovine oocytes. Microsc Res Tech 69:799−807.

Lodde V, Modina S, Galbusera C, Franciosi F, Luciano AM. 2007. Large-scale chromatin remodeling in germinal vesicle bovine oocytes: Interplay with gap junction functionality and developmental competence. Mol Reprod Dev 74:740−749.

Lodde V, Modina S, Maddox-Hyttel P, Franciosi F, Lauria A, Luciano AM. 2008. Oocyte morphology and transcriptional silencing in relation to chromatin remodeling during the final phases of bovine oocyte growth. Mol Reprod Dev 75:915−924.

Lodde V, Modina SC, Franciosi F, Zuccari E, Tessaro I, Luciano AM. 2009. Localization of DNA methyltransferase-1 during oocyte differentiation, in vitro maturation and early embryonic development in cow. Eur J Histochem: EJH 53:e24.

Lomberk G, Wallrath L, Urrutia R. 2006. The Heterochromatin Protein 1 family. Genome Biol 7:228.

Luciano AM, Franciosi F, Modina SC, Lodde V. 2011. Gap Junction-Mediated Communications Regulate Chromatin Remodeling During Bovine Oocyte Growth and Differentiation Through cAMP-Dependent Mechanism(s). Biol Reprod 85:1252−1259.

Luciano AM, Lodde V. 2013. In: Coticchio G, Albertini DF, De Santis L, editors. Changes of Large-Scale Chromatin Configuration During Mammalian Oocyte Differentiation. London: Oogenesis: Springer. p 93−108.

Luciano AM, Lodde V, Franciosi F, Tessaro I, Corbani D, Modina S. 2012. Large-scale chromatin morpho-functional changes during mammalian oocyte growth and differentiation. Eur J histochem: EJH 56:e37.

Ma JY, Li M, Luo YB, Song S, Tian D, Yang J, Zhang B, Hou Y, Schatten H, Liu Z, Sun QY. 2013. Maternal factors required for oocyte developmental competence in mice: Transcriptome analysis of non-surrounded nucleolus (NSN) and surrounded nucleolus (SN) oocytes. Cell Cycle 12:1928−1938.

Marzluff WF, Wagner EJ, Duronio RJ. 2008. Metabolism and regulation of canonical histone mRNAs: Life without a poly(A) tail. Nat Rev Genet 9:843−854.

Mattson BA, Albertini DF. 1990. Oogenesis: Chromatin and microtubule dynamics during meiotic prophase. Mol Reprod Dev 25:374−383.

McGraw S, Vigneault C, Tremblay K, Sirard MA. 2006. Characterization of linker histone H1FOO during bovine in vitro embryo development. Mol Reprod Dev 73:692−699.

Monti M, Zanoni M, Calligaro A, Ko MS, Mauri P, Redi CA. 2013. Developmental arrest and mouse antral not-surrounded nucleolus oocytes. Biol Reprod 88:2.

Pan H, O'Brien MJ, Wigglesworth K, Eppig JJ, Schultz RM. 2005. Transcript profiling during mouse oocyte development and the effect of gonadotropin priming and development in vitro. Dev Biol 286:493−506.

Pfeiffer MJ, Siatkowski M, Paudel Y, Balbach ST, Baeumer N, Crosetto N, Drexler HC, Fuellen G, Boiani M. 2011. Proteomic analysis of mouse oocytes reveals 28 candidate factors of the "reprogrammome". J Proteome Res 10:2140−2153.

Potireddy S, Vassena R, Patel BG, Latham KE. 2006. Analysis of polysomal mRNA populations of mouse oocytes and zygotes: Dynamic changes in maternal mRNA utilization and function. Dev Biol 298:155−166.

Robert C, Nieminen J, Dufort I, Gagne D, Grant JR, Cagnone G, Plourde D, Nivet AL, Fournier E, Paquet E, Blazejczyk M, Rigault P, Juge N, Sirard MA. 2011. Combining resources to obtain a comprehensive survey of the bovine embryo transcriptome through deep sequencing and microarrays. Mol Reprod Dev 78:651−664.

Rodman TC, Bachvarova R. 1976. RNA synthesis in preovulatory mouse oocytes. J Cell Biol 70:251−257.

Sanchez R, Marzluff WF. 2004. The oligo(A) tail on histone mRNA plays an active role in translational silencing of histone mRNA during Xenopus oogenesis. Mol Cell Biol 24: 2513−2525.

Sternlicht AL, Schultz RM. 1981. Biochemical studies of mammalian oogenesis: Kinetics of accumulation of total and poly(A)-containing RNA during growth of the mouse oocyte. J Exp Zool 215:191−200.

Subtelny AO, Eichhorn SW, Chen GR, Sive H, Bartel DP. 2014. Poly(A)-tail profiling reveals an embryonic switch in translational control. Nature 508:66−71.

Tan JH, Wang HL, Sun XS, Liu Y, Sui HS, Zhang J. 2009. Chromatin configurations in the germinal vesicle of mammalian oocytes. Mol Hum Reprod 15:1−9.

Thelie A, Pascal G, Angulo L, Perreau C, Papillier P, Dalbies-Tran R. 2012. An oocyte-preferential histone mRNA stem-loop-binding protein like is expressed in several mammalian species. Mol Reprod Dev 79:380−391.

Townley-Tilson WH, Pendergrass SA, Marzluff WF, Whitfield ML. 2006. Genome-wide analysis of mRNAs bound to the histone stem-loop binding protein. RNA 12:1853−1867.

Vandesompele J, De Preter K, Pattyn F, Poppe B, Van Roy N, De Paepe A, Speleman F. 2002. Accurate normalization of real-time quantitative RT-PCR data by geometric averaging of multiple internal control genes. Genome Biol 3: RESEARCH 0034.

Wang S, Kou Z, Jing Z, Zhang Y, Guo X, Dong M, Wilmut I, Gao S. 2010. Proteome of mouse oocytes at different developmental stages. Proc Natl Acad Sci U S A 107:17639−17644.

Wang ZF, Ingledue TC, Dominski Z, Sanchez R, Marzluff WF. 1999. Two Xenopus proteins that bind the 3' end of histone mRNA: Implications for translational control of histone synthesis during oogenesis. Mol Cell Biol 19:835−845.

Wassarman PM, Letourneau GE. 1976. RNA synthesis in fully-grown mouse oocytes. Nature 261:73−74.

Whitfield ML, Kaygun H, Erkmann JA, Townley-Tilson WH, Dominski Z, Marzluff WF. 2004. SLBP is associated with histone mRNA on polyribosomes as a component of the histone mRNP. Nucleic Acids Res 32:4833−4842.

Worrad DM, Ram PT, Schultz RM. 1994. Regulation of gene expression in the mouse oocyte and early preimplantation embryo: developmental changes in Sp1 and TATA box-binding protein, TBP. Development 120:2347−2357.

Zuccotti M, Merico V, Sacchi L, Bellone M, Brink TC, Bellazzi R, Stefanelli M, Redi CA, Garagna S, Adjaye J. 2008. Maternal Oct-4 is a potential key regulator of the developmental competence of mouse oocytes. BMC Dev Biol 8:97.

SUPPORTING INFORMATION

Additional supporting information may be found in the online version of this article at the publisher's web-site.

MRD

molecular human reproduction

ORIGINAL ARTICLE

Differences in cumulus cell gene expression indicate the benefit of a pre-maturation step to improve *in-vitro* bovine embryo production

Cecilia Dieci[1,†], Valentina Lodde[1,†], Rémi Labreque[2], Isabelle Dufort[2], Irene Tessaro[1,3], Marc-André Sirard[2], and Alberto M. Luciano[1,*]

[1]Reproductive and Developmental Biology Laboratory, Department of Health, Animal Science and Food Safety, University of Milan, Via Celoria 10, 20133 Milan, Italy [2]Centre de Recherche en Biologie de la Reproduction, Département des Sciences Animales, Université Laval, 2440, boulevard Hochelaga, Québec, (Québec) G1V 0A6, Canada [3]Present address: I.R.C.C.S. Istituto Ortopedico Galeazzi, Via R. Galeazzi, 4, 20161 Milan, Italy

*Correspondence address. Dipartimento di Scienze Veterinarie per la Salute, la Produzione Animale e la Sicurezza Alimentare, Università degli Studi di Milano, Via Celoria, 10, 20133 Milano, Italy. E-mail: alberto.luciano@unimi.it

STUDY QUESTION: Does the gene expression profile of cumulus cells (CC) accompanying oocytes with different degrees of chromatin compaction within the germinal vesicle (GV) reflect the oocyte's quality and response in culture during *in-vitro* embryo production (IVP).

SUMMARY ANSWER: The transcriptomic profile of the CC is related to oocyte competence, setting the stage for the development of customized pre-maturation strategies to improve IVP.

WHAT IS KNOWN ALREADY: Oocytes complete the acquisition of their competence during antral follicle development. During this period, the chromatin configuration within the GV changes dynamically and is indicative of oocyte's developmental potential. The interactions between somatic and germ cells modulate chromatin morphology and function and are critical for acquisition of oocyte competence.

STUDY DESIGN, SIZE, DURATION: Bovine cumulus–oocyte complexes (COC) were isolated from 0.5 to 6 mm antral follicles. Surrounding CC were separated from the oocyte and classified as GV0, GV1, GV2 and GV3 according to the degree of the oocyte's chromatin compaction.

PARTICIPANTS/MATERIALS, SETTING, METHOD: RNA extracted from CC of each group was amplified and hybridized on a bovine embryo-specific 44 K Agilent slide. The CC_GV1, CC_GV2 and CC_GV3 classes were each hybridized against the CC_GV0 class, representing an early oocyte differentiation stage with poor development competence. The data were normalized and fold changes of the differentially expressed genes were determined. Microarray data were validated using quantitative RT-PCR on selected targets. Microarray data were further analyzed through: (i) between-group analysis (BGA), which classifies the samples according to their transcriptomic profiles; (ii) cluster analysis according to the expression profile of each gene; and (iii) Ingenuity Pathway Analysis (IPA) to study gene regulation patterns and predicted functions. Furthermore, CC of each GV group were cultured and apoptotic cells were assessed after 3 h by caspase analysis. Finally, based on the analysis of CC transcriptomic profiles and the relationship between morphological features of the COC and the oocyte chromatin configuration, a customized, stage-dependent oocyte pre-maturation (pre-IVM) system was used to improve oocyte developmental potential before IVM. For this, the blastocyst rate and quality were assessed after *in-vitro* maturation and fertilization of pre-matured oocytes.

MAIN RESULTS AND THE ROLE OF CHANCE: Overall, quantitative RT-PCR results of a subset of five selected genes were consistent with the microarray data. Clustering analysis generated 16 clusters representing the main profiles of transcription modulation. Of the 5571 significantly differentially expressed probes, the majority (25.49%) best fitted with cluster #6 (downregulation between CC_GV0 and CC_GV1 and stable low levels in successive groups). IPA identified the most relevant functions associated with each cluster. Genes included in cluster #1 were mostly related to biological processes such as 'cell cycle' and 'cell death and survival', whereas genes included in cluster #5 were mostly related to 'gene expression'. Interestingly, 'lipid metabolism' was the most significant function identified in clusters #6, #9 and

---

† Contributed equally.

#12. IPA of gene lists obtained from each contrast (i.e., CC_GV0 vs. CC_GV1; CC_GV0 vs. CC_GV2; CC_GV0 vs. CC_GV3) revealed that the main affected function in each contrast was 'cell death and survival'. Importantly, apoptosis was predicted to be inhibited in CC_GV1 and CC_GV2, but activated in CC_GV3. Caspase analysis indicated that a low percentage of CC_GV0 was prone to undergo apoptosis but apoptosis increased significantly in CC from oocytes with condensed chromatin, reaching a peak in CC_GV3 ($P < 0.05$). Finally, the tailored oocyte pre-maturation strategy, based on morphological features of the COC and the oocyte chromatin configuration, demonstrated that pre-IVM improved the developmental capability of oocytes at early stages of differentiation (GV1-enriched COC) but was detrimental for oocytes at more advanced stages of development (GV2 and GV3-enriched COC).

LARGE SCALE DATA: The data are available through the GEO series accession number GSE79886.

LIMITATIONS, REASONS FOR CAUTION: This study was conducted with bovine samples. Whether or not the results are applicable to human oocytes requests further elucidation. Embryo transfer experiments are required to determine whether the improvement in blastocyst rates in the tailored system leads to increased live birth rates.

WIDER IMPLICATIONS OF THE FINDINGS: The identification of multiple non-invasive biomarkers predictive of oocyte quality can greatly strengthen the pre-IVM approach aimed to improve IVM outcomes. These results have potentially important implications in treating human infertility and in developing breeding schemes for domestic mammals.

STUDY FUNDING/COMPETING INTEREST(S): This work was supported in part by NSERC Strategic Network EmbryoGENE, Canada and in part by CIG—Marie Curie Actions—Reintegration Grants within the EU 7FP (n. 303640, 'Pro-Ovum'). The authors declare no potential conflict of interest.

Key words: oocyte / chromatin / follicle / granulosa cells / cumulus cells / apoptosis / pre-maturation / embryo development

Introduction

In-vitro embryo production (IVP) remains inefficient in both clinical applications of human reproduction and animal breeding. In particular, the development of suitable conditions for *in-vitro* oocyte maturation (IVM) that supports high quality oocyte production is a major challenge in assisted reproductive technologies (Smitz *et al.*, 2011). In the bovine, although many attempts to increase the number of transferable embryos have been made in recent decades, the efficiency of IVP techniques, calculated as the proportion of immature oocytes aspirated from middle antral follicles (2–8 mm in diameter) that reach the blastocyst stage of embryonic development, is struggling to overcome a 35% threshold (Lonergan and Fair, 2008), unless very specific hormonal programming is used, that can double this rate (Blondin *et al.*, 2002; Nivet *et al.*, 2012, Landry *et al.*, 2016). In fact, oocytes retrieved from non-treated animals reveal heterogeneous cellular and molecular features as well as distinct embryonic developmental capabilities (Pavlok *et al.*, 1992; Blondin and Sirard, 1995). On the other hand, it is well known that oocytes enclosed in early antral follicles (<2 mm in diameter) have not yet acquired the competence to spontaneously resume meiosis once isolated from the follicular compartment (Pavlok *et al.*, 1992; Blondin and Sirard, 1995); thus, they are generally not used in standard IVP protocols.

The diversity of oocyte competence is mainly due to the intrinsic heterogeneity of the cohort of follicles from which cumulus–oocyte complexes (COC), to be subjected to standard IVP procedures, are isolated (Merton *et al.*, 2003; Vassena *et al.*, 2003). In cows, as in humans, only one oocyte is released at each reproductive cycle while the remaining follicles undergo atresia (Gougeon, 1986; Lussier *et al.*, 1987). It is widely accepted that one of the main factors that impairs oocyte ability to become an embryo *in vitro* is the precocious meiotic resumption that occurs when oocytes are isolated from the follicles. This, indeed, interrupts the process of oocyte capacitation

(Hyttel *et al.*, 1997; Gilchrist *et al.*, 2008; Coticchio *et al.*, 2015) and creates an asynchrony between the nuclear and the cytoplasmic events that are required for oocyte differentiation program before ovulation (Eppig *et al.*, 1994). In addition, a large proportion of these oocytes have already started an atretic process (Gougeon, 1996; Adams *et al.*, 2008; Monniaux *et al.*, 2014).

Oocyte quality heterogeneity is reflected in differences in the large-scale configuration of the chromatin enclosed in the germinal vesicle (GV) of immature oocytes (reviewed in Zuccotti *et al.*, 2005; De La Fuente, 2006; Luciano and Lodde, 2013; Luciano *et al.*, 2014). In cows, oocytes isolated from early to middle antral follicles have four different patterns of chromatin configuration, from GV0 to GV3, which are characterized by progressive increases in chromatin compaction (Lodde *et al.*, 2007), transcriptional silencing (Lodde *et al.*, 2008; Luciano *et al.*, 2011) and global DNA methylation (Lodde *et al.*, 2009). Notably, oocytes with a GV0 configuration (isolated from early antral follicles) display a very limited capability to resume meiosis, while virtually all of the GV1, GV2 and GV3 oocytes (isolated from mid-antral follicles) are capable of reaching the metaphase II (MII) stage *in vitro*, regardless their GV configuration (Lodde *et al.*, 2007). However, only a limited proportion of GV1 oocytes reach the blastocyst stage after IVF, while GV2 and GV3 oocytes have significantly higher embryonic developmental potentials (Lodde *et al.*, 2007). Thus, large-scale chromatin configuration is a marker of oocyte differentiation and competence.

It is clear that a better characterization of the molecular determinants of oocyte heterogeneity would be beneficial in understanding basic oocyte biology as well as in improving IVP efficiency. With this view, we have recently analyzed the transcriptomic profile of bovine oocytes with different chromatin configurations to identify changes in mRNA expression in the oocyte during the GV0-to-GV3 transition (Labrecque *et al.*, 2015). The present study aimed to expand this knowledge by assessing the transcriptomic profile of cumulus cells (CC) isolated from oocytes with different chromatin configurations. In

fact, proper assessment of the oocyte 'signature' cannot overlook features of the surrounding CC. It is well established that the CC play a fundamental role in the modulation of oocyte competence acquisition. During folliculogenesis, oocyte growth and differentiation rely upon the establishment of a microenvironment generated by bidirectional paracrine regulatory signals, and intercellular heterologous gap junction communications between oocytes and somatic cells are pivotal (Eppig, 2001; Matzuk *et al.*, 2002; Gilchrist *et al.*, 2008). Moreover, previous studies show that the tight association between oocyte and companion CC is required for the progressive suppression of transcriptional activity, chromatin remodeling and competence acquisition during the final phase of oocyte growth in mice (De La Fuente and Eppig, 2001), cows (Luciano *et al.*, 2011) and humans (Sanchez *et al.*, 2015).

Furthermore, based on the results of our microarray analysis, in a second part of this study, we hypothesize that each class of oocytes responds differently to the cultural environment during IVP. To test this hypothesis, and considering that it is technically not possible to identify the chromatin configuration without DNA staining after removal of CC, we first looked for possible morphological markers that could be related to the chromatin configuration of the corresponding oocyte, and used these criteria to select a population of COC enriched in GV1 oocytes (which are less competent compared with GV2 and GV3). Then, on the basis of the microarray results, we designed a culture system specifically formulated to fulfill the specific needs of the oocyte at a specific stage and to support *in-vitro* development. This system was used as proof-of-concept of an *in-vitro* differentiation strategy, the so-called 'pre-maturation' system, in order to improve oocyte developmental potential before IVM. This, in turn, confirmed the hypothesis that each class of oocytes responds differently to the cultural environment during IVP.

Materials and Methods

All chemicals and reagents were purchased from Sigma-Aldrich, St. Louis, MO USA., unless otherwise stated.

COC collection

Ovaries were recovered at the abattoir (INALCA Spa, Ospedaletto Lodigiano, LO, IT 2270 M CE, Italy) from 4 to 8 years old Holstein dairy cows and COC were retrieved from early (0.5–2 mm) and middle antral follicles (2–8 mm) as previously described (Lodde *et al.*, 2007). All the COC collected were then washed in medium 199 (M199) supplemented with HEPES 20 mM, 1790 units/L Heparin and 0.4% of bovine serum albumin (HM199) and examined under a stereomicroscope. Only COC suitable for standard IVP procedures were used. Precisely, only oocytes medium-brown in color, with homogenous or finely granulated ooplasm and surrounded by five or more complete layers of CC were included in the study (Luciano *et al.*, 2005). The same morphological selection criteria are commonly accepted by the scientific community and applied in the commercial settings worldwide (Gordon, 2003; Stringfellow and Givens, 2010).

CC isolation

COC were individually vortexed (2 min, 35 Hz) in HM199 supplemented with 5% of calf serum (Gibco, Thermo Fisher Scientific, Waltham, MA USA) to isolate CC. In order to assess the chromatin configuration of oocytes corresponding to each cumulus, the denuded oocytes (DO) were individually washed in HM199, stained in HM199 containing 1 μg/ml

Hoechst 33342 for 5 min in the dark, and then transferred into a 5-μl drop of the same medium, overlaid with mineral oil and observed under an inverted fluorescence microscope (Olympus IX50, Olympus Italia S.r.l., Segrate, Italy, magnification ×40). Oocytes were classified according to the degree of chromatin compaction within the nuclear envelope as previously described (Lodde *et al.*, 2007): the GV0 stage is characterized by a diffuse filamentous pattern of chromatin in the whole nuclear area; the GV1 and GV2 configurations represent early and intermediate stages, respectively, of chromatin remodeling, a process starting with the appearance of few foci of condensation in GV1 oocytes and proceeding with the formation of distinct clumps of condensed chromatin in GV2 oocytes; the GV3 is the stage where the maximum level of condensation is reached with chromatin organized into a single clump.

For transcriptomic and gene expression analyses, CC isolated from each COC were individually collected in RNAse-free tubes, washed twice in cold PBS followed by centrifugation at 10.600 g for 1 min at 4°C. After the removal of the supernatant, CC pellets (in the minimum volume of PBS possible) were snap-frozen in liquid nitrogen and stored at −80°C until RNA extraction. For the assessment of pan-caspase activity, CC were isolated following the same experimental procedure with the exception that they were removed by pipetting to avoid cell damage. Then, CC isolated from a single COC were transferred into culture medium and assayed as described below.

RNA extraction

Groups of CC isolated from 10 oocytes with the same chromatin configuration were pooled and processed for total RNA extraction. Total RNA was extracted and purified with the Pico-Pure RNA Isolation Kit (ARCTURUS®, Thermo Fisher Scientific) following the manufacturer's protocol, with minor modifications. Briefly, 10–30 μl of extraction buffer was added to each tube containing CC pellet from a single COC and incubated 30 min at 42°C. Following incubation, extraction reaction mixtures from 10 tubes with CC isolated from oocytes bearing the same chromatin configuration were pooled and equal volumes of EtOH 70% were added to each tube. Then, 250 μl of the RNA sample and EtOH mixture was loaded into the preconditioned purification columns and centrifuged for 2 min at 100g; this step was repeated until all the RNA/EtOH mixtures were loaded into the columns. Finally, the columns were centrifuged at 16 000g for 30 s to remove the flow-through and bind RNA. Following these steps, the procedure was performed according to manufacturer's instructions and including DNase treatment (Qiagen Italia, Milano, Italy) on the purification columns. Four pools for each chromatin configuration (CC_GV0, CC_GV1, CC_GV2 and CC_GV3) were used for microarray analysis and an additional four pools for each chromatin configuration (from independent collections) were used for microarray validation by quantitative reverse-transcriptase-PCR (qRT-PCR). Total RNA purity, integrity and concentration were evaluated using a 2100-Bioanalyzer (Agilent Technologies, Palo Alto, CA, USA) with the RNA PicoLab Chip (Agilent Technologies). All extracted samples were of good quality with an RNA integrity number of >7.4.

RNA amplification, sample labeling and microarray hybridization

To generate enough material for the hybridization, RNA samples were linearly amplified according to the EmbryoGene pipeline. Antisense RNA (aRNA) was produced using the RiboAmp HS RNA amplification kit (Applied Biosystems, Thermo Fisher Scientific). After two amplification rounds of 6 h each, the aRNA output was quantified using the NanoDrop ND-1000 (NanoDrop Technologies, Wilmington, DE, USA) (Gilbert *et al.*, 2009, 2010). Then, for each sample, 4 μg of aRNA was labeled using the
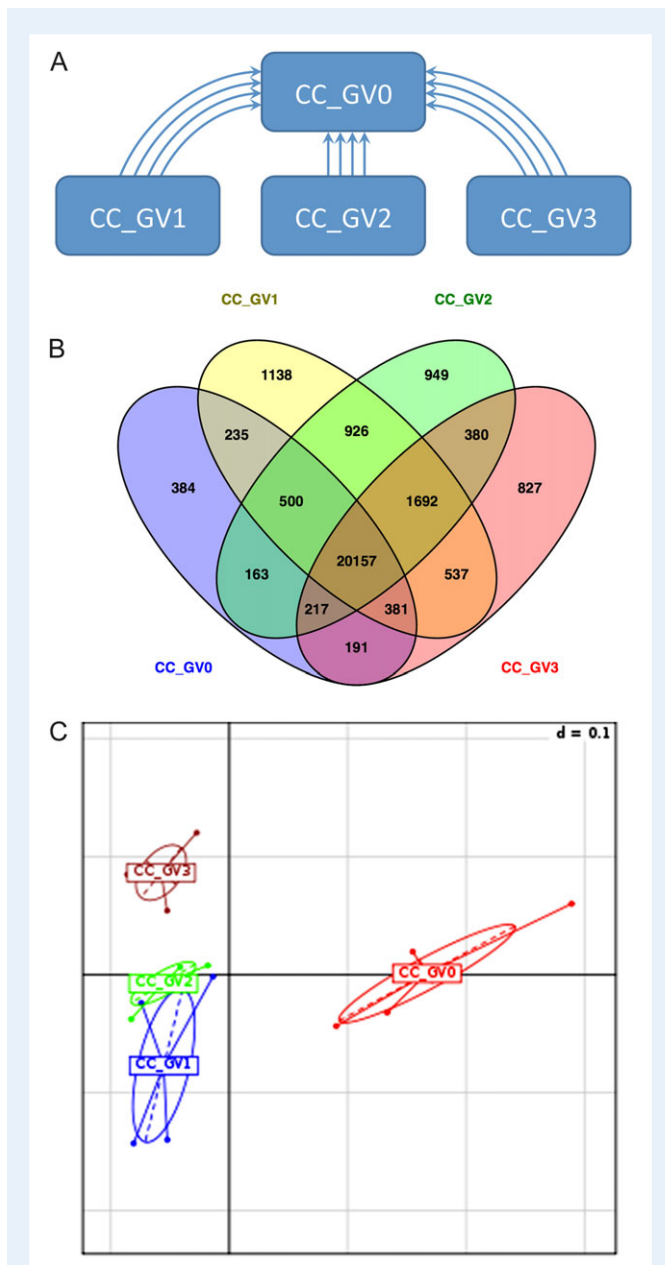
Figure 1 Microarray analysis of CC isolated from oocytes with different large-scale chromatin configuration. (**A**) Experimental design. CC associated with oocytes with GV0, GV1, GV2 and GV3 chromatin configuration were isolated and subjected to microarray analysis. The hybridizations were performed using a reference design, where CC isolated from oocytes with GV1, GV2 and GV3 chromatin configuration were compared with CC isolated from GV0 oocytes (CC_GV0 vs. CC_GV1; CC_GV0 vs. CC_GV2; CC_GV0 vs. CC_GV3). In each contrast, the CC_GV0 group represents the reference group. Overall, 12 hybridizations corresponding to the 4 biological replicates and 3 comparisons were performed. (**B**) Venn's diagram showing commonly expressed probes in the four experimental groups. Diagram was generated using the online tool VENNY 2.0 (*Oliveros, J.C. (2007–2015) Venny. An interactive tool for comparing lists with Venn's diagrams.* http://bioinfogp.cnb.csic.es/tools/venny/index.html), in which the lists of expressed probes in each group were uploaded. (**C**) BGA of the CC microarray data, in which the samples

ULS Fluorescent Labeling Kit for Agilent arrays (with Cy3 and Cy5) (Kreatech Diagnostics, Amsterdam, The Netherlands). The labeled product was then purified with the Pico-Pure RNA Isolation Kit. Labeling efficiency was measured using the Nano-Drop ND-1000. Samples from the four biological replicates, representing six different weeks of CC collection, were hybridized on a custom bovine embryo-specific Agilent 44 K microarray slide (Robert *et al.*, 2011). The hybridizations were performed using a reference design, where CC isolated from oocytes bearing the GV1, GV2 or GV3 chromatin configuration were compared with CC isolated from GV0 oocytes (CC_GV0 vs. CC_GV1; CC_GV0 vs. CC_GV2; CC_GV0 vs. CC_GV3). Thus, the reference group in the contrast is always represented by the CC_GV0 group. Overall, 12 hybridizations corresponding to the 4 biological replicates and 3 comparisons were performed (Fig. 1A). A total of 825 ng of each labeled sample (Cy3 and Cy5) was incubated in a solution containing 10× blocking agent and 25× fragmentation buffer in a volume of 55 μl at 60°C for 15 min and were put on ice immediately after. Then, 55 μl of 2× GEx Hybridization Buffer HI-RPM was added for a total volume of 110 μl. The hybridization mix (100 μl) was added onto the array and hybridization was performed at 60°C for 17 h using an Agilent Hybridization chamber in a rotating oven. After washing and drying steps, the slides were scanned using the Tecan PowerScanner microarray scanner (Tecan Group Ltd, Männerdorf, Switzerland) and features were extracted using ArrayPro 6.4 Analyzer (Media Cybernetics, Bethesda, MD, USA).

Microarray data analysis

Microarray data analysis was performed according to the EmbryoGENE pipeline. Intensities files were uploaded to ELMA software (EmbryoGENE LIMS Microarray Analysis, http://elma.embryogene.ca/), to run the quality control module.

To detect the presence or absence of the signal for each spot present on the slide, microarray data sets generated by ELMA were analyzed and an arbitrary cut-off corresponding to the mean intensity of the background level plus twice the standard deviation (SD) of the background was used. A Venn diagram was created using the online tool VENNY to show present and common probes between groups. Moreover, a between-group analysis (BGA) was performed to classify the samples according to their transcriptomic profiles (Culhane *et al.*, 2002).

To calculate the gene expression fold change for each contrast individually (CC_GV0 vs. CC_GV1; CC_GV0 vs. CC_GV2; CC_GV0 vs. CC_GV3) microarray data sets generated by ELMA were analyzed with the FlexArray microarray analysis software, Version 1.6.1 (Blazejczyk *et al.*, 2007). Briefly, raw data were subjected to a simple background subtraction, normalized within each array (Loess) and a Limma simple analysis was performed to obtain the fold change values. The reference group in the contrasts is represented by the CC_GV0 group.

In addition, data sets generated by ELMA were subjected to microarray analysis of variance (MAANOVA) that was conducted considering the four experimental groups and by using the CC_GV0 as a reference group. Differences were considered as statistically significant with a *P*-value of

are classified according to their transcriptomic profile (Culhane *et al.*, 2002) using the online tool available within the EmbryoGENE LIMS and Microarray Analysis (ELMA) pipeline. The plot illustrates the global distribution of transcriptome data (expressed probes) from the four experimental groups (CC from GV0, GV1, GV2 or GV3 oocytes) and the four biological replicates (dots in each group). The relative distance between each group indicates the global transcriptional differences among CC isolated from oocytes with different chromatin configurations.

<0.05. After MANOVA analysis, probes were grouped in clusters according to their expression profile using the mFuzz Bioconductor package (Kumar and Futschik, 2007).

Finally, the gene lists generated by our analysis were examined using Ingenuity Pathway Analysis (Ingenuity Systems, Mountain View, CA, USA). All statistically significant genes (*P*-value < 0.05) were uploaded to the application. The functional analysis identified the biological functions that were most significant to the molecules in the database.

cDNA preparation and qRT-PCR

The validation of microarray results was performed by qRT-PCR using four independent biological replicates (each pool containing CC derived from 10 COC). For each sample, 1 ng of total RNA was reverse transcribed using the SuperScript First-Strand Synthesis for RT-PCR (Invitrogen—Thermo Fisher Scientific) with oligo-dT primers following the manufacturer's recommendations. Primer sequences used for real-time RT-PCR are provided in Supplementary Table 1. Primers were designed using the Primer3 online tool (http://primer3.ut.ee/) from sequences obtained using the UMD3.1 assembly of the bovine genome. Specificity of each primers pair was confirmed by electrophoresis analysis on a standard 2% agarose gel and sequencing analysis.

The PCR products were purified with the QIAquick PCR Purification kit (Qiagen), quantified using the Qbit 2.0 fluorometer and Qubit dsDNA HS Assay Kit (Invitrogen—Thermo Fisher Scientific). Serial dilutions of the PCR products (ranging from 2×10^{-4} to 2×10^{-8} ng/µl) were then used to create the standard curves for the evaluation of the amplification efficiencies. Quantitative real-time PCR was performed on an iQ5 (Bio-Rad, Laboratories S.r.l., Segrate, Italy) using SYBR incorporation. Each qPCR, in a final volume of 20 µl, contained the cDNA corresponding to 1 ng of RNA extracted, 0.1 µM of each primer and 1× SYBR mix (iTaq Universal SyBR Green Supermix, Bio-Rad). The PCR conditions used for all genes were as follows: a denaturing step of 30 s at 95°C, followed by 40 PCR cycles (95°C for 30 s; 57°C for 1 min), a melting curve (55°C for 1 min and a step cycle starting at 55°C, up to 94.5°C). PCR specificity was confirmed by melting-curve analysis.

For each gene tested, four independent biological replicates were used. Analysis of gene expression stability over the four groups was performed using the GeNorm algorithm (Vandesompele *et al.*, 2002) through Biogazelle's qBase+ software (Biogazelle, Zwijnaarde, Belgium). Beta actin (ACTB), glyceraldehyde-3-phosphate dehydrogenase (GAPDH) and hypoxanthine phosphoribosyl transferase 1 (HPRT1) were identified as the most stable genes among the different groups, with *M*-value <1.5, and thus used as reference genes. Complementary DNA quantification was performed with the iQ5 Optical System Software Version 2.0 (Bio-Rad) using the delta—delta Ct method, where CC from GV0 were used as a reference group.

Active caspase-positive cells analysis

Dispersed CC preparations (Luciano *et al.*, 2000) isolated from single oocytes with different chromatin configurations (CC_GV0, CC_GV1, CC_GV2 and CC_GV3) were collected as described above and processed through the CaspaTag™ Pan-Caspase *In-Situ* Assay Kit (Merck Millipore, Billerica, MA, USA), a methodology based on Fluorochrome Inhibitors of Caspases (FLICA) to detect active caspase in cells undergoing apoptosis, following the manufacturer's specification sheet with slight modifications. Briefly, dispersed CC were plated in four-well plate for 3 h in TCM199 supplemented with 0.68 mM L-glutamine, 25 mM NaHCO$_3$, 0.2 mM sodium pyruvate and 0.4% fatty acid-free BSA at 38.5°C and 5% CO$_2$, to allow them to adhere to the plate. Subsequently, cells were cultured for one additional hour in the presence of a carboxyfluorescein-labeled inhibitor of caspases. After washings and fixation in 10% formaldehyde, cells

were detached by gently pipetting and moved on a glass slide. When dried, cells were covered with the antifade medium Vecta Shield (Vector Laboratories, Burlingame, CA, USA) supplemented with 1 µg/ml 40,6-diamidino-2-phenylindole (DAPI) and analyzed under fluorescent microscopy (Nikon Eclipse E600). For each sample, 10/15 fields were randomly chosen and results were expressed as the number of active caspase-positive cells over the total number of cells observed.

Assessment of the relationship between COC features and oocyte chromatin configuration

In order to establish morphological criteria that would allow for the collection and/or selection of a population of COC enriched in one of the three GV chromatin configurations (GV1, GV2 or GV3), the relationship between the oocyte chromatin configuration and either (i) the size of the follicle from which the COC was isolated or (ii) the morphology of the corresponding COC was assessed.

With this aim, in a first set of experiments, follicle sizes were determined with a ruler by measuring their visible diameter on the surface of the ovary. COC were collected from 2 to 4 mm, 4–6 or >6 mm antral follicles. In the second set of experiments, COC were collected from 2 to 8 mm antral follicles. In any case, only COC suitable for standard IVP procedure were included in the study. After the first selection, COC were further divided into three groups on the basis of morphological characteristics previously described (Blondin and Sirard, 1995; Hazeleger *et al.*, 1995): Class 1, with homogeneous ooplasm and compact CC; Class 2, with minor granulation of the ooplasm with compact CC; Class 3, with highly granulated ooplasm and slight expansion of CC layers (Fig. 6B) (Gordon, 2003; Stringfellow and Givens, 2010).

In both cases, COC were finally denuded, fixed in a methanol and Dulbecco's Phosphate-Buffered Saline (DPBS) solution (60:40), and stained with DAPI for the assessment of chromatin configuration under fluorescence microscopy as above described.

Glucose-6-phosphate dehydrogenase activity determination by brilliant cresyl blue staining

COC isolated from 2 to 8 mm antral follicles and selected as above described were separated into two groups based on the morphological criteria as Class 1 and Class 2/3 (Fig. 6B). COC were then stained with brilliant cresyl blue (BCB) as previously described (Torner *et al.*, 2008), with slight modifications. Briefly, COC were incubated in 26 µM BCB diluted in DPBS with calcium and magnesium, and supplemented with 0.4% of BSA for 90 min at 38.5°C in humidified air atmosphere. After washing, CC were removed and oocytes were examined under a stereomicroscope. Oocytes were classified as BCB negative (BCB−), when the oocyte showed a colorless cytoplasm, or BCB positive (BCB+) where oocytes showed different grades of blue/violet color.

In-vitro pre-maturation, IVM, IVF and embryo culture

For IVP experiments, only COC from 2 to 8 mm middle antral follicles collected as above described were used. After isolation and selection, COC were divided based on the morphological criteria as Class 1, Class 2 and Class 3 as above described. Groups of 20–30 COC belonging to Class 1, Class 2/3 or unsorted COC (a mix of Class 1, Class 2 and Class 3, corresponding to the population of COC that is commonly used in standard IVP procedures) were subjected to standard IVP (IVM, IVF and in-vitro embryo culture (IVC)) with or without a *In-vitro* pre-maturation (pre-IVM) culture step (Franciosi *et al.*, 2014). To avoid meiotic resumption before pre-IVM,

COC were classified in HM199 supplemented with the non-selective PDE inhibitor 3-isobutyl-1-methyl-xanthine (IBMX) at the final concentration of 0.5 mM (Lodde *et al.*, 2013). Pre-IVM consisted of culture for 6 h in M199 added with 0.68 mM L-glutamine, 25 mM NaHCO$_3$, 0.4% BSA fatty acid free, 0.2 mM sodium pyruvate, 10^{-4} IU/ml of r-hFSH (Gonal-F, Serono, Rome, Italy) and 10 µM cilostamide in humidified air under 5% CO$_2$ at 38.5°C (Franciosi *et al.*, 2014).

For IVM, COC (immediately after collection or after 6 h of pre-IVM) were cultured for 22 h in M199 added with 0.68 mM L-glutamine, 25 mM NaHCO$_3$, 0.4% BSA fatty acid free, 0.2 mM sodium pyruvate and 0.1 IU/ml of r-hFSH (Gonal-F, Merck Serono, Darmstadt, Germany) at 38.5°C in 5% CO$_2$ as described by Luciano *et al.* (2005).

IVF and IVC were carried out as previously described (Luciano *et al.*, 2005). At the end of culture period ($d + 8$), the blastocyst rate was assessed under a stereomicroscope. The embryos were then fixed in 60% methanol in DPBS and the cell nuclei were counted under a fluorescence microscope after staining with 0.5 mg/ml of propidium iodide (Luciano *et al.*, 2005).

Table I **Number of differentially expressed probes ($P < 0.05$).**

	Total	Fold change >2[a]	Fold change >−2[a]
CC_GV0 vs. CC_GV1	112	77	35
CC_GV0 vs. CC_GV2	127	42	85
CC_GV0 vs. CC_GV3	204	82	122

[a]Note: that CC_GV0 represents the reference group; therefore, positive fold change means upregulation in GV1, GV2 or GV3 when compared with CC_GV0, while negative fold change means downregulation in GV1, GV2 or GV3 when compared with CC_GV0.

Statistical analysis

Experiments were repeated at least three times. Data were analyzed by one-way ANOVA followed by Newman–Keuls Multiple Comparison test using Graph Pad Prism version 6.0 h. Data are presented as mean ± SEM. P values < 0.05 were considered as statistically significant. For each experiment, the specific test used is indicated in the figure legend.

Results

Microarray results

To gain insights into transcriptomic profiles of CC associated with oocytes with different large-scale chromatin configurations, three microarray comparisons using the EmbryoGENE bovine microarray were performed. This microarray includes 42 242 probes, of which 31 138 represent reference genes, novel untranscribed regions, 3′-untranslated region variants and alternatively spliced exons (Robert *et al.*, 2011).

As shown in Fig. 1A, the hybridizations were performed using a reference design, where the CC isolated GV1, GV2 or GV3 chromatin configuration were compared with CC from GV0 oocytes (CC_GV0 vs. CC_GV1; CC_GV0 vs. CC_GV2; CC_GV0 vs. CC_GV3; the reference group in the contrast is represented by the CC_GV0 group). Microarray data were deposited in the National Center for Biotechnology Information (NCBI)'s Gene Expression Omnibus (Edgar *et al.*, 2002), and are accessible through GEO series accession number GSE79886 (http://www.ncbi.nlm.nih.gov/geo/query/acc.cgi?acc=GSE79886).

Considering the threshold used to detect the presence/absence of the spots on the microarray slides, a total of 20 155 probes were commonly expressed in all the four groups (Fig. 1B), while 384, 1138, 949 and 827 were expressed only in CC_GV0, CC_GV1, CC_GV2 and CC_GV3, respectively. As shown in Fig. 1C, the BGA revealed the
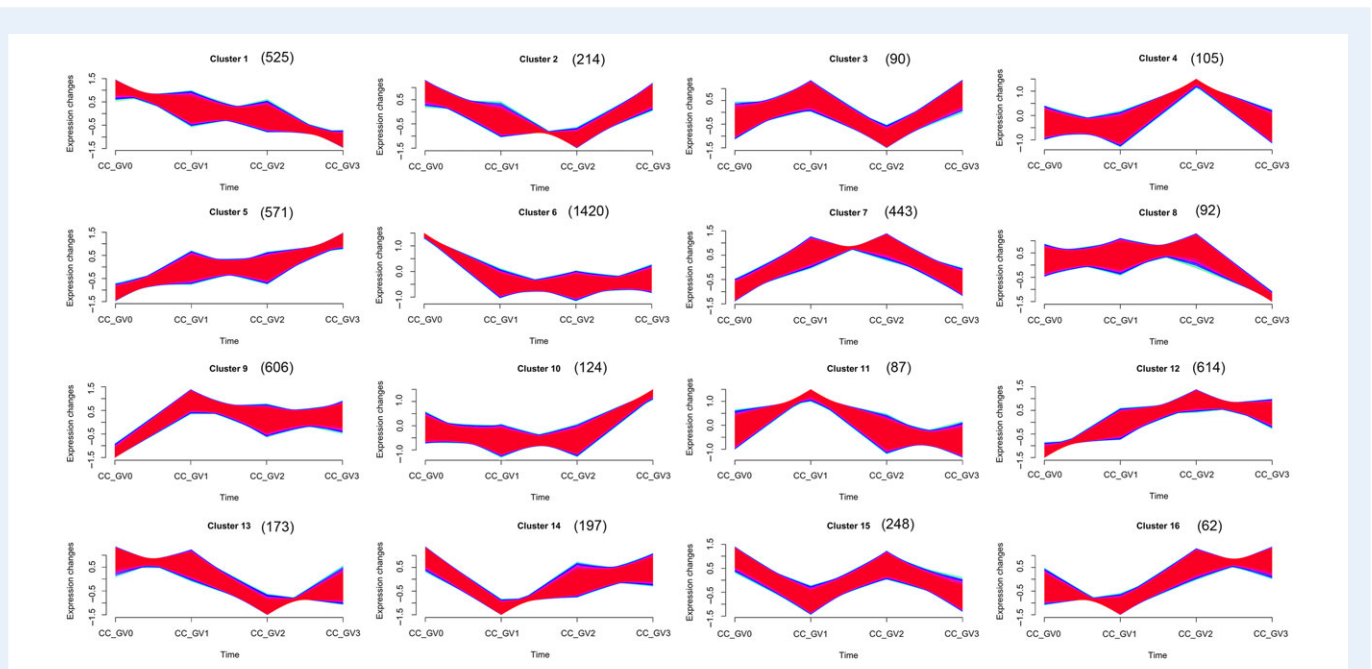

Figure 2 Clusters analysis. Graphs represent the 16 clusters generated by the mFuzz clustering analysis (Kumar and Futschik, 2007). For each cluster, the number of statistically significant probes that best fit to each profile is indicated between brackets. Note: cluster #6 is the one with the higher number of best fit probes.
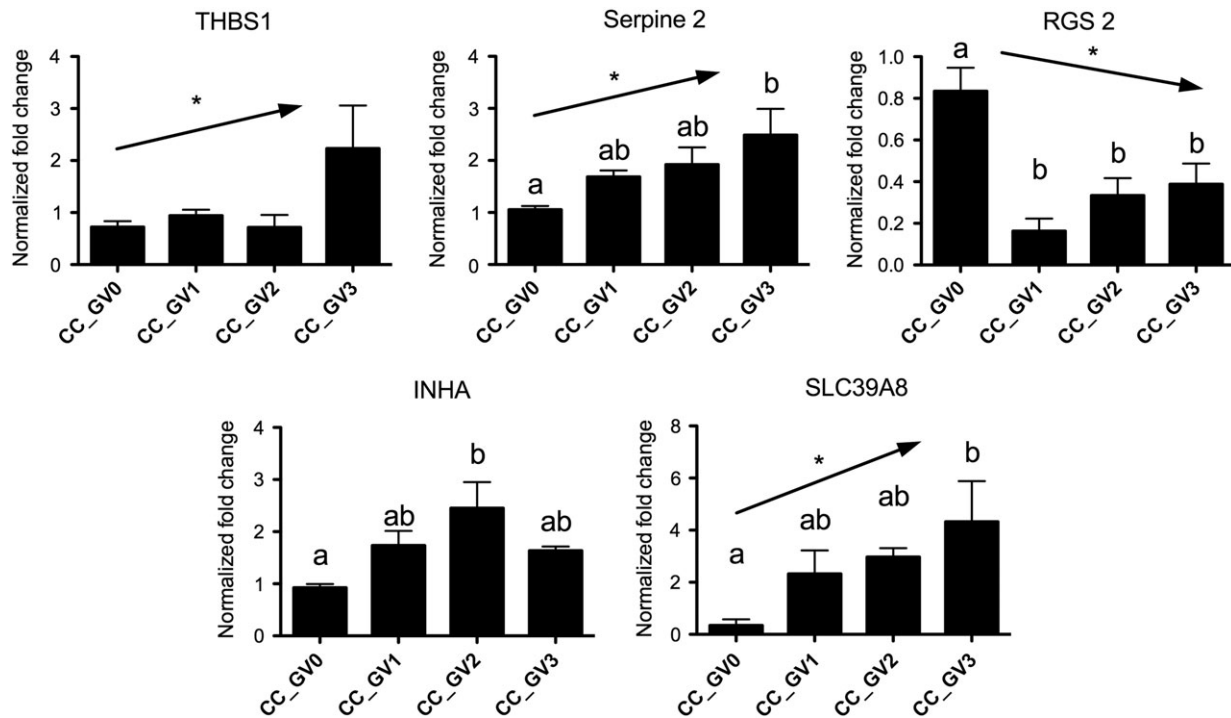
Figure 3 qRT-PCR validation of the microarray results. Validation of microarray data by means of qRT-PCR. Graphs indicate relative expression levels of selected genes in CC isolated from oocytes with GV0, GV1, GV2 or GV3 chromatin configuration; expression levels for each gene were normalized using ACTB, GAPDH and HPRT1 as reference genes. Relative fold changes were calculated using the delta–delta Ct method using CC_GV0 as a reference group. Data were analyzed by one-way ANOVA followed by Newman–Keuls multiple comparison test and are expressed as means $\pm$ SEM. Different superscripts indicate significant differences between groups ($P < 0.05$). Where applicable, test for linear trend was also conducted (*, $P < 00.5$). Note: the selected genes, with accession number, primer sequences, annealing temperature and product size are as in Supplementary Table 1.

global transcriptional differences among CC isolated from oocytes with different chromatin configurations. Considering the biological replicates (dots) within each group, the CC_GV0 and CC_GV1 groups displayed more variation (increased distance between the dots) compared with GV2 and GV3. Moreover, CC_GV0 and CC_GV3 groups were characterized by unique gene expression profiles, while some minimal overlapping existed between CC_GV1 and CC_GV2 groups.

The MAANOVA algorithm revealed that 5571 probes were significantly differentially expressed ($P < 0.05$) between groups, of which 112, 127 and 204 presented a fold change difference more than ±2 in CC_GV0 vs. CC_GV1, CC_GV0 vs. CC_GV2 and CC_GV0 vs. CC_GV3, respectively (Table I). Clustering analysis with the mFuzz Bioconductor package generated 16 clusters representing the main profiles of transcription modulation (Fig. 2). Of the 5571 significantly differentially expressed probes, 25.49% best fitted with cluster #6 profile (downregulation between CC_GV0 and CC_GV1 and relatively stable low levels in successive groups). Clusters #1 (constant decrease from CC_GV0 to CC_GV3), cluster #5 (constant increase from CC_GV0 to CC_GV3), cluster #9 (upregulation between CC_GV0 and CC_GV1 and relatively stable levels in successive groups) and cluster #12 (upregulation from CC_GV0 to CC_GV2 and relatively stable levels from CC_GV2 to CC_GV3) each included ~10% of the total probes, while the other clusters included low numbers of probes (Fig. 2).

A subset of five genes was selected, according to their significant changes in the three comparisons after FlexArray analysis and their known biological functions, to validate the microarray results by qRT-PCR. The chosen genes were Thrombospondine 1 (THBS1), Serpine 2, regulator of G-protein signaling 2 (RGS2), inhibin alpha (INHA) and solute carrier family 39, member 8 (SLC39A8, Supplementary Table 1). Overall, qRT-PCR results were consistent with the microarray data (Fig. 3).

IPA-based functional analysis

Lists of genes that best fitted each of the main clusters (#1, #5, #6, #9 and #12) were submitted to IPA in order to identify the most relevant molecular and cellular functions associated with each cluster (Table II). The genes included in cluster #1 were related to biological processes such as 'cell cycle' and 'cell death and survival', whereas genes included in cluster #5 were more related to molecular processes such as 'gene expression', 'RNA post transcriptional modification' and 'protein synthesis'. Interestingly, 'lipid metabolism' and 'small molecule biochemistry' were the most significant functions identified in clusters #6, #9 and #12.

Moreover, in order to gain insights into the molecular and cellular pathways that were likely affected in CC during oocyte chromatin compaction, gene lists obtained from each contrast individually by

Table II Molecular and cellular functions of best fit genes in most represented clusters identified by IPA ($P < 0.05$).

Molecular and cellular functions	P-value	#Molecules
Cluster 1 (↘↘↘) (constant decrease from CC_GV0 to CC_GV3)		
Cell cycle	1.73E-02–3.49E-09	74
Cellular assembly and organization	1.73E-02–3.49E-09	48
DNA replication, recombination and repair	1.73E-02–3.49E-09	67
Cellular movement	1.73E-02–5.10E-06	30
Cell death and survival	1.73E-02–6.41E-06	99
Cluster 5 (↗↗↗) (constant increase from CC_GV0 to CC_GV3)		
RNA post-transcriptional modification	1.24E-02–2.06E-05	17
Protein synthesis	8.88E-03–3.87E-05	43
Gene expression	1.88E-02–5.04E-05	72
Cell signaling	1.88E-02–3.43E-04	15
Vitamin and mineral metabolism	1.88E-02–3.43E-04	8
Cluster 6 (↘→→) (downregulation between CC_GV0 and CC_GV1 and relatively stable low levels in successive groups)		
Lipid metabolism	2.16E-02–8.40E-05	103
Small molecule biochemistry	2.23E-02–8.40E-05	141
Cellular assembly and organization	2.13E-02–2.01E-04	60
Cellular development	2.31E-02–2.23E-04	176
Cellular growth and proliferation	2.31E-02–2.23E-04	260
Cluster 9 (↗→→) (upregulation between CC_GV0 and CC_GV1 and relatively stable levels in successive groups)		
Lipid metabolism	1.97E-02–2.65E-05	32
Small molecule biochemistry	1.97E-02–2.65E-05	46
Molecular transport	1.97E-02–2.81E-05	69
Cellular assembly and organization	1.97E-02–1.22E-04	31
Cellular function and maintenance	1.97E-02–1.22E-04	37
Cluster 12 (↗↗→) (upregulation from CC_GV0 to CC_GV2 and relatively stable levels from CC_GV2 to CC_GV3)		
Lipid metabolism	2.18E-02–8.79E-05	49
Small molecule biochemistry	2.18E-02–8.79E-05	71
Vitamin and mineral metabolism	2.15E-02–8.79E-05	23
Cell-to-cell signaling and interaction	2.15E-02 - 8.79E-05	59
Cellular movement	1.86E-02–9.96E-05	43

FlexArray (CC_GV0 vs. CC_GV1; CC_GV0 vs. CC_GV2; CC_GV0 vs. CC_GV3) were uploaded to IPA and analyzed considering the fold change difference for each gene. Interestingly, one of the main affected functions in each contrast was 'cell death and survival' (Table III). Moreover, as shown in Fig. 4, the number of apoptosis-related genes that were deregulated increased substantially from CC_GV0 vs. CC_GV1 to CC_GV0 vs. CC_GV3 contrasts. Importantly, IPA revealed that apoptosis is predicted to be inhibited in CC_GV1 and CC_GV2, while it is activated in CC_GV3 (Fig. 4, gene lists shown in Fig. 4 are provided as Supplementary Table 2).

Active caspase-positive cells analysis

In order to validate the *in-silico* functional prediction (generated by IPA) that CC_GV3 is more prone to apoptosis, we analyzed the susceptibility of CC isolated from oocytes with different chromatin configurations to undergo apoptosis.

It has been shown that apoptotic cell death of granulosa cells is the molecular mechanism underlying follicle atresia (Jolly *et al.*, 1994).

A previous study demonstrated that the dissociation of both mural granulosa cells and CC triggers apoptosis in both cell subsets (Luciano *et al.*, 2000). Therefore, we used CC dissociation as a 'stress test' in order to assess whether chromatin compaction (from GV0 to GV3) was associated with an increased tendency of the oocyte's associated CC to undergo apoptosis. CC isolated from single oocytes with different chromatin configurations (CC_GV0, CC_GV1, CC_GV2 and CC_GV3) were isolated and *in-vitro* cultured for 3 h and then assayed for pan-caspase activity. As shown in Fig. 5, the percentage of caspase-positive cells was significantly lower in CC from GV0 oocytes, whereas it increased in CC from GV1 and GV2 oocytes, reaching the highest value in CC from GV3 oocytes, as predicted by IPA.

Relationship between COC features and oocyte chromatin configuration

The findings that CC isolated from oocytes with different chromatin configurations differ in their transcriptomic profiles and in their

Table III Molecular and cellular functions identified by IPA ($P < 0.05$, fold change higher than ± 2) in each contrast (CC_GV0 vs. CC_GV1, CC_GV0 vs. CC_GV2, CC_GV0 vs. CC_GV3, where CC_GV0 represents the reference group).

Molecular and cellular functions	*P*-value	#Molecules
CC_GV0 vs. CC_GV1		
Cell death and survival	4.23E-03–2.69E-08	60
Cellular function and maintenance	4.28E-03–3.48E-07	64
Cellular movement	4.31E-03–5.75E-07	42
Cellular growth and proliferation	3.51E-03–7.05E-07	63
Cell-to-cell signaling and interaction	4.17E-03–9.85E-07	49
CC_GV0 vs. CC_GV2		
Cell death and survival	7.77E-03–2.51E-08	73
Cellular function and maintenance	8.19E-03–4.69E-08	60
Cellular growth and proliferation	7.51E-03–5.65E-07	76
Cellular movement	7.72E-03–9.42E-07	49
Cell morphology	8.19E-03–1.12E-05	53
CC_GV0 vs. CC_GV3		
Cell death and survival	1.78E-03–1.22E-15	107
Cellular development	1.95E-03–7.66E-11	109
Cell cycle	1.78E-03–1.10E-10	61
Cellular growth and proliferation	1.95E-03–1.25E-10	114
Cell morphology	1.70E-03–1.16E-08	67

susceptibility to undergo apoptosis, lead us to hypothesis that COC isolated from middle antral follicles bearing oocytes with different chromatin configurations (GV1, GV2 or GV3) could respond differently to specific *in-vitro* cultural conditions.

To test this hypothesis, and considering that it is technically not possible to directly identify the chromatin configuration without DNA staining after CC removal, we first looked for possible morphological markers that could be related to the chromatin configuration of the corresponding oocyte, and that therefore could be used to isolate a population of COC from middle antral follicle enriched in one of the GV stages (GV1, GV2 or GV3). Precisely, we considered the possible relationship between chromatin configuration and (i) the size of the follicle and (ii) the morphology of the COC, using morphological criteria commonly accepted by the scientific community and clearly recognizable under a stereomicroscope. These studies revealed a relationship between the oocyte chromatin configuration and the morphology of the COC but not with the size of the follicle from which they originate (Fig. 6). In fact, oocytes with GV1, GV2 and GV3 chromatin configuration were equally distributed in follicle of 2–4, 4–6 and > 6 mm in diameter (Fig. 6A). On the other hand, as shown in Fig. 6B, when isolated and additionally sub-grouped into three classes based on their morphology (Blondin and Sirard, 1995), Class 1 COC (with homogeneous ooplasm and compact CC) was the only one in which oocytes with GV1 chromatin configuration could be found,

while oocytes with GV1 chromatin configuration were almost absent in Class 2 and 3 COC (minor granulation of the ooplasm with compact CC, or highly granulated ooplasm and/or few outer layers CC showing expansion in Classes 2 and 3, respectively),

Furthermore, BCB staining of Classes 1, 2 and 3 COC indicated that Class 1 COC are in an earlier stage of differentiation when compared with Class 2 and 3 COC, giving additional (indirect) confirmation that chromatin compaction is associated with oocyte (and accompanying CC) differentiation. Indeed as shown in Fig. 6C, the percentage of BCB-negative oocytes was significantly higher in Class 1 than in Class 2/3 COC ($P < 0.05$).

## Effect of pre-IVM treatment on oocyte developmental competence

Having established that Class 1 and Class 2/3 COC differ in the relative percentage of oocytes with different chromatin configuration, and that Class 1 was the only class enriched with GV1 oocytes, we tested the hypothesis that these classes respond differently to specific *in-vitro* cultural conditions.

As shown in Fig. 7, when subjected to standard IVP procedures (within a regular IVM protocol), Class 1 COC showed a limited embryonic developmental competence (Fig. 7). Indeed after 7 days of culture both the blastocyst rate and mean blastocyst cell number per embryo were significantly lower in Class 1 COC when compared with the Class 2/3 groups ($P < 0.05$). As expected, the group composed of the mix of Class 1, 2 and 3 COC, which correspond to the unsorted group of COC commonly used in IVP protocols, showed intermediate values between Class 1 and Class 2/3 COC. On the other hand, pre-IVM treatment increased significantly the developmental capability (blastocyst rate and mean blastocyst cell number per embryo) of Class 1 COC and had no effect on the mixed group, while it reduced the developmental competence of Class 2/3 COC.

Discussion

The present work provides the first comprehensive transcriptome analysis of bovine CC associated with oocytes with a specific large-scale chromatin configuration. This is particularly relevant as chromatin configuration is indicative of the state of oocyte differentiation in the antral follicle before dominance emergence in naturally cycling animals (Lodde *et al.*, 2007, 2008, 2009). Transcriptomic data analysis confirmed the hypothesis that features of the cumulus oophorus investment change along with oocyte chromatin compaction. Interestingly, results of the BGA analysis, that gives information on the overall transcriptomic profile of each biological sample, are in accordance with the global change in distribution of transcriptomic data obtained from oocytes with different chromatin configurations (compare Fig. 1C of the present study and Fig. 2 in Labrecque *et al.*, 2015). Collectively, these data, and in particular the relative distance between each group, effectively confirm that global transcriptional differences exist among oocytes with different chromatin configurations as well as in their surrounding CC. Thus, the transcriptome of the whole COC changes along with the increase in chromatin compaction.

According to our previous morphological and functional studies, the present clustering analysis of microarray data revealed that major changes in terms of CC transcript differences occur during the
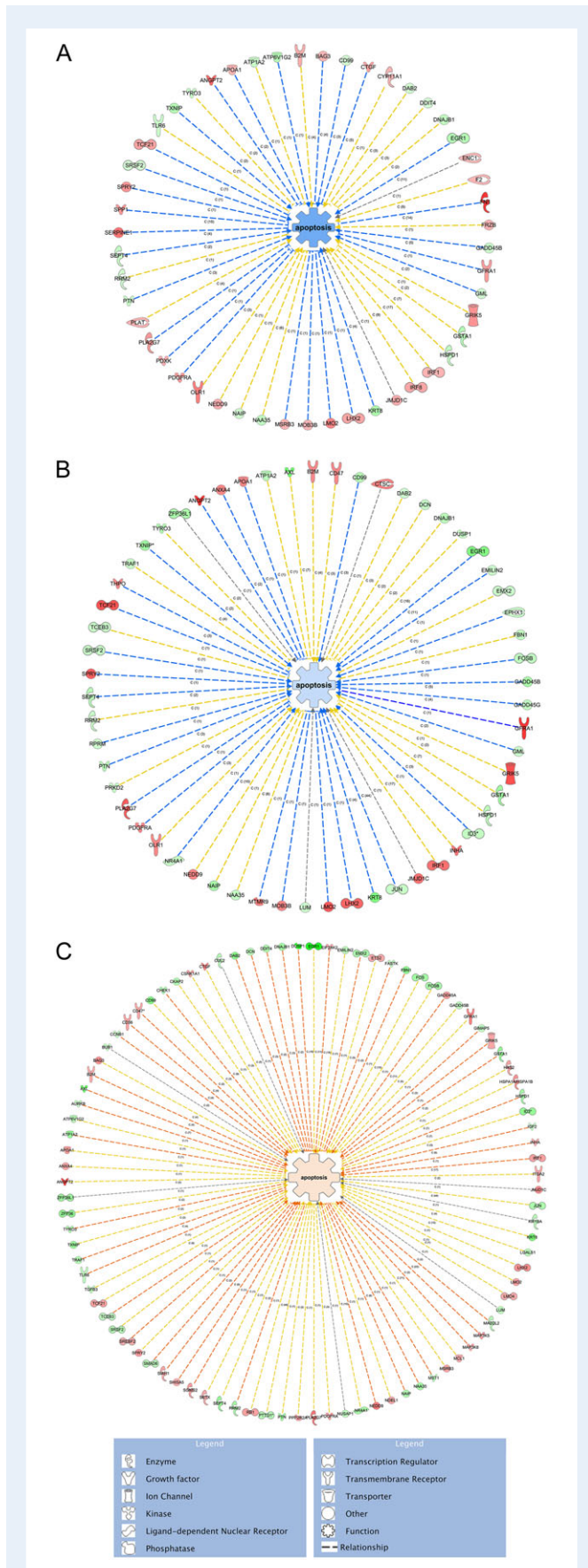
GV0-to-GV1 transition (Fig. 2). Indeed, the cluster profiles #6 and 9 (downregulation or upregulation between CC_GV0 and CC_GV1 and relatively stable low levels in successive groups) collect ~36% of the differentially expressed probes. Interestingly, *in-silico* functional analysis through IPA of the subsets of genes that best fitted with these two profiles revealed a major change of CC transcripts involved in lipid metabolism during the GV0-to-GV1 transition. Recent works showed that the lipid content in CC reflects the quality of the female gamete (Montani *et al.*, 2012; Auclair *et al.*, 2013) both in human (Matorras *et al.*, 1998) and in bovine (Kim *et al.*, 2001). It has been also recently reported that CC are able to protect the oocyte by storing elevated levels of free fatty acids from follicular fluid (Aardema *et al.*, 2013). In addition, studies in mice revealed that oocytes are deficient in cholesterol production and require CC to provide products of the cholesterol biosynthesis pathway, and suggest that oocytes promote cholesterol biosynthesis in CC through oocyte-derived paracrine factors, probably to compensate for their deficiency (Su *et al.*, 2008). Altogether, these data sustain the general idea that defective lipid metabolism inside the COC may be in part responsible for the lower meiotic and developmental competence of the oocyte. In this view, we can speculate that CC acquire the 'competence' of metabolizing lipids during the GV0–GV1 transition, which occurs during the early-to-middle stage of follicle development, and that the inability of GV0 oocytes to mature and develop into an embryo might be, at least in part, from an inappropriate capacity of the surrounding CC to metabolize lipids. Nevertheless, this hypothesis remains to be confirmed experimentally.

Gene expression profiles in CC have attracted great interest in the last years. In fact, a small biopsy of the cumulus oophorus could be easily collected before IVM, without perturbing oocyte viability, and assayed for expression of genes used as markers to predict the corresponding oocyte's quality. With this view, the present study confirms several previously reported markers associated with poor or high embryonic developmental potential in cattle, such as GATM or MAN1A1 (Bunel *et al.*, 2014, 2015). Notably, a similar approach has been conducted in the primed mouse model by comparing the transcriptomic profiles of CC isolated from antral oocytes with a non-surrounded nucleolus configuration (NSN, less compacted chromatin) and surrounded nucleolus configuration (SN, more compacted chromatin) (Zuccotti *et al.*, 1995; Vigone *et al.*, 2013). Compared to the present study in the cow, Vigone *et al.* found a relatively low number of differentially expressed genes with fold changes higher than 2. The difference of the animal model of course could explain this difference. Moreover, we cannot exclude that taking advantages of the gradual chromatin remodeling by considering two intermediate stages of compaction (GV1 and GV2) between the two extremes (GV0 and GV3) allowed the identification of a higher number of differentially expressed

Figure 4 Functional analysis. IPA generated diagrams representing deregulated apoptosis-related genes (*P* < 0.05; fold change higher than ±2) in CC_GV0 vs. CC_GV1 (**A**), CC_GV0 vs. CC_GV2 (**B**) and CC_GV0 vs. CC_GV3. Note that apoptosis is predicted to be inhibited (blue) in CC_GV1 and CC_GV2, while it is activated (orange) in CC_GV3. Gene lists are provided in Supplementary Table 2; genes in red are upregulated; genes in green are downregulated.
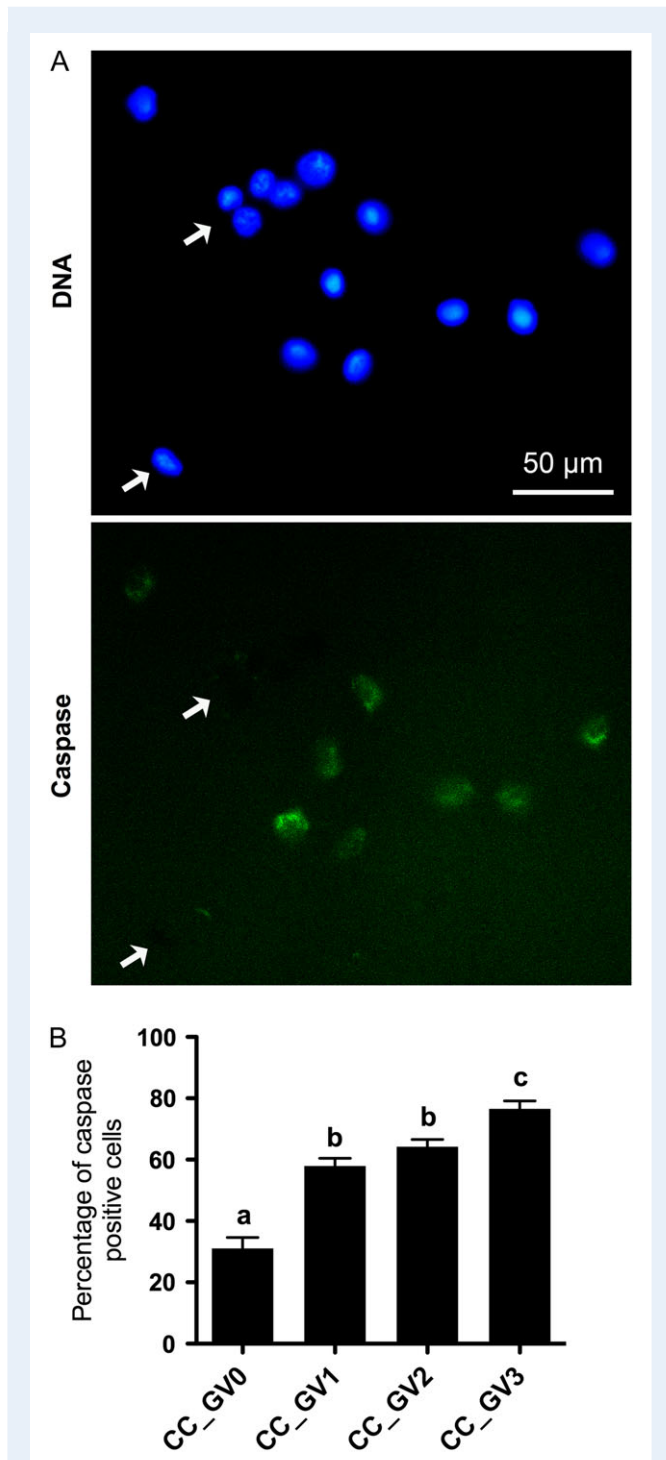
Figure 5 Assessment of caspase activity in cells isolated from oocytes with different chromatin configurations. CC associated with oocytes with GV0, GV1, GV2 and GV3 chromatin configuration were isolated and assayed for Caspase activity after 3 h of culture using the CaspaTag™ Pan-Caspase In Situ Assay Kit. (**A**) Representative pictures show active caspase in cells undergoing apoptosis and negative (arrows) cells. (**B**) Graph shows the percentage of caspase-active cells in each GV category; data from three independent experiments were analyzed by one-way ANOVA followed by Newman–Keuls multiple comparison test; data are expressed as means ± SEM; a,b,c: different superscripts indicate significant differences between groups ($P < 0.05$).

genes. It may be possible indeed that mouse oocytes with intermediated configurations (Bouniol-Baly et al., 1999; Bonnet-Garnier et al., 2012), which are generally grouped together with one of the two extremes may limit the capacity for revealing certain differences. On the other hand, we found correspondence with some of the genes identified by Vigone et al., such as Has2, which is upregulated in bovine CC_GV3 and mouse SN oocytes when compared to GV0 and NSN oocytes, respectively. This sets the stage for further comparative studies between the mouse and the bovine models.

Importantly, besides the assessment and confirmation of genes with known function in the reproductive system, our analysis provides multiple new biomarkers that are potentially involved in oocyte competence acquisition. For example, our data indicate that SLC39A8 is one of the genes whose expression constantly increases in CC during the GV0-to-GV3 transition. SLC39A8, also known as ZIP8, encodes for a member of the SLC39 family of solute-carrier genes, which shows structural characteristics of zinc transporters (Wang et al., 2012). Recently, it has been shown that the oocyte zinc content exerts important roles in oocyte function in mice, especially during meiotic maturation and fertilization (Kim et al., 2010, 2011; Bernhardt et al., 2011, 2012; Kong et al., 2012; Tian and Diaz, 2012). Moreover, Lisle et al. suggested that CC regulate the amount of free Zinc in the oocyte during maturation (Lisle et al., 2013). Interestingly, findings in mice show that acute dietary zinc deficiency during preconception (i.e. restricted to 3–5 days before ovulation) disrupts oocyte chromatin methylation and alters transcriptional regulation of repetitive elements, which is associated with severe defects of pre- and post-implantation embryonic development as well as of placental development (Tian and Diaz, 2013; Tian et al., 2014). This is important since the period in which the mice were fed with a zinc deficiency diet in these studies corresponds to the final oocyte growth phase, when chromatin remodeling occurs (Albertini, 1992; Debey et al., 1993; Zuccotti et al., 1995; Bouniol-Baly et al., 1999; De La Fuente et al., 2004; Bonnet-Garnier et al., 2012). These data clearly indicate that zinc plays important roles also before meiotic resumption and our data might set the stage for further investigation on the role of SLC39A8 as a possible player acting in the somatic compartment and involved in the control of oocyte zinc content, which is in turn important for the establishment of the oocyte epigenetic signature. Interestingly, in the mouse model, the zinc transporter SLC39A10 was found to be upregulated in CC from SN oocytes, when compared to NSN oocytes (Vigone et al., 2013).

Importantly, besides the identification of single gene's function, the present data set gives the opportunity to find pathways and mechanisms that are set in place in the somatic compartment that ultimately affect oocyte quality. This has paramount implications in the development of oocyte culture systems specifically formulated to fulfill the specific needs of the oocyte at a specific stage and support their in-vitro development. For example, in-silico analysis of differentially expressed genes in the three contrasts through IPA, revealed that apoptosis is predicted to be inhibited in CC of GV1 and of GV2 (even if at a lower extent) while it is predicted to be activated in CC of oocytes with the highest degree of chromatin compaction (GV3). Among the apoptosis-related genes identified by IPA, angiopoietin 2 (ANGPT2) was the most upregulated gene in CC_GV3 when compared to CC_GV0. ANGPT2 is an antagonist of the angiogenic factor ANGPT1 that signals through the endothelial cell-specific Tie2 receptor tyrosine kinase. ANGPT2 disrupts the vascular remodeling ability of ANGPT1
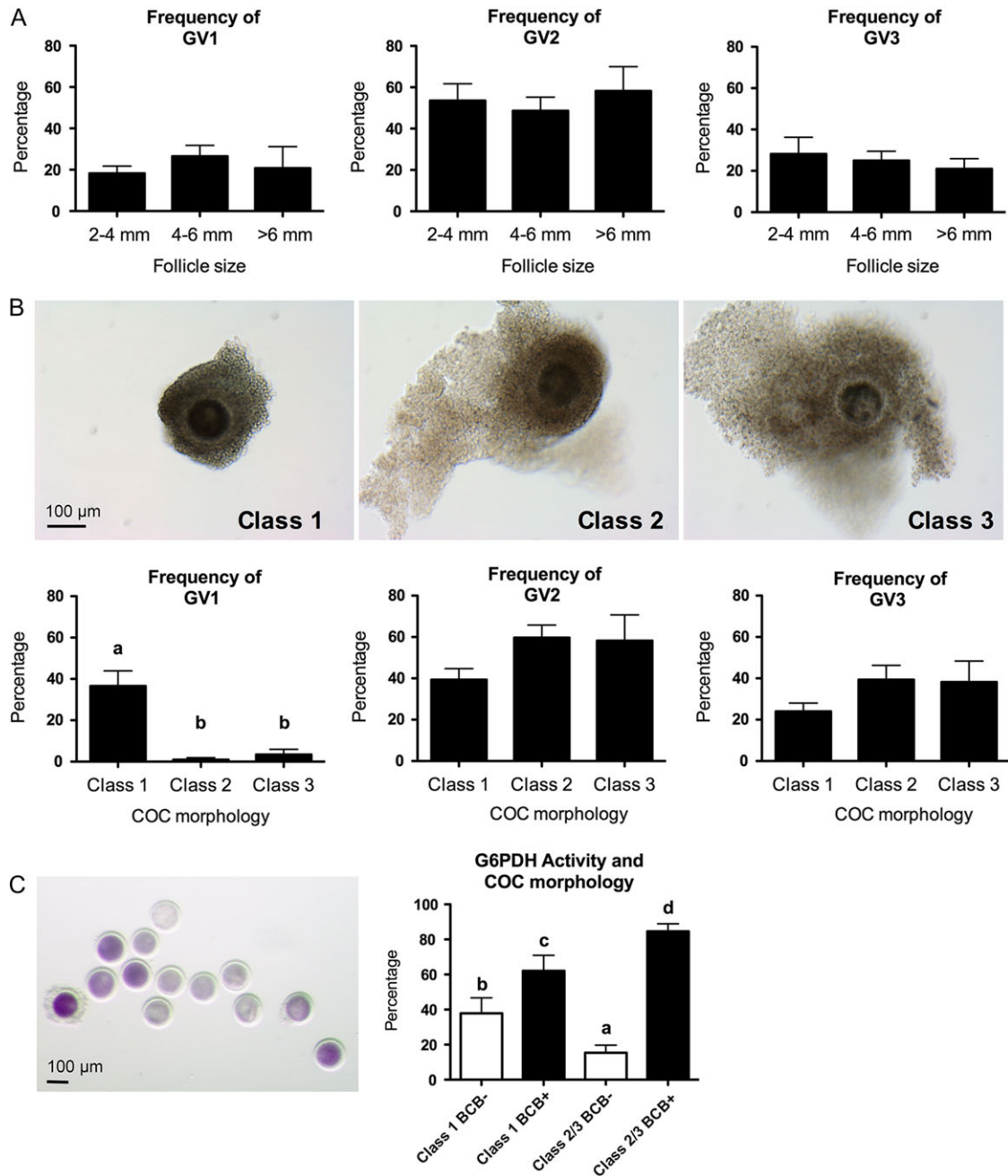
Figure 6 Relationship between large-scale chromatin configuration, follicle size, COC morphology and oocyte glucose-6-phosphate dehydrogenase (G6PDH) activity. (**A**) COC were collected from follicles of different diameter and chromatin configurations were assessed after CC removal. Graphs show the frequency of GV1, GV2 and GV3 chromatin configurations in each follicle size category. A total of 277 oocytes (167, 52 and 52 from small, medium and large antral follicle, respectively) were used in this study in three independent experiments. Data were analyzed by one-way ANOVA. (**B**) After collection, COC were separated according to morphological criteria as shown in the representative pictures (*Class 1*: homogeneous ooplasm and absence of expansion of outer layer CC; *Class 2*: minor granulation of the ooplasm and/or beginning of expansion of outer layer CC; *Class 3*: highly granulated ooplasm and few CC layers showing expansion). After classification, CC were removed and the chromatin configuration was assessed. Graphs show the frequency of GV1, GV2 and GV3 chromatin configurations in each class. A total of 300 oocytes (101 Class 1, 119 Class 2 and 80 Class 3) were used in this study in three independent experiments. Data were analyzed by one-way ANOVA followed by Newman–Keuls multiple comparison test; a,b: different letters indicate significant differences, $P < 0.05$). (**C**) After collection, COC were separated into Class 1 and Class 2/3 on the basis of their morphology and subjected to Brilliant Cresyl Blue staining (BCB). After removal of CC, oocytes were classified as BCB+ or BCB− as shown in the representative picture. Graph shows the percentage of BCB+ and BCB− oocytes in Class 1 and 2/3 COC. A total of 337 COC were analyzed (126 Class 1 and 211 of Class 2/3) in nine independent experiments. Data were analyzed by one-way ANOVA followed by Newman–Keuls multiple comparison test; data are expressed as means ± SEM; a, b, c, d: different letters indicate significant differences ($P < 0.05$).
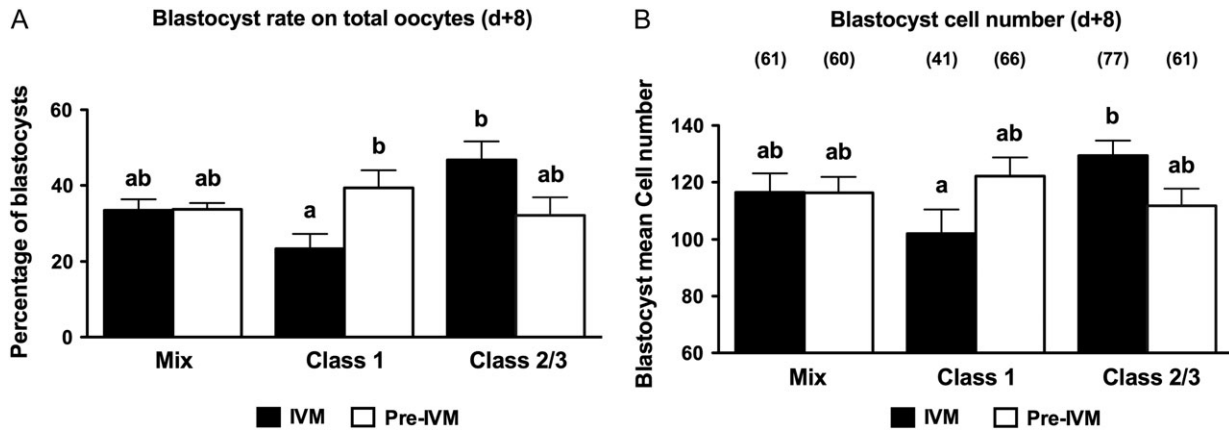
Figure 7 Effect of pre-maturation treatment on COC with different morphology. After collection, COC were separated into Class 1 and Class 2/3 on the basis of their morphology and *in vitro* matured with or without the pre-IVM treatment. Then, oocytes were *in-vitro* fertilized and *in-vitro* cultured for 8 days. Groups of unsorted COC (mix of Class 1/2/3) were subjected to the same experimental procedure and were used as controls. Graphs show the effect of the pre-IVM treatment on the blastocyst rate (**A**) and mean cell number per blastocyst (**B**). A total of 947 oocytes were analyzed in this study (292 mixed oocytes, 321 Class 1 and 334 Class 2/3) in six independent experiments. Data were analyzed by one-way ANOVA followed by Newman–Keuls multiple comparison test; data are expressed as means ± SEM; a, b: different letters indicates significant differences ($P < 0.05$).
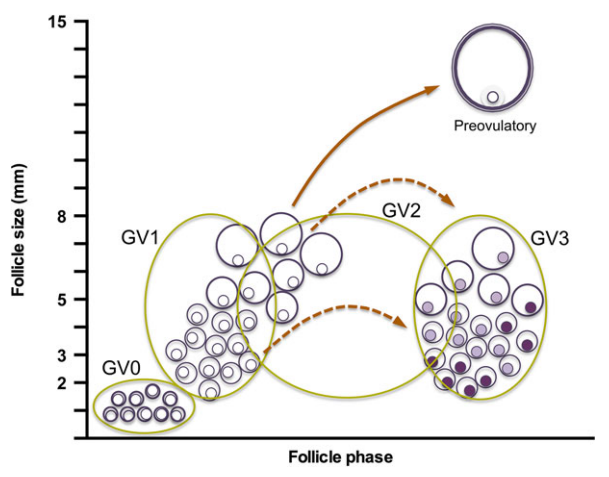

Figure 8 Chromatin remodeling during follicular development: a model. The figure shows chromatin remodeling, as it would occur during the bovine estrous cycle. Follicles with white oocytes are non-atretic, while follicles with pink oocytes are early atretic and those with purple oocytes are atretic. The growing follicles would be mainly GV1, the plateau phase would be mainly GV2 and the early atretic would be GV3. Adapted from Merton et al. (2003).

and may induce endothelial cell apoptosis (Maisonpierre et al., 1997). In the cyclic ovary, ANGPT1, ANGPT2, Tie1 and Tie2, play important roles in the modulation of vascular growth and regression (Goede et al., 1998; Hazzard et al., 1999; Wulff et al., 2000, 2001a, b) and studies in cow revealed a function of this system in the remodeling of the vascular network specifically in the ovarian follicle (Hayashi et al., 2003, 2004). Strikingly, ANGPT2 was found to be upregulated in early atretic follicles (Hayashi et al., 2003; Girard et al., 2015), thus supporting our finding that CC_GV3 are more prone to apoptosis.

These *in-silico* predictions are experimentally confirmed by the fact that the CC's susceptibility to apoptosis increases with oocyte's chromatin compaction. Moreover, these data are in agreement with previous findings indicating that functional gap junction-mediated communication between the oocyte and the surrounding CC is impaired in COC enclosing a GV3 oocyte and with signs of early cellular degeneration observed in GV3 oocytes at the ultrastructure level (Lodde et al., 2007, 2008). On the other hand, the present findings support the general idea that COC enclosing a GV1 oocyte are in an earlier stage of oocyte differentiation. In fact, Class 1 COC, which was originally characterized as the one with no morphological signs of degeneration and lower developmental competence (Blondin and Sirard, 1995; Hazeleger et al., 1995) and whose oocytes were found to be in an earlier stage of differentiation as assessed by BCB staining (present study), was the only class enriched in GV1 oocytes.

On the basis of our findings, we designed a tailored culture system, which confirmed that the success of *in-vitro* cultural strategies aimed at improving oocyte developmental capability is 'stage dependent', i.e. mainly due to the characteristic of the COC that are subjected to the procedure. Indeed we demonstrated that standard IVM conditions are inappropriate to support pre-implantation embryonic development of GV1-enriched Class 1 COC, while their developmental competence is positively affected by a 6 h period of inhibition of meiotic resumption through cAMP modulators. On the contrary, the same treatment negatively affected Class 1 and 2 COC developmental competence, which is consistent with the findings that these classes only contain GV2 and GV3 oocytes. This in turn confirms earlier studies in which prolonged Pre-IVM (24 h) increased GV0 meiotic and developmental competencies (Luciano et al., 2011). These data are consistent with one of the concepts beyond pre-maturation strategies (Gilchrist, 2011; Sirard, 2011; Smitz et al., 2011; Franciosi et al., 2014; Gilchrist et al., 2016), i.e. the prolongation of GJ-mediated communication between the somatic and germinal compartments is expected to be more effective in COC with a functional oocyte-CC coupling (as in GV0 and GV1 (Lodde et al., 2007)).

An important finding of the present work is that, in naturally cycling animals, COC selection based on follicle size does not allow isolation of a homogeneous population in terms of chromatin configuration. This implies that at each follicular wave, GV1-to-GV2 transition, which marks the acquisition of a high embryonic developmental potential, occurs at almost any size as the growth of the follicle slows down before dominant follicle emergence and concomitantly with decline in the FSH level (Adams *et al.*, 2008; Forde *et al.*, 2011). After the highest FSH level is attained in the preovulatory peak, the atretic events would start and GV2-to-GV3 transition eventually occurs. The timing of such a sequence would fit the preparation of the oocyte for ovulation or atresia, which requires chromatin compaction in both cases. This further confirms a previously postulated hypothesis that 'GV3 oocytes represent that proportion of gametes, which have reached a high developmental capability during follicular growth, and that, at the time of collection, were undergoing early events of atresia' (Lodde et al., 2007, 2008). These concepts are summarized in a tentative model illustrated in Fig. 8 which relates well with an average competence of 33% and early atresia improving developmental potential (Blondin and Sirard, 1995). If each follicle would contain a GV2 stage oocyte at its plateau phase and such status would be permissive for further development, it would explain the extraordinary stable blastocyst rate observed with bovine IVM since 1995. The growing follicles would be mainly GV1, the plateau phase would be (low FSH) GV2 and the early atretic would be GV3 with respectively low, high and medium developmental competence.

In conclusion, our data support the idea that the synchrony between nuclear, cytoplasmic and molecular events is finely tuned during the final phase of oocyte growth. Our results also demonstrate the necessity of a deep knowledge of the biological process occurring in CC during the final growth of the oocyte for the refinement of customized culture systems, which should consider the metabolic requirements of the heterogeneous population of oocytes that are submitted to IVM. This is mandatory to significantly improve assisted reproductive technologies. Very recently, a high similarity in the process of chromatin remodeling occurring in bovine and human immature oocytes, which reflects a high cellular and molecular heterogeneity in human oocytes, have been reported (Sanchez *et al.*, 2015). Thus, the present work may have important consequences for human IVM in which the results are still suboptimal compared to conventional IVF (Coticchio *et al.*, 2012). In addition to avoiding the primary adverse effects caused by ovarian stimulation, further improvements in IVM effectiveness and efficiency may help broaden the use of IVM for fertility preservation and in infertile patients.

Supplementary data

Supplementary data are available at *Molecular Human Reproduction* online.

Acknowledgements

Authors' roles

All authors contributed substantially to this manuscript. A.M.L., V.L. and M.A.S. designed the study; C.D., V.L., R.L., I.D., I.T. and A.M.L. executed experiments; C.D., R.L., V.L., A.M.L. and M.A.S. analyzed the data; V.L., C.D. and A.M.L. wrote the manuscript. All authors revised and approved the final manuscript.

Funding

Conflict of interest

None declared.

References

Aardema H, Lolicato F, van de Lest CH, Brouwers JF, Vaandrager AB, van Tol HT, Roelen BA, Vos PL, Helms JB, Gadella BM. Bovine cumulus cells protect maturing oocytes from increased fatty acid levels by massive intracellular lipid storage. *Biol Reprod* 2013;**88**:164.

Adams GP, Jaiswal R, Singh J, Malhi P. Progress in understanding ovarian follicular dynamics in cattle. *Theriogenology* 2008;**69**:72–80.

Albertini DF. Cytoplasmic microtubular dynamics and chromatin organization during mammalian oogenesis and oocyte maturation. *Mutat Res* 1992;**296**:57–68.

Auclair S, Uzbekov R, Elis S, Sanchez L, Kireev I, Lardic L, Dalbies-Tran R, Uzbekova S. Absence of cumulus cells during in vitro maturation affects lipid metabolism in bovine oocytes. *Am J Physiol Endocrinol Metab* 2013;**304**:E599–613.

Bernhardt ML, Kim AM, O'Halloran TV, Woodruff TK. Zinc requirement during meiosis I-meiosis II transition in mouse oocytes is independent of the MOS-MAPK pathway. *Biol Reprod* 2011;**84**:526–536.

Bernhardt ML, Kong BY, Kim AM, O'Halloran TV, Woodruff TK. A zinc-dependent mechanism regulates meiotic progression in mammalian oocytes. *Biol Reprod* 2012;**86**:114.

Blazejczyk M, Miron M, Nadon R *FlexArray: A* Statistical Data Analysis Software for Gene Expression Microarrays. Montreal, Canada: Genome Quebec, 2007.

Blondin P, Bousquet D, Twagiramungu H, Barnes F, Sirard MA. Manipulation of follicular development to produce developmentally competent bovine oocytes. *Biol Reprod* 2002;**66**:38–43.

Blondin P, Sirard MA. Oocyte and follicular morphology as determining characteristics for developmental competence in bovine oocytes. *Mol Reprod Dev* 1995;**41**:54–62.

Bonnet-Garnier A, Feuerstein P, Chebrout M, Fleurot R, Jan HU, Debey P, Beaujean N. Genome organization and epigenetic marks in mouse germinal vesicle oocytes. *Int J Dev Biol* 2012;**56**:877–887.

Bouniol-Baly C, Hamraoui L, Guibert J, Beaujean N, Szollosi MS, Debey P. Differential transcriptional activity associated with chromatin configuration in fully grown mouse germinal vesicle oocytes. *Biol Reprod* 1999;**60**:580–587.

Bunel A, Jorssen EP, Merckx E, Leroy JL, Bols PE, Sirard MA. Individual bovine in vitro embryo production and cumulus cell transcriptomic analysis to distinguish cumulus-oocyte complexes with high or low developmental potential. *Theriogenology* 2015;**83**:228–237.

Bunel A, Nivet AL, Blondin P, Vigneault C, Richard FJ, Sirard MA. Cumulus cell gene expression associated with pre-ovulatory acquisition of

developmental competence in bovine oocytes. *Reprod Fertil Dev* 2014; **26**:855–865.

Coticchio G, Dal Canto M, Mignini Renzini M, Guglielmo MC, Brambillasca F, Turchi D, Novara PV, Fadini R. Oocyte maturation: gamete-somatic cells interactions, meiotic resumption, cytoskeletal dynamics and cytoplasmic reorganization. *Hum Reprod Update* 2015; **21**:427–454.

Coticchio G, Dal-Canto M, Guglielmo MC, Mignini-Renzini M, Fadini R. Human oocyte maturation in vitro. *Int J Dev Biol* 2012; **56**:909–918.

Culhane AC, Perriere G, Considine EC, Cotter TG, Higgins DG. Between-group analysis of microarray data. *Bioinformatics* 2002; **18**:1600–1608.

De La Fuente R. Chromatin modifications in the germinal vesicle (GV) of mammalian oocytes. *Dev Biol* 2006; **292**:1–12.

De La Fuente R, Eppig JJ. Transcriptional activity of the mouse oocyte genome: companion granulosa cells modulate transcription and chromatin remodeling. *Dev Biol* 2001; **229**:224–236.

De La Fuente R, Viveiros MM, Burns KH, Adashi EY, Matzuk MM, Eppig JJ. Major chromatin remodeling in the germinal vesicle (GV) of mammalian oocytes is dispensable for global transcriptional silencing but required for centromeric heterochromatin function. *Dev Biol* 2004; **275**:447–458.

Debey P, Szollosi MS, Szollosi D, Vautier D, Girousse A, Besombes D. Competent mouse oocytes isolated from antral follicles exhibit different chromatin organization and follow different maturation dynamics. *Mol Reprod Dev* 1993; **36**:59–74.

Edgar R, Domrachev M, Lash AE. Gene Expression Omnibus: NCBI gene expression and hybridization array data repository. *Nucleic Acids Res* 2002; **30**:207–210.

Eppig JJ. Oocyte control of ovarian follicular development and function in mammals. *Reproduction* 2001; **122**:829–838.

Eppig JJ, Schultz RM, O'Brien M, Chesnel F. Relationship between the developmental programs controlling nuclear and cytoplasmic maturation of mouse oocytes. *Dev Biol* 1994; **164**:1–9.

Forde N, Beltman ME, Lonergan P, Diskin M, Roche JF, Crowe MA. Oestrous cycles in Bos taurus cattle. *Anim Reprod Sci* 2011; **124**:163–169.

Franciosi F, Coticchio G, Lodde V, Tessaro I, Modina SC, Fadini R, Dal Canto M, Renzini MM, Albertini DF, Luciano AM. Natriuretic peptide precursor C delays meiotic resumption and sustains gap junction-mediated communication in bovine cumulus-enclosed oocytes. *Biol Reprod* 2014; **91**:61.

Gilbert I, Scantland S, Dufort I, Gordynska O, Labbe A, Sirard MA, Robert C. Real-time monitoring of aRNA production during T7 amplification to prevent the loss of sample representation during microarray hybridization sample preparation. *Nucleic Acids Res* 2009; **37**:e65.

Gilbert I, Scantland S, Sylvestre EL, Dufort I, Sirard MA, Robert C. Providing a stable methodological basis for comparing transcript abundance of developing embryos using microarrays. *Mol Hum Reprod* 2010; **16**:601–616.

Gilchrist RB. Recent insights into oocyte-follicle cell interactions provide opportunities for the development of new approaches to in vitro maturation. *Reprod Fertil Dev* 2011; **23**:23–31.

Gilchrist RB, Lane M, Thompson JG. Oocyte-secreted factors: regulators of cumulus cell function and oocyte quality. *Hum Reprod Update* 2008; **14**:159–177.

Gilchrist RB, Luciano AM, Richani D, Zeng HT, Wang X, Vos MD, Sugimura S, Smitz J, Richard FJ, Thompson JG. Oocyte maturation and quality: role of cyclic nucleotides. *Reproduction* 2016; **152**:R143–157.

Girard A, Dufort I, Douville G, Sirard MA. Global gene expression in granulosa cells of growing, plateau and atretic dominant follicles in cattle. *Reprod Biol Endocrinol* 2015; **13**:17.

Goede V, Schmidt T, Kimmina S, Kozian D, Augustin HG. Analysis of blood vessel maturation processes during cyclic ovarian angiogenesis. *Lab Invest* 1998; **78**:1385–1394.

Gordon I. *Laboratory Production of Cattle Embryos*, 2nd edn. Cambridge MA (USA): CABI Publishing, 2003.

Gougeon A. Dynamics of follicular growth in the human: a model from preliminary results. *Hum Reprod* 1986; **1**:81–87.

Gougeon A. Regulation of ovarian follicular development in primates: facts and hypotheses. *Endocr Rev* 1996; **17**:121–155.

Hayashi KG, Acosta TJ, Tetsuka M, Berisha B, Matsui M, Schams D, Ohtani M, Miyamoto A. Involvement of angiopoietin-tie system in bovine follicular development and atresia: messenger RNA expression in theca interna and effect on steroid secretion. *Biol Reprod* 2003; **69**:2078–2084.

Hayashi KG, Berisha B, Matsui M, Schams D, Miyamoto A. Expression of mRNA for the angiopoietin-tie system in granulosa cells during follicular development in cows. *J Reprod Dev* 2004; **50**:477–480.

Hazeleger NL, Hill DJ, Stubbing RB, Walton JS. Relationship of morphology and follicular fluid environment of bovine oocytes to their developmental potential in vitro. *Theriogenology* 1995; **43**:509–522.

Hazzard TM, Molskness TA, Chaffin CL, Stouffer RL. Vascular endothelial growth factor (VEGF) and angiopoietin regulation by gonadotrophin and steroids in macaque granulosa cells during the peri-ovulatory interval. *Mol Hum Reprod* 1999; **5**:1115–1121.

Hyttel P, Fair T, Callesen H, Greve T. Oocyte growth, capacitation and final maturation in cattle. *Theriogenology* 1997; **47**:23–32.

Jolly PD, Tisdall DJ, Heath DA, Lun S, McNatty KP. Apoptosis in bovine granulosa cells in relation to steroid synthesis, cyclic adenosine 3',5'-monophosphate response to follicle-stimulating hormone and luteinizing hormone, and follicular atresia. *Biol Reprod* 1994; **51**:934–944.

Kim AM, Bernhardt ML, Kong BY, Ahn RW, Vogt S, Woodruff TK, O'Halloran TV. Zinc sparks are triggered by fertilization and facilitate cell cycle resumption in mammalian eggs. *ACS Chem Biol* 2011; **6**:716–723.

Kim AM, Vogt S, O'Halloran TV, Woodruff TK. Zinc availability regulates exit from meiosis in maturing mammalian oocytes. *Nat Chem Biol* 2010; **6**:674–681.

Kim JY, Kinoshita M, Ohnishi M, Fukui Y. Lipid and fatty acid analysis of fresh and frozen-thawed immature and in vitro matured bovine oocytes. *Reproduction* 2001; **122**:131–138.

Kong BY, Bernhardt ML, Kim AM, O'Halloran TV, Woodruff TK. Zinc maintains prophase I arrest in mouse oocytes through regulation of the MOS-MAPK pathway. *Biol Reprod* 2012; **87**:11–12.

Kumar L, Futschik ME. Mfuzz: a software package for soft clustering of microarray data. *Bioinformation* 2007; **2**:5–7.

Labrecque R, Lodde V, Dieci C, Tessaro I, Luciano AM, Sirard MA. Chromatin remodelling and histone mRNA accumulation in bovine germinal vesicle oocytes. *Mol Reprod Dev* 2015; **82**:450–462.

Landry DA, Bellefleur AM, Labrecque R, Grand FX, Vigneault C, Blondin P, Sirard MA. Effect of cow age on the in vitro developmental competence of oocytes obtained following FSH stimulation/coasting treatments. *Theriogenology* 2016; **86**:1240–1246.

Lisle RS, Anthony K, Randall MA, Diaz FJ. Oocyte-cumulus cell interactions regulate free intracellular zinc in mouse oocytes. *Reproduction* 2013; **145**:381–390.

Lodde V, Franciosi F, Tessaro I, Modina SC, Luciano AM. Role of gap junction-mediated communications in regulating large-scale chromatin configuration remodeling and embryonic developmental competence acquisition in fully grown bovine oocyte. *J Assist Reprod Genet* 2013; **30**:1219–1226.

Lodde V, Modina S, Galbusera C, Franciosi F, Luciano AM. Large-scale chromatin remodeling in germinal vesicle bovine oocytes: interplay with gap junction functionality and developmental competence. *Mol Reprod Dev* 2007; **74**:740–749.

Lodde V, Modina S, Maddox-Hyttel P, Franciosi F, Lauria A, Luciano AM. Oocyte morphology and transcriptional silencing in relation to

chromatin remodeling during the final phases of bovine oocyte growth. *Mol Reprod Dev* 2008;**75**:915–924.

Lodde V, Modina SC, Franciosi F, Zuccari E, Tessaro I, Luciano AM. Localization of DNA methyltransferase-1 during oocyte differentiation, in vitro maturation and early embryonic development in cow. *Eur J Histochem* 2009;**53**:e24.

Lonergan P, Fair T. In vitro-produced bovine embryos: dealing with the warts. *Theriogenology* 2008;**69**:17–22.

Luciano AM, Franciosi F, Dieci C, Lodde V. Changes in large-scale chromatin structure and function during oogenesis: a journey in company with follicular cells. *Anim Reprod Sci* 2014;**149**:3–10.

Luciano AM, Franciosi F, Modina SC, Lodde V. Gap junction-mediated communications regulate chromatin remodeling during bovine oocyte growth and differentiation through cAMP-dependent mechanism(s). *Biol Reprod* 2011;**85**:1252–1259.

Luciano AM, Lodde V. Changes of large-scale chromatin configuration during mammalian oocyte differentiation. In: Coticchio G, Albertini DF, De Santis L (eds). *Oogenesis*. London: Springer, 2013:93–108.

Luciano AM, Lodde V, Beretta MS, Colleoni S, Lauria A, Modina S. Developmental capability of denuded bovine oocyte in a co-culture system with intact cumulus-oocyte complexes: role of cumulus cells, cyclic adenosine 3',5'-monophosphate, and glutathione. *Mol Reprod Dev* 2005;**71**:389–397.

Luciano AM, Modina S, Gandolfi F, Lauria A, Armstrong DT. Effect of cell-to-cell contact on in vitro deoxyribonucleic acid synthesis and apoptosis responses of bovine granulosa cells to insulin-like growth factor-I and epidermal growth factor. *Biol Reprod* 2000;**63**:1580–1585.

Lussier JG, Matton P, Dufour JJ. Growth rates of follicles in the ovary of the cow. *J Reprod Fertil* 1987;**81**:301–307.

Maisonpierre PC, Suri C, Jones PF, Bartunkova S, Wiegand SJ, Radziejewski C, Compton D, McClain J, Aldrich TH, Papadopoulos N et al. Angiopoietin-2, a natural antagonist for Tie2 that disrupts in vivo angiogenesis. *Science* 1997;**277**:55–60.

Matorras R, Ruiz JI, Mendoza R, Ruiz N, Sanjurjo P, Rodriguez-Escudero FJ. Fatty acid composition of fertilization-failed human oocytes. *Hum Reprod* 1998;**13**:2227–2230.

Matzuk MM, Burns KH, Viveiros MM, Eppig JJ. Intercellular communication in the mammalian ovary: oocytes carry the conversation. *Science* 2002;**296**:2178–2180.

Merton JS, de Roos AP, Mullaart E, de Ruigh L, Kaal L, Vos PL, Dieleman SJ. Factors affecting oocyte quality and quantity in commercial application of embryo technologies in the cattle breeding industry. *Theriogenology* 2003;**59**:651–674.

Monniaux D, Clement F, Dalbies-Tran R, Estienne A, Fabre S, Mansanet C, Monget P. The ovarian reserve of primordial follicles and the dynamic reserve of antral growing follicles: what is the link? *Biol Reprod* 2014;**90**:85.

Montani DA, Cordeiro FB, Regiani T, Victorino AB, Pilau EJ, Gozzo FC, Ferreira CR, Fraietta R, Lo Turco EG. The follicular microenviroment as a predictor of pregnancy: MALDI-TOF MS lipid profile in cumulus cells. *J Assist Reprod Genet* 2012;**29**:1289–1297.

Nivet AL, Bunel A, Labrecque R, Belanger J, Vigneault C, Blondin P, Sirard MA. FSH withdrawal improves developmental competence of oocytes in the bovine model. *Reproduction* 2012;**143**:165–171.

Pavlok A, Lucas-Hahn A, Niemann H. Fertilization and developmental competence of bovine oocytes derived from different categories of antral follicles. *Mol Reprod Dev* 1992;**31**:63–67.

Robert C, Nieminen J, Dufort I, Gagne D, Grant JR, Cagnone G, Plourde D, Nivet AL, Fournier E, Paquet E et al. Combining resources to obtain a comprehensive survey of the bovine embryo transcriptome through deep sequencing and microarrays. *Mol Reprod Dev* 2011;**78**:651–664.

Sanchez F, Romero S, De Vos M, Verheyen G, Smitz J. Human cumulus-enclosed germinal vesicle oocytes from early antral follicles reveal heterogeneous cellular and molecular features associated with in vitro maturation capacity. *Hum Reprod* 2015;**30**:1396–1409.

Sirard MA. Follicle environment and quality of in vitro matured oocytes. *J Assist Reprod Genet* 2011;**28**:483–488.

Smitz JE, Thompson JG, Gilchrist RB. The promise of in vitro maturation in assisted reproduction and fertility preservation. *Semin Reprod Med* 2011;**29**:24–37.

Stringfellow DA, Givens MD. Manual of the International Embryo Transfer Society: A Procedural Guide and General Information for the Use of Embryo Transfer Technology Emphasizing Sanitary Procedures, 4th edn, IETS Publisher, Savoy, IL (USA), 2010.

Su YQ, Sugiura K, Wigglesworth K, O'Brien MJ, Affourtit JP, Pangas SA, Matzuk MM, Eppig JJ. Oocyte regulation of metabolic cooperativity between mouse cumulus cells and oocytes: BMP15 and GDF9 control cholesterol biosynthesis in cumulus cells. *Development* 2008;**135**:111–121.

Tian X, Anthony K, Neuberger T, Diaz FJ. Preconception zinc deficiency disrupts postimplantation fetal and placental development in mice. *Biol Reprod* 2014;**90**:83.

Tian X, Diaz FJ. Zinc depletion causes multiple defects in ovarian function during the periovulatory period in mice. *Endocrinology* 2012;**153**:873–886.

Tian X, Diaz FJ. Acute dietary zinc deficiency before conception compromises oocyte epigenetic programming and disrupts embryonic development. *Dev Biol* 2013;**376**:51–61.

Torner H, Ghanem N, Ambros C, Holker M, Tomek W, Phatsara C, Alm H, Sirard MA, Kanitz W, Schellander K et al. Molecular and subcellular characterisation of oocytes screened for their developmental competence based on glucose-6-phosphate dehydrogenase activity. *Reproduction* 2008;**135**:197–212.

Vandesompele J, De Preter K, Pattyn F, Poppe B, Van Roy N, De Paepe A, Speleman F. Accurate normalization of real-time quantitative RT-PCR data by geometric averaging of multiple internal control genes. *Genome Biol* 2002;**3**:RESEARCH0034.

Vassena R, Mapletoft RJ, Allodi S, Singh J, Adams GP. Morphology and developmental competence of bovine oocytes relative to follicular status. *Theriogenology* 2003;**60**:923–932.

Vigone G, Merico V, Prigione A, Mulas F, Sacchi L, Gabetta M, Bellazzi R, Redi CA, Mazzini G, Adjaye J et al. Transcriptome based identification of mouse cumulus cell markers that predict the developmental competence of their enclosed antral oocytes. *BMC Genomics* 2013;**14**:380.

Wang CY, Jenkitkasemwong S, Duarte S, Sparkman BK, Shawki A, Mackenzie B, Knutson MD. ZIP8 is an iron and zinc transporter whose cell-surface expression is up-regulated by cellular iron loading. *J Biol Chem* 2012;**287**:34032–34043.

Wulff C, Wiegand SJ, Saunders PT, Scobie GA, Fraser HM. Angiogenesis during follicular development in the primate and its inhibition by treatment with truncated Flt-1-Fc (vascular endothelial growth factor Trap (A40)). *Endocrinology* 2001a;**142**:3244–3254.

Wulff C, Wilson H, Largue P, Duncan WC, Armstrong DG, Fraser HM. Angiogenesis in the human corpus luteum: localization and changes in angiopoietins, tie-2, and vascular endothelial growth factor messenger ribonucleic acid. *J Clin Endocrinol Metab* 2000;**85**:4302–4309.

Wulff C, Wilson H, Rudge JS, Wiegand SJ, Lunn SF, Fraser HM. Luteal angiogenesis: prevention and intervention by treatment with vascular endothelial growth factor trap(A40). *J Clin Endocrinol Metab* 2001b;**86**:3377–3386.

Zuccotti M, Garagna S, Merico V, Monti M, Alberto Redi C. Chromatin organisation and nuclear architecture in growing mouse oocytes. *Mol Cell Endocrinol* 2005;**234**:11–17.

Zuccotti M, Piccinelli A, Giorgi Rossi P, Garagna S, Redi CA. Chromatin organization during mouse oocyte growth. *Mol Reprod Dev* 1995;**41**:479–485.